Development of lentiviral vectors targeted to P38MAPK inhibition and Akt activation in motor neurons of a mouse model of familial amyotrophic lateral sclerosis

Thesis

The Open University, UK

— Advanced School of Pharmacology —
Dean, Enrico Garattini M D

Mario Negri Institute for
Pharmacological Research

DEVELOPMENT OF LENTIVIRAL VECTORS TARGETED TO P38MAPK INHIBITION AND AKT ACTIVATION IN MOTOR NEURONS OF A MOUSE MODEL OF FAMILIAL AMYOTROPHIC LATERAL SCLEROSIS

Marco Peviani

Degree of Doctor of Philosophy

The Open University of London

Submitted: 30th September 2009

ProQuest LLC.
789 East Eisenhower Parkway
P.O. Box 1346
Ann Arbor, MI 48106 – 1346

ABSTRACT

Amyotrophic lateral sclerosis (ALS) is a neurodegenerative disease characterised by progressive loss of motor neurons in the cortex, brainstem and spinal cord. This leads to weakness and muscular atrophy that evolves to paralysis and death. Studies on patients and animal models of ALS suggest that the pathology is the consequence of the unbalance between pro-degenerative (p38MAPK) and pro-survival (Akt) pathways in motor neurons. In order to re-equilibrate this complex interplay, the major objective of this study was to develop a gene-based approach to target, in vivo, these two intracellular signaling proteins.

We demonstrated for the first time that a construct derived from Hb9 promoter can be used in lentivectors to restrict transgene expression to motor neurons in vivo; moreover we found that induction of Akt pathway, through expression of constitutively activated Akt3 in motor neurons, prevents neuronal loss in SOD1G93A mice, although it does not influence their premature death. On the other hand, we used RNAi to downregulate p38MAPKalpha in a mouse model of ALS. We revealed that expression of p38MAPK-targeted shRNA in the spinal cord of presymptomatic mice reduces motor neuronal loss in the early phases of the pathology, but then it is not able to sustain neuronal survival during disease progression, eventually resulting in worsening of symptoms and shortening of life span. We found preliminary evidences that hyperactivation of microglial cells may be responsible for this more aggressive phenotype, suggesting that a fine tuning of microglial reactivity may be important to avoid pro-degenerative effects. Overall these data support the hypothesis that modulation of pro-degenerative and pro-survival pathways may help counteracting motor neuronal degeneration, and strengthen the evidence that preservation of neuronal perikaria is not sufficient to ameliorate disease progression in ALS. The peripheral compartment (axons, muscles) should be regarded as an additional target for potential therapeutic approaches.

ACKNOWLEDGMENTS

I wish to express my gratitude to Dr. Caterina Bendotti for the great academic and personal support given to me in all these years spent in her laboratory, and to my supervisor Prof. Robert J. Williams for helpful discussions and great availability during my PhD.

My sincere gratitude also goes to Dr. Roberto Piva for his mentorship and helpful advice for lentiviral vector development, and to his collaborators for welcome and support during the period spent in Turin for work in his laboratory.

I thank the Mario Negri Institute for Pharmacological Research for giving me the opportunity to undertake my PhD.

Finally, the most special thought to all the people that have been the body and the soul of the laboratory of Molecular Neurobiology in the last seven years.

I dedicate this thesis to my wife Marialuisa and all the people who believe in me.

To the beloved memory of Antonio and Emilia.

INDEX

ABSTRACT 1

ACKNOWLEDGMENTS 2

INDEX 3

LIST OF ABBREVIATIONS 8

LIST OF TABLES 13

LIST OF FIGURES 14

CHAPTER 1 - GENERAL INTRODUCTION 18

1.1 AMYOTROPHIC LATERAL SCLEROSIS 19

1.1.1 Symptomatology 20

1.1.2 Diagnosis 23

1.1.3 Neuropathology 26

1.1.4 Epidemiology 31

1.1.5 Genetics 33

1.2. EXPERIMENTAL MODELS OF ALS 44

1.2.1 In vitro models of MND 45

1.2.2 Animal models of MND 46

1.3. PATHOGENETIC HYPOTHESES OF ALS 54

1.3.1 Oxidative stress 54

1.3.2 Excitotoxicity 57

1.3.3 Mitochondrial dysfunction 59

1.3.4 Protein aggregation 60

1.3.5 Alterations of cytoskeleton and axonal transport 62

1.3.6 Evidence for ALS as a non-cell autonomous disease 65

1.3.7 Aberrant regulation of pro-degenerative and anti-apoptotic pathways 68

1.4 THE p38-MAPK PATHWAY 73
1.4.1 Overview of p38 MAPK pathway 73
1.4.2 Physiological roles of p38 MAPK pathway 78
1.4.3 p38 MAPK pathway in physiology and pathology in the nervous system 80
1.4.4 Strategies for targeting p38MAPK 83
1.5 THE PI3K/AKT PATHWAY 89
1.5.1 Overview of the PI3K/AKT pathway 89
1.5.2 Physiological roles of Akt pathway 101
1.5.3 PI3K/Akt pathway in health and disease of the nervous system 103
1.5.4 Strategies for targeting PI3K/Akt pathway 106
1.6 USE OF LENTIVIRAL VECTORS FOR TREATMENT OF NEURODEGENERATIVE DISEASES 111
1.6.1. From Lentivirus to a Lentiviral Vector 111
1.6.2 Features of lentiviral vectors 122
1.6.3 Targeting the Central Nervous System (CNS) is problematic 124
1.6.4 Strategies for broadening infectivity and increasing specificity 126
1.7 HYPOTHESIS OF THE STUDY 132
1.8 AIMS OF THE STUDY 132
CHAPTER 2 - MATERIALS AND METHODS 134
2.1 MATERIALS AND REAGENTS 135
2.1.1 Plasmids 135
2.1.2 Antibodies 139

2.1.3 Reagents for molecular biology 141

2.1.4 Cell lines 142

2.2 METHODS 142

2.2.1 Lentiviral vector production 142

2.2.2. G93A transgenic mouse model of ALS 143

2.2.3 Surgical procedures for delivery of lentiviral vectors in vivo 146

2.2.4 Analysis of motor performance and disease progression .. 149

2.2.5 Immunohistochemistry 150

2.2.6 Primary cell cultures 154

2.2.7 Infection of cell cultures 156

2.2.8 Transfection of cell cultures 156

2.2.9 Semi-quantitative PCR 157

2.2.10 Detection of viral genome integrated in host cells 159

2.2.11 Immunoblotting 160

2.2.12 PCR-cloning experiments 162

2.2.13 Data handling and statistical analysis 163

CHAPTER 3 - DEVELOPMENT OF STRATEGIES FOR TARGETING MOUSE SPINAL CORD MOTOR NEURONS IN VIVO 166

3.1 Protocol for production of lentiviral vectors at high titre 168

3.2 Direct injection into spinal cord parenchyma 169

3.3 Use of neuron-specific promoters in lentiviral vectors 170

3.3.1 Assessment of viral vectors carrying the rNSE promoter .. 170

3.3.2 Preparation of lentiviral vectors with motor neuron-restricted expression 172

3.4. Discussion 182

CHAPTER 4 - INDUCTION OF THE AKT PATHWAY 186

4.1 Generation of constitutively activated Akt constructs 189

4.2 Effect of induction of Akt pathway in vivo, in SOD1G93A mice.... 190

4.3 Discussion 202

CHAPTER 5 - USE OF RNA INTERFERENCE FOR TARGETING P38MAPK PATHWAY 206

5.1 RNAi, an introduction 207

5.2 RNAi as a tool to study the molecular mechanisms involved in ALS pathogenesis 208

5.3 Screening of p38-targeted shRNA candidate sequences 210

5.4 shRNA nr.7 selectively inhibits TNFα induced p38MAPK phosphorylation 212

5.5 shRNA nr.7 protects cultured neurons against colchicine induced toxicity 214

5.6 Effect of p38MAPK downregulation in vivo, in SOD1G93A mice... 215

5.7 Discussion 237

CHAPTER 6 - DEVELOPMENT OF NON-INVASIVE APPROACHES FOR DELIVERY OF VIRAL VECTORS TO SPINAL CORD MOTOR NEURONS 242

6.1 Delivery in cerebrospinal fluid 244

6.1.1 Injection in cerebral lateral ventricles (ICV delivery)..... 244

6.1.2 Injection in subarachnoid space of spinal cord at lumbar level (ITL delivery)..... 245

6.1.3 Effect of mannitol-induced BBB disruption on viral vector bioavailability after ITL delivery 246

6.2 Rabies-G pseudotyping..... 247

6.2.1 Set up of a protocol for production of Rabies-G lentiviral vectors at high titre 249

6.2.2 Delivery of Rabies-G pseudotyped vectors in peripheral muscles 250

6.3 Discussion 256

CHAPTER 7 - GENERAL DISCUSSION AND CONCLUSIONS 260

7.1 GENERAL DISCUSSION 261

7.2. CONCLUSIONS 268

BIBLIOGRAPHY 270

LIST OF PUBLICATIONS 302

LIST OF ABBREVIATIONS

Abeta	Amyloid beta
AMPA	α-Amino-3-Hydroxy-5-Methyl-4-Isoxazole Propionic Acid
ANOVA	Analysis of Variance
ATP	Adenosine Triphosphate
BCA	Bicinchoninic Acid Assay
BDNF	Brain derived neurotrophic factor
Bp	Base pair
BSA	Bovine Serum Albumin
CCS	Copper Chaperone for Superoxide Dismutase
CD11b	Cluster of Differentiation 11 beta
CDK5	Cyclin-Dependent Kinase 5
cDNA	Complementary DNA
ChAT	Choline Acetyl Transferase
CHOP	C/EBP Homologous Protein
CM	Centimeters
CMV	Cytomegalovirus
CNS	Central Nervous System
CNPase	2',3'-cyclic nucleotide 3'-phosphodiesterase
CNTF	Ciliary neurotrophic factor
COX-2	Cyclooxygenase 2
Cra1 mice	Cramping mice
CSF	Cerebrospinal Fluid
DAB	3'-3-Diaminobenzidine Tetrahydrocholride
DIV	Divisions
DNA	Deoxyribonucleic Acid
DNAse	Deoxyribonuclease
dNTPs	Deoxynucleotide Triphosphates
dsRNA	Double strand RNA

DTT	Dithiothreitol
EAAT	Excitatory Amino Acid Transporter
ECL	Enhanced Chemiluminescence
EDTA	Ethylenediamine-N,N,N',N'-Tetraacetic Acid
EF1α	Elongation factor 1 alpha
EGTA	Ethylene glycol tetraacetic acid
EMG	Electromyography
ENU	N-ethyl N-nitrosourea
ER	Endoplasmic Reticulum
ERK	Extracellular signal-regulated kinase
FCS	Fetal calf serum
FGF2	Fibroblast growth factor
FTD	Frontotemporal Dementia
FTDP	Frontotemporal Dementia with Parkinsonism
FTLD	Frontotemporal Lobar Degeneration
GDNF	Granulocyte-derived neurotrophic factor
GEF	Guanine Exchange Factor
GFAP	Glial Fibrillary Acidic Protein
GFP	Green Fluorescent Protein
GluR2	Glutamate receptor 2
GPCR	G-protein coupled receptor
GSK3β	Glycogen synthase kinase 3 beta
GTP	Guanosine-triphosphate
GTPase	GuanilTriphosphatase
H	Hour
HAtag	Hemagglutinin tag
hnRNP	heterologous ribonucleoprotein
hPGK	Human phosphoglycerate kinase
HRP	Horseradish Peroxidase

ICV	Intracerebro-ventricular
IGF	Insulin Growth Factor
IL-1	Interleukine 1
IL-10	Interleukine 10
IL-12	Interleukine 12
IL-18	Interleukine 18
IP	Intra-peritoneal
ISL-1	Islet-1
IT	Intrathecal
IV	Intravenous
JNK	C-jun N-terminal kinase
Kb	Kilobase
KDa	KiloDalton
LDH	Lactate dehydrogenase
LMN	Lower Motor Neurons
Loa mice	Leg at odd angles mice
LPS	lipopolysaccharide
LTR	Long terminal repeat
LV	Lentiviral vector
MAPK	Mitogen Activated Protein Kinase
MCK	Muscle creatine kinase
M-CSF	Macrophage colony stimulating factor
Min	Minute
miRNA	microRNA
miRNP	Micro-ribonucleoprotein complex
MLC	Myosine light chain
MND	Motor Neuron Disease
MND mice	Motor Neuron Degeneration mice
MRI	Magnetic Resonance Imaging

mRNA	Messenger RNA
MuLV RT	Moloney Murine Leukaemia Virus Reverse Transcriptase
nAChR	Nicotinic acetylcholine receptor
NCAM	Neuronal cell adhesion molecule
NF-H	High molecular weight Neurofilament
NFkB	Nuclear Factor-Kappa B
NF-L	Low molecular weight Neurofilament
NGS	Normal Goat Serum
NM	nanometers
NMD mice	Neuromuscular Degeneration mice
NMDA	N-methyl D-aspartic acid
NMJ	Neuromuscular junctions
NO	Nitric Oxide
NOS	Nitric Oxide Synthase
NTg mice	Non-Transgenic mice
NTS	Nucleotydes
P75NTR	p75 neurotrophin receptor
PBS	Phosphate Buffered Saline
PC12	Pheocromocytoma cell line
PCR	Polymerase Chain Reaction
PDK	3-phosphoinositide dependent kinase
PFA	Paraformaldheyde
PI3K	Phosphatidyl-inositole 3-phosphate
PKA	Protein kinase A
PKB	Protein kinase B
Poli-Q	Poliglutamine-extension
rAAV	Recombinant Adeno-associated viral vector
RCC	Regulator of chromosome condensation
rLV	Recombinant lentivirus

RNA	Ribonucleic Acid
RNase	Ribonuclease
rNSE	Rat Neuron specific enolase
ROS	Reactive Oxygen Species
RPM	Revolutions per minute
RRE	Rev responsive element
RT	Room Temperature
RTK	Receptor tyrosine kinase
RT-PCR	Reverse-Transcriptase Polymerase Chain Reaction
S.E.	Standard error
sALS	Sporadic ALS
SDS	Sodium Dodecyl Sulfate
Sec	Second
shRNA	Small hairpin RNA
siRNA	small interfering RNA
SOD1G93A mice	Mice transgenic for human SOD1 carrying G93A mutation
SOD1wt mice	Mice transgenic for human wild type SOD1
TBS	Tris Buffered Saline
TBST	TBS + 0.1% Tween-20
TDP-43	TAR-DNA-binding Protein 43
TNB	TBS 0.1 M, Blocking reagent 0.5%
TNFα	Tumor Necrosis Factor alpha
TNT	TBS 0.1 M, Triton X-100 0.05%
Tris	Tris(hydroxymethyl)methylamine
tRNA	Transfer RNA
TU	Transducing units
UMN	Upper Motor Neurons
VAChT	Vescicular acetyl-choline transporter
VEGF	Vascular Endothelial Growth Factor

Vol	Volume
VSVG	Vescicular Stomatitis Virus Glycoprotein

LIST OF TABLES

Table 1.1 - Features of Motor Neuron Diseases 20

Table 1.2 - Revised El Escorial Criteria 25

Table 1.3- Causative genes and Mendelian loci for familial ALS 34

Table 1.4 - Mouse models with motor neuron dysfunction 52

Table 1.5 - Effect of selective expression of mutant SOD1 in neurons, astrocytes or muscles 68

Table 1.6 - Effect of selective downregulation of mutant SOD1 in specific cell types 68

Table 1.7 - Features of the most commonly used p38MAPK pharmacologic inhibitors 88

Table 1.8 - Akt activation in human cancer 103

Table 1.9 - Classification of retroviruses 112

Table 1.10 - Properties of viruses used to derive gene transfer vectors 124

Table 1.11 - Tropism modification of lentiviral vectors by pseudotyping 128

Table 2.1 - List of the different vectors produced and utilised in the project 138

Table 3.1 - High titre production of VSVG pseudotyped lentiviral vectors ... 169

Table 5.1 - List of candidate shRNA sequences targeting murine p38MAPK alpha 211

Table 6.1 - High titre production of Rabies pseudotyped lentiviral vectors .. 249

LIST OF FIGURES

Figure 1.1 - Outline of neuro-anatomic pathways involved in ALS 23

Figure 1.2 - SOD1-mediated chemistry 56

Figure 1.3 - Converging molecular mechanisms involved in motor neuron death in fALS 65

Figure 1.4 - Dysregulation of pro-degenerative and anti-apoptotic pathways in motor neurons in ALS 72

Figure 1.5 - Signalling cascades leading to activation of the MAPKs 76

Figure 1.6 - Downstream targets of p38MAPK 77

Figure 1.7 - Overview of PI3K/Akt pathway 90

Figure 1.8 - Structural features of the three Akt isoforms 95

Figure 1.9 - Akt activation pathway 98

Figure 1.10 - Cellular functions mediated by ten Akt substrates 99

Figure 1.11 - Schematic cross section through a retroviral particle 113

Figure 1.12 - Scheme of reverse transcription process 115

Figure 1.13 - Genome organization of HIV-1 118

Figure 1.14 - Scheme of the life cycle of HIV-1 119

Figure 1.15 - Diagram of wild type HIV-1 and plasmids for production of recombinant LVs 122

Figure 1.16 – Overview of genesis and function of miRNA sequences 131

Figure 2.1 – Scheme of the site of lumbar intrathecal injection 147

Figure 2.2 – Visualisation of the site of laminectomy 148

Figure 2.3 – Scheme of the injection sites in spinal cord parenchyma 148

Figure 3.1 – Pattern of GFP reporter gene expression after injection in the spinal cord parenchyma 174

Figure 3.2 – Tropism of VSVG-pseudotyped lentiviral vector after delivery in the spinal cord parenchyma 175

Figure 3.3 – Use of rNSE promoter leads to specific transgene expression in neurons, in vitro 176
Figure 3.4 – Viral vectors carrying the rNSE promoter efficiently infect cells, in vitro 176
Figure 3.5 – Viral vectors carrying the rNSE promoter can infect cells in vivo, in the mouse 177
Figure 3.6 – Scheme of the 3.6Kb enhancer from original 11Kb Hb9 promoter 178
Figure 3.7 – Hb9_3.6Kb-GFP can drive selective expression of transgene after transfection in vitro 178
Figure 3.8 – Scheme of the new constructs derived from 3.6Kb enhancer... 179
Figure 3.9 – Neuron specific expression of transgene after transfection of Bg.AB and Bg.1.6 constructs in mixed co-cultures 179
Figure 3.10 – Viral vectors carrying the Hb9.AB promoter can infect motor neurons in vivo but lead to ectopic expression in non neuronal cells 180
Figure 3.11 – Viral vectors carrying the Hb9.1.6Kb promoter display higher specificity for ventral horn neurons in the spinal cord in vivo 181
Figure 4.1 – Preparation of constitutively activated AKT constructs and validation in vitro 193
Figure 4.2 – Lentiviral vectors containing the Myr.AKT3 construct are fully infective and functional in vitro 194
Figure 4.3 – Treatment of SOD1G93A mice with W.1.6.Myr.AKT3 lentivector does not significantly modify survival 195
Figure 4.4 – Effect of Myr.AKT3 expression on disease progression in SOD1G93A mice 195
Figure 4.5 – End-point analysis of deficits in SOD1G93A mice after treatment with W.1.6.Myr.AKT3 or empty vector 198

Figure 4.6 – Expression of Myr.AKT3 increases motor neuron survival in SOD1G93A animals 199

Figure 4.7 – Intraspinal injection of W.1.6.Myr.AKT3 lentivector in SOD1G93A animals results in specific expression of the transgene in motor neurons... 200

Figure 4.8 – Myr.AKT3 expression results in increased P-Akt staining in motor neurons of SOD1G93A animals 201

Figure 5.1 – Screening of candidate shRNA sequences targeting p38MAPK alpha, in vitro 221

Figure 5.2 – Schematic representation of shRNA nr.7* sequence 222

Figure 5.3 – Test of the selected shRNA sequences on primary cultured mouse astrocytes 222

Figure 5.4 – TNFα-mediated induction of p38MAPK and JNK in murine astrocyte cultures; effect of shRNA nr.7 223

Figure 5.5 – Test of shRNA nr.7 on rat neuronal cultures 224

Figure 5.6 – Test of shRNA nr.7-mediated effects at short term: schematic representation of the injection in the spinal cord 225

Figure 5.7 – Higher susceptibility of SOD1G93A motor neurons to intraspinal injection of an empty viral vector 226

Figure 5.8 – Protection of motor neurons in the spinal cord side injected with shRNA nr.7 226

Figure 5.9 – Treatment of SOD1G93A mice with lentivectors expressing shRNA nr.7 significantly reduces life span 227

Figure 5.10 – Effect of shRNA nr.7 on disease progression in SOD1G93A... 228

Figure 5.11 – End-point analysis of deficits in SOD1G93A mice after treatment with shRNA nr.7; comparison with sham operated group 231

Figure 5.12 – End-point analysis of deficits in SOD1G93A mice after treatment with shRNA nr.7; comparison with shRNA nr.7* treated group 232

Figure 5.13 – Expression of shRNA nr.7 causes a mild decrease of motor neuron survival in SOD1G93A animals 233
Figure 5.14 – Analysis of motor neuron survival in treated SOD1G93A mice at different spinal cord levels 234
Figure 5.15 – Effect of shRNA nr.7 expression on reactive astrocytosis in SOD1G93A mice..... 235
Figure 5.16 – Effect of shRNA nr.7 expression on reactive microgliosis in SOD1G93A mice..... 236
Figure 6.1 – Pattern of GFP reporter gene expression in CNS after ICV delivery 252
Figure 6.2 – Trypan-blue dye distribution after IT delivery at lumbar level.. 252
Figure 6.3 – GFP expression in spinal cord after IT delivery of lentivectors at lumbar level..... 253
Figure 6.4 – Evan Blue dye distribution after IT delivery and concomitant BBB disruption..... 254
Figure 6.5 – Efficient trasduction of spinal cord motor neurons after delivery of Fluorogold in peripheral muscles 254
Figure 6.6 – Rabies lentivector can retrogradelly infect neuronal cells after delivery in brain parenchyma 255

CHAPTER 1

GENERAL INTRODUCTION

1.1 AMYOTROPHIC LATERAL SCLEROSIS

Amyotrophic Lateral Sclerosis (ALS) initially known as *Charcot's sclerosis*, is a form of muscular atrophy that was first described in 1869 by the French neurobiologist and clinician Jean-Martin Charcot. It belongs to a wide group of syndromes called Motor Neuron Diseases (**Table 1.1**). The term "*amyotrophic*" refers to muscle atrophy, weakness and fasciculations appearing as a consequence of degeneration of the motor neurons. The term "*lateral sclerosis*" derives from Charcot's observation of a distinct "myelin pallor" and hardness of the lateral columns of spinal cord, at autopsy. This is due to the loss of axons of upper motor neurons as they descend from the brain to connect to the lower motor neurons within the spinal cord, and to the massive gliosis following degeneration of the cortico-spinal tract.

In the United States ALS is commonly termed Lou Gehrig's disease, after the famous baseball player who died of this syndrome in the late 1930s. The term Motor Neuron Disease (MND) is instead mainly used in the United Kingdom to refer to this pathology.

Currently ALS is defined as a fatal progressive neurodegenerative disorder involving primarily the motor neurons of the cerebral cortex (upper motor neurons, UMN), brainstem and spinal cord (lower motor neurons, LMN). This causes a reduction of the input signals delivered to the voluntary muscles, leading to initial weakness. As the disease progresses, widespread limb and trunk weakness and atrophy lead to a dramatic decline in physical function, finally resulting in complete paralysis. Patients usually die for respiratory failure, due to denervation of the diaphragm and respiratory muscles.

ALS is the most common motor neuron disease. The majority of ALS cases are sporadic (sporadic ALS or sALS), although in 5-10% of cases the pathology is

inherited (familial ALS or fALS). Sporadic and familial forms share similar pathological hallmarks.

Despite extensive efforts to study and understand the molecular mechanisms that lead to this disease, ALS still lacks a truly effective therapy *(Boillee et al., 2006a; Aggarwal and Cudkowicz, 2008; Raibon et al., 2008).*

Table 1.1. Features of Motor Neuron Diseases

Affected region	Motor Neuron Disease
Combined UMN and LMN involvement	Amyotrophic Lateral Sclerosis
Pure LMN involvement	Progressive Muscular Atrophy, Progressive Bulbar Palsy, Spinal Muscular Atrophy
Pure UPM involvement	Primary Lateral Sclerosis, Pseudo-bulbar Palsy, Hereditary Spastic Paraplegia
Mixed motor and sensory involvement	Charcot Marie Tooth Disease, Distal hereditary motor neuropathy, ALS with fronto-temporal dementia

1.1.1 SYMPTOMATOLOGY

Symptoms of ALS are associated with dysfunction of lower and upper motor neurons (**Figure 1.1**). LMN involvement initially determines weakness and fatigue. As disease progresses, muscular deficits, due to loss of innervation, appear more evident: muscular atrophy, reduced muscle tone and absence of tendon reflexes, fasciculations (muscular twitching and shaking of contiguous groups of muscle fibers) and fibrillations (muscular twitching and shaking involving individual muscle fibers acting without coordination). UMN involvement instead causes weakness, incoordination, stiffness and slowing of movement, with spasticity (persistent contraction of muscle), increased tendon reflexes, clonus (alternating contractions and relaxations) and extensor plantar responses.

ALS probably begins a long time before its clinical manifestations, since a substantial number of motor neurons can be lost before any clinical signs develop. In fact, several studies on animal models have shown that motor neuron dysfunction precedes the onset of symptoms and that compensatory reinnervation from nearby motor neurons permits a good maintenance of the motor function, although with an enlargement of motor units, until more than 50% of motor units have been lost; at this point symptoms appear and the number of motor units declines rapidly *(Cote et al., 1993; Kennel et al., 1996).*

No neuropathological, neurophysiological or biochemical markers are yet available to identify a patient as potentially susceptible for ALS prior to symptom onset *(Swash and Desai, 2000).*

At the onset, ALS can appear with LMN involvement, UMN involvement or bulbar involvement. Limb onset is the most frequent, and is found in 75-80% of cases, while bulbar onset is evidenced in only 20-25% *(Wijesekera and Leigh, 2009).*

At the early stages of the pathology there is great variability in the extent and localization of motor system involvement in different patients, thus complicating the diagnosis. However, as the disease progresses, the clinical expression of ALS becomes quite uniform, with extreme muscular wasting, spasticity and paralysis.

The most common initial presentation of ALS is focal asymmetric distal weakness and muscular atrophy. For example, the patient may report a history of unexpected tripping, dragging of a foot and ultimately more diffuse weakness of the leg. When upper limbs are involved, symptoms may appear as difficulty with buttoning clothes, turning keys in doors or simply poor coordination while performing fine movements.

Bulbar motor neuron degeneration leads to difficulty in swallowing (dysphagia) and breathing, and slurred or thick speech (dysarthria), associated with fasciculation of the tongue. Bulbar signs are often closely related to respiratory deficits, due to the involvement of the diaphragm. This leads to a poor prognosis and to a shorter life expectancy.

With the progression of the illness, the disease spreads to contiguous muscle segments. The progressive loss of motor function results in increasing disability and paralysis, ultimately leading to a bed-bound state.

Recent findings have revealed that the selectivity of ALS for the motor system is not absolute. In fact, some reports describe cognitive impairment in a subgroup of ALS patients. A battery of neuropsychological tests has shown a cognitive impairment in about 30% of ALS patients, ranging from mild impairment to frontotemporal lobar degeneration (FTLD). The main symptoms are executive dysfunction with deficits in verbal and non-verbal fluency and concept formation *(Lomen-Hoerth et al., 2003; Kilani et al., 2004; Abrahams et al., 2005; Schreiber et al., 2005; Rippon et al., 2006).* However, in the majority of cases, the rate of cognitive decline is very slow as compared to the devastating motor deterioration. Eye and bladder muscles, along with sexual function, are not normally affected.

Average life expectancy for ALS patients is 2-5 years from diagnosis, with the cause of death being respiratory failure, most often hastened by pneumonia.

When swallowing and respiratory muscle activity appear to be insufficient during disease progression, patients need to use tube feedings and mechanised ventilation, respectively. Through these supporting systems patients can generally be maintained for several years, although the quality of life is decreased.

Figure 1.1. Outline of neuro-anatomic pathways involved in ALS

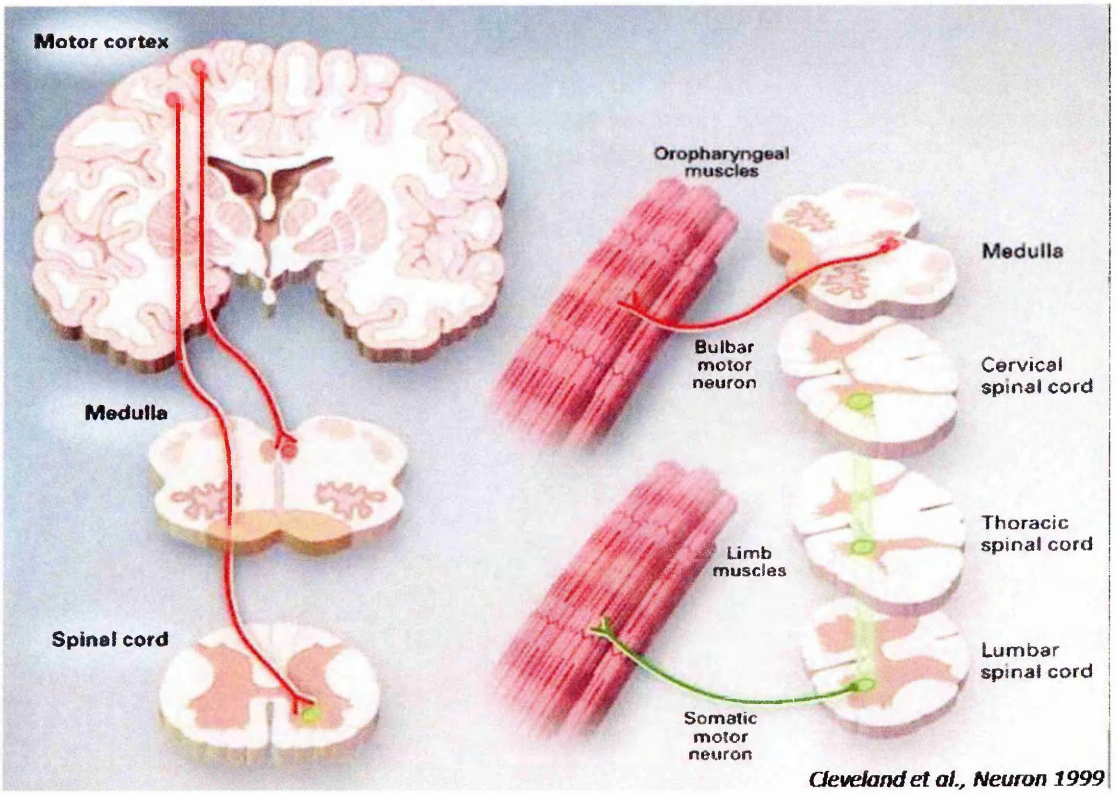

1.1.2 DIAGNOSIS

ALS is a very difficult disease to diagnose. Clinical findings early in the course of the disease are often variable, and to date there is no biological diagnostic marker or procedure to ultimately establish the diagnosis of ALS. This often compromises the certainty of the diagnosis in clinical practice and therapeutic trials.

It is through a clinical examination and series of diagnostic tests, often ruling out other diseases that mimic ALS, that a diagnosis can be established.

These tests include genetic screening (in case of suspected familiarity), muscle and nerve biopsy, spinal tap, X-rays, MRI's and electromyography (EMG).

A set of diagnostic criteria for ALS was established in 1994 by the World Federation of Neurology during a meeting in El Escorial, Spain, and it was subsequently updated at Airlie Conference Center, Warrenton, Virginia in 1998.

Based on these criteria, diagnosis of ALS requires:

- ✓ The presence of:
  1) Evidence of LMN degeneration, assessed by clinical, electrophysiological or neuropathological examination;
  2) Evidence of UMN degeneration, by clinical examination;
  3) Progressive spread of symptoms or signs within a region or to other regions, as determined by history or examination;

- ✓ Together with the absence of:
  1) Electrophysiological or pathological evidence of other disease processes that might explain the signs of LMN and/or UMN degeneration;
  2) Neuroimaging evidence of other disease processes that might explain the observed clinical and electrophysiological signs.

The so-called "Revised El-Escorial criteria" **(Table 1.2)** classify the probability for a patient to be affected by ALS according to the level of clinical certainty, as compared to other similar pathologies *(Brooks et al., 2000)*.

Table 1.2. Revised El Escorial Criteria

Level of certainty	Clinical presentation
Clinically definite ALS	Presence of UMN and LMN signs in the bulbar region and at least two spinal regions. Alternatively, presence of UMN and LMN signs in three spinal regions
Clinically probable ALS	UMN and LMN signs in at least two regions with some UMN signs necessarily rostral to the already detected LMN signs
Clinically probable ALS – Laboratory supported	Clinical signs of UMN and LMN dysfunction are only in one region. Alternatively, UMN signs alone are present in one region, and LMN signs (defined by EMG criteria) are present in at least two regions. Neuroimaging and clinical laboratory protocols must be applied in this case to exclude other causes.
Clinical Possible ALS	Signs of UMN and LMN dysfunction together in only one region. Alternatively LMN signs are found rostral to UMN signs and the diagnosis of Clinically Probable ALS-Lab.supported cannot be proven in conjunction with laboratory studies.

When ALS occurs in association with other features, such as Parkinsonism (5% of cases) or dementia (3% of cases), or when there is a pure UMN or LMN syndrome, it is often considered an atypical variant of Charcot ALS.

Atypical ALS cases are also characterised by one or more of the following features:

- Geographic clustering (Western Pacific, Guam, Kii Peninsula, North Africa, Madras)
- Extrapyramidal signs (bradykinesia; cogwheel rigidity; tremor)
- Cerebellar degeneration (spinocerebellar abnormalities)
- Autonomic nervous system involvement (abnormal cardiovascular reflexes; bowel or bladder control problems)

- Sensory abnormalities (decreased vibration; sharp/dull discrimination; blunting of cold sensation)
- Ocular movement abnormalities
- Syndromes that mimic ALS (adult onset proximal spinal muscular atrophy; Kennedy syndrome; delayed post-poliomyelitis; multifocal motor neuropathy with or without conduction block; endocrinopathies; lead intoxication; infections).

Such patients are usually excluded from clinical trials *(Eisen and Calne, 1992; Kew and Leigh, 1992; Brooks et al., 2000; Swash and Desai, 2000).*

1.1.3 NEUROPATHOLOGY

A better understanding of the neuropathology of the disease has taken advantage of immunohistochemical and ultrastructural studies performed on post mortem tissues of ALS patients. However, post-mortem examinations are conducted on tissues that represent the final stage of the pathology; thus the observed alterations reflect a very advanced state of neuronal degeneration and give little information about the events that trigger cell death.

The major pathological features of ALS are:

1) Upper motor neuron abnormalities
2) Myelin pallor in the corticospinal tracts
3) Reduction in both size and number of lower motor neurons in the spinal ventral horns and in the bulbar nuclei *(Robert H. Brown, 2000).*

1) UMN involvement

Upper motor neurons localized in the motor cortex exert supranuclear control over lower motor neurons.

The degree of degeneration observable at autopsy in the motor cortex of ALS patients is variable and may not always be evident, even in the presence of clear upper motor neuron signs. In the most severely affected cases, an evident loss of giant Betz cells in cortical layer 5, associated with an extensive astrogliosis and microgliosis, is reported. Since there are not good markers to distinguish upper motor neurons and other pyramidal cell types in the cortex, the identification of the Betz cell is often based on morphological and size criteria. Neuron cell bodies appear atrophied *(Kiernan and Hudson, 1991)*, with shorter fragmented dendrites *(Hammer et al., 1979)*. Intracellular alterations are rarely identified in the spared Betz cells in classical ALS; occasionally, ubiquitinated neurofilament inclusions are reported. Pathological changes are rarely evident in somatosensory cortex, prefrontal cortex and premotor areas *(Kiernan and Hudson, 1991)*.

2) Myelin pallor in the corticospinal tract

Axonal degeneration of the descending corticospinal tract results in clear demyelination. As a consequence, the spinal cord of ALS patients shows a pallor with myelin stain. Corticospinal fibers also show marked axonal swelling and spheroids *(Chou, 1992)*. An extensive gliosis is present, causing the typical sclerosis of lateral spinal cord tracts.

3) LMN involvement

Loss of large motor neurons localized in the lower brainstem and in the spinal cord are clearly observed at autopsy. Shrinkage and atrophy of the cell body precedes neuronal death *(Kiernan and Hudson, 1991)*; the phenomenon is associated with alterations of axon and dendrite structures, which become thinner *(Nakano and Hirano, 1987)*.

Certain motor neuron groups, such as those controlling eye movements and the Onuf's nucleus of the sacral spinal cord (that regulates the pelvic floor musculature) are largely spared by the disease.

The remaining motor neurons display several abnormalities, listed below.

Ubiquitinated inclusions

Ubiquitin-positive inclusions are found very frequently in the susceptible LMN groups of the spinal cord and brainstem of most cases and are defined as *skein-like* or *Lewy body-like* inclusions. The former are a specific hallmark of ALS whereas the latter are also found in other disorders, like Parkinson's disease *(Jellinger, 2008)*. Both inclusions probably represent two different morphological stages of protein aggregation, from diffuse filamentous forms to dense and compact inclusions. The major protein constituent of these inclusions is unknown, but they do not immunostain for tau, alpha-synuclein or cystatin C, that represent components of inclusions in other neurodegenerative diseases *(Ince, 2000)*. Besides phosphorylated neurofilaments and ubiquitin, in some cases Lewy body-like inclusions also contain cyclin-dependent kinase 5 (CDK5) *(Nakamura et al., 1997)*, or dorfin, a RING finger-type E3 ubiquitin ligase *(Hishikawa et al., 2003)*.

More recently, the nuclear factor TDP-43 (TAR-DNA-binding protein 43) has been identified as a major component of ubiquitinated inclusions in sporadic ALS cases *(Neumann et al., 2006b)*. TDP-43 is thought to function as a regulator of transcription and alternative splicing *(Buratti and Baralle, 2001; Buratti et al., 2004; Mercado et al., 2005)*. Ubiquitin-positive inclusions are localized both in normal appearing motor neurons and in some shrunken cells.

Bunina bodies

Bunina bodies are small, eosinophilic, irregularly shaped inclusions localized in the soma of motor neurons; probably they have a lysosomal derivation *(Sasaki and Maruyama, 1993)*. At the ultrastructural analysis, they appear like electron-dense, amorphous structures surrounded by vesicles, endoplasmic reticulum

(ER) fragments, lipofuscin granules. They immunostain positive for cystatin C, a protein inhibitor of lysosomal cysteine proteases, and transferrin, an iron-binding protein, but they are usually negative for ubiquitin, and do not contain TDP-43 *(Okamoto et al., 2008)*. Bunina bodies are reported to be present in 30-50% of cases; since they are not described in other disorders, they seem to be specific for ALS.

Some authors have hypothesised that Bunina Bodies may be a special type of autophagic vacuole, probably deriving from altered mitochondria *(Hart et al., 1977)*, or that they may originate from smooth endoplasmic reticulum or the Golgi apparatus *(Okamoto et al., 1993)*. However their pathogenesis and their relationship to neurodegeneration is controversial and has not yet been unravelled.

Golgi fragmentation

Both upper and lower motor neurons of ALS cases show signs of fragmentation of the Golgi apparatus, that is dispersed into numerous small isolated elements *(Mourelatos et al., 1994; Fujita and Okamoto, 2005)*, as evidenced by MG-160 staining, that recognises a 160-Kda sialoglycoprotein of medial cisternae of the Golgi apparatus *(Mourelatos et al., 1990)*.

Hyaline conglomerate inclusions

Hyaline conglomerate inclusions consist of large aggregates of phosphorylated and non phosphorylated neurofilaments associated with other "entrapped" cytoplasmic proteins and organelles *(Schochet et al., 1969; Leigh et al., 1989; Sasaki and Maruyama, 1991)*. They have been identified in sporadic and familial ALS; however, they seem to be less specific for this pathology, since they have been found in other neurological disorders, like multiple system atrophy and in normal patients *(Leigh et al., 1989; Sobue et al., 1990)*.

Globules, spheroids and somatic accumulation of phosphorylated neurofilaments

Diffuse accumulation of phosphorylated neurofilaments has been observed in the perikarya of motor neurons, especially in sporadic ALS *(Hirano et al., 1984)*. They can also be found packed in axonal swellings in the anterior horns of spinal cord of ALS patients *(Corbo and Hays, 1992; Toyoshima et al., 1998)*. Spheroids are larger structure that tend to be localized in proximal axons and dendrites, whereas globules are smaller and usually are more peripheral in the ventral horn. Both might represent focal abnormalities of axonal cytoskeleton regulation due to a failure of axonal transport.

Mitochondrial alterations

In recent years, morphological alterations of mitochondria in the motor neurons of ALS patients have been observed. These include dense conglomerates of aggregates, dark mitochondria, swelling and vacuolization *(Hirano et al., 1984; Swerdlow et al., 1998)*.

4) Involvement of other cell types

Clear morphological and neurochemical evidence demonstrates the proliferation and activation of the microglial and astrocytic populations in the areas characterized by motor neuronal loss *(Kawamata et al., 1992)*. The concept of selective motor neuronal death has been challenged by studies reporting the loss of small neurons in the spinal cord of ALS cases *(Oyanagi et al., 1989; Raynor and Shefner, 1994)*. In a recent report by Stephens and colleagues, the morphometric examination of the lumbar spinal cord of sporadic ALS patients revealed a substantial loss of ventral interneurons in addition to motor neurons. Therefore, the interneuronal population may degenerate to a similar extent and contemporary with the motor neuronal one *(Stephens et al., 2006)*.

5) Non-motor system pathology

Autopsy examination revealed in some ALS patients alterations in extra-motor regions of the CNS, such as in the sensory system (Hudson, 1981), substantia nigra and hippocampus *(Wharton, 2003).*

6) Non-CNS pathology

Profound atrophy of the skeletal muscles is one of the earliest pathological changes in ALS patients *(Mitsumoto H, 1998).* Interestingly, other alterations are reported in the skin, in which collagen cross-linking is changed *(Kolde et al., 1996).*

1.1.4 EPIDEMIOLOGY

Three classifications of ALS have been described:

- Sporadic - the most common form of ALS in the United States - 90 to 95% of all cases.
- Familial - occurring more than once in a family lineage (genetic dominant inheritance) accounts for a very small number of cases in the United States - 5 to 10% of all cases.
- Guamanian - an extremely high incidence of ALS was observed in Guam and the Trust Territories of the Pacific in the 1950's.

ALS is considered as a rare disease: it occurs in about 1-3 people per 100,000 per year with a prevalence of about 5-7 per 100,000, *(McGuire et al., 1996; Mitsumoto H, 1998).* The average survival for sporadic ALS patients is approximately 3-5 years after the first symptoms. Onset of ALS in patients younger than 50 years of age is generally associated with a longer survival.

The incidence of ALS increases with age, with a peak occurring between 55 and 75 years of age; therefore, aging is the most significant risk factor. ALS occurs

predominantly in males, with a male to female ratio of 3:2. Male predominance is particularly marked in some lower motor neuron variants. After the menopause the male to female ratio approaches 1:1, suggesting a neuro-protective effect exerted by estrogens *(Worms, 2001; Mitchell and Borasio, 2007)*.

Environmental risk factors are inconsistently reported in ALS; this may reflect a complex interaction between several environmental risk factors and specific genetic susceptibilities.

People of all races and ethnic backgrounds are affected by ALS and, with the exception of specific endemic areas in the Western Pacific, its worldwide frequency is uniform. Four geographic areas with a high prevalence (approximately 100-150 fold higher than the other regions) of ALS are described *(Kurland and Molgaard, 1982; Oyanagi and Wada, 1999)*:

- Guam and Rota islands
- 2 areas in the Kii peninsula
- Irian Jaya (Indonesia)
- Area of the Gulf of Carpentaria (North Australia)

Western Pacific ALS is considered a distinct disease because it is often associated with Parkinsonism Dementia, with pathological alterations resembling Alzheimer's disease (neurofibrillary tangles).

Although familial ALS is almost indistinguishable from the sporadic form in terms of clinical phenotype, some features differentiate it from an epidemiological point of view *(Mitsumoto H, 1998)*: the average onset of fALS cases is approximately 47 years, a decade earlier than the sporadic type, and the mean survival is shorter; moreover, it occurs equally in males and females. Finally, in fALS, symptoms more frequently begin in the lower extremities compared to sporadic ALS.

1.1.5 GENETICS

ALS is predominantly sporadic; familial ALS accounts only for 5-10% of cases. Studies in families have led to identification of genes responsible for the disease and of potential genetic loci (**Table 1.3**). Although these studies are not exhaustive, they helped identify molecular pathways that may be involved in the neuropathology of the sporadic forms of the disease.

Table 1.3. Causative genes and Mendelian loci for familial ALS

Designation	Genetic locus	Gene	Clinical features	Main reference
ALS1	21q21	SOD1	Autosomal dominant; typical ALS	*(Rosen et al., 1993)*
ALS2	2q33	ALSin	Autosomal recessive; jouvenile onset, slowly progressive	*(Hadano et al., 2001)*
ALS3	18q21	Unknown	Autosomal dominant	*(Hand et al., 2002)*
ALS4	9q34	SETX	Autosomal dominant; juvenile onset, slowly progressive, non fatal	*(Blair et al., 2000)*
ALS5	15q15.1-q21.1	Unknown	Autosomal recessive; juvenile onset, slowly progressive	*(Hentati et al., 1998)*
ALS6	16q12.1-q12.2	FUS/TLS	Autosomal dominant	*(Ruddy et al., 2003; Kwiatkowski et al., 2009; Vance et al., 2009)*
ALS7	20pter	Unknown	Autosomal dominant	*(Sapp et al., 2003)*
ALS8	20q13.3	VAPB	Autosomal dominant	*(Nishimura et al., 2004)*
ALS10 ALS/FTLDU	1p36	TARDBP	Frontotemporal lobar degeneration with ubiquitinated tau-negative inclusions	*(Sreedharan et al., 2008)*
ALS11	6q21	FIG4	Autsomal recessive; prominence of corticospinal tract involvement	*(Chow et al., 2009)*
ALS/FTD/P	17q21 9q21-22	MAPT	Autosomal dominant ; frontotemporal dementia and parkinsonism with amyotrophy	*(Siddique and Hentati, 1995; Hosler et al., 2000; Wilhelmsen et al., 2004)*
MND, dynactin type	2p13	DCTN1	Autosomal dominant ; adult onset, slowly progressive, with vocal cord paralysis	*(Puls et al., 2003; Munch et al., 2005)*
Recently identified genetic loci	12q24	DAO	Autosomal dominant; typical ALS	*(Mitchell et al.)*
	3p11.2	CHMP2B	Familial transmission not analysed; predominant LMN phenotype	*(Cox et al.)*

1) ALS1: Copper-zinc superoxide dismutase gene (SOD1)

The first discovery of a mutation in the SOD1 gene linked with ALS dates back to 1993 *(Rosen et al., 1993)*. This is the most common form of inherited ALS, accounting for about 20% of all familial ALS forms (2-3% of all ALS cases).

SOD1 enzyme is a superoxide dismutase: it scavanges superoxide ion, a free radical that is formed during mitochondrial respiration, by catalyzing the reaction $4O^{2-} + 2H^{+} \rightarrow H_2O_2 + O_2$. SOD1 is a 153aa, homodimeric protein ubiquitously expressed. At the subcellular level it is found mainly in the cytoplasm, but it has also been detected in the intermembrane space in mitochondria, and in the nucleus.

Up today 125 ALS-linked mutations have been identified in the SOD1 gene. They are distributed in all five exons of the protein, with practically no region being spared of mutations. The majority are missense mutations; a few mutations cause stop-codons leading to generation of a truncated protein *(Andersen et al., 2003)*.

All mutations are associated with autosomal dominant fALS, except for D90A and D96N, which can cause both dominant and recessive ALS *(Andersen et al., 1995; Robberecht et al., 1996; Orrell, 2000)*. The most frequent SOD1 mutation is A4V.

Penetrance, clinical manifestations, age of onset, disease progression and survival vary greatly among specific mutations. For example, A4V and A4T are associated with an aggressive fALS type *(Aksoy et al., 2003)*, whereas G37R, D90A, G93C and G93V mutations show a slower progression over 10-15 years *(Arisato et al., 2003)*.

These genetic studies have opened the field to the generation of transgenic mice overexpressing human SOD1 carrying the mutations found in human ALS patients. These mice develop a progressive motor syndrome that recapitulates

several aspects of the pathology and symptoms found in human ALS, described in section 1.2.2 *(Gurney et al., 1994)*.

Initially it was hypothesised that mutations in SOD1 led to a loss of catalytic enzyme activity. However, subsequent studies on transgenic mice revealed that the enzymatic activity was not reduced, but was rather unchanged or even increased *(Gurney et al., 1994; Ripps et al., 1995; Wong, 1995; Bruijn et al., 1997b)*. Moreover knock out of endogenous SOD1 in mice does not lead to spontaneous motor neuron disease *(Reaume et al., 1996)*. Collectively, this strongly suggests that reduced catalytic SOD1 activity does not account for the observed pathology.

Currently, it is believed that mutated SOD1 either acquires a toxic gain of function, or loses some protective property such as the ability to reach the nucleus to scavenge DNA-damaging free radicals *(Sau et al., 2007)*.

2) ALS2: ALSin

ALS2 variant is a recessively inherited form of ALS characterized by juvenile onset and slow progression, with a symptomatology in which spasticity of facial and limb muscles are predominant. In 2001 the gene linked with this form of ALS was identified: ALSin *(Hadano et al., 2001; Yang et al., 2001)*. Two transcripts of this gene can be detected: long alsin (1659 aminoacids) and short alsin (396 aminoacids). Alsin is predicted to have a molecular mass of 184 Kda; it is ubiquitously expressed and is abundant in neurons, where it is localized to the cytosolic portion of the endosomal membrane. With the exception of the liver, which appears to show selective augmentation of the short form, the distribution of both splice variants appears to be similar.

The aminoterminal of alsin contains three guanine exchange factor (GEF) domains: the RCC1-like (regulator of chromosome condensation 1) domain (termed RLD), a diffuse B cell lymphoma (Dbl) homology/pleckstrin homology (DH/PH) domain, and a vacuolar protein sorting 9 (VPS9) domain. The

carboxyterminal of alsin contains two further domains, which are similar to those of the Rho G-protein family that modulates dynamic actin assembly.

The majority of the mutations appear to result in the generation of a premature stop codon, leading to protein instability and a loss of function *(Yamanaka et al., 2003)*. However, although mutations in ALS2 lead to clinical variations of motor dysfunction in humans, mice lacking alsin surprisingly did not recapitulate the symptoms of motor neuron disease, but showed only subtle deficits in motor performances, probably because of potential compensatory mechanisms within the mouse genome *(Cai et al., 2005; Hadano et al., 2006; Yamanaka et al., 2006)*.

The function of alsin is not fully understood, although some recent studies have shed light on some of its activities. Alsin has been shown to act as an exchange factor for the small GTPase Rab5 in vitro *(Otomo et al., 2003; Topp et al., 2004)*, suggesting a possible involvement in vesicle trafficking. In addition, alsin can interact with the small Rho GTPase Rac1 *(Otomo et al., 2003; Topp et al., 2004; Tudor et al., 2005)*, mediating actin dynamics related to neuritic outgrowth. Interestingly, it has been shown that alsin can bind to different mutant variants of SOD1 through the RhoGEF domain *(Kanekura et al., 2004)* and, in a cell culture paradigm, alsin overexpression can suppress mutant SOD1 toxicity *(Kanekura et al., 2005)*. Moreover, it has been demonstrated that loss of alsin altered the subcellular localization of glutamate receptor interacting protein (GRIP1), which correlated with a reduction of GluR2 (a subunit of AMPA glutamate receptors) at the cell/synaptic surface of ALS2−/− neurons, resulting in an increased vulnerability of these neurons to excitotoxicity *(Lai et al., 2006)*.

3) ALS4: Senataxin (SETX)

The gene encodes a 303 KDa protein that contains a DNA/RNA helicase domain with strong homology to human RENT1 and IGHMBP2, two proteins known to have roles in RNA processing *(Chen et al., 2004)*. Missense mutations in SETX cause an autosomal dominant, juvenile onset motor neuron disease with very

slow progression of distal limb atrophy and motor neuron loss; the lifespan is not reduced *(Blair et al., 2000)*.

4) ALS6: Fused in sarcoma/Translocation in liposarcoma (FUS/TLS)

FUS is an ubiquitously expressed, predominantly nuclear, protein that is involved in DNA repair and the regulation of transcription, RNA splicing, and export to the cytoplasm. The N terminus has a transcriptional activation domain and contains a glycine rich region; the C terminus contains an RNA recognition motif (RRM), an Arg-Gly-Gly (RGG) repeat rich region, and zinc finger domains involved in RNA processing. FUS binds to the motor proteins kinesin (KIF5) and myosin-Va and is involved in mRNA transport. The vast majority of ALS-linked mutations are clustered in the extreme C terminus. Mutations in FUS/TLS occur in 4-5% of familial ALS cases; mutations are all missense changes except for two, both of which are located in the glycine-rich region and correspond to an insertion or a deletion of two glycines in a 10 glycine-long tract *(Lagier-Tourenne and Cleveland, 2009)*. Patients develop classical ALS with no cognitive deficits. Except for the recessive mutation in a family of Cape Verdean origin, the inheritance pattern is dominant.

Analysis of the brains and spinal cords of ALS patients with FUS/TLS mutations revealed normal staining of FUS/TLS in the nuclei of many neurons and glial cells but aggregates of FUS/TLS in the cytoplasm of lower motor neurons *(Kwiatkowski et al., 2009; Vance et al., 2009)*.

5) ALS8: Vesicular associated protein B (VAPB)

VAPB gene encodes an ubiquitously expressed homodimer, which belongs to a family of intracellular vesicle-associated/membrane-bound proteins. It associates with microtubules and is presumed to regulate vesicle transport. In particular, VAPB has been shown to act during the transport through the endoplasmic reticulum, Golgi apparatus and secretion. The P56S mutation dramatically

disrupts the sub-cellular distribution of VAPB and induces the formation of intracellular protein aggregates *(Nishimura et al., 2004)*.

6) ALS10: TAR DNA binding protein 43 (TARDBP)

TARDBP contains 6 exons; it encodes for an ubiquitously expressed RNA/DNA binding protein, named TDP-43. This protein exerts a regulatory function for transcription and splicing, and probably also for miRNA biogenesis *(Buratti and Baralle, 2008)*. It is a 414 amino acid nuclear protein with two highly conserved RNA recognition motifs (RRM1 and RRM2), a nuclear-localisation signal, a predicted nuclear-export signal and a C-terminal tail with a typical glycine-rich region that mediates protein-protein interactions, including interactions with other heterogeneous ribonucleoprotein (hnRNP) family members. TDP-43 is the major protein found in ubiquitinated inclusions in neurons and glia in patients suffering of frontotemporal lobar degeneration (FTLD) and ALS. Ubiquitinated inclusions in the perikarion and proximal axons of surviving spinal cord motor neurons represent a pathological hallmark of ALS, and are also prominent in cortical neurons within the frontal and temporal lobes in patients with tau-negative FTLD. Moreover, FTLD patients can develop ALS and ALS patients often suffer from a dementia consistent with FTLD, thus TDP-43 may provide a molecular link between these two types of disorder *(Murphy et al., 2007)*. The brains and spinal cords of patients with TDP-43 proteinopathy present a biochemical signature that is characterized by abnormal hyperphosphorylation and ubiquitination of TDP-43 and the production of ~25kDa C-terminal fragments that are missing their nuclear targeting domains, thus cytoplasmic sequestration of TDP-43 is supposed to play a role in neurodegeneration *(Arai et al., 2006; Neumann et al., 2006b)*.

Interestingly mislocalisation of TDP43 is found both in familial and sporadic cases of ALS, thus representing a common feature of the neurodegenerative process in ALS. A total of 30 different dominant mutations are now known in 22

unrelated families (~3% of familial ALS cases) and in 29 sporadic cases of ALS (~1.5% of sporadic cases). All mutations are missense, except Y374X that leads to a truncation. It is now recognized that aberrant accumulation of TDP-43 is not just a byproduct of the neurodegenerative process, but it can represent a primary cause of ALS *(Lagier-Tourenne and Cleveland, 2009).*

7) ALS11: phosphoinositide 5-phosphatase (FIG4)

FIG4 is a phosphoinositide 5-phosphatase also called SAC3. This enzyme regulates the cellular levels of $PI(3,5)P_2$, a lipid involved in signalling processes and retrograde trafficking of endosomal vescicles to the trans-Golgi network *(Rutherford et al., 2006).* Mutations in FIG4 are responsible for a variant of Charcot Marie Tooth (CMT) disease, a peripheral-nerve disorder *(Chow et al., 2007).* Interestingly inactivation of FIG4 in mice determines massive degeneration of neurons in sensory nad autonomic ganglia, motor cortex, striatum and other regions of the CNS, recapitulating some of the pathologic features observed in human patients affected by CMT *(Rutherford et al., 2006).* Mutations in FIG4 have been recently identified also in patients with ALS, suggesting that this gene is another contributor to this disease *(Chow et al., 2009).*

8) ALS/FTD/P: Microtubule associated protein Tau (MAPT)

Tau is a member of the microtubule-associated protein family, which binds to tubulin and has the principal function of stabilizing microtubules and promoting their assembly. In addition, tau is likely to regulate motor protein-mediated transport of vesicles and organelles along the microtubules by modulating their stability *(Sato-Harada et al., 1996; Ebneth et al., 1998).* In frontotemporal dementia with parkinsonism (FTD/P), the mutation of tau gene affects the alternative splicing of exon 10, resulting in an excess of four repeat tau isoforms; this may cause a reduced binding of tau to microtubules in axons. No pure ALS

case has been associated with tau mutations *(Siddique and Hentati, 1995; Hosler et al., 2000; Wilhelmsen et al., 2004).*

9) Dynactin 1 (DCTN1)

The gene encodes for the p150 subunit of the transporter dynactin. This protein is a component of the dynein complex, implicated in the retrograde axonal transport of vesicles and organelles along microtubules. A dominantly transmitted missense mutation (G59S) was identified in 2003. The mutation appears to affect the binding of the dynactin-dynein motor complex to microtubules. It causes an adult onset, slowly progressive atypical motor neuron disorder with vocal cord paresis, and weakness of facial and hand muscles *(Puls et al., 2003).*

10) Recently identified genes

In 2010 two new genes have been associated with ALS: charged multivescicular protein 2B (CHMP2B) *(Cox et al.)* and D-amino acid oxidase (DAO) *(Mitchell et al.).* CHMP2B is a member of ESCRT-III (endosomal sorting complex required for transport III), which is required for formation of the multivesicular body, a late endosomal structure involved in lysosome-mediated degradation of endocitosed proteins and in autophagy. It has been hypothesized that mutations of CHMP2B may contribute to motor neuron injury through dysfunction of the autophagic clearance of cellular proteins, and the formation of ubiquitin positive inclusions *(Cox et al.).* DAO is an enzyme which controls the levels of D-serine, a coagonist at the glycine site of the NMDA glutamate receptor. Increased levels of D-serine and its producing enzyme, serine racemase, have been found in the spinal cord of ALS patients and SOD1G93A mice *(Sasabe et al., 2007).* It has been proposed that mutations in DAO, in ALS patients, participate to the buildup of D-serine in the CNS, thus contributing to excitotoxicity *(Mitchell et al.).*

11) Susceptibility and modifier genes

Although a number of genes have been identified as being causative in familial ALS (**Table 1.3**), the genetics of the sporadic form of the disease is poorly understood. Several candidate genes have been proposed to increase the risk of ALS; a list of these genes is provided below. Although the results are still controversial and preliminary, studying these genes may give further insight into the possible pathogenetic mechanisms involved in ALS.

- Vascular endothelial growth factor (VEGF): identified as a candidate gene on the basis of a transgenic mouse model that showed progressive motor neuron degeneration as a consequence of deletion of the hypoxia response element in the promoter of VEGF. A number of studies initially associated specific haplotypes of the VEGF promoter with increase risk of ALS, however a recent report failed to confirm any association between polymorphisms in the VEGF promoter and sALS thus ruling out a causative role in the pathology *(Oosthuyse et al., 2001; Gros-Louis et al., 2003; Lambrechts et al., 2003; Chen et al., 2006).*

- Apurinic endonuclease gene (APEX1): initially selected on the basis of its protective role against oxidative stress. A variant of this gene showed moderate association with ALS *(Hayward et al., 1999).*

- Angiogenin (ANG): an angiogenesis factor that shares functional similarity with VEGF. It was selected because it is a neighbouring gene found in the genetic locus of APEX1. A variant of this gene was associated with increased risk of disease in the Irish and Scottish ALS populations, although this observation was not confirmed in subsequent studies on a large cohort of patients from America, Sweden, England and Italy. These data are not sufficient to support the hypothesis that ANG is relevant in

the pathogenesis of ALS *(Greenway et al., 2004; Greenway et al., 2006; Corrado et al., 2007; Del Bo et al., 2008).*

- Peripherin (PRPH): an intermediate filament protein primarily expressed in autonomic nerves and in peripheral sensory neurons. PRPH mutations have been found in two sporadic ALS patients. Immunohistochemical analysis of their spinal cord showed the presence of aggregates containing peripherin within surviving motor neurons *(Gros-Louis et al., 2004; Leung et al., 2004).*

- Survival motor neuron 1 and 2 (SMN1, SMN2): Survival motor neuron is a neuron-specific protein involved in RNA processing. Deletions or mutations of SMN1 cause child-onset spinal muscular atrophy, whereas variations in SMN2 copy number affect disease severity. A study conducted on 600 sporadic ALS cases found that altered copy numbers of SMN1 occurred more frequently in cases than in controls. It has been suggested that disruptions to the genomic organization of the SMN region may result in lower total SMN protein levels, thus increasing susceptibility of ALS *(Corcia et al., 2002; Veldink et al., 2005; Corcia et al., 2006).*

- Kinesin-Associated Protein 3 (KIFAP3): KIFAP3 is an ubiquitously expressed protein that associates with kinesin to mediate anterograde transport of vesicles along microtubules. A wide genetic study conducted on sporadic ALS cases from the United States and Europe revealed two variants (one in the gene sequence and one in the promoter) that lead to reduced expression of KIFAP3 gene, and conferred a 14 month survival advantage to the ALS patients. This suggests that decreased expression of KIFAP3 is associated with an increase in survival in sporadic ALS *(Landers et al., 2009).*

1.2. EXPERIMENTAL MODELS OF ALS

A number of studies have been performed on ALS patients to try to gain a better understanding of the pathology of the disease. Approaches have involved the collection of cerebro-spinal fluid (CSF) and peripheral blood *(Sussmuth et al., 2008; Bonetto et al., 2009; Mantovani et al., 2009; Wuolikainen et al., 2009)*, neuroimaging techniques *(Pyra et al., 2009)*, and histopathological studies on nerve and muscle biopsies or on post-mortem tissues *(Belsh, 1999; Soraru et al., 2008)*. Although these techniques can give useful information on the status of the pathology at a defined stage of the progression of the disease, they provide only a rather limited contribution towards understanding the overall pathogenic mechanisms.

One of the major breakthroughs in the field of ALS research derived from the development of animal models of disease, that proved useful both for the study of pathogenetic mechanisms and for testing potential pharmacological approaches. Rodent models are clearly not precise replicas of the human condition, but the key issue in working with these models is that the cellular and biochemical pathways remain largely conserved between humans and mice.

In order to investigate the cellular processes involved in the pathology ALS, in vitro model systems such as primary neuronal cell cultures and spinal cord organotypic cultures have been developed. Although these experimental models have intrinsic drawbacks, thanks to their relative ease of manipulation they have often been regarded as the starting point for testing pharmacologic treatments, or for studying the toxic effects induced by expression of mutant genes linked with ALS.

1.2.1 In vitro models of MND

The main advantage offered by in vitro systems is the possibility to dissect specific molecular pathways in defined cell populations.

- **Cell cultures**

In vitro cell cultures are the most widely used system developed to study individual cell types under stress conditions. Several neuronal or glial cell lines have been created. Usually, to study features of ALS, these cell lines, derived from immortalization of neurons, astrocytes or microglial cells, are transiently or stably transfected with human mutated SOD1 *(Raimondi et al., 2006; Liu et al., 2009)*. As an alternative approach, primary neuronal or glial cell cultures have been produced starting from transgenic animals expressing human mutated SOD1 *(Spalloni et al., 2004; Tortarolo et al., 2004)*. Recently, with the aim of deepening the knowledge of physiological as well as pathological interactions between neurons and the surrounding glial cells, co-cultures systems have been established *(Ferri et al., 2004; Bilsland et al., 2008)*.

- **Organotypic cultures**

Organotypic spinal cord cultures are thin slices of spinal cord (300-400 μm thickness) prepared from 9-days old mouse pups. These cultures can be mantained in vitro for up to 3 months *(Rothstein et al., 1993)*. This system is used to analyze the reaction of motor neurons to pharmacological treatments, with the advantage that the slice preserves, at least in part, the spinal cord architecture, with maintanance of the interconnectivity between neuronal cells and surrounding glial cells. However, these culture systems have some drawbacks: to obtain the culture the slice must be removed from the animal, which means that multiple axotomies are performed not only on peripheral connections of anterior horn cells, but also on descending tracts and inputs from

dorsal ganglia, leaving the motor neurons deafferented; moreover, since the motor neurons in the slice lack their target (the muscles), they project their large-caliber axons back into the white matter of the spinal cord, thus producing artifactual axonal fascicula that encircle the slice culture. Recently technical improvements have led to the establishment of organotypic cell cultures from embryonic mouse spinal cord, that contain some muscle fibres originating from peripheral tissues dissected during the explant. It has been demonstrated that this culture system can represent a valuable in vitro model to study the mechanisms of neurogenesis, glial differentiation, myelination, muscle formation, and synaptogenesis *(Avossa et al., 2003)*. The possibility of establishing organotypic cultures from the spinal cord of SOD1-G93A expressing mice has further helped study the role of motor neuron vulnerability in ALS pathogenesis *(Avossa et al., 2006; Kosuge et al., 2009)*.

1.2.2 Animal models of MND

In vivo models can be subdivided into:

- spontaneous mutants, derived from natural mutations occurring in genes that lead to impairment of the motor system;
- targeted mutants; transgenic animals (mice and rats) expressing mutated genes linked with ALS or knock-out mice, in which one gene has been deleted by homologous recombination;
- ENU-induced mutants, obtained by induction of point mutations in the genome through exposure to a mutagen.

- **Spontaneous mutants**

  - **MND mouse**

    MND (motor neuron degeneration) is a spontaneous, dominant mutation localized to chromosome 8 in the coding region of the gene Cln8,

belonging to the family of neuronal ceroid lipofuscinose-related genes *(Ranta et al., 1999)*. MND mice exhibit an adult-onset, progressive deterioration of motor function with spastic paralysis moving from caudal to cranial spinal cord levels. They undergo a premature death at 10-12 months *(Messer et al., 1987)*. However, the number of choline acetyl transferase (ChAT) immuno-positive lumbar motor neurons is not different from normal mice, consistent with the fact that these mice do not show the flaccid paralysis and muscle atrophy typical of skeletal muscle denervation due to spinal motor neuron loss *(Mennini et al., 2002)*. Neuropathological hallmarks are inclusion bodies containing ubiquitin, mitochondrial alterations, lipofuscin accumulation and neurofilament abnormalities. However, the presence of abnormal autofluorescent cytoplasmic inclusions rich in lipofuscin found in neurons, as well as in many other somatic organs, makes these animals a useful model for human neuronal ceroid lipofuscinosis rather than for ALS *(Bronson et al., 1993)*.

- **PMN mouse**

PMN (paralysé natural mutant) mice carry an autosomal recessive mutation on chromosome 13 *(Brunialti et al., 1995)*. Two groups identified the PMN mutation as a Trp to Gly substitution at the last residue of the tubulin-specific chaperone (Tbce) protein *(Bommel et al., 2002; Martin et al., 2002)* that is essential for correct tubulin assembly and for the maintenance of microtubules in motor axons. Distal axonopathy with paralysis of the limbs and muscular atrophy are the most relevant clinical signs, while motor neuron cell bodies and proximal axons are relatively preserved *(Schmalbruch et al., 1991)*. Symptomatic phase begins at 3 weeks of age and evolves rapidly to death by 7 weeks of age.

- **Wasted mouse**

Wasted (wst) is a spontaneous autosomal recessive mutation in which the gene encoding translation elongation factor eEF1A2 is deleted *(Chambers et al., 1998)*. The symptom onset is around 2 weeks of age, with homozygous mice showing tremors and disturbances of gait. The progression is very fast, leading to death within a month. Recent studies have demonstrated that spontaneous loss of eEF1A2 expression that occurs in Wst mutant mice triggers the dying-back pathways in lower motor neurons in vivo: synaptic loss at the NMJ is an early event, accompanied by gliosis in the spinal cord, followed by motor neuron pathology (with vacuolisation and perikarial accumulation of neurofilaments) with a rostrocaudal progression, and finally death *(Newbery et al., 2005; Murray et al., 2008)*. Only spinal and brainstem motor neurons are lost, while UMN are not affected *(Doble and Kennel, 2000)*.

- **Wobbler mouse**

The wobbler mouse represents another model of motor neuron disease *(Mitsumoto and Bradley, 1982)*. It shows a progressive forelimb weakness and atrophy, beginning at about 1 month of age, accompanied by a marked decrease of muscular strength and motor ability with no involvement of the hind limbs. The symptoms are associated with proximal axonal degeneration and vacuolar changes within the motor neurons of the cervical spinal cord with little involvement of the brain. Death occurs at about 1 year of age. In this case, the autosomal recessive genetic defect responsible for this syndrome has been mapped on chromosome 11 and it has recently been identified as a missense mutation in Vps54 (Vacuolar Vesicular Protein Sorting) involved in the

transport of vesicles from late endosomes to the Golgi apparatus *(Schmitt-John et al., 2005).*

- **NMD mouse**

NMD (neuromuscular degeneration) mice carry an autosomal recessive mutation localized on the gene coding for the ATPase/DNA helicase, also known as SMbp2 *(Cook et al., 1995; Cox et al., 1998).* These mice develop rapidly progressive hind limb weakness, beginning at 2 weeks of age. Pathological examination reveals motor neuron cell body degeneration in the spinal cord. Death occurs by 4 weeks of age.

➢ **Targeted mutants**

To obtain transgenic animals, exogenous genes are introduced by microinjection of purified DNA in the male pronucleus of fertilized mouse eggs. The integration of foreign DNA is random, with multiple copies of DNA usually integrating at a single site. On the other hand, it is possible to delete a gene (knock-out) in order to study the effect of its ablation on the organism. To obtain knock-out mice, a murine stem cell line is engineered in vitro to obtain substitution of the gene of interest with a very similar sequence carrying modifications that make the gene inoperable. The knock-out stem cells are then inserted into a mouse blastocyst and reimplanted into a foster mother. Mice carrying the gene deletion in germline cells are selected from the offspring and used for colony expansion.

The most widely used animal model of ALS is represented by transgenic mice expressing human SOD1 gene with mutations found in human patients (see section 1.1.5). Recently transgenic rats expressing human mutant SOD1 have been also generated. These models will be described in detail; other transgenic animals showing features of motor neuron disease are listed in **Table 1.4**.

- **SOD1 mutant mice**

To date seven lines expressing different mutations of SOD1 have been generated *(Shibata, 2001)*. The most extensively studied are the lines over-expressing human SOD1 with G93A, G37R or G85R mutations *(Dal Canto and Gurney, 1994; Wong, 1995)*. A line expressing mouse SOD1 with G86R mutation has been also produced *(Ripps et al., 1995)*. These animals develop a phenotype that closely resembles ALS, with an adult onset progressive motor paralysis, muscle wasting and reduced lifespan. Pathological changes mainly consist of depletion of motor neurons in the spinal cord, gliosis, axonal swelling and presence of ubiquitin-positive inclusions in surviving motor neurons, and muscular atrophy. In contrast, mice overexpressing wild type SOD1 remain clinically normal, although some changes have been reported at two years of age *(Jaarsma et al., 2000)*. Transgenic mice carrying 23 copies of human SOD1 with Gly93Ala mutation (SOD1G93A mice) are considered the standard model of ALS in therapeutic studies *(Bendotti and Carri, 2004)*. The model develops a motor system disease prevalently affecting lower motor neurons. Ultrastructural and microscopical analysis reveals that the earliest pathological sign in these mice is the vacuolization of large neurons in the anterior horns of the spinal cord *(Bendotti et al., 2001a)*; it has been hypothesized that these vacuoles originate from the dilatation of rough endoplasmic reticulum and from degenerating mitochondria. At the end stage, motor neuronal depletion is evident and hyaline, filamentous inclusions immuno-positive for ubiquitin and neurofilaments are present in some of the surviving neurons *(Gurney et al., 1994; Migheli et al., 1999)*.

Transgenic mice expressing low levels of SOD1 G37R mutant show a motor disease restricted to lower motor neurons, whereas higher copy number causes more severe abnormalities and affects a variety of other neuronal populations. The most evident cellular abnormality is the presence of

vacuoles derived from degenerating mitochondria in axons and dendrites *(Wong, 1995)*.

Transgene expression of mutant human SOD1 G85R or its murine counterpart G86R develops a very aggressive pathology with a rapid progression to paralysis and death within two weeks from the first symptoms. In G85R mice, inclusions that are immunopositive for ubiquitin and SOD1 appear within motor neurons and astrocytes *(Bruijn et al., 1997b)*. Differences in disease progression and survival in various SOD1 mutant mice is dependent on the mutation and the copy number of the transgene. The age of onset, the duration and several pathological features also vary and are dependent on the gender and the mouse strain in which the mutation is expressed; this background effect suggests the existence of strong modifying genetic factors *(Alexander et al., 2004; Heiman-Patterson et al., 2005)*.

- **SOD1 mutant rats**

Recently two lines of rats expressing transgenes for mutant SOD1 protein with two different ALS-associated mutations (H46R and G93A) have been established. As in the human disease and transgenic ALS mice, pathological analysis shows selective loss of motor neurons in the spinal cords of these transgenic rats. In addition, typical neuronal Lewy body-like hyaline inclusions as well as astrocytic hyaline inclusions are observed in the spinal cords *(Nagai et al., 2001; Aoki et al., 2005)*. An interesting feature of this animal model is the variability of phenotype manifestation. For example motor deficits and atrophy can initially appear in the fore-limbs, or in the hind-limbs, and then spread to other areas of the body. Alternatively symptoms can be more generalized, with both fore- and hind-limbs affected. One of the reasons for this inter-individual variability of phenotype manifestation is that these lines of rats are on an outbred genetic

background (Sprague-Dawley), suggesting that naturally occurring polymorphisms in some genes may be implicated *(Matsumoto et al., 2006a).*

Table 1.4. Mouse models with motor neuron dysfunction

Mouse	Symptomatology and pathologic changes	References
Mutant NF-L (point missense mutation in the gene for Neurofilament Light chain)	Perikaryal and axonal NF accumulations with trapped organelles in motor neuron and sensory neurons. No degeneration of sensory neurons but massive degeneration of spinal motor neurons. Motor impairment and atrophy of skeletal muscles.	*(Lee et al., 1994b)*
NF-L knock-out	Perikaryal accumulation of NF-M and NF-H. Loss of motor axons; decresed caliber of myelinated axons; altered nerve conductivity. Mild sensorimotor dysfunction but no signs of paresis.	*(Zhu et al., 1997; Dubois et al., 2005)*
hNF-H overexpressor	Perikaryal accumulations and axonal atrophy. Altered conductivity but no neuronal loss. Progressive axonopathy and muscle atrophy.	*(Cote et al., 1993; Kriz et al., 2000)*
Peripherin overexpressor	Progressive accumulation of intermediate filament aggregates in perikarya and axons of motor neurons. 40% loss of spinal motor neurons, and manifestation of motor dysfunction late in life (after 2 years of age).	*(Beaulieu et al., 1999)*
Dynamitin overxpressor	Late-onset progressive motor neuron degenerative disease characterized by decreased strength and endurance, motor neuron degeneration and loss, axonal intermediate filament swellings, and denervation of muscles.	*(LaMonte et al., 2002)*
Short Tau overexpressors	Spheroidal inclusions containing tau, NFs and tubulin. Axonal degeneration of spinal neurons and motor weakness.	*(Ishihara et al., 1999)*
VEGF -/- (deletion of Hypoxia responsive element within VEGF promoter)	Neurofilament accumulations in the spinal and brainstem motor neurons; vacuolisation and abnormal mitochondria and organelles in affected motor neurons. Severe motor deficits at 5–7months of age with signs of severe muscle weakness and limb paresis.	*(Oosthuyse et al., 2001)*
Als2 knock-out	Slow progressive loss of cerebellar Purkinje Cells and reduction in ventral motor axons during aging; astrogliosis and evidence of deficits in endosome trafficking. Mild phenotype with age-dependent deficits in motor coordination.	*(Cai et al., 2005; Hadano et al., 2006)*

➢ **ENU-induced mutants**

N-Ehtyl-N-nitrosurea (ENU) is a chemical mutagen that produces point mutations in the genome, which enables identification of the causal gene by methods such as positional candidate cloning, and is currently being used to generate new mouse models of MND *(Chen et al., 2000; Brown and Balling, 2001; Hafezparast et al., 2003a).* So far this approach has successfully created the mouse Legs at odd angles (Loa), and the cramping mouse (Cra1).

- **Loa mice**

  In these mice, a missense autosomal dominant mutation in the cytoplasmic dynein heavy chain gene (Dnchc1) causes defects in retrograde axonal transport and motor neuron degeneration. Heterozygous mice display age-related progressive loss of muscle tone and locomotor ability without major reduction in life-span. Homozygous Loa mice show a more severe phenotype with an inability to feed and move, and die within 24 hours of birth. Homozygous Loa/Loa animals have neuronal inclusion bodies that are positive for SOD1, CDK5, neurofilaments and ubiquitin *(Hafezparast et al., 2003b).*

- **Cra1 mice**

  These mice carry a missense autosomal dominant mutation in gene Dnchc1, different from the one described for Loa mice. Heterozygous mice show the same phenotype described for Loa. In homozygous Cra1 animals also large dorsal root ganglion neurons are affected *(Hafezparast et al., 2003b).*

1.3. PATHOGENETIC HYPOTHESES OF ALS

To date, the aetiology of ALS remains unknown. Most current knowledge on the mechanisms leading to the degeneration of motor neurons in ALS has come from the study of fALS cases, in which mutations in single genes have been identified. Since the discovery of SOD1 mutations as causative genetic factor for fALS, in 1993, several hypotheses have been formulated on the possible molecular players involved in the neurodegeneration; however, even in this defined genetic subgroup the pathways leading to neuronal death appear to be complex.

Studies performed on human ALS autopsy samples or on animal models have suggested that ALS may be considered as a multifactorial disease in which a complex interplay between multiple mechanisms including genetic factors, oxidative stress, excitotoxicity, mitochondrial damage, protein aggregation, and alterations of axonal transport determine the motor neuronal death. Interestingly, since the clinical and pathological profiles of sporadic and familial ALS are similar, it can be predicted that evidence emerging from studies on ALS-causing gene mutations may apply also to sporadic ALS. However, one biochemical difference appears to be the absence of pathologic TDP-43 (a hallmark of affected neurons in sALS and frontotemporal dementia) in fALS cases due to SOD1 mutation *(Mackenzie et al., 2007)*. However this observation remains controversial since there are contrastating results on human cases and mutant SOD1 mice *(Robertson et al., 2007; Turner et al., 2008; Shan et al., 2009)*.

1.3.1 Oxidative stress

The role of oxidative stress in the pathogenesis of ALS remains controversial. Increases in markers of oxidative damage have been reported in human patients affected by both sporadic and inherited forms of ALS *(Beal et al., 1997; Ferrante*

et al., 1997; Liu et al., 1999) and in transgenic mouse models of the disease *(Ferrante et al., 1997; Andrus et al., 1998)*. However in other independent studies no significant modifications of markers of oxidative damage were reported *(Shaw et al., 1995a; Bruijn et al., 1997a)*.

Concerning ALS linked to SOD1 mutations, it has been hypothesized that mutated SOD1 may acquire a toxic function, thus becoming the source of oxidative stress. It is possible that mutations may alter protein folding, leading to aberrant copper-mediated catalysis, or to the release of redox active metals leading to unregulated oxidative reactions.

A number of chemical models have been proposed to explain mechanisms by which oxidative stress could be generated by mutant SOD1 (**Figure 1.2**):

- **Peroxidase hypothesis:** the reduced form of mutant SOD1 (Cu^{1+}-bound state) may accept hydrogen peroxide as a substrate thus producing hydroxyl radical OH- (an extraordinarily reactive oxigen species), leading to a cascade of peroxidation *(Wiedau-Pazos et al., 1996)*;
- **Peroxynitrite hypothesis:** mutant SOD1 may accept abnormal substrates such as peroxynitrite, provoking aberrant tyrosine nitration *(Beckman et al., 1993)*;
- **Backward catalysis:** mutations of SOD1 may reduce the amount of bound zinc, thus destabilizing the structure of the enzyme, and allowing a rapid reduction of Cu^{2+} to Cu^{1+}. The reduced SOD1 mutant would then run the normal catalytic step backwards, converting oxygen to superoxide. Finally, the superoxide produced would combine in the enzymatic active site with freely diffusing nitric oxide, thereby producing peroxynitrite, which would promote intracellular damage, including protein nitration *(Estevez et al., 1999)*.

Figure 1.2. SOD1-mediated chemistry

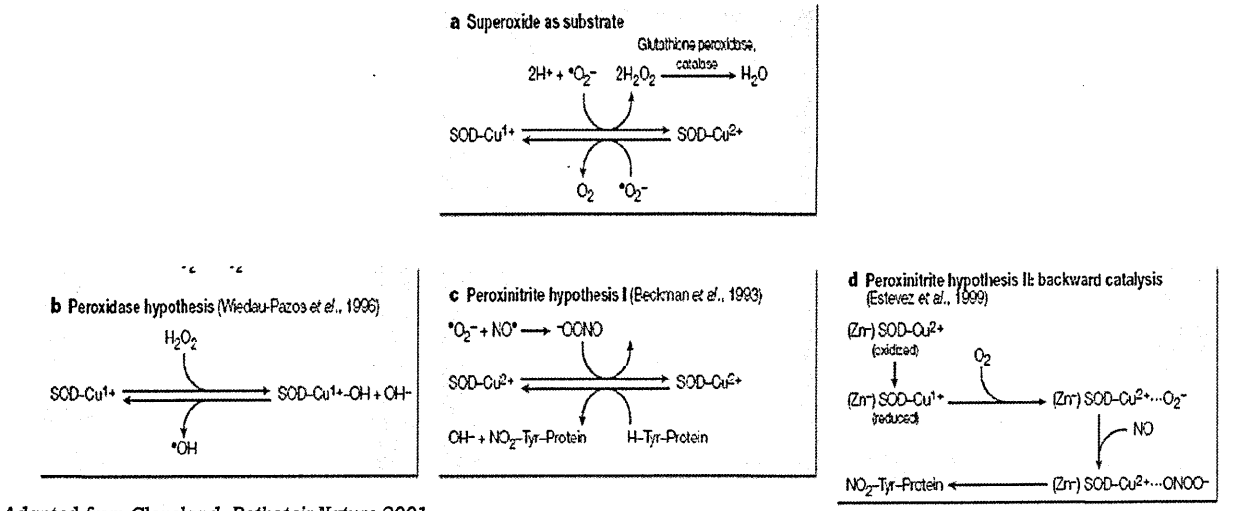

Adapted from Cleveland, RothsteinNature 2001

SOD1 enzyme normally uses superoxide ion as a substrate, producing H_2O_2 and molecular oxygen as products (a). fALS linked SOD1 mutants may acquire aberrant chemical reactivity, thus leading to production of highly reactive hydroxyl radicals (b) or to nitration of other proteins (c,d).

Several experiments in SOD1 mutant mice have tried to address the question as to whether the toxicity of mutant SOD1 can be explained by aberrant oxidative chemistry.

In particular, manipulation of wild type SOD1 activity levels in mice have provided some evidence that the peroxynitrite hypothesis is unlikely to play a central role in the pathology: in SOD1G85R mice (carrying a mutation that confers only a ~10% increase in SOD1 activity over the wild-type SOD1) neither elimination nor chronic elevation (by about sixfold) of wild-type SOD1 activity affected disease onset, progression or pathology *(Bruijn et al., 1998).* In contrast, the expression of elevated levels of wild-type human SOD1 in SOD1G93A, L126Z or A4V mice unexpectedly accelerated the disease onset *(Jaarsma et al., 2000; Deng et al., 2006).* The fact that toxicity cannot be ameliorated by increased wild-type SOD1 activity challenges the hypothesis that damage arises from superoxide or any reactive oxygen species derived from it, though it may be argued that oxidative stress contributes to the degenerative process.

Another set of experiments were aimed at modifying copper loading into SOD1 in vivo, to address the question whether the toxic activity of mutated SOD1 is dependent on aberrant chemistry catalyzed by the copper atom. One of the key players involved in copper loading into the enzyme is the copper chaperone (CCS). Deletion of CCS in mice has been shown to reduce copper loading into SOD1, thus affecting the enzyme activity *(Wong et al., 2000)*. Interestingly, mutant SOD1 transgenic mice with a CCS knock out possess only very low levels of SOD1-bound copper and have drastically reduced dismutase activity, but still develop motor neuron disease *(Subramaniam et al., 2002)*. However, CCS over-expression in G93A mice produces severe mitochondrial pathology and strongly accelerates disease progression *(Son et al., 2007)*.

The most plausible interpretation is that copper-mediated oxyradical chemistry is not required for the motor neuron pathology provoked by mutant SOD1, although it has been proposed that mutant SOD1 might exert aberrant catalysis through copper loaded on the surface of the protein in a CCS-independent fashion *(Bush, 2002)*.

1.3.2 Excitotoxicity

Glutamate-induced excitotoxicity is considered another mechanism that may play a major role in the aetiology of ALS. An over-stimulation of neuronal glutamate receptors can cause neuronal death by increasing the calcium influx in the cytosol, thus activating death pathways, involving calpain, protein kinase C, lipases, endonucleases, xanthine oxidase and nitric oxide synthase. This phenomenon may be exacerbated by the regulation of the activity or of the subunit composition of glutamate receptors, which can render them more permeable to Ca^{2+} and Zn^{2+} influx.

To prevent the aberrant activation of glutamate receptors, glial cells express glutamate transporters that facilitate removal of glutamate from the synaptic cleft. EAAT2 is the major glutamate transporter, and is localized exclusively in

glia. Changes in the equilibrium of this system may result in harmful events to the motor neurons in ALS.

Evidence of abnormalities in glutamate handling in ALS arose from the discovery of large increases in the levels of glutamate in the plasma *(Plaitakis and Caroscio, 1987)* and in the cerebrospinal fluid of a subset of ALS patients *(Rothstein et al., 1991; Shaw et al., 1995b)*. Direct measurement of functional glutamate transport in ALS revealed a marked reduction in the affected brain regions, which was the result of a pronounced loss of the astroglial EAAT2 protein *(Rothstein et al., 1995)*. Interestingly, EAAT2 is a target for oxidative regulation and glutamate transport is impaired by mutant SOD1 in an in vitro model *(Trotti et al., 1999)*. The loss of glutamate transporters has been confirmed in mutant SOD1-transgenic mice and rats *(Bendotti et al., 2001b; Howland et al., 2002)*.

Glutamate-induced excitotoxicity provides another possible explanation for the selective vulnerability of motor neurons in ALS. In fact, motor neurons have a diminished capacity to buffer calcium *(Alexianu et al., 1994)*. Additionally, although motor neurons express a range of glutamate receptors (NMDA, AMPA, kainate and metabotropic), in vitro studies have demonstrated that they are particularly sensitive to glutamate excitotoxicity mediated through AMPA receptors *(Carriedo et al., 1996)*. A defect in the RNA editing of the AMPA GluR2 subunit, or a lack of this receptor subunit, are likely to be involved in the selective vulnerability of motor neurons in ALS by conferring calcium permeability to AMPA-gated channels *(Kawahara et al., 2004)*. Indeed, treatments with AMPA receptor antagonists slow the disease progression and increase survival of mutant SOD1 transgenic mice, suggesting that AMPA receptors may represent promising targets for therapies *(Van Damme et al., 2003; Tortarolo et al., 2006)*.

Riluzole, the only drug currently approved for treatment of ALS patients, is believed to antagonize glutamate-mediated excitotoxicity although the precise mechanism of action is rather controversial.

1.3.3 Mitochondrial dysfunction

Alterations in mitochondrial function are an attractive candidate for involvement in ALS pathogenesis because changes in mitochondrial morphology are seen at pre-symptomatic stages in SOD1 mutant mice *(Bendotti et al., 2001a; Jung et al., 2002)* and in cultured cells expressing the mutant protein *(Carri et al., 1997; Beal et al., 2000)*. Interestingly, mitochondrial abnormalities have also been observed in motor axon terminals of muscle biopsies from patients with early-diagnosed sporadic ALS *(Siklos et al., 1996; Beal et al., 2000)* and in proximal axons *(Hirano et al., 1984)* and in anterior horns of the spinal cord in post mortem tissues of sALS patients *(Sasaki and Iwata, 1996)*. Biochemical studies have highlighted defects in the activity of the respiratory chain complex IV in sALS spinal motor neurons *(Borthwick et al., 1999)* and in complexes I and IV in spinal cord and brainstem homogenates of G93A mice *(Browne et al., 1998)*.

Recent studies have indicated that mutant SOD1 could directly damage mitochondria. The presence of SOD1 in mitochondria of eukaryotic cells has been confirmed by several groups using a variety of experimental approaches. In particular, using immuno-gold electron microscopy, it has been demonstrated that both wild type and mutant SOD1 localize in the mitochondria of motor neurons in the spinal cord of transgenic mice *(Jaarsma et al., 2001; Higgins et al., 2002)*. Liu and colleagues have proposed that mutant SOD1 progressively accumulates and aggregates on the mitochondrial outer membrane, altering the protein translocation machinery of the organelle *(Liu et al., 2004)*. It has also been hypothesized that mutant SOD1 aggregates could damage the mitochondrion through abnormal interaction with mitochondrial proteins such as Bcl-2 *(Pasinelli et al., 2004)*.

Whether mitochondrial dysfunction and pathology represents a primary or secondary pathological event is unknown, as mitochondrial abnormalities can both result from or cause oxidative toxicity. In either circumstance, the

pathological mitochondria may contribute to cell death by releasing calcium into the cytoplasm, through bioenergetic failure due to production of inadequate levels of ATP, and by releasing cytochrome c, a trigger of pro-degenerative apoptotic pathways.

Interestingly, the disease in mutant SOD1 mice is slowed by interventions that improve mitochondrial function like for example, creatine, which inhibits opening of the mitochondrial transition pore, and minocycline, which blocks leakage of cytochrome c *(Klivenyi et al., 1999; Zhu et al., 2002).*

1.3.4 Protein aggregation

As previously described one of the pathological hallmarks of ALS, as well as of SOD1 mutant mice, is the formation of proteinaceous inclusions in the motor neurons and sometimes in the surrounding astrocytes *(Migheli et al., 1990; Bruijn et al., 1997b; Kato et al., 1999).* These inclusions are composed of different proteins, such as SOD1, ubiquitin, dorfin, neurofilaments, peripherin and p38 MAPK; additionally, chaperones and proteasome subunits may also be sequestered *(Watanabe et al., 2001; Strong et al., 2005).*

Given that ubiquitin-containing aggregates are a frequent feature both in sporadic and familial cases, this could link the mechanisms of the two forms of ALS. As regards to fALS cases linked to SOD1 mutations, another set of hypotheses propose that mutant SOD1 acquires conformational instability and becomes prone to aggregation.

Actually, SOD1 mutants display a general structural instability *(Lindberg et al., 2002)* and are less thermostable than the wild type enzyme *(Rodriguez et al., 2002).* Some studies suggest that SOD1 mutations perturb the folding pathway of the protein by destabilizing the precursor monomers or weaken the dimer interface; the result is a shift of the folding equilibrium toward poorly structured monomers. Another characteristic that could promote aggregation of mutant SOD1 is a decrease of the net negative charge of the polypeptide observed in

several ALS-associated mutations; this phenomenon is further exacerbated in cellular environments that are more acidic than the cytosol, such as mitochondria and the trans-Golgi network *(Lindberg et al., 2005).*

Generally, the mutation can determine both local perturbations of the secondary, tertiary or quaternary structure and the loss of metal ion binding; the common result is a destabilization of the enzyme that leads to non-native interactions with itself, or other proteins, and aggregation. Many in vitro and in vivo data support this hypothesis. Studies in cell culture have shown that, in contrast to the stable wild type protein, the mutant protein oligomerizes to form small pore-like structures *(Chung et al., 2003; Ray et al., 2004; Matsumoto et al., 2005; Matsumoto et al., 2006b).* Inclusions of SOD1 are found in primary cultured motor neurons expressing several different SOD1 mutations; the formation of such inclusions correlates with a loss of viability *(Durham et al., 1997).*

Studies in the spinal cord of G93A mice have demonstrated the progressive appearance of aggregates in dendrites, periaxonal processes of oligodendrocytes and neuronal and astrocytic perikarya *(Stieber et al., 2000).* The aggregation of SOD1 into insoluble high molecular weight species is an early event occurring in G93A mice *(Johnston et al., 2000)* and their abundance increases as the disease progresses.

Correlations between protein aggregation and clinical phenotype have been reported in familial ALS and mutations associated with more severe forms of the disease which present with a short half-life are more likely to form aggregates *(Lindberg et al., 2005; Sato et al., 2005).*

Aggregate formation could be a primary event in the disease pathogenesis and could drive neurotoxicity. Alternatively, aggregation could occur secondary to the primary neurotoxic event and it has been hypothesized that inclusions could be the product of a cellular defence mechanism that occurs when the burden of misfolded or damaged protein exceeds the capacity of the protein degradation machinery to eliminate them. The formation of inclusion bodies may act as a

cellular defence mechanism in the attempt to actively reduce the concentration of smaller, more toxic aggregates *(Ross and Poirier, 2005)*.

Various hypotheses have been proposed regarding the cytotoxicity of SOD1 aggregates, including the disruption of axonal transport *(Stokin et al., 2005)*, the aberrant binding of apoptosis regulators *(Pasinelli et al., 2004; Tomik et al., 2005)*, perturbations in mitochondrial function and calcium homeostasis *(Hervias et al., 2006; Sumi et al., 2006)* and inhibition or overload of the ubiquitin-proteasome pathway *(Cleveland and Rothstein, 2001)*. Consistent with the latter hypothesis, accumulation of ubiquitinated aggregates have been detected in SOD1 mutant mice *(Stieber et al., 2000; Watanabe et al., 2001; Bendotti et al., 2004)*. Since one of the roles of ubiquitin is to label and target misfolded and inactive proteins to the proteasome machinery, it has been hypothesized that proteasome activity could be inhibited by SOD1, leading to accumulation of aberrantly folded forms of SOD1 and other proteins *(Cleveland and Rothstein, 2001)*.

1.3.5 Alterations of cytoskeleton and axonal transport

The idea that cytoskeleton abnormalities may play a role in ALS pathology arises from early reports of neurofilament accumulations in the cell bodies and proximal axons of motor neurons of both sporadic and familial ALS *(Hirano et al., 1984)*. Subsequent studies have shown that over-expression of NF-H or NF-L subunits in mice causes the selective degeneration and death of motor neurons *(Cote et al., 1993; Xu et al., 1993)*. Other studies on transgenic mice have demonstrated that neurofilament content and organization strongly influence the disease induced by mutant SOD1 *(Couillard-Despres et al., 1998; Williamson et al., 1998; Couillard-Despres et al., 2000; Kong and Xu, 2000)*. In particular, deletion of the NF-L subunit increases the survival of SOD1 mutant mice, while increased expression of the NF-L or NF-H subunits slows SOD1 mutant-mediated disease. The protective effects of increased NF-H content in perikarya may be due

to the ability of neurofilaments to "buffer" against a cascade of aberrant and harmful events in the cell body *(Couillard-Despres et al., 1998)*. Mice that over-express peripherin, another intermediate filament protein, develop a late onset motor neuron degeneration and show disruption of neurofilament assembly *(Beaulieu et al., 1999)*, however, alteration of peripherin levels in SOD1 mutant mice does not modify the disease course *(Lariviere et al., 2003)*.

Currently it has not yet been clarified whether neurofilament disorganization represents a secondary product of the pathological processes or whether it directly contributes to the death of the motor neurons. However, it is clear that motor neurons are particularly dependent on axonal transport of molecules and organelles for their activity and survival *(De Vos et al., 2008)*. For example, axonal proteins are synthesized in the cell body and must be transported in an anterograde manner along the axons and dendrites to reach synapses, whereas substances such as trophic factors synthesized at the muscular level must be transported backward centrally from the synaptic regions by retrograde transport. Kinesin and the dynein-dynactin complex represent the molecular motors for anterograde and retrograde transport, respectively.

Several factors indicate that defects in axonal transport might contribute to the degeneration of motor neurons in ALS. First, anterograde transport is slowed in G93A and G37R transgenic mice prior to disease onset and the deficits are exacerbated as the disease progresses *(Borchelt et al., 1998; Williamson and Cleveland, 1999)*. Also retrograde transport is disrupted in SOD1 mutant mice *(Murakami et al., 2001)*.

It has been hypothesized that the aggregation of neurofilaments in proximal axons (spheroids) might physically compromise the transport apparatus *(Sasaki and Iwata, 1996)*. On the other hand, defects in retrograde transport in ALS mice has been attributed to the mis-localization and disruption of dynein function *(Ligon et al., 2005)*. In two lines of mice (Loa and Cra1) point mutations in the dynein heavy chain impaired motor neuron functionality and viability *(Witherden*

et al., 2002; Hafezparast et al., 2003b). In addition, disruption of the dynein–dynactin complex in mice, by the forced expression of dynamitin, a subunit of dynactin, also produces a late onset motor neuron disease *(LaMonte et al., 2002).* Interestingly, introduction of the dynein mutations that generate either the legs at odd angles or the cramping phenotypes into SOD1G93A ALS mice significantly ameliorates the motor neuron disease and the slowing of axonal transport *(Kieran et al., 2005; Teuchert et al., 2006).* Consistent with these observations, a recent study by Teuling and collegues demonstrated that neuron-specific expression of Bicaudal D2 N-terminus (a protein that chronically impairs dynein/dynactin function) in SOD1G93A ALS transgenic mice increased life span *(Teuling et al., 2008).* The mechanism underlying this is unclear, although the implication is that *Loa* and *Cra*-mutant dyneins compensate or counteract axonal transport abnormalities triggered by mutant SOD1 *(Kieran et al., 2005).* Alternatively, dynein/dynactin inhibition may attenuate functions that are potentially harmful to mutant SOD1-expressing motor neurons such as retrograde transport of axonal debris or protein aggregates *(Johnston et al., 2002; Ravikumar et al., 2005),* or deleterious retrograde signalling *(Cavalli et al., 2005; Hanz and Fainzilber, 2006).* These diverse observations favour the view that disturbances and attenuation of axonal transport might be a unitary feature of all forms of ALS and potentially a primary pathogenic event in this disease.

Figure 1.3.

Converging molecular mechanisms involved in motor neuron death in fALS

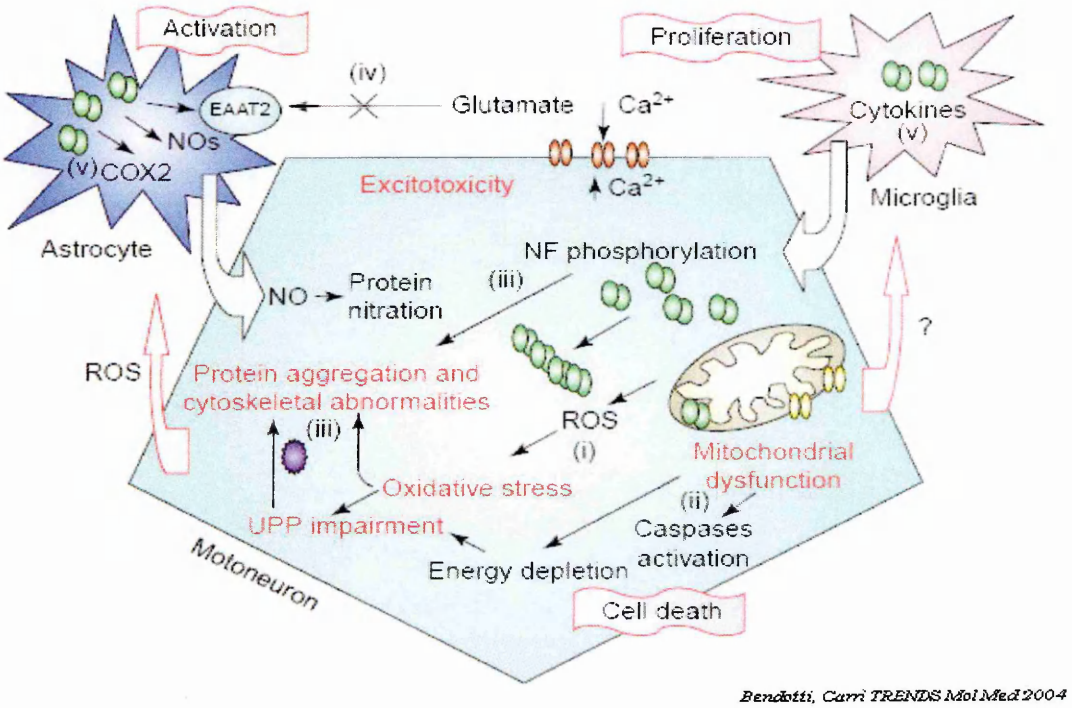

Mutant SOD1 might act at different levels to induce neuronal death: (i) by exacerbating the production of oxygen radicals and nitrotyrosine with consequent alterations of intracellular proteins and lipids (oxidative stress); (ii) by inducing mitochondrial dysfunction and the further production of reactive oxygen species (ROS), the activation of caspases and energy depletion, which results in the impairment of different ATP-dependent cellular processes, such as the ubiquitin–proteasome pathway (UPP); (iii) by facilitating the formation of ubiquitinated aggregates due to the misfolding of mutant protein and increased phosphorylation of cytoskeletal proteins; (iv) by inhibiting the activity of the glial glutamate transporter EAAT2; (v) by activating microglia and astrocytes to produce and release pro-inflammatory cytokines and other potential toxic factors (nitric oxide, NO).

1.3.6 Evidence for ALS as a non-cell autonomous disease

Evidence from experimental models supports the view that a functional cross-talk between neurons and non-neuronal cells is crucial for the induction of motor neuronal death in ALS. Although motor neurons are induced to die by expression of mutant SOD1, other cell types actively participate in the generation of the pathological phenotype by releasing neurotoxic factors, such as inflammatory cytokines, glutamate and nitric oxide (NO) *(Raoul et al., 2002)*. An early event in the neurodegeneration process is the inflammatory response. Indeed,

accumulation of reactive microglia and astrocytes has been documented in the spinal cord and in the motor cortex of ALS patients and in pre-symptomatic animal models of the disease *(Kawamata et al., 1992; Hall et al., 1998).* Moreover a broad spectrum up-regulation of pro-inflammatory genes, such as COX-2 (Cyclooxygenase 2), NOS (nitric oxide synthase) and cytokines, for example TNF□, is reported in the spinal cord of G93A mice *(Hensley et al., 2002).* The concept that glial cells are activated early in fALS SOD1 mice suggests that neuroinflammation has a relevant role in the cascade of events that trigger the death of motor neurons.

Several authors have tried to dissect the features of the pathologic interplay between motor neurons and surrounding glial cells, in ALS. The most interesting results have emerged from the use of transgenic mice with expression of mutant SOD1 in specific cell populations of the nervous system (**Table 1.5**), or from chimeric mice with mixed populations of cells expressing either endogenous or transgenic mutant SOD1 (**Table 1.6**). Transgenic mice possessing SOD1 G37R cDNA under the prion gene promoter express mutant SOD1 in neurons, astrocytes and muscles, but not in the macrophage lineage. They develop motor neuron disease *(Wang et al., 2005),* thus indicating that the presence of the mutant protein in the motor neuron/muscle circuit, along with supporting astrocytes, is sufficient to induce the disease. However, expression of mutant SOD1 only in neurons or in glia failed to trigger motor neuron degeneration *(Gong et al., 2000; Pramatarova et al., 2001).* This might reflect insufficient expression of mutant SOD1 in these experimental paradigms, as demonstrated by a subsequent study *(Jaarsma et al., 2008).*

Interestingly, through chimeric mice it has been demonstrated that the toxicity to motor neurons requires damage from mutant SOD1 acting within non-neuronal cells: in fact, wild type motor neurons surrounded by SOD1 mutated glia showed ubiquitin-positive inclusions, indicative of neuronal stress, whereas, on the other hand, degeneration of motor neurons expressing mutant SOD1 was delayed or

prevented when they were surrounded by wild type glia *(Clement et al., 2003).* Consistent with these data, experiments in co-culture systems have recently provided evidence that astrocytes expressing mutant SOD1 are able to cause the death of both wild type and mutant motor neurons probably through release of soluble toxic factors *(Di Giorgio et al., 2007; Nagai et al., 2007).*

Microglia also appear to be important in the pathological processes. Deletion of mutant SOD1 only in microglia and peripheral macrophages did not change the onset of the disease, but increased the survival, whereas deletion of mutant SOD1 only within motor neurons extended survival by delaying the onset and the early phase of disease process *(Boillee et al., 2006b).* In another study the presence of G93A only in microglia was not capable of inducing motor neuron disease, while the substitution of mutated microglia with the wild type in G93A mice significantly slowed the motor neuron loss, prolonging the disease duration and the survival *(Beers et al., 2006).*

In a recent paper from Fischer the authors highlighted denervation of peripheral muscles before loss of neuronal cell body occurred in SOD1 pre-symtpomatic transgenic mice, and confirmed this observation in a single human sALS case *(Fischer et al., 2004).* These evidences support the hypothesis that the pathology presents feature of a distal axonopathy, thus suggesting that alterations of peripheral nervous system may also be involved in the neurodegenerative process in ALS. Actually, though the mutant SOD1-mediated damage within muscles has been ruled out by recent studies *(Miller et al., 2006),* the contribution of Schwann cells in the maintenance and delivery of supporting factors to axons has emerged *(Lobsiger et al., 2009).* Overall these data support the hypothesis that alterations within motor neuronal cell body (as outlined in **Figure 1.3**) or in the peripheral axons, may be the triggering event of the pathologic process. Then aberrant activation of glial cells and release of toxic factors may play a role in the progression and worsening of the disease.

Table 1.5.

Effect of selective expression of mutant SOD1 in neurons, astrocytes or muscles

Mouse	mSOD1 is expressed in...	alterations of non-neuronal cells	MN loss	MND phenotype	Reference
GFAP_SOD1^{G85R}	astrocytes	astrocytosis	no	no	*Gong, J.Neurosc. 2000*
NFL_SOD1^{G87R}	motor neurons	not described	no	no	*Pramatarova, J.Neurosc. 2001*
Thy1.2_SOD1^{G93A}	neurons	astrocytosis	yes	yes	*Jaarsma, J.Neurosc. 2009*
MLC_SOD1^{G93A}	muscles	muscle atrophy	no	no	*Dobrowolny Cell Metab. 2008*

Table 1.6.

Effect of selective downregulation of mutant SOD1 in specific cell types

Mouse	mSOD1 is reduced in...	Biochemical/histological alterations	Disease progression	Reference
Isl1-$^{Cre+}$ x Lox-SOD1^{G37R}	motor and dorsal root ganglion neurons	not described	delayed onset, extended survival	*Boillée Science 2006*
CD11b-$^{Cre+}$ x Lox-SOD1^{G37R}	microglial cells	astrocytosis, microgliosis	no effect on onset, extended survival	*Boillée Science 2006*
GFAP-$^{Cre+}$ x Lox-SOD1^{G37R}	astrocytes	astrocytosis, delayed microgliosis	no effect on onset, extended survival	*Yamanaka Nat.Neurosc. 2008*
P_0-$^{Cre+}$ x Lox-SOD1^{G37R}	schwann cells	lack of IGF-I induction in sciatic nerves	no effect on onset, decreased survival	*Lobsiger PNAS 2009*
MCK-$^{Cre+}$ x Lox-SOD1^{G37R}	scheletal muscles	not described	no effects on onset and survival	*Miller PNAS 2006*

1.3.7 Aberrant regulation of pro-degenerative and anti-apoptotic pathways

Cells respond to a multitude of external stimuli using a limited number of signalling pathways activated by plasma membrane receptors, such as G protein-coupled receptors (GPCRs), receptor tyrosine kinases (RTKs) and ligand-gated ion channels. These pathways do not simply transmit, but process, encode and integrate external signals with the events occurring at different locations within the cytoplasm. Signalling by RTKs plays a central role in the development and maintenance of neurons and glia through a wide range of processes, including survival, proliferation, differentiation, neurite outgrowth, and synaptogenesis *(Romanelli and Wood, 2008).*

Typically, upon stimulation, RTKs undergo dimerization and allosteric modification resulting in activation of the intrinsic tyrosine kinase catalytic

activity. Subsequent phosphorylation of multiple tyrosine residues transmits a biochemical message to a number of cytoplasmic proteins, in a cascade fashion. Cascades of coupled phosphorylation/dephosphorylation cycles, such as mitogen-activated protein kinase (MAPK) pathways, allows the integration and propagation of signals efficiently from the plasma membrane to intracellular target organelles, such as the nucleus. Typically, this signalling cascade comprises MAPK, MAPK kinase (MAP2K) and MAP2K kinase (MAP3K). MAP2K is activated by MAP3K at the cell membrane and then it interacts with downstream MAPK phosphorylating it on two conserved threonine and tyrosine residues. Various phosphatase activities oppose these phosphorylation events resulting in tightly regulated signalling. The specific outcome of the overall process is determined by the temporal and spatial dynamics of downstream signalling components *(Kholodenko, 2006; Markevich et al., 2006).*

It can be easily argued that the neuron, being a highly polarized cell, spend a lot of energy and take advantage of several molecular systems, like trafficking of phosphorylated kinases within endocytic vesicles or non-vesicular signaling complexes with molecular motors *(Kholodenko, 2002; Perlson et al., 2005),* to assure signal propagation from periphery to the cellular body. This is particularly true for motor neurons, that in some cases (like the neurons in the sciatic nerve) have to connect district that can be very far from each other (axons of LMN can be 1 meter long in the human).

Taking into account the several mechanisms found to be implied in ALS pathogenesis, and already described in the previous paragraphs, it can be hypothesized that excitotoxic stimuli, factors released by glial cells (like cytokines), or defects in the delivery of trophic factors from muscles to the perikarion due to axonal transport impairment or energy failure, may perturb homeostasis of the motor neuronal cell, thus influencing the dynamic of intracellular signalling pathways. In recent years great attention has been

concentrated on pathways that may account for the selective vulnerability of motor neurons.

In particular, a motoneuron-specific cell death pathway downstream of the Fas death receptor, in which synthesis of nitric oxide (NO) is an obligate step has been described *(Raoul et al., 1999; Raoul et al., 2005a).* In cultured motoneurons exogenous NO triggers expression of Fas ligand (FasL). Interestingly in motoneurons from G93A and G85R mice this up-regulation results in activation of Fas, leading through Daxx to phosphorylation of p38MAPK and further NO synthesis. This Fas/NO feedback amplification loop is implicated in selective death of motor neurons in vitro. Consistent with these observations, G93A and G85R mice show increased accumulation of Daxx in nuclear bodies within motor neurons before disease onset. Moreover, FasL up-regulation is reduced in the presence of transgenic dominant-negative Daxx. It is possible that chronic low-level activation of the Fas/NO feedback loop may underlie the motoneuron loss that characterizes familial ALS and may help to explain its slowly progressive nature *(Raoul et al., 2006).*

Interestingly p38MAPK appears to be the converging key point of several pro-degenerative stimuli activated in ALS, including FasL and TNFα *(Bendotti et al., 2005).* Activated p38MAPK (phospho-p38) has been found in motor neurons of post mortem spinal cord samples of ALS patients. Colocalization of p38MAPK with phosphorylated neurofilaments inside neuronal cell bodies has been also described *(Ackerley et al., 2004).* Analyses performed on spinal cord from SOD1G93A overexpressing mice report an increase in both p38MAPK protein levels and phosphorylation status even at a presymptomatic stage. Phospho-p38 is mainly localized inside motor neurons and during disease progression it also appears in neurons with signs of degeneration (vacuolization and perikaryal accumulation of phosphorylated neurofilaments) and in reactive glial cells (hypertrophic astrocytes and mostly activated microglia) *(Tortarolo et al., 2003; Wengenack et al., 2004).* Moreover activation of p38 in both neuronal and glial

cells determines the transcription of several pro-degenerative genes: nitric-oxide synthase, IL-1, TNFα and TNFα receptors. This highlights an active role for p38MAPK in the pathways that trigger neuronal death, or, at least, in those processes that produce a pro-degenerative environment around neurons. Consistent with these observations, treatment of SOD1G93A mice with minocycline or TNFα inhibitors retarded neuronal death and extended life span *(Zhu et al., 2002; West et al., 2004)*. These effects have been linked to a reduction of p38MAPK activation, suggesting that p38MAPK may be considered a good target for the design of selective inhibitors of pro-degenerative pathways.

Although several lines of evidence highlight an induction of pro-degenerative pathways in motor neurons in ALS, the extent of activation of pro-survival and anti-apoptotic pathways, such as the PI3K/Akt, are also worthy of consideration. In the nervous system, PI3K is usually activated by binding of neurotrophic factors to the cognate receptors. Active PI3K produces phosphatidyl-inositol-3-phosphate (PIP3) that recruits Akt (a Ser/Thr kinase) to the cell membrane via a plextrin homology domain. Akt is then activated by phosphorylation by PDK1 and PDK2, detaches from the membrane and can remain in the cytosol or translocate to the nucleus, to exert anti-apoptotic activities. Studies on human post-mortem tissues have revealed that although PI3K was activated in homogenates from spinal cord of ALS patients, the levels of phospho-Akt were not altered. This suggests that there may be some obstacle in the transduction of signals from PI3K to Akt in the spinal cord of ALS affected individuals *(Wagey et al., 1998)*. Moreover analyses on late onset SOD1G93A mice show that the total levels of Akt are reduced at the onset of symptoms *(Warita et al., 2001)*.

Therefore, neuronal dysfunction and death in ALS may be determined not only by the activation of pro-degenerative processes, but also by an impaired activation of pro-survival pathways (**Figure 1.4**). Several neurotrophic factors are able to activate the Akt pathway. Indeed, viral mediated deliver of GDNF and IGF to spinal motor neurons in G93A mice, that produced amelioration of the

pathology and elongation of life span, have been linked to the activation of Akt in the nervous system *(Wang et al., 2002; Kaspar et al., 2003).*

Figure 1.4.

Dysregulation of pro-degenerative and anti-apoptotic pathways in motor neurons in ALS

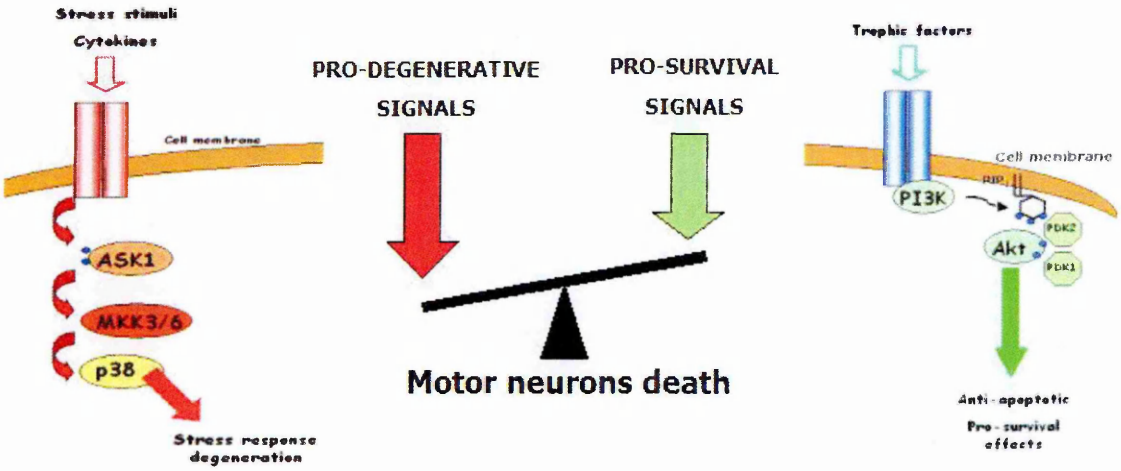

Several evidences point out the possibility that motor neuronal death may result from over-activation of pro-degenerative pathways, not counterbalanced by induction of anti-apoptotic molecules.

Since modulation of the p38MAPK and Akt pathways are the main aim of this thesis, further description of these pathways will be provided in the following sections.

1.4 THE p38-MAPK PATHWAY

Mitogen-activated protein kinase (MAPK) pathways are utilised by cells to respond to extracellular stimuli. MAPKs are members of discrete signalling cascades and serve as focal points which a variety of extracellular stimuli eventually converge on. Four distinct subgroups within the MAPK family have been described: 1) extracellular signal-regulated kinases (ERKs); 2) c-jun N-terminal kinases (JNKs), also called stress-activated protein kinases (SAPK); 3) ERK/big MAP kinase 1 (BMK1), and 4) the p38MAPK group of protein kinases.

1.4.1 Overview of p38 MAPK pathway

p38 MAPK was first isolated as a 38KDa protein that is rapidly tyrosine phosphorylated in response to LPS stimulation *(Han et al., 1994).* To date four isoforms of the p38 MAPK family have been identified: p38MAPK alpha, p38MAPK beta, p38MAPK gamma (or ERK6, SAPK3), and p38MAPK delta (or SAPK4). Each isoform shares about 60% identity within the p38MAPK group but only 40-45% to the members of other MAPK families *(Zarubin and Han, 2005).*

All p38MAPK kinases are characterised by a Thr-Gly-Tyr (TGY) dual phosphorylation motif. p38MAPK alpha and beta are ubiquitously expressed, while p38gamma is localized mainly in muscles and heart and p38MAPK delta is mainly in kidneys and lungs.

Structural features of p38MAPK

p38 MAPK is a proline-directed serine/threonine kinase. Crystal structure of p38MAPK alpha in the unphosphorylated, inactive, form has been resolved. The enzyme is characterized by two domains separated by a deep channel where potential substrates might bind. The N-terminal domain creates a pocket for binding of the adenine ring of ATP. The C-terminal domain contains the

presumed catalytic base, magnesium binding sites, and the phosphorylation lip, a 13 residues segment containing the Thr^{180}-Gly-Tyr^{182} motif *(Wilson et al., 1996).* Both Thr^{180} and Tyr^{182} are already exposed to solvent in p38MAPK structure; this suggests that these residues are readily accessible by the upstream activating kinases. Moreover it is believed that the sequence and structural variation of the lip among protein kinases could provide a specific recognition element for the upstream kinases in the cellular activation cascade. Also each MAP kinase is specific for the site that recognises the target proline-containing peptide substrate (P+1 site). The position of the P+1 site is known to be adjacent to the Lip, and the residues that form the P+1 pocket (Val^{183}-Arg^{189}) are all conserved among the MAPKs.

Interestingly, the domains of p38 MAPK are oriented so that the side chains of some key catalytic residues are misaligned, and a portion of the p38MAPK activation lip blocks the peptide substrate binding channel. The combination of these regulatory mechanisms ensures that the kinase activity of p38 MAPK is minimal before activation *(Wilson et al., 1996; Wang et al., 1997).*

Upstream activators of p38 MAPK pathway

p38MAPK proteins are considered stress-activated kinases, as they are reported to be activated mainly by UV light exposure, heat, osmotic shock and inflammatory cytokines. The pathway that leads to the final activation of p38 MAPK is a multistep cascade that involves several upstream kinases, each with a cell-type specific expression level and a tightly regulated activity.

The canonical activation of p38 MAPKs occurs via dual phosphorylation of their Tyr-Gly-Thr motif, in the activation loop, by two MAP kinase kinases (MKKs), MKK3 and MKK6. In some circumstances, such as ultraviolet radiation, MKK4, an upstream kinase of JNK, can aid in the activation of p38MAPK alpha and p38MAPK delta in specific cell types *(Jiang et al., 1997; Brancho et al., 2003).* A further upstream step of regulation is represented by the MKK kinases (MAP3K).

These include TAK1, ASK1 or MAPKKK5, MLKs, and some members of the MEKK family *(Ichijo et al., 1997; Kyriakis and Avruch, 2001; Gallo and Johnson, 2002; Cheung et al., 2003)*. MAP3K overexpression leads to activation of both p38 MAPK and JNK pathways *(Ogura and Kitamura, 1998; Zarubin and Han, 2005)* suggesting that the selective induction of p38MAPK, and other MAPK pathways, is dependent on the specific modulation of MKKs.

Interestingly low molecular weight GTP-binding proteins of the Rho family, such as Rac1 and Cdc42, are also involved in upstream activation of p38 MAPK. Rac1 binds to MEKK1 or MLK1 while Cdc42 can only bind to MLK1 and both result in activation of p38 MAPK via MAP3Ks *(Zhang et al., 1995; Tibbles et al., 1996)*. P21-activated kinases (PAKs) are another reported group of p38MAPK activators *(Bagrodia et al., 1995)*.

The major pathway for p38 MAPK regulation is via MKKK-MKK in mammalian cells although two other possible mechanisms of activating p38MAPK alpha have been described. In one case, MKK-independent activation is achieved by autophosphorylation of p38MAPK after its interaction with TAB1 (trasforming growth factor beta-activated protein kinase 1 (TAK1)-binding protein). This mechanism appears to be involved in activation of p38MAPK alpha in ischemic heart *(Li et al., 2005)* although the overall importance of this pathway in other cells/tissues is unknown and in fibroblasts and epithelial cells this is not involved *(Brancho et al., 2003)*. Other MKK-independent mechanisms of activation of p38 have been observed and in T cells stimulated through the T cell antigen receptor (TCR) phosphorylation of p38MAPK alpha on a non-canonical residue, Tyr323, has been reported *(Salvador et al., 2005)*.

Under physiological conditions, p38 MAPK activation occurs very rapidly, but is transient and dephosphorylation of the kinase plays an important role in the downregulation of MAPK pathway. This process is mediated by dual-specificity MAP kinase phosphatases (MKPs), or by PP2C (Ser/Thr phosphatase) and PTP (Tyr phosphatase) *(Takekawa et al., 1998; Keyse, 2000)*. p38MAPK alpha and

p38MAPK beta can be efficiently dephosphorylated, but to date p38MAPK gamma and p38MAPK delta appear to be resistant to all known MKP family members.

Figure 1.5. Signaling cascades leading to activation of the MAPKs.

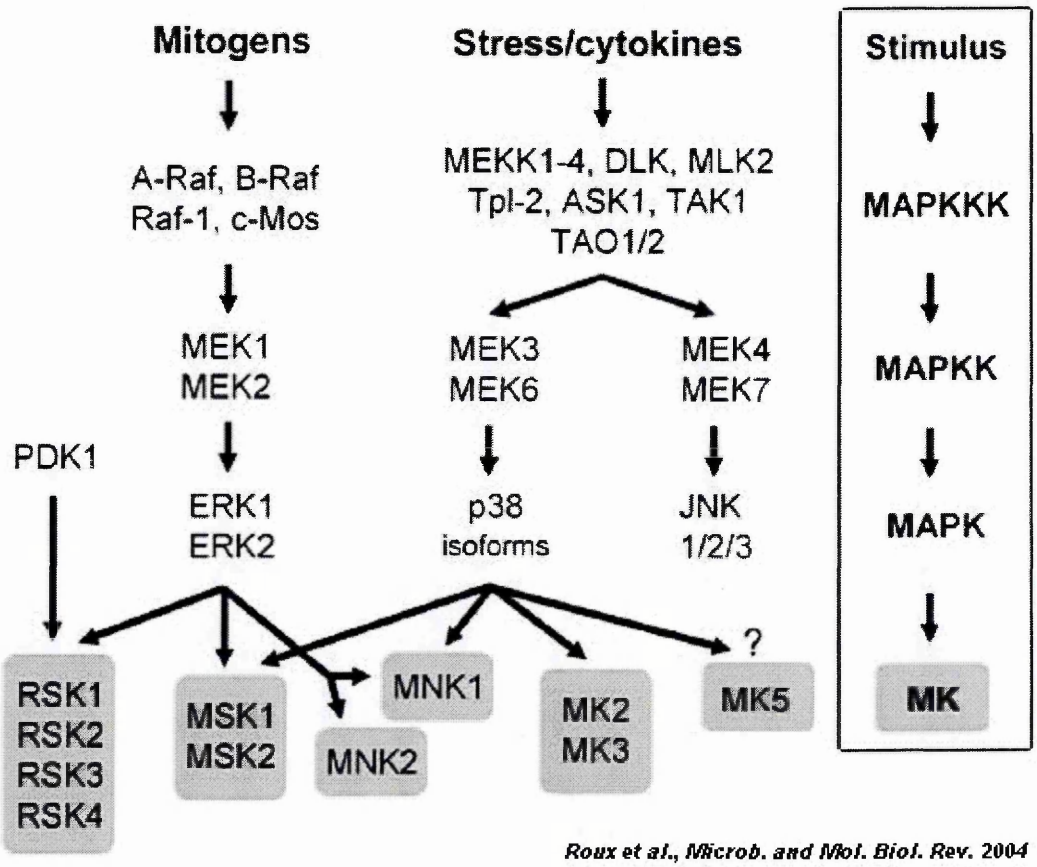

Downstream targets of p38MAPK pathway

p38MAPK has a huge variety of downstream targets, ranging from protein kinases, to other enzymes and transcription factors. Some p38MAPK alpha and beta physiological substrates are summarised in **Figure 1.6**. These are transcription factors, other protein kinases (such as MAPKAP-K2/3, or MNK1/2 or MSK1/2) that in turn phosphorylate trascription factors, cytoskeletal proteins, components of the translational machinery and other proteins such as metabolic enzymes, glycogen synthase or cytosolic phospholipase A2 *(Roux and Blenis, 2004)*. Na/H exchanger isoform-1 (NHE-1), Tau and Keratin 8, and stathmin

have also been reported as substrates for p38MAPK alpha *(Zarubin and Han, 2005)*.

Figure 1.6. Downstream targets of p38 MAPK.

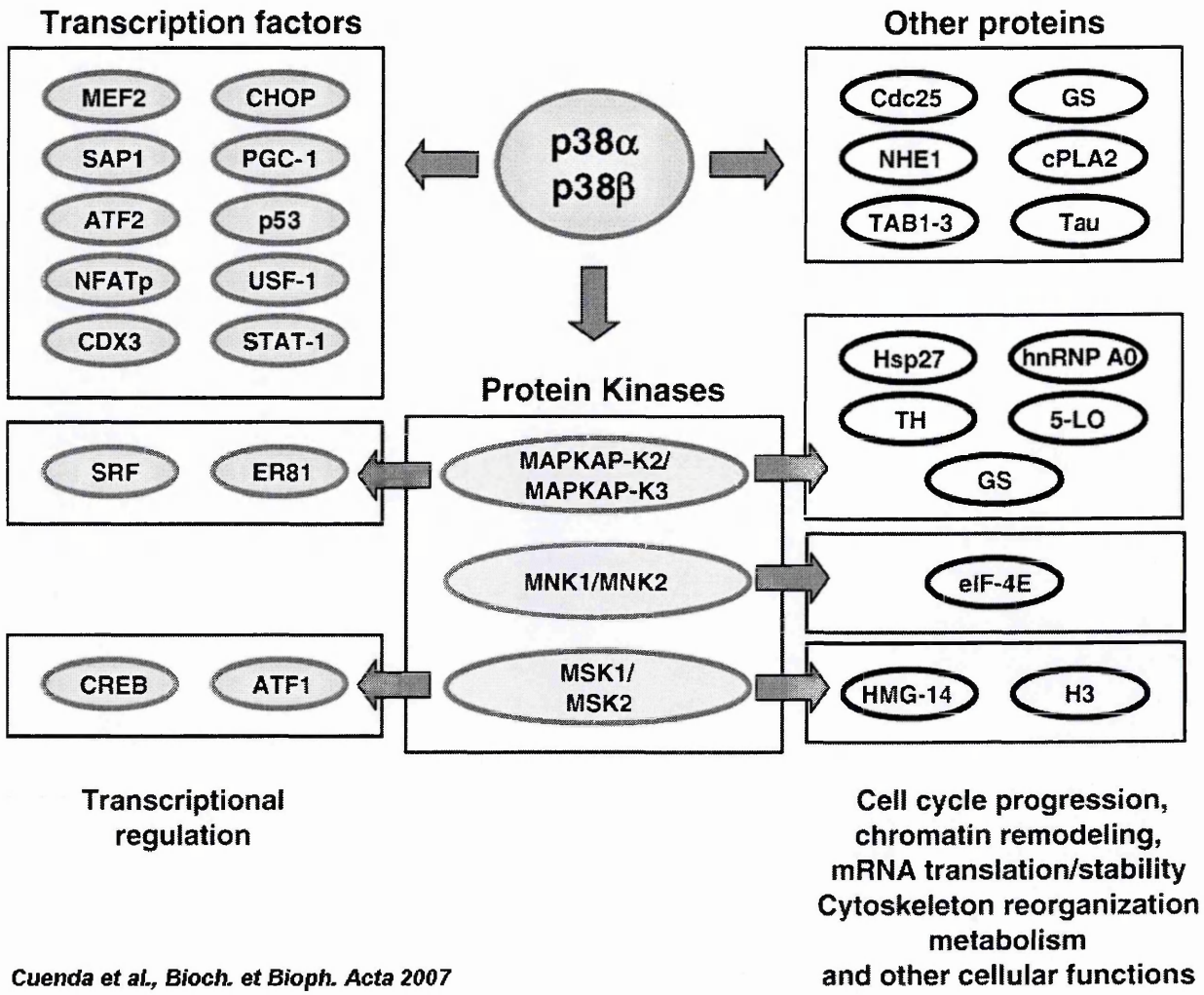

Potential substrates of p38 alpha and p38 beta MAPKs. CHOP, CCAAT/enhancer-binding protein-homologous protein; MEF, myocyte enhancing factor; PGC, peroxisome proliferators activated receptor γ coactivator; SAP, serum response factor accessory protein; HBP, high mobility group-box transcription factor; NFAT, nuclear factor of activated T-cells; ATF, activating transcription factor; MAPKAP-K, mitogen activated protein kinase activated protein kinase; MSK, mitogen and stress activated protein kinase; MNK, mitogen activated protein kinase-interacting protein; TAK, transforming growth factor-β-activated kinase.

1.4.2 Physiological roles of p38 MAPK pathway

p38 MAPK is strongly activated in response to many types of stress, like UV irradiation, osmotic and oxidative stress *(Han et al., 1994; Tibbles and Woodgett, 1999)*. It is also activated in response to proinflammatory cytokines and is involved in cytokine synthesis. Indeed, p38MAPK is centrally involved in IL-1beta and TNFα production in human monocytes following lipopolysaccharide treatment *(Lee et al., 1994a)*. Recent work in knock-in mice in which either p38MAPK alpha or p38MAPK beta kinase carry a mutation that provide resistance to the effects of specific inhibitors, has demonstrated that specific inhibition of p38MAPK alpha in vivo is sufficient and necessary for suppression of increased peripheral proinflammatory cytokine levels after lipopolysaccharide challenge *(O'Keefe et al., 2007)*. p38MAPK alpha is generally thought to be the major isoform involved in mediating cytokine production since mice lacking p38MAPK beta did not show deficits in cytokine production or in immune function *(Beardmore et al., 2005)*. No involvement in inflammation has been reported for the other two isoforms of p38MAPK.

An interesting mechanism of regulation of inflammatory mediators is exerted by p38 MAPK at a post-transcriptional level. In fact, several cytokines genes share an ARE (AU-rich element) in the 3'-untranslated region of their mRNA. The presence of this element is known to shorten the half-life of the mRNA and in some cases, such as for TNFα, blocks the translation. p38MAPK activation determines phosphorylation of specific ARE-binding proteins that aid in stabilizing the mRNA, thus enhancing its translation, and mice lacking the ARE of TNFα were incapable of p38-mediated TNFa translation after exposure to LPS *(Kontoyiannis et al., 1999)*.

In addition to immune-modulatory function, p38MAPK alpha has been proposed to regulate some cellular processes unrelated to the stress response, for example, the differentiation and/or survival of several cell types *(Morooka and Nishida,*

1998; Cuenda and Cohen, 1999; Zetser et al., 1999). Knockout mice for p38MAPK alpha have been generated; this leads to a lethal phenotype, mainly due to defects in placental organogenesis *(Adams et al., 2000).* In contrast, p38MAPK beta, p38MAPK gamma, p38MAPK delta and double p38MAPK gamma/delta knockout mice develop normally into adulthood, suggesting reduntant functions among these isoforms *(Beardmore et al., 2005; Kim et al., 2005; Sabio et al., 2005).* It appears that p38MAPK alpha is important for myogenesis, since myoblasts from mice lacking p38MAPK alpha, but not those lacking p38MAPK beta or p38MAPK delta, do not differentiate to multinucleated myotubes *(Perdiguero et al., 2007).* Given that p38MAPK gamma is highly expressed in skeletal muscle, and that endogenous p38MAPK gamma protein levels increase as myoblasts differentiate, it is not surprising that p38MAPK gamma also plays a key role in skeletal muscle differentiation. Indeed, over-expression of p38MAPK gamma in skeletal muscle cells leads to differentiation from myoblast to myotubes, and a dominant-negative mutant of p38MAPK gamma prevents this differentiation process *(Lechner et al., 1996).* A role for p38MAPK alpha in various aspects of cardiogenesis including the regulation of cardiomyocyte differentiation, apoptosis, and hypertrophy has also been suggested *(Wang et al., 1998; Mackay and Mochly-Rosen, 1999; Davidson and Morange, 2000).* Some reports have also suggested a role for p38MAPK delta in keratinocyte differentiation, or in induction of cell death upon exposure to hydrogen peroxide *(Eckert et al., 2003; Efimova et al., 2003).* Other processes in which p38 MAPKs have been implicated in either positive or inhibitory roles are: early stages of osteoclastogenesis from bone marrow precursors *(Huang et al., 2006),* adipogenesis *(Aouadi et al., 2006),* intestinal epithelial cells differentiation *(Houde et al., 2001)* cell proliferation (Maher, 1999), cytoskeletal reorganization *(Rousseau et al., 1997),* cell-cycle regulation *(Takenaka et al., 1998)* and neuronal plasticity *(Butler et al., 2004; Pickering et al., 2005).*

1.4.3 p38 MAPK pathway in physiology and pathology in the nervous system

p38MAPK alpha and p38MAPK beta are the two isoforms most abundant in the nervous system. They are highly expressed in most brain areas, including cerebral cortex, hippocampus, cerebellum and a few nuclei of the brainstem *(Lee et al., 2000)*. In the spinal cord, p38MAPK alpha is found in most neurons, whereas p38MAPK beta is localized in microglial cells throughout the spinal cord parenchyma and in ventral horn motor neurons *(Svensson et al., 2005)*. At the subcellular level p38MAPK alpha is localised in dendrites and in cytoplasmic and nuclear regions of neuronal soma, while p38MAPK beta is concentrated in the nucleus of neurons, suggesting that the two isoforms may play different physiological functions in the CNS.

In the nervous system, in vitro studies have implicated the p38 MAPK pathway in neuronal cell fate decision, in migration during development, and in the control of synaptic function and excitability. For example, p38 MAPK signaling has been found to participate in NGF-induced neuronal differentiation of PC12 cells and selective inhibition of p38 MAPK results in defective NGF-induced neurite outgrowth in this model. Moreover constitutive activation of ASK1, or expression of a dominant negative form of TAK1, both upstream activators of p38 MAPK, leads to induction or inhibition of neurite outgrowth in PC12 cells respectively *(Takeda et al., 2000; Yanagisawa et al., 2001)*. In addition in MN9D dopaminergic neuronal cells expression of calbindin-D28K, a member of the calmodulin superfamily of calcium binding proteins, induces neurite outgrowth in a p38-dependent manner *(Choi et al., 2001)*.

p38 MAPK has been shown to regulate cytoskeletal reorganization in neuronal cells, during development of CNS. This role is mediated primarily by phosphorylation of Hsp27 and Rac GTPase *(Rousseau et al., 1997)*. p38MAPK also participates in the induction of metabotropic glutamate receptor (mGluR)-dependent long term depression (LTD) at excitatory synapses between CA3 and

CA1 pyramidal neurons in the hippocampus *(Bolshakov et al., 2000).* Neuronal function is also regulated by p38 MAPK through the modulation of recycling of AMPA subtype glutamate receptors (AMPARs) which are internalized in response to various extracellular stimuli and are recycled back to the plasma membrane or targeted to the degradative pathway. This trafficking is thought to play a critical role in synaptic plasticity *(Carroll et al., 2001).* The small GTPase Rab5 is involved in this early endocytic trafficking of AMPARs. Interestingly, p38 MAPK has been identified as activator of guanyl-nucleotide dissociation inhibitor (GDI), a protein involved in relocalization of Rab5 to the appropriate target membrane. The p38MAPK induced formation of GDI:Rab5 complex has been found to accelerate endocytosis *(Cavalli et al., 2001).*

Several studies have shown that the p38MAPK pathway may exert opposite effects on cell survival/death decision, depending on the stress-status of the cell. Neuronal activity may control the p38MAPK pathway to mediate cell survival. For example, the p38MAPK pathway activates the MEF2 transcription factor in response to physiological calcium influx in cerebellar granule cells, and activated MEF2 regulates neuronal survival *(Mao et al., 1999; Okamoto et al., 2000).* On the other hand, under pathophysiological conditions the p38MAPK pathway may be induced through activation of ASK1 to mediate neuronal degeneration *(Matsuzawa and Ichijo, 2001).*

Aberrant activation of the p38 MAPK pathway has been linked to several neurodegenerative diseases, such as stroke, Alzheimer's disease (AD) and Amyotrophic Lateral Sclerosis.

Acute neuronal injuries, such as trauma or ischemia, are characterized by activation of microglial cells and the release of pro-inflammatory cytokines, that ultimately contribute to the degenerative process observed in neurons in the affected area. The p38 MAPK pathway is involved in this process, as demonstrated by the fact that p38 MAPK inhibitors are protective in animal models of ischemia and reperfusion injury *(Piao et al., 2003; Melani et al., 2006;*

Bu et al., 2007). It has also been proposed that the p38MAPK pathway is involved in the release of pro-inflammatory cytokines from aberrantly activated microglia in AD brains. In this case, microglial activation seems to be triggered by deposition of amyloid beta peptide, a hallmark of the disease *(Culbert et al., 2006).* Another pathological hallmark of AD and other disorders called "tauopathies" is the accumulation of neurofilaments composed of the microtubule-associated protein Tau. Hyperphosphorylation of Tau is one of the mechanisms leading to its aberrant accumulation in neurons, and p38 MAPK is one of the kinases thought to be involved in this process *(Ferrer et al., 2005).*

Among the different proteins found altered in the degenerative process in ALS, p38 MAPK has acquired increasing importance. Activated p38 MAPK has been found in degenerating motor neurons and reactive astrocytes of post mortem spinal cord samples of ALS patients: the intracellular immunostaining appears in some neurons as filamentous skein-like and ball-like inclusions, with an immunohistochemical pattern identical to that of ubiquitin *(Bendotti et al., 2004).* Another study found overlapping labelling of abnormally phosphorylated neurofilaments and p38 MAPK alpha in the motor neurons of ALS patients, and provided evidence that the alpha isoform may be particularly relevant for the formation of perikarial aggregates in affected motor neurons *(Ackerley et al., 2004).* Interestingly, p38 MAPK protein levels and phosphorylation has been reported as enhanced in spinal cord homogenates from SOD1G93A overexpressing mice even at a presymptomatic stage. Phospho-p38 immunostaining is mainly localized in motor neurons with phosphorylated neurofilaments and vacuolized perikaria and neurites. During disease progression, active p38 MAPK also accumulates in reactive glial cells (hypertrophic astrocytes and mostly activated microglia) *(Tortarolo et al., 2003; Wengenack et al., 2004).* Activation of p38 MAPK has been confirmed in cortical neurons of SOD1G93A animals, thus strengthening the hypothesis that this pathway may play a role in the degeneration of both upper and lower motor

neurons *(Holasek et al., 2005)*. In a recent report activation of the p38 MAPK pathway in spinal motor neurons of SOD1G93A mice was associated with selective upregulation of TNFα receptors *(Veglianese et al., 2006)*, moreover Fas-signalling pathway was found to converge on p38 MAPK activation selectively in motor neurons in SOD1G93A mice *(Raoul et al., 2002; Raoul et al., 2006)*. These data suggest that the p38 MAPK pathway may increase the susceptibility of motor neurons to inflammatory cytokines released by surrounding glial cells. In summary, this pathway may represent a key factor in the degeneration of motor neurons in ALS, and may therefore be considered as a good target for therapeutic intervention. Indeed, treatment of SOD1 mutant mice with anti-inflammatory molecules, such as minocycline, nordihydroguaiaretic acid, thalidomide and its analog lenalidomide, or Fas siRNAs and Semapimod, provide neuronal protection and extend life span *(Zhu et al., 2002; West et al., 2004; Kiaei et al., 2006; Dewil et al., 2007a; Locatelli et al., 2007)*. For treatment with minocycline, Fas siRNAs and Semapimod a reduction in p38 MAPK activation has been reported. Moreover it has been recently demonstrated in vitro that riluzole, the only drug approved for treatment of ALS, is protective against glutamate induced changes to neurofilament phosphorylation and transport, through inhibition of p38 MAPK and ERK *(Stevenson et al., 2009)*.

1.4.4 Strategies for targeting p38MAPK

Aberrant production of inflammatory cytokines, and subsequent activation of the p38 MAPK pathway, has been linked with several inflammatory disorders, including chronic pathologies such as rheumatoid arthritis and Chron's disease, or acute injuries such as heart failure, ischaemic retinopathies and the development of insulin resistance in diabetes *(Cuenda and Rousseau, 2007)*. Because of this, commercial drug discovery programs have focussed considerable effort designing small inhibitory molecules targeting the p38 MAPK pathway. Generally the lead compounds target p38 MAPK directly, although a lack of

selectivity for a specific isoform is often reported. Moreover, many molecules appear to interact with other unrelated kinases, thereby causing adverse effects. Nevertheless some of these drugs have reached clinical application, mainly for treatment of reumatoid arthritis or Chron's disease (**Table 1.7**).

Alternative approaches for targeting p38 MAPK have been developed in the last few years, although these have been only utilised in basic research and have not yet been tested in a clinical setting. For example, RNAi represents an intriguing strategy for targetting p38 MAPK . Through the accurate design of siRNAs it is possible to selectively downregulate p38 MAPK at the mRNA level, thus reducing the risk of non-specific effects *(Hirose et al., 2003; Gao et al., 2004)* and providing the opportunity to better dissect the role played by each p38 MAPK isoform in the pathologic process. As an alternative approach, dominant negative mutants of p38 MAPK or its upstream regulatory kinases (such as ASK1) have been generated. Usually these mutants are kinase-dead enzymes, which can be phosphorylated (activated) but are not able to catalyze the phosphorylation of their downstream targets. This strategy has been effectively used to dissect the role played by specific kinases *in vitro (Muthumani et al., 2005).* These strategies have been used to study the neurodegenerative process in ALS and have provided strong evidence for a central role of p38 MAPK and the upstream kinase ASK1 *(Raoul et al., 2002; Raoul et al., 2006; Nishitoh et al., 2008).*

The design and use of small molecule inhibitors will be described in more detail as some of these compounds have reached clinical application for peripheral inflammatory disorders although to date there are no reports of p38 MAPK inhibitors in clinical trials for neurodegeneration.

Pharmacological inhibition of the p38 MAPK pathway

Most of the available molecules targeting p38 MAPK have been designed for use in inflammatory disorders, since p38 MAPK has been considered as a key player

in the over-production of proinflammatory cytokines in these diseases. Some of these drugs have also been proposed as possible treatments for neurodegenerative diseases, although bioavailability particularly in relation to penetration of the blood-brain-barrier is a challenge.

Pyridinil imidazoles

4-pyridinylimidazoles represent the main pharmacophore for p38 MAPK inhibitors. The lead structure is the imidazothiazole SK&F 86002, originally conceived as an hybrid structure from the antiinflammatory imidazole derivative tiflamizole and the bicyclic immunomodulator levamisole. This compound displayed a specific and unexpected mechanism of action, since it was a weak inhibitor of the metabolism of arachidonic acid, but exerted an antiinflammatory effect through inhibition of IL-1 and TNFα production. Later p38 MAPK was discovered as the target of this compound *(Lee et al., 1988; Lee et al., 1993)*. The pyridinil imidazoles bind competitively at the ATP binding site of p38 MAPK. However, unlike ATP, these inhibitors bind with similar affinity to both the phosphorylated and unphosphorylated form of the enzyme. The Thr^{106} residue of p38 MAPK appears to be the determinant for the potency and selectivity of these compounds versus other kinases. In fact pyridinyl imidazoles display similar affinities for isoforms p38MAPK alpha and p38MAPK beta, carrying a Thr in this position, but are not effective towards p38MAPK gamma and p38MAPK delta, displaying a bulkier Met residue, or ERK2, displaying a Gln *(Bolos, 2005)*.

Subsequent modifications of the structure of SK&F 86002 led to the 2,4,5-triaryl-imidazoles, more potent and selective compounds *(Bolos, 2005)*. Within this group, SB 203580 displayed good oral efficacy for several models of cytokine inhibition and inflammatory diseases and became the prototypical standard for other p38 MAPK inhibitors *(Badger et al., 1996)*. The main drawback of these compounds was their interaction with cytochrome P-450 isoenzymes, a mechanism that led to hepatotoxicity and potential carcinogenicity in pre-clinical

trials *(Howard et al., 1991; Adams et al., 1998).* Structural modifications have subsequently been introduced with the aim of reducing this side effect: the morpholinopropyl derivative SB 210313 represents an example, with potent in vivo oral activity and reduced interaction with most cytochrome P-450 isoenzymes *(Boehm et al., 1996).*

Pyrimidinil imidazoles

Based on the fact that pyrimidine is a weaker cP-450 inhibitor compared to pyridine, and that it still maintains the ability to interact with p38 MAPK, new imidazoles derivatives have been generated with pyrimidine substitution. SB 242235 and SB 239063 are two examples; SB 242235 has entered phase I clinical trials *(Bolos, 2005).*

Other classes of p38MAPK inhibitors

Although the imidazole ring plays a structural role in keeping the correct conformation for interaction with the active site of the enzyme, its substitution with heterocyclic scaffolds has been shown to maintain similar electronic and spatial features. Interestingly, these non-imidazole pyridinyl heterocycle derivatives, like pyridinyl oxazole, are orally active potent inhibitors of p38 MAPK devoid of inhibition of cP-450. A different structural class is constituted by molecules with a pyrimidopyridazinone nucleus and other related bicyclic analogues. VX 745 is representative compound of this family; it was the first inhibitor of p38 MAPK to undergo clinical trials in patients with rheumathoid arthritis. However safety concerns about some adverse neurologic effects observed in dogs in long term toxicological studies led to the discontinuation of its use *(Bolos, 2005).* This nervous system toxicity was related to extensive penetration across the blood-brain-barrier, which has been attributed to the high lipophilicity of VX 745. Another class of p38 MAPK inhibitors is represented by N,N'-diaryl ureas. These molecules exhibit a unique mode of binding to the

enzyme: they interact with a site near to the ATP pocket but distinct from it. The diaryl ureas represent allosteric inhibitors, since their binding determines a modification of the enzyme conformation, inducing structural hindrance at the ATP binding site. This mechanism of action accounts for much slower binding and dissociation rates as compared to imidazoles derivatives *(Bolos, 2005)*.

In contrast to VX 745, compounds belonging to the other inhibitor classes are not blood-brain-barrier permeable. This represents a severe limitation for the application of p38 inhibitors in neurodegenerative disorders.

Recently CNI-1493, a tetravalent guanylhydrazone called Semapimod, has attracted considerable interest for the treatment of neurodegenerative disorders due to its ability to cross the BBB after i.p. delivery. This compound has been used since 1995 for its antiinflammatory properties *(Bianchi et al., 1995)*, with quite encouraging results for the treatment of Crohn's disease. The effect seems to be mediated by inhibition of both p38 and JNK MAPKs *(Hommes et al., 2002)*. In the last few years Semapimod has also been used in models of neurodegenerative disorders, such as AD and ALS. In an animal model of AD, treatment with semapimod produced a significant reduction of Abeta deposition, plaque formation and cognitive deterioration *(Bacher et al., 2008)*. In the SOD1G93A mouse model of ALS, this compound resulted in downregulation of p38 MAPK pathway and substantial protection of motor neurons in the spinal cord, but did not modify disease progression in a significant way, although did cause a slight extension of life span *(Dewil et al., 2007a)*. In fact , JNK and p38 MAPKs are not direct targets of Semapimod. A detailed *in vitro* study has determined that the molecular target of this compound is c-Raf, an upstream kinase canonically involved in the activation of the ERK pathway. It was shown that Semapimod, through inhibition of c-Raf isoform, was able to reduce activation of ERK, JNK and p38 MAPKs in cytokine-stimulated macrophages, but not in T cells *(Lowenberg et al., 2005)*. Therefore, it is likely that Semapimod

may rather represent a good candidate for treatment of disorders in which c-Raf mediated inflammatory response is involved.

Table.1.7

Features of the most commonly used p38 pharmacologic inhibitors

	Structural class	Mechanism of action	Compound	Target	Interaction with P-450 enzymes	BBB perm.
1	**Pyridinyl imidazole**	ATP competitive inhibitor	SK&F 86002 SB203580 SB210313 SB235699* RWJ-67657*	P38a/b (+) P38a/b (++) P38a/b (++) P38a/b (+++) P38a/b (+++)	++++ +++ ++ + +	No No No No No
2	**Pyrimidinyl imidazole**	Same as class 1	RPR203494 RPR238677 SB220025 SB242235* SB239063	P38a/b (+++) P38a/b (+++) P38a/b (+++) P38a/b (+++) P38a/b (+++)	+/- +/- +/- +/- +/-	No No No No No
3	**Non-imidazole pyridinyl heterocycle**	Same as class 1	Pyridinyl-oxazole L167307 RWJ68354*	P38a/b (+++) P38a/b (+++) P38a/b (+++)	- - -	No No No
4	**Pyrimidopyridazinone**	ND	VX 745*	P38a/b (+++)	ND	Yes
5	**N,N'-diaryl urea**	ATP allosteric inhibitor	BIRB 796** (doramapimod)	P38a/b (++++)	ND	ND
6	**Dyaril ketone**	Same as class 1	RO 320 1195*	P38a/b (+++)	ND	ND
7	**Aromatic carboxamide**	Same as class 1	SCIO 323* SCIO 469*	P38a/b (+++) P38a (++++)	ND ND	ND
8	**Guanylhydrazone**	c-Raf inhibitor	CNI-1493* (semapimod)	P38a/b (+++)	ND	Yes

ND=not described; *=early phases of clinical trials; **=phase III in clinical trials *(Sitaraman et al., 2003; Bolos, 2005).*

1.5 THE PI3K/AKT PATHWAY

Phosphoinositide 3-kinase (PI3K) and Akt, also called protein kinase B (PKB) are key players in the transduction of signals from membrane receptors to intracellular and nuclear targets. The PI3K-dependent Akt signalling pathway is of great importance since it participates in a myriad of cellular processes, such as cell growth, differentiation, motility, insulin action and cell survival. Understanding the complex mechanism of regulation of these kinases is an essential step in defining a strategy for the manipulation of this pathway in disease.

1.5.1 Overview of the PI3K/AKT pathway

PI3K comprises a family of agonist-stimulated lipid signaling enzymes that are activated by growth factor receptors through binding of their regulatory subunit to phosphotyrosine residues in the receptor. Upon activation the catalytic subunit of PI3K phosphorylates Phospho-Inositides (PI) at the 3-position of the inositol ring to generate Phosphatidyl-Inositol-3-phosphate (PI3P), $PI(3,4)P_2$, and $PI(3,4,5)P_3$.

Akt possesses a plextrin homology (PH) domain in its structure that allows interaction with PIP_3, thus mediating the membrane translocation of Akt. The interaction of Akt with PIP_3 does not directly activate Akt but is thought to induce a conformational change in the kinase that facilitates its phosphorylation on Thr^{308} and Ser^{473} by the upstream kinases phosphoinositide-dependent kinase 1 and 2 (PDK1 and PDK2). Once activated, Akt then dissociates from the plasma membrane and phosphorylates many substrates in the cytoplasm and the nucleus, leading to activation of the appropriate physiological response (**Figure 1.7**) *(Toker, 2000; Rodgers and Theibert, 2002).*

Figure 1.7. Overview of PI3K/Akt pathway.

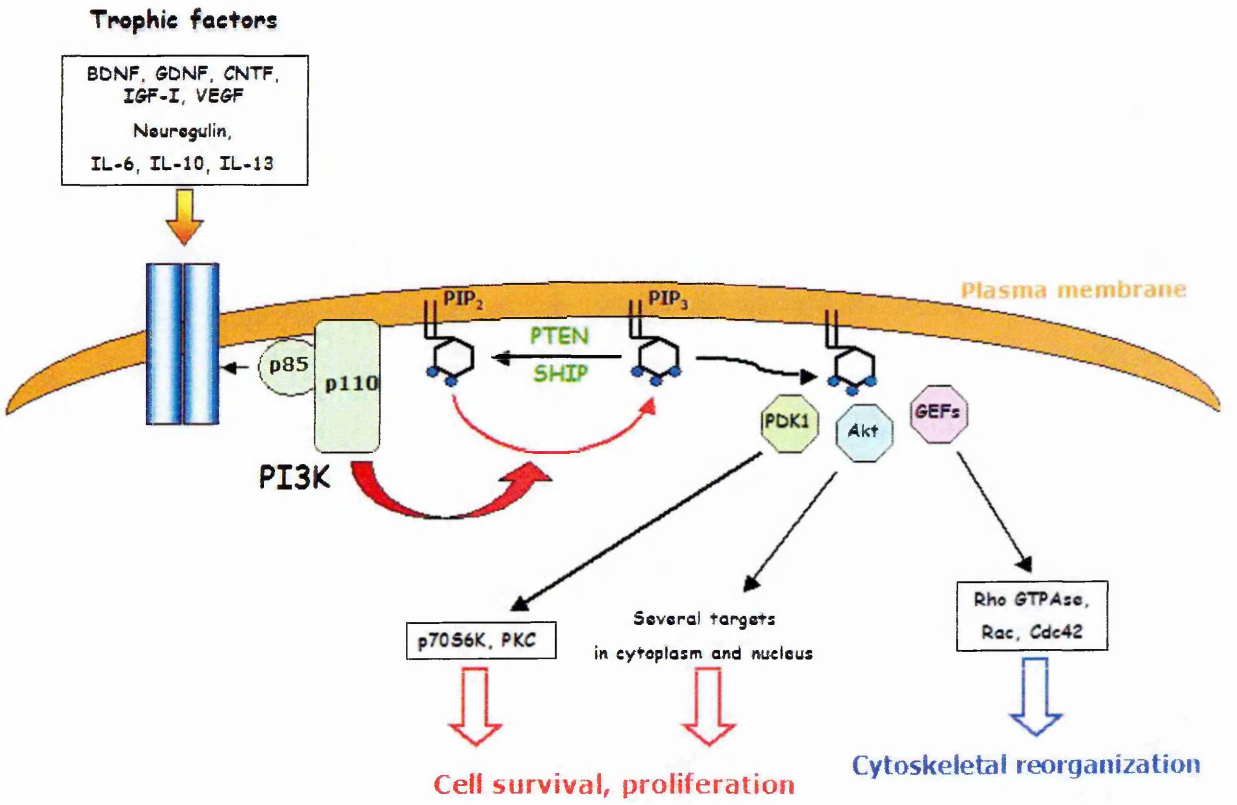

Adapted from Rodgers et al., Int.J.Devl.Neurosc. 2002

Features of PI3Ks

Several isoforms of these kinases have been described. They have been grouped under three classes, according to their specificity of function and their preferential substrates.

Class I

This class comprises kinases that preferentially phosphorylate PIP2, thus generating PIP3 as the final product. These proteins are composed of a catalytic subunit and a regulatory adapter subunit. This class of enzymes has been implicated in a wide range of cellular responses, including cell cycle progression, growth, survival, motility and adhesion.

Class II

PI3Ks that use PI or PIP as substrates, thus producing PIP or PIP2, respectively. These enzymes share homology with the class I catalytic domain, but are larger proteins that also contain structural domains involved in calcium/lipid interactions.

Class III

This class comprises enzymes that only phosphorylate PI, thus producing PIP as final product.

Enzymes of class II and III are believed to be required mainly for vescicular trafficking. It has also been hypothesized that PI3Ks class III are involved in induction of autophagy-mediated neuronal death *(Petiot et al., 2000)*. Therefore, it is likely that the balance between PI3K class I activity and PI3K class III may represent another mechanism of modulation of cellular homeostasis.

Class I PI3Ks will be described in more detail, since they are the most studied, and appear to be the class of proteins mainly involved in survival pathways in the CNS. Studies conducted *in vitro* on cell lines and primary neuronal cultures have identified a wide range of factors that activate PI3K in neurons, such as NGF, BDNF, IGF-1, GDNF, Fractalchine and neurotransmitters. In astrocytes, PI3K is instead activated by Neuregulins, members of the family of GDNF and IGF-I, and cytokines such as IL-10, and neurotransmitters *(Rodgers and Theibert, 2002)*.

Regulation of PI3K

The enzyme is composed of a catalytic subunit (p110) and a regulatory subunit (p85). Four isoforms of p110 have been identified: alpha, beta, gamma and delta,

and three different genes code for the regulatory subunit: p85alpha, p85beta, and p55gamma. The p85alpha gene can be alternatively spliced to produce p50alpha and p55alpha. All of the regulatory and catalytic subunits are expressed in the nervous system. The regulatory subunit binds to the catalytic subunit and mediates the interaction with upstream signaling proteins. Isoform diversity seems to modulate the specificity of PI3K-mediated responses through differential subcellular localization, variable kinetics of activation and recruitment of specific receptor signaling pathways.

Mechanisms of activation of PI3K

Three main strategies of activation have been described. These systems overall take advantage of protein-protein interactions to determine translocation of PI3K to the plasma membrane, where PI3K functions by phosphorylating its PI substrates.

Activation through membrane receptor-tyrosine kinases (RTK)

Extracellular neurotrophic factors interact with specific RTKs. Upon binding, the intracytoplasmatic domain of the RTK undergoes phosphorylation of specific Tyr residues. In some cases these residues are recognised by the regulatory subunit p85, through interaction with two SH2 (src-homology 2) domains. Alternatively, several adaptor proteins (Shc, Grb-2, Gab-1, IRS1/2) can be recruited to the phosphorylated domains of the RTK. These adaptors then recruit PI3K through interaction with SH2 domains of the regulatory subunit. In motor neurons growth-factor dependent activation of PI3K can also be mediated by calmodulin, a protein involved in calcium homeostasis *(Soler et al., 1998).*

Activation through non-receptor tyrosine kinases

Some cytoplasmic kinases, such as JAK (Janus Kinases), Syk, Src and ZAP70, have been reported to mediate the activation of PI3K, through recruitment to membrane associated receptors .

Activation through G-protein coupled receptors (GPCRs) and ionotropic receptors

GPCRs have been shown to recruit PI3K to the plasma membrane, through interaction of the catalytic subunit p110 with the beta-gamma subunit of the G proteins. Moreover ionotropic receptors also appear to be able to interact with p85 regulatory subunit, thus recruiting PI3K to the plasma membrane *(Rodgers and Theibert, 2002).*

Activation of PI3K leads to production of PIPs. These molecules diffuse within the lipid bilayer of the plasma membrane, thus propagating the original extracellular signal. From this point of view they are considered "second messengers". The signal is then transduced to intracellular targets by PDK-1 and PDK-2 (phosphoinositide-dependent-kinase-1 and 2). These enzymes, as well as the downstream target proteins, interact with the membrane-bound PIPs, thus becoming closely associated. In this way PDK can phosphorylate and activate the downstream proteins, such as Akt.

Modulation of the PI3K pathway can also be mediated through the phosphatase PTEN, that dephosphorylates PIP2 and PIP3, or by SHIP, that excusively dephosphorylates PIP3. It has been also proposed that PDKs can be phosphorylated and inactivated by intracellular enzymes *(Toker, 2000; Toker and Newton, 2000a).*

As shown in **Figure 1.7**, among the several targets of PI3K and PDKs:

- Akt/PKB is mainly involved in cellular survival
- PKC plays a central role for cellular growth
- Rho, Rac and Cdc42 are proteins that coordinate cytoskeletal reorganization
- P70S6K is involved in the stabilization of ribosomal complexes, thus influencing synthesis of novel proteins *(Rodgers and Theibert, 2002).*

Features of Akt

Akt, also termed PKB or RAC, is a serine/threonine kinase belonging to the "AGC kinase" superfamily. This group of kinases share similarity within their catalytic domain structure and in their mechanism of activation. Akt was first identified in 1991 by three groups, independently: one group cloned the cellular homologue of the v-akt oncogene from a transforming retrovirus (AKT8), and called this protein c-Akt; in two other studies, the authors cloned the cDNA of a new protein while searching for novel members of the protein kinase C (PKC) and protein kinase A (PKA) superfamily as possible participants in signal transduction cascades. Accordingly, the novel kinase was called RAC (related to A and C kinases) or PKB (protein kinase B) *(Bellacosa et al., 1991; Coffer and Woodgett, 1991; Jones et al., 1991).*

In mammals, there are three isoforms of Akt; they share a high degree of aminoacid identity, but are expressed in different tissues

Akt1/PKBalpha:	predominant isoform; ubiquitous expression
Akt2/PKBbeta:	expressed at high levels in insulin-responsive tissues (skeletal muscles, heart, liver, kidney, adipose)
Akt3/PKBgamma:	highly expressed in the central nervous system and testis

These isoforms are composed of three functionally distinct relevant regions (**Figure 1.8**):

- A PH (Pleckstrin homology) N-terminal domain.

  This region is responsible for interaction with membrane-bound phoosphoinositides.

- A catalytic core.

  This domain contains the serine/threonine kinase activity of the enzyme. Thr^{308}, within this region, is target of phosphorylation, and represents a regulatory site.

- A C-terminal region containing a hydrophobic motif (HM).

  HM is a regulatory domain involved in interaction with other proteins that modulate Akt activity. Moreover, HM contains Ser^{473}, target of phosphorylation, that represents an additional regulatory site.

Figure 1.8. Structural features of the three Akt isoforms.

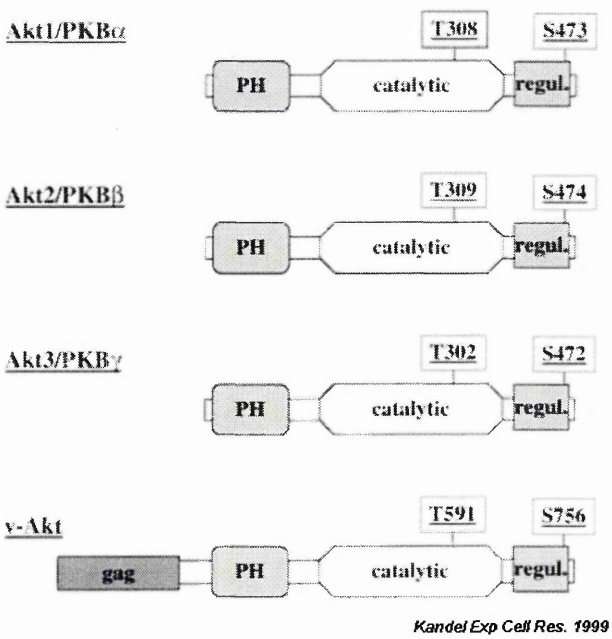

Structural organization of the three major Akt isoforms is shown in comparison to virally encoded v-Akt. v-Akt is an in-frame fusion of Akt-1 with a portion of retroviral group-specific antigen (gag). Amino acid positions are shown for mouse proteins. Threonine and serine residues whose phosphorylation is important for regulation of enzymatic activity are indicated.

Mechanism of activation of Akt

Akt is activated by, and dependent on, multisite phosphorylation. In fact Akt usually resides in the cytoplasm in an inactive state. Activation occurs only when both the Thr^{308} and Ser^{473} sites within Akt are phosphorylated.

Akt is mantained in inactive form in the cytosol, through conformational modifications induced by the PH and HM domains: the PH domain occupies the catalytic domain, thus preventing Thr^{308} phosphorylation by PDK-1; HM interacts with an hydrophobic groove in the N-terminal domain of Akt, thus stabilizing the inactive conformation. Upon receptor binding by extracellular signaling molecules, PI3K is recruited to the membrane and second messengers PIP3 and PIP2 are produced. The PH domain of Akt can interact specifically with phosphates in position D3 and D4 (but not D5) of the inositol ring, when PIP2 and/or PIP3 are produced thus the PH domain of Akt recognizes membrane-bound phosphoinosites inducing translocation of the protein from cytosol to the plasma membrane. The same happens for PDK-1, that also contains a PH domain in its structure. In this way Akt and PDK-1 are brought into close contact on a lipid-micelle surface. Phosphorylation of Ser^{473} occurs first although the mechanism leading to phosphorylation of Ser^{473} is still not completely understood. Some studies have hypothesized that interaction of the PH domain with membrane-bound phosphoinositides induces a conformational change allowing autophosphorylation of Ser^{473} *(Toker and Newton, 2000b).* It has also been reported that phosphorylation may be catalysed by other kinases, including the integrin-linked kinase (ILK), DNA-dependent protein kinase and the target of Rapamycin complex 2 (TORC2) *(Persad et al., 2001; Feng et al., 2004; Sarbassov et al., 2005).* What is clear is that Ser^{473} phosphorylation induces a conformational change in the HM domain, thus allowing interaction of HM with a pocket in PDK-1. This interaction brings PDK-1 into close proximity to Thr^{308} of Akt thus enhancing PDK-1 dependent phosphorylation of Thr^{308}. This modification causes a charge-induced change in conformation allowing binding of

ATP, and complete activation of Akt *(Scheid and Woodgett, 2003)*. The total amount of negative charges due to the phosphate on Thr^{308} and the three phosphates from the ATP could compensate the four phosphates of the PIP3 head group, and thus trigger the detachment of the PH domain, and Akt, from the membrane. In this stable form, Akt can target substrates located in the cytoplasm and then in the nucleus (**Figure 1.9**) *(Calleja et al., 2009)*. A PI3K-independent activation of Akt has also been described: PKA agonists can induce an increase of intracellular calcium levels, determining activation of CaMKK (calcium/calmodulin dependent kinase kinase). This enzyme is then able to phosphorylate Akt at Thr^{308} in a PDK-1 independent manner *(Datta et al., 1999; Toker, 2000)*.

FRET analysis has shown that upon stimulation a wave of Akt phosphorylation starts from the plasma membrane, then propagates to the cytoplasm and finally to the nucleus. Moreover, there is a turnover of Akt activation whereby new molecules of inactive Akt translocate to the plasma membrane to be activated, whereas previously activated molecules detach, and eventually become dephosphorylated. This movement of protein continues as long as 3-phosphoinositides are being generated *(Kunkel et al., 2005)*.

Mechanism of deactivation of Akt

Negative modulation of Akt is achieved through okadaic acid-sensitive phosphatases, such as PP2A. These enzymes de-phosphorylate Ser^{473} and Thr^{308} thus returning Akt to the inactive state. More recently, a family of okadaic acid-insensitive phosphatases, PHLLP, have been found to promote de-phosphorylation of Ser^{473} *(Gao et al., 2005)*. An additional mechanism of regulation by phosphorylation of Tyr^{474} has also been proposed. It has been hypothesized that phospho-Tyr^{474} blocks the action of the putative Ser^{473}-directed kinase, or it may prevent HM from packaging into the PIF-pocket, thus increasing its susceptibility to the action of phosphatases *(Conus et al., 2002)*.

In addition to dephosphorylation, deactivation of Akt may also be achieved through cleavage and in a cellular model of oxidative-stress-induced apoptosis Akt has been shown to be cleaved and inactivated by caspase 3 *(Luo et al., 2003)*. In contrast, Heat Shock Proteins seem to play a central role for the maintenance of Akt activation. Indeed it has been reported that Hsp90 and Hsp25 can interact with Akt, and stabilize the phosphorylated (activated) form, thus increasing duration of the enzymatic activity *(Murashov et al., 2001; Newton, 2003)*.

Figure 1.9. Akt activation pathway.

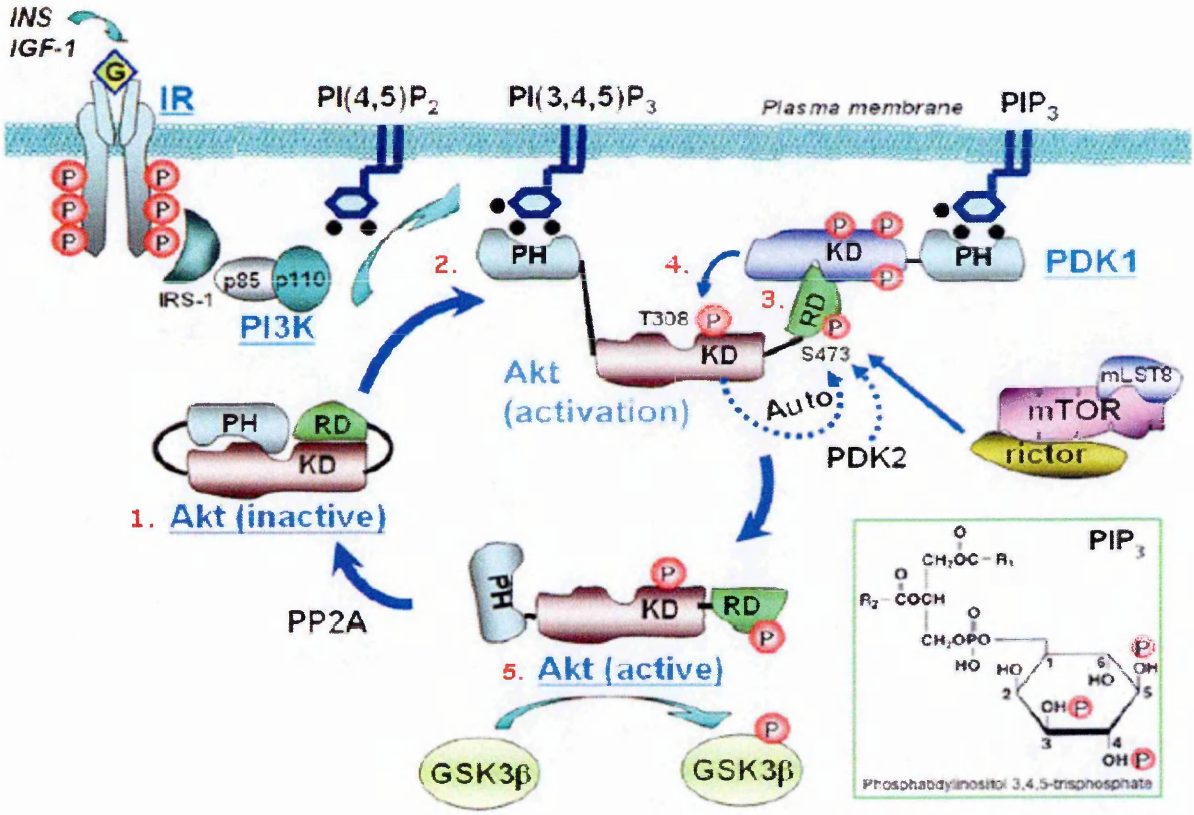

adapted from Lee et al., Mol Biol of the Cell 2009

Scheme of Akt activation pathway: 1.in its inactive form Akt is in the cytoplasm; 2.upon PI3K activation Akt interacts with membrane-bound phosphoinositides and translocates to the plasma membrane; 3. phosphorylation of Ser^{473} within regulatory domain (RD) occurs, then RD interacts with PDK1; 4. PDK1 catalyzes phosphorylation of Thr^{308} in Akt catalytic domain (KD); 5. fully active Akt detaches from the plasma membrane and goes back to the cytoplasm or to the nucleus to phosphorylate its targets, such as GSK3β.

Downstream targets of Akt

Akt activates numerous proteins involved in metabolism, angiogenesis, cell proliferation, growth and survival, as outlined in **Figure 1.10** *(Manning and Cantley, 2007)*. The substrates usually contain a conserved R-X-R-X-X-S/T-B recognition motif (where X represents any aminoacid and B stands for a bulky hydrophobic residue) *(Alessi et al., 1996a)*.

Figure 1.10 Cellular functions mediated by ten Akt substrates.

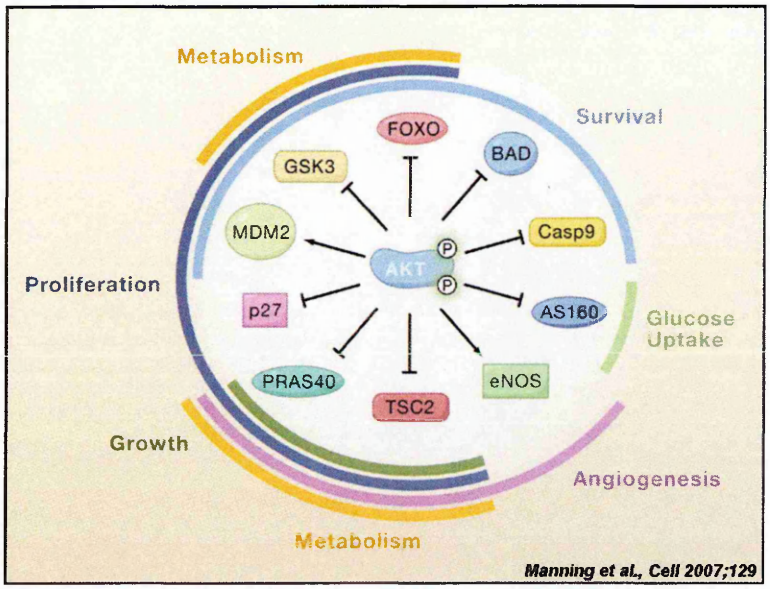

Scheme of the major processes known to be regulated by the Akt pathway. Ten of the Akt substrates are shown (arrow denotes activation; blocking arrow denotes inhibition)

A number of Akt substrates are particularly important in regulating nervous system physiology, or have been found to be altered in neurodegenerative diseases.

Among them:

- **GSK3β** (Glycogen Synthase Kinase 3) is a cytosolic enzyme that can phosphorylate several proteins, including Glycogen Synthase and Tau, in the nervous system. Phosphorylation of Tau has been found to reduce binding of the protein to microtubules. This modification has been implicated in formation of toxic protein inclusions in neurones *(Hong and Lee, 1997)*. Akt phosphorylates GSK3β at Ser^9, controlling inhibition of the

kinase, and thus provides protection of the cell against the formation of inclusions and promotes cellular metabolism.

- **Glut-4** is a glucose-transporter highly expressed in in the hypothalamus as well as in skeletal muscle and adipose tissue. It is another substrate of Akt, that translocates to the membrane upon phosphorylation in a IGF-I mediated manner. At this level it allows entrance of glucose molecules thus increasing cellular metabolism *(Komori et al., 2005).*
- **P70S6K** (p70 ribosomal protein S6 kinase) is another target of Akt phosphorylation, and activation of **P70S6K** increases protein synthesis and thus is important in cell growth and differentiation *(Toker, 2000; Brunet et al., 2001).*
- **Caspase 9** can be phosphorylated, and inhibited, by Akt. This interferes with the apoptotic pathway downstream of cytochrome c release *(Zhou et al., 2000).*
- Akt can selectively phosphorylate **BAD** at Ser^{136}. BAD is a pro-apoptotic protein that can sequester the pro-survival protein Bcl-xL. Upon phosphorylation at Ser^{136}, BAD enters a complex with a chaperone protein 14-3-3, thus releasing Bcl-xL. Bcl-xL is then free to interact with the mithochondrial membrane and inhibit the release of cytochrome c *(Zhou et al., 2000).*
- **IKK-α** is another substrate of Akt. Phosphorylation of IKKα leads to activation of NF-kB transcription factor, that is involved in transcription of pro-survival genes.
- In the nucleus Akt can phosphorylate and activate **CREB** transcription factor, that is implicated in transcription of survival genes.
- On the other hand, the forkhead transcription factors, in particular the **FOXOs** (forkhead transcription factors, class O), represent transcription factors involved in induction of pro-apoptotic and proinflammatory genes, including BIM (Bcl-2-interacting mediator of cell death) that is implicated

in the release of cytochrome c, or Fas, Fas Ligand, TNFα and its receptors. FOXOs are targets of Akt. Their phosphorylation by this kinase determines nuclear exclusion and recruitment in inhibitory complexes with the 14-3-3 protein *(Brunet et al., 2001).*

- **ASK1** is a MAPK3K involved in the activation of p38MAPK and JNK pathways. Phosphorylation of ASK1 at Ser^{83}, catalysed by Akt, inhibits ASK1 activity, suggesting that there is a link between the Akt pathway and the family of stress-activated kinases *(Kim et al., 2001).* In fact it has also been demonstrated that Akt1 can bind to **JIP1** (JNK-interactor protein 1) in neurons. This interaction prevents binding of JIP1 to JNK, and acts as a regulatory gate preventing JNK activation *(Kim et al., 2002).*

1.5.2 Physiological roles of Akt pathway

PI3K/Akt pathway is a key mediator of cell proliferation, survival and insulin responsiveness. Since 2001, the availability of transgenic mice obtained by knock out of specific isoforms of Akt has helped to deepen the knowledge about the functions of this kinase in different tissues. Interestingly, although three isoforms of Akt are described, in certain tissues loss of function of one of these isoforms is not compensated by the others, so determining relevant dysfunctions. Akt1 KO mice are small and have increased spontaneous apoptosis in the thymus, and display increased neonatal mortality (about 40%). Akt1 has been found to be the predominant isoform in placenta. Its ablation results in absence of spongiotrophoblast cells and loss of vascularization. This negatively affects placental development and maintenance *(Chen et al., 2001; Cho et al., 2001).* Akt2 KO mice display a more striking phenotype: they develop severe diabetes, with hyperglycaemia, hyperinsulinaemia and glucose intolerance. In fact Akt2 is the most abundant isoform in insulin-responsive organs and tissues, such as liver, skeletal muscles and adipose, and appears to be an isoform specialized in regulation of glucose homeostasis *(Yang et al., 2003).* In line with the evidence of

an involvement of Akt1 and Akt2 in growth and development, double knock out mice of Akt1/2 show a more obvious phenotype than the single knock-outs. They display severe growth defects and impaired skin development, skeletal muscle atrophy and abnormal bone development *(Peng et al., 2003)*. Akt3 deficient mice do not exhibit increased perinatal mortality neither apparent growth retardation, however they display dramatic reduction of brain size and weight (25%). Interestingly the reduced brain weight is caused by significant reduction of cell number and cell size, suggesting that Akt3 is critically implicated in postnatal development of the brain *(Easton et al., 2005)*. Accordingly double knock outs for Akt1/3 leads to a drastically more severe phenotype, resulting in embryonic lethality *(Yang et al., 2005)*.

On the other hand, tissue-specific overexpression of Akt in mice has highlighted that this pathway is critical for the modulation of heart growth *(Matsui et al., 2002)*, for mammary gland development during lactation *(Schwertfeger et al., 2003)*, and for growth of pancreatic islet beta cells and insulin production *(Tuttle et al., 2001)*. Interestingly, overexpression of Akt in T lymphocytes or prostate epithelial cells leads to tumorigenesis *(Malstrom et al., 2001; Majumder et al., 2003)*. Actually overexpression or overactivation of Akt has been documented in many solid tumours and hematological malignancies, such as prostate cancer, ovarian carcinomas, pancreatic carcinomas, gliomas as well as non-Hodgkin's lymphoma (**Table 1.8**) *(Altomare and Testa, 2005)*. Several studies have highlighted that Akt can phosphorylate a number of targets implicated in cell/cycle regulation, including p27, p21, Mdm2 and Myt1, resulting in cell-cycle progression and probably contributing to invasiveness of malignant cells *(Brazil et al., 2004)*. Among the three isoforms, Akt2 has been found more frequently deregulated in tumours. This sheds light on the possible involvement of this isoform in mediating PI3K-dependent effects on cellular adhesion, motility, invasion and metastasis formation *(Altomare and Testa, 2005)*. For these reasons

the Akt pathway has attracted increasing interest as a molecular target for cancer therapy.

Table.1.8 Akt activation in human cancer

Tumor type	*% Tumors with active AKT*
Glioma	~55
Thyroid carcinoma	80–100
Breast carcinoma	20–55
Small-cell lung carcinoma	~60
Non-small-cell lung carcinoma	30–75
Gastric carcinoma	~80
Gastrointestinal stromal tumors	~30
Pancreatic carcinoma	30–70
Bile duct carcinoma	~85
Ovarian carcinoma	40–70
Endometrial carcinoma	>35
Prostate carcinoma	45–55
Renal cell carcinoma	~40
Anaplastic large-cell lymphoma	100
Acute myeloid leukemia	~70
Multiple myeloma	~90
Malignant mesothelioma[a]	~65
Malignant melanoma[b]	43–67

(Altomare and Testa, 2005).

1.5.3 PI3K/Akt pathway in health and disease of the nervous system

Akt1 and Akt3 are the isoforms mainly expressed in the nervous system. Studies conducted on animals in which either or both of these kinases were ablated reported that Akt is critically involved in neuronal cell survival during developmental stages, thus influencing normal growth of the brain. Similarly, PI3K, the canonical upstream activator of Akt, plays a pivotal role in maintenance of neuronal survival; in fact its expression is already detected throughout the nervous system during development stages, and it is increased in the adult brain *(Rodgers and Theibert, 2002).*

In the adult nervous system, the PI3K/Akt pathway plays a crucial role in the transduction of survival signals in neurones, and in mediating protection against toxic insults. This is particularly evident in some acute neurodegenerative

disorders, including epilepsy, cerebral ischemia or peripheral nerve damage. In an experimental paradigm of epilepsy, rats were challenged by microinjection of kainic acid in the amygdala. The kainic-induced epileptic insult causes neuronal death in the hippocampus. In dying neurons within this brain area a strong activation of pro-apoptotic proteins such as Bax and BAD has been reported. Interestingly, in the cerebral cortex (an area that displays resistance to seizure-induced neurodegeneration) neuronal cells show strong activation of Akt, and increased BAD phosphorylation at Ser^{136} *(Henshall et al., 2002)*. In the case of cerebral ischemia, neurodegeneration occurs as a consequence of reduced oxygen supply. Experimentally this is usually obtained by temporary or permanent occlusion of an afferent cerebral artery. Hypoxic insults are known to be potent inducers of neuronal apoptosis. Often the clinical outcome is complicated by propagation of death-inducing signals from the ischemic core to the boundary regions (penumbra). Studies on an experimental model of permanent focal ischemia have reported that early after the middle cerebral artery occlusion, in the surviving neurons of the penumbra there is a transient activation of Akt, paralleled by reduced caspase 3 activation. This suggests that induction of the Akt anti-apoptotic pathway is important in sustaining neuroprotection after cerebral ischemia *(Jin et al., 2000; Shibata et al., 2002)*. Similarly, in transient ischemia of the spinal cord in the rabbit, an activation of both cell death and survival pathways have been detected. Interestingly, the activation of Akt early after reperfusion appears to be one of the factors responsible for retarding neuronal death after injury *(Sakurai et al., 2001)*. On the other hand, acute injury of peripheral nerves (such as crush or axotomy) represents a common paradigm of acute damage to the neuronal cells of brain stem or spinal cord. Axotomy of rat hypoglossal nerve has highlighted different susceptibilities of motor neurons to injury: at the postnatal stage injury to peripheral axons leads to neuronal death, whereas, in contrast, if damage occurs in the adult neurons do not die, but rather start a regenerative process *(Ito et al.,*

1996; Namikawa et al., 2000). Also in this case the survival of neurons has been associated with concomitant activation of Akt pathway. This is true also for axotomy of the sciatic nerve; in this case injury determines induction of Akt in surviving motor neurons of the lumbar spinal cord *(Murashov et al., 2001).*

While induction of Akt seems to represent a physiological response of surviving neurons to acute injury, in the case of chronic neurodegenerative diseases, such as Huntington's Disease (HD), Alzheimer's Disease (AD), or Amyotrophic Lateral Sclerosis, a lack of induction of this pathway is often reported.

HD is characterized by polyQ expansion in huntingtin protein, which leads to aggregation of the mutated protein in the nucleus and selective apoptosis of striatal neurons in the brain *(Saudou et al., 1998).* Analysis of Akt in brain samples from HD patients revealed the presence of both the full-length Akt and of a shorter form predicted to be generated by caspase 3-mediated cleavage of the full-length kinase. This suggests that compromised Akt pathway may accentuate the progression of HD. Accordingly, treatment with IGF-I, and induction of Akt activation, is protective for striatal neurons, and prevents formation of intranuclear inclusions. Akt-mediated phosphorylation of Ser^{421} on mutated huntingtin is required for the IGF-I mediated protective effect *(Humbert et al., 2002).* Altered distributions of Akt and PTEN have also been reported in AD, with a reduction of the levels of activated Akt *(Griffin et al., 2005; Steen et al., 2005; Lee et al., 2009).* Accordingly, it has been recently reported that intracellular amyloid-beta can directly interfere with Akt pathway activation, by preventing the interaction between Akt and PDK-1. The authors demonstrated, in vitro, that amyloid-beta acts upstream of Akt by inhibiting PDK-1 activity *(Lee et al., 2009).* Analysis of post mortem samples from patients that died with ALS showed increased activities and protein levels of PI3K in membrane fractions of spinal cord, compared to controls. However the downstream targets, such as Akt and S6K, were not upregulated in ALS tissues, suggesting that there may be an impairment of this signal transduction cascade in the disease *(Wagey et al.,*

1998). In a subsequent study, the same group revealed a reduction of PI3K levels and activity, with no modification of Akt, in the spinal cord of pmn mice (a mouse model of ALS) *(Wagey et al., 2001).* Instead, analysis of homogenates from late onset SOD1G93A transgenic mice showed reduction of PI3K and total Akt protein levels even at the presymptomatic stage *(Warita et al., 2001).* In a recent report, downregulation of phospho-Akt has also been detected in the spinal cord motor neurons of presymptomatic SOD1G93A mice; moreover this has been confirmed by immunohistochemistry in post-mortem samples obtained from ALS patients *(Dewil et al., 2007b).* Reduced activation of Akt has been described in muscles from ALS patients, suggesting a link between inhibition of this pathway and progressive atrophy in this tissue *(Leger et al., 2006).* Although there are some discrepancies between these studies, overall they highlight that an impairment of the PI3K/Akt pathway in motor neurons may be a common feature in ALS. Nevertheless, further studies are needed to better dissect the role played by these kinases in the disease process.

1.5.4 Strategies for targeting PI3K/Akt pathway

Several strategies have been developed to target specific components of the PI3K/Akt pathway. Given that aberrant activation of one or more Akt isoform has been detected in cancer, most of the efforts have been spent trying to inhibit this pathway, through small molecule inhibitors, antisense technology or RNAi. On the other hand, since increasing evidence reports a downregulation of the pathway in neurodegenerative disorders, it has been hypothesized that induction of Akt may be beneficial. In this case growth factors upstream of PI3K/Akt pathway have been regarded as potential therapeutic molecules *(Sale and Sale, 2008).*

Small-molecule inhibitors

In recent years, a number of pharmacological inhibitors against Akt have been described. However, these molecules often present limited specificity over the three Akt isoforms, or side effects due to interaction with unrelated kinases, or poor bioavailability. Despite these drawbacks, great efforts have been spent to develop new molecules, since targeting of the PI3K/Akt pathway is considered a good therapeutic strategy for cancer.

Inhibitors targeting the ATP-binding site

These compounds include H-89 and analogues, NL-71–01 and indazole-pyridine-based compounds *(Reuveni et al., 2002; Luo et al., 2005).* They show moderate to high selectively for Akt over PKA, which has 50% identity in the kinase domain and 70% identity in the 25-residue ATP-binding site *(Kumar and Madison, 2005).* However, since the ATP-binding site shows 96–100% identity amongst Akt isoforms, developing isoform-specific inhibitors acting at the ATP binding site is difficult.

Allosteric inhibitors

These molecules represent a new class of inhibitor recently described. They interact with multiple domains on Akt, and do not show inhibitory effects on a range of unrelated kinases. Moreover, some molecules display specificity for Akt1, or Akt2, or both *(Barnett et al., 2005; DeFeo-Jones et al., 2005).* They are PH domain dependent and are also postulated to bind to the linker region that connects the PH domain to the kinase domain, consistent with the sequence diversity of this region. The main limitation of these compounds is their poor pharmokinetic profile and low solubility, that have prevented their evaluation in animal models *(Kumar and Madison, 2005).*

Chemically modified peptide substrate mimetic inhibitors

These compounds target the substrate-binding site. This strategy avoids the potential specificity problems of targeting the kinase active site but does not provide specificity over the three isoforms of Akt *(Litman et al., 2007)*.

Phosphatidylinositol ether lipid analogue (PIA) inhibitors

These molecules inhibit Akt activation by targeting the PH domain *(Castillo et al., 2004; Gills and Dennis, 2004)*. However these compounds show poor solubility, only moderate potency, aggregation and weak pharmacokinetics. Moreover, as PH domains are present in many proteins there is also concern about the specificity of PIAs.

A number of other compounds have been reported to inhibit the activation of Akt, like curcumin *(Chaudhary and Hruska, 2003)*, deguelin *(Chun et al., 2003)*, indo-3-carbinol *(Chinni and Sarkar, 2002)* and CMEP *(Zhang et al., 2007)*. However the molecular mechanism of action of these molecules still remains unclear.

Knock-down by genetic approaches

Dominant negative mutants of Akt have been generated. These construct have Ser^{473} and Thr^{308} substituted by Ala, an un-charged aminoacid; as an alternative a mutation in K179→D generates a kinase-dead mutant *(Andjelkovic et al., 1997)*. A number of antisense oligonucleotides (typically 18mers) have been developed that enable the specific and potent knock-down of endogenous Akt isoforms individually or in various combinations *(Sale et al., 2006)*. Knock-down of the targeted isoform is routinely higher than 95%, making these extremely powerful tools. Akt-targeted siRNAs have also been validated, with quite good results, in a number of studies *(Jiang et al., 2003; Katome et al., 2003)*.

Strategies aimed at activating the Akt pathway

Akt is activated by several growth factors, that are involved in induction of proliferation or cell survival. Administration of these compounds has been regarded as a possible therapeutic strategy for a number of neurodegenerative diseases, with some encouraging results. As an alternative approach, genetic manipulation has been used to obtain activation of the pathway by overexpression of constitutively activated mutants of Akt. This approach has been widely used experimentally, to dissect the functions of the Akt pathway, however difficulties in manipulating these constructs have limited their development in therapy.

Growth factors

A number of growth factors are able to activate PI3K/Akt pathway, including IGF-I, GDNF, CNTF, VEGF, EGF, BDNF and FGF2 *(Brunet et al., 2001; Rodgers and Theibert, 2002; Johnson-Farley et al., 2007).* Some of these molecules have been successfully used in experimental models of ALS. CNTF intrathecal delivery through encapsulated engineered xenogenic cell lines was protective in animal models of ALS, and went into early stage of clinical trials *(Aebischer et al., 1996b; Aebischer et al., 1996a).* Intramuscular delivery of an Adeno-Associated Viral vector expressing GDNF to G93A mouse model of ALS delayed motorneuron loss, preserving neuromuscular junctions and reducing muscle atrophy *(Wang et al., 2002).* Delivery of IGF-I, using the same viral vector-mediated approach, was protective in the G93A transgenic mouse. The authors reported an increase of activated Akt in the spinal cord of animals that received IGF-I, suggesting that induction of this pathway may be the key element for delay of the neurodegeneration *(Kaspar et al., 2003).* These results were confirmed by another group that used direct intrathecal delivery of IGF-I in the same mouse model. An induction of both Akt and ERK activation were reported in

this case *(Nagano et al., 2005)*. Another growth factor, VEGF, displayed protective effects against mutant SOD1-induced neuronal death in vitro, by inducing activation of Akt *(Li et al., 2003)*. Intracerebroventricular treatment of SOD1G93A rats with VEGF improved motor performances and prolonged the survival. The authors also provided evidence that VEGF treatment resulted in an increase of activated Akt in the spinal cords of the animals *(Storkebaum et al., 2005; Dewil et al., 2007b)*.

One of the main drawbacks of the use of growth factors is that usually these molecules are effective on several cell types, thus exerting pleiotropic effects in the organism. This has led to the failure of all the clinical trials that used growth factors in ALS, due to strong collateral effects.

Constitutively activated mutants of Akt

Studies conducted to investigate the molecular features of Akt protein have led to the generation of mutants that display constitutive activity in the cells. One approach is fusion of a myristylated/palmitylated sequence at the N-terminal of Akt. This modification induces constitutive translocation of the kinase to the membrane, and subsequent continuous activation, in a PH and PI3K independent manner. As an alternative, Ser^{473} and Thr^{308} of Akt are substituted by Asp, that provides the negative charge mimicking phosphorylation. This mutant displays constitutive activity independently of membrane translocation *(Alessi et al., 1996b; Andjelkovic et al., 1997; Brodbeck et al., 1999)*. These mutants have been shown to be functional in several in vitro culture systems, and to mediate cell survival against mutant SOD1 toxicity in cell lines *(Kanekura et al., 2005)*. Although these constructs have been widely used to dissect molecular mechanisms related to Akt pathways in vitro, they have raised great concern for use in vivo, since constitutive activation of Akt pathway is implicated in oncogenicity *(Aoki et al., 1998; Mende et al., 2001)*.

1.6 USE OF LENTIVIRAL VECTORS FOR TREATMENT OF NEURODEGENERATIVE DISEASES

1.6.1. From Lentivirus to a Lentiviral Vector

The genus " lentiviridae"

Genus "Lentiviridae" belongs to the Retroviridae family, a large family of enveloped RNA viruses. The virions are 80–100 nm in diameter, and their outer lipid envelope incorporates and displays the viral glycoproteins. The viral genome is a linear, single-stranded, non-segmented RNA; it is 7–12 kb in size with positive polarity. The hallmark of the family is its replicative strategy whose essential steps are reverse transcription of the virion RNA into linear double-stranded DNA and its subsequent integration into the genome of the host cell. Retroviruses are subdivided into seven groups defined by evolutionary relatedness, each with the taxonomic rank of *genus* (**Table 1.9**). Most of the members of this family are known for their oncogenic potential. In contrast, Lentiviruses generally cause a slowly progressive disease (lenti = slow) by killing or inducing loss of function of specific cells and tissues. A representative example of this family is human immunodeficiency virus (HIV), the etiological agent of acquired immunodeficiency syndrome (AIDS) *(Coffin, 1997).*

Table 1.9. Classification of Retroviruses

Genus		Example	Virion morphology	Genome
1.	Avian sarcoma and leukosis viruses	Rous sarcoma virus	central, spherical core "C particles"	simple
2.	Mammalian B-type viruses	mouse mammary tumor virus	eccentric, spherical core "B particles"	simple
3.	Murine leukemia-related viruses	Moloney murine leukemia virus	central, spherical core "C particles"	simple
4.	Human T-cell leukemia–bovine leukemia viruses	human T-cell leukemia virus	central, spherical core	complex
5.	D-type viruses	Mason-Pfizer monkey virus	cylindrical core "D particles"	simple
6.	Lentiviruses	human immunodeficiency virus	cone-shaped core	complex
7.	Spumaviruses	human foamy virus	central, spherical core	complex

The genome of all retroviruses contains long terminal repeats at the 5' and 3' ends (5'LTR and 3'LTR), a packaging signal located 3' of the 5'LTR (psi) and three major domains encoding the virion proteins: *gag*, which directs the synthesis of the virion proteins forming the matrix, the capsid, and the nucleoprotein structures; *pol*, which codes the reverse transcriptase and integrase enzymes; *env*, with information for the surface and transmembrane proteins that constitute the viral envelope. An additional coding domain present in all retroviruses is *pro*, which encodes the virion protease (**Figure 1.11**). After integration, these structural genes are expressed through a strong promoter located in the 5'LTR. Retroviruses are divided into two main categories (simple and complex), according to the organization of their genomes *(Coffin, 1992; Blesch, 2004)*. Simple retroviruses usually carry only the elementary genomic domains described above, whereas complex retroviruses (like lentiviruses) code for additional regulatory non-virion proteins derived from multiply spliced messages.

Figure 1.11

Schematic cross section through a retroviral particle.

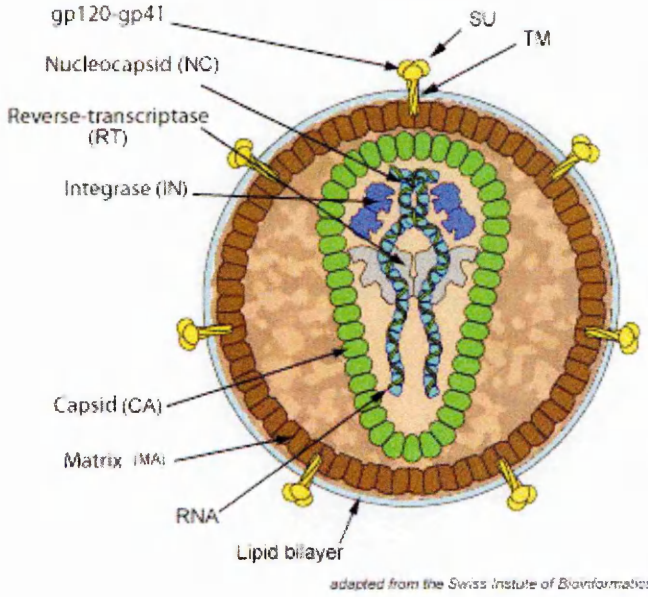

The viral envelope is formed by a cell-derived lipid bilayer into which proteins encoded by the env region of the viral genome are inserted. These consist of the transmembrane (TM) and the surface (SU) components linked together by disulfide bonds. Internal non-glycosylated structural proteins are encoded by the gag region of the viral genome. They are the matrix (MA) protein, capsid (CA) protein, and nucleocapsid (NC) protein. Major products of the pol-coding region are reverse transcriptase (RT) and integrase (IN).

The retroviral replication cycle follows the general pattern of enveloped viral infections, with some specific features *(Coffin, 1996)*. Retroviruses enter the host cell through the attachment of their surface glycoproteins to specific plasma membrane receptors, which leads to fusion of virus and cell membranes. The interaction of virus and cell surfaces is highly specific; it constitutes the main determinant of viral host range, defining susceptible animal species and target cells within the host. After penetration into the cell, the RNA genome, still contained in a core complex of non-glycosylated proteins and associated with the virion reverse transcriptase, is retro-transcribed. Reverse transcription takes place in the cytoplasm; and it is the fundamental step that leads to generation of a double stranded DNA viral genome, ready for random integration into the genome of host cell.

The steps of the retrotranscription process can be summarized as follows (**Figure 1.12**):

1. Minus-strand DNA synthesis is initiated using the 3'-end of a partially unwound transfer RNA which is annealed to the primer-binding site (PBS) in genomic RNA, as a primer. Minus-strand DNA synthesis proceeds until the 5'-end of genomic RNA is reached (R-U5), generating a DNA intermediate of discrete length termed minus-strand strong-stop DNA (sssDNA).
2. The RNA:sssDNA duplex formed during this first step synthesis is degraded by RNase H, thus leaving the sssDNA free to anneal to the 3'-end of a viral genomic RNA. This transfer is mediated by identical sequences known as the repeated (R) sequences, which are present at the 5'- and 3'-ends of the RNA genome. The 3'-end of sssDNA was copied from the R sequences at the 5'-end of the viral genome and therefore contains sequences complementary to R. The annealing reaction appears to be facilitated by the nucleocapsid protein.
3. Once the sssDNA has been transferred to the 3'-R segment on viral RNA, minus-strand DNA synthesis resumes, accompanied by RNase H digestion of the template strand. This degradation is not complete, however, because the RNA genome contains a short polypurine tract (PPT) that is relatively resistant to RNase H degradation.
4. A defined RNA segment derived from the PPT primes plus-strand DNA synthesis. Plus-strand synthesis is halted after a portion of the primer tRNA is reverse-transcribed, yielding a DNA called plus-strand strong-stop DNA (+sssDNA).
5. RNase H removes the primer tRNA, exposing sequences in +sssDNA that are complementary to sequences at or near the 3'-end of plus-strand DNA.
6. Annealing of the complementary PBS segments in +sssDNA and minus-strand DNA constitutes the second strand transfer.
7. Plus- and minus-strand syntheses are then completed, with the plus and minus strands of DNA each serving as a template for the other strand.

8. At the end of the process a double stranded DNA is generated. It encompasses the entire viral genome, plus two Long Terminal Repeats (LTR) at both extremities, each composed of the regions U5-R-U3.

Figure 1.12

Scheme of reverse transcription process

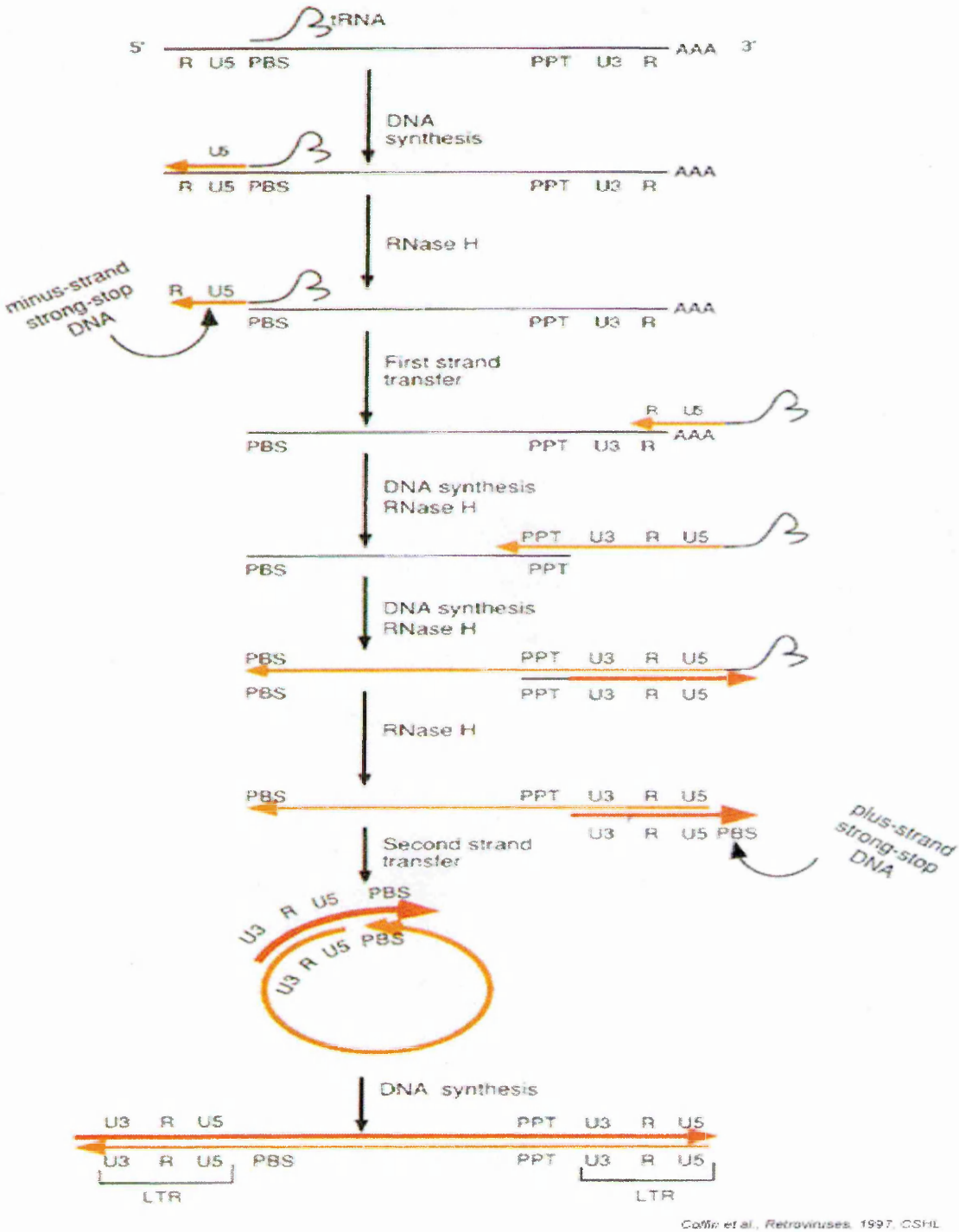

Coffin et al., Retroviruses, 1997, CSHL

After retro-transcription, the viral DNA is translocated into the nucleus where the linear copy of the retroviral genome is inserted into chromosomal DNA with the aid of the virion integrase, thus generating a stable provirus. With integration, the proviral genome achieves the status of a cellular gene: it is expressed through RNA polymerase II and is replicated by cellular enzymes together with chromosomal DNA. Viral messages are translated on cellular ribosomes. The translation products, together with progeny RNA, are assembled at the cell periphery into viral particles that are released from the cell by budding of the plasma membrane. Budding of viruses is followed by proteolytic cleavage of virion polyproteins by a viral protease and by cellular proteases.

Lentivirus: genome organization and steps of the replication cycle

The genome organization and replication cycle of HIV-1 will be described in this section, as HIV-1 is the most extensively studied lentivirus, and it represents the prototype for generation of lentiviral vectors.

HIV-1 is a complex retrovirus whose genome comprises nine genes: Gag, Pol, Env, that represent the conventional three open reading frames of all retroviruses; Tat, Rev, Vif, Vpr, Vpu, and Nef that are generated by alternative splicing of the original genome RNA. These accessory genes are used by the virus to control its own gene expression, allowing temporal separation into early and late phases, and to manipulate the host cell for virus entry, for integration of the genetic material into the cell genome, and for virus production.

The HIV-1 genome, like almost all retroviruses, contains a single RNA polymerase II-dependent promoter in the 5'LTR. It drives transcription of an initial genome-length RNA that also acts as an mRNA for translation of Gag and Pol genes. In the case of HIV-1, this initial transcript can also be processed into fully spliced transcripts encoding Tat and Rev regulatory proteins, and the auxiliary protein Nef. Alternatively this transcript can be processed into partially spliced mRNAs

encoding the other auxiliary proteins Vif, Vpu and Vpr *(Cullen, 2009)* (**Figure 1.13**).

The Tat protein regulates the promoter activity of the 5'LTR and is necessary for the transcription from the 5'LTR. It recognises a 50bp transactivation response element (TAR) located immediately 3' to the transcription start site of viral genome. Tat first interacts with a cellular factor called cyclin T1, which, along with the kinase cdk9, constitutes the positive transcription elongation factor b (P-TEFb). The complex of Tat and P-TEPb binds the HIV TAR, thus increasing the stability of RNA-polymerase II. This allows the transcription of the entire viral genome *(Kao et al., 1987; Barboric and Peterlin, 2005).*

The HIV replication cycle requires that the single initial transcript is exported out of the nucleus in several different spliced forms, but eukaryotic cells do not normally permit the nuclear export of intron-containing mRNAs. The strategy used by the virus to circumvent the risk of nuclear retention of not fully spliced RNAs resides in the features of the viral protein Rev. Rev is translated from a fully spliced mRNA that is constitutively exported from the nucleus. Once synthesized, it enters the nucleus and binds to the rev responsive element (RRE) within the viral RNA. Rev then interacts with cellular proteins involved in nucleocytoplasmic transport, thus allowing the export of unspliced RNA out of the nucleus *(Cullen, 2009).*

Figure 1.13

Genome organization of HIV-1

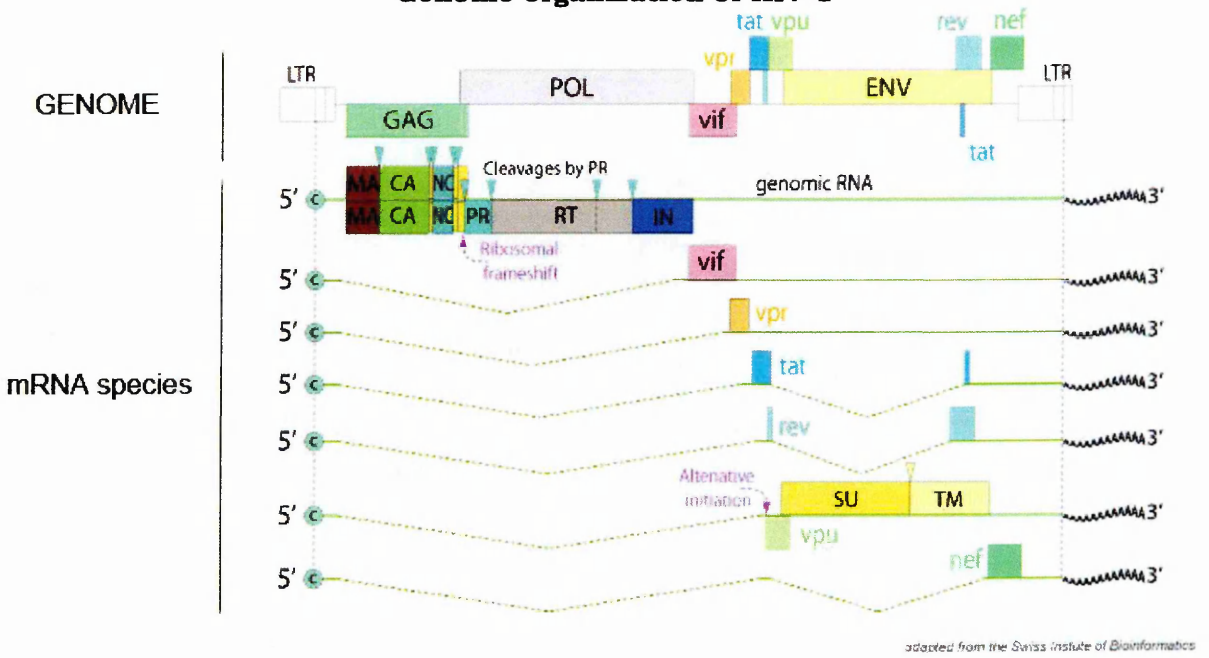

The overall life cycle of HIV-1 can be summarized as follows (**Figure 1.14**):

1. Virus attaches to host receptor CD4 through the SU glycoprotein (gp120), with subsequent interaction with a chemokine coreceptor. TM glycoprotein (gp41) mediates fusion with cell membrane.
2. The viral particle is then internalized through the cellular endosomal compartment; this process is followed by partial uncoating of the nucleocapsid.
3. Once in the cytoplasm, the ssRNA(+) genome is copied into a linear dsDNA molecule by the viral reverse transcriptase.
4. Subsequently the viral dsDNA is transferred into the nucleus, where it is covalently and randomly integrated into the cell's genome by the integrase (provirus). The provirus can stay in this form throughout the life of the cell
5. During productive infection the provirus is transcribed by Pol II, thus producing viral spliced and unspliced RNAs.
6. Translation of spliced viral RNAs produces tat, rev, and nef proteins.
7. Rev mediates nuclear export of the uncompletely spliced RNAs.

8. Translation of unspliced viral RNAs produces Env, Gag and Gag-Pol polyproteins.
9. Virions are then assembled at the host cellular membrane, followed by packaging of the viral RNA genome.
10. Budding through the plasma membrane and release of the virions.
11. Proteolytic processing of the precursors polyproteins by viral protease and maturation of the virions.

Figure 1.14

Scheme of the life cycle of HIV-1

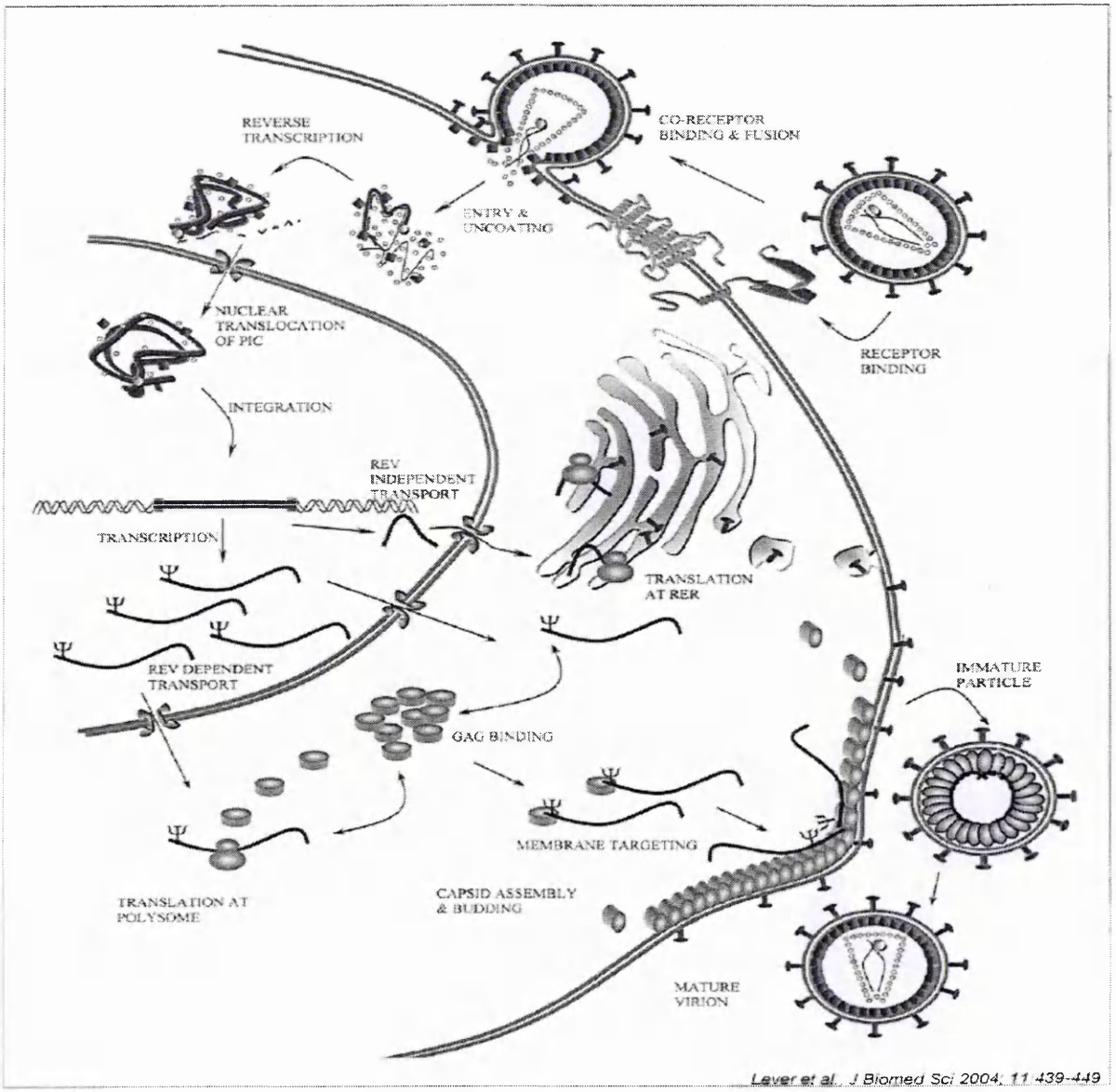

Generation of a lentiviral vector

Lentiviral vectors (LVs) are recombinant lentiviruses produced in vitro; they represent valuable tools for administration of genes of interest to specific cellular targets.

Two major points need to be considered when generating a viral vector starting from a vital virus: 1. the viral vector should retain the infection properties of the virus it derives from; 2. the viral vector should be deprived of the information necessary to produce a replication-competent retrovirus, for safety considerations.

The strategy for generation of viral vectors consists of preparation of a transfer vector plasmid derived from the original viral genome, after deletions of the majority of gag coding region, and of the complete coding regions for pol and env genes. In this way the viral genome is reduced to a backbone containing the 5' and 3' LTR, the packaging signal (psi) and a small part of the gag coding region that enhances the packaging of viral RNA (psi+). Transgenes of interest are cloned inside this backbone to allow insertion into viral particles, with the only restriction of the lentiviral genome maximal length (not higher than 9 kilobases). Information needed for packaging of viral particles are provided in trans, generally on different plasmids, to prevent the risk of wild-type virus production through recombination *(Blesch, 2004)*. In this way the new-formed viral particles will contain the structural proteins needed to allow infection of host cells, but the information needed for replication in host cells will not be present.

The first generation of lentiviral vectors was initially produced by transient trasfection of three different plasmids in producer cell lines: one construct contained the wild type HIV genome deprived of the packaging signal (psi) sequence and env gene, and with 5'LTR replaced by an heterologous promoter and a polyadenylation signal instead of 3'LTR; an helper plasmid provided envelope information, and a third plasmid contained an expression cassette for the transgene of interest, 5'- and 3'-LTR and psi. There have been several

technological improvements since then, with the aim of increasing the biosafety of the system: vpr, vpu, nef and vif have been deleted in second generation lentiviral vectors, as these auxiliary genes are crucial for HIV virulence but do not influence in vitro production *(Kim et al., 1998)*; in third generation vectors the U3 region in the 5'LTR has been replaced by a heterologous enhancer. In this way the activity of 5'LTR is independent of the tat gene *(Dull et al., 1998)*. Moreover a deletion has been introduced into the U3 region of the 3'LTR resulting in a self-inactivating (SIN) vector *(Miyoshi et al., 1998; Zufferey et al., 1998)*. In fact, removal of the enhancer in U3 leads to a deleted U3 region in 5'LTR after reverse transcription, thereby eliminating the potential influences of LTR on neighbouring genes. However, to allow expression of the transgene of interest, an heterologous promoter needs to be added in the transfer vector. To further diminish the likelihood of recombination, the rev gene has been cloned into a separate expression plasmid *(Dull et al., 1998)*. Moreover, to increase infectivity of lentiviral vectors, a central polypurine tract (cPPT) is included in the transfer vector *(Follenzi et al., 2000)*; to enhance transgene expression in infected cells, the post-transcriptional response element of the Woodchuck hepatitis virus (WPRE) is cloned downstream of the gene of interest *(Donello et al., 1998)*.

Figure 1.15

Diagram of wild type HIV-1 and plasmids for production of recombinant LVs

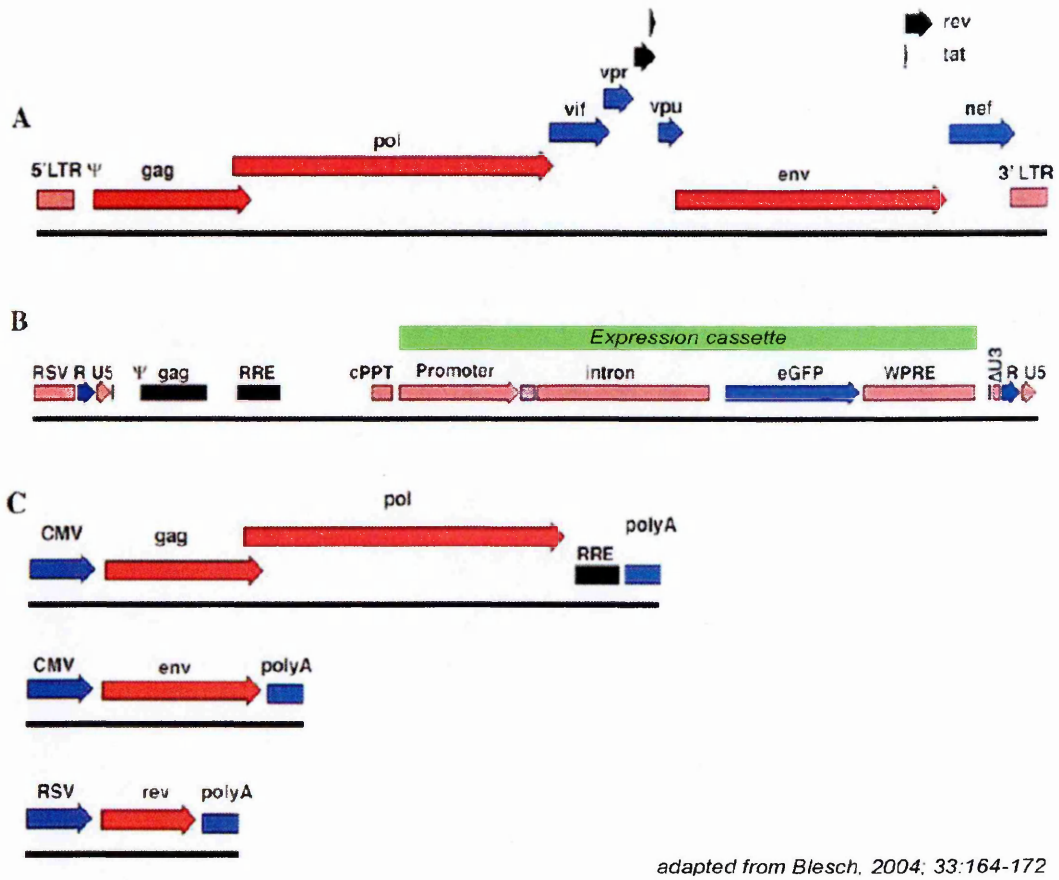

A. Diagram of the genome of wild type HIV-1. B. Scheme of a third generation lentiviral transfer vector: enhancer in 5'LTR has been substituted by an heterologous promoter from Rous Sarcoma Virus; U3 region in 3'LTR has been deleted, to generate a SIN vector; cPPT and WPRE have been added to increase viral infectivity and transgene expression. C. Adjuvant plasmids carrying information needed for packaging.

1.6.2 Features of lentiviral vectors

The main feature of lentiviral vectors is that, in contrast with vectors derived from other retroviruses, they can easily transduce slowly and non-dividing cells (such as neurons). Moreover, LVs have an highly manipulable genome with a quite high size of gene-carrying capacity (7-8Kb), and show very low levels of pro-inflammatory activity, at variance with other virus-derived vectors like adenoviruses, known to be highly immunogenic in humans.

Recent studies have also demonstrated that, due to the fact that the virus integrates into the host genome, LVs can maintain long-lasting expression in the brain for several months *(Bosch et al., 2000; Deglon et al., 2000; Kordower et al., 2000)*. For these reasons LVs are considered attractive for gene transfer to the central nervous system (CNS) and hold great potential as a therapeutic gene delivery strategy for neurological disorders.

However, due to the characteristics of native lentiviruses, the use of LVs for gene therapy presents some drawbacks:

1. Although random integration of vector DNA into the host cell genome allows long lasting gene expression, this process is at high risk of deregulating neighbouring genes within the genome. Several modifications have been introduced into the original viral genome (as described above), however the site of integration still cannot be controlled.
2. Most of the studies are based on lentiviral vectors derived from HIV-1, that is a human pathogen. This poses great concern for the risk of recombination with wild type lentivirus. Fortunately, over years, sequence analysis tools have led to the generation of vectors containing very short homology between transfer vector sequence and adjuvant genes from the wild-type virus. Moreover, there is accumulating evidence of the possibility of generating lentiviral vectors starting from non-human pathogen viruses, like Simian Immunodeficiency Virus (SIV) *(Mangeot et al., 2000; Schnell et al., 2000)* or non-primate lentiviruses, like Equine Infectious Anaemia Virus (EIAV) *(Mitrophanous et al., 1999; Ikeda et al., 2002)*, Feline Immunodeficiency Virus (FIV) *(Curran et al., 2000; Brooks et al., 2002)* , or Bovine Immunodeficiency Virus (BIV) *(Takahashi et al., 2002)*.
3. Use of lentiviral vectors in vivo requires high titre preparations. Although great technological improvements have lead to the generation of titres in the range 10^9-10^{10} Transfection Unit/mL, vectors based on other viruses (like Adenovirus or Adeno-Associated-Virus) appear to be best suited, from this point of view (**Table 1.10**).

Table 1.10.

Properties of Viruses Used to Derive Gene Transfer Vectors

Virus	Genome	Insert capacity (kb)	Specific integration	Long-term maintenance	RNA intermediate	Titre[a]
Retroviruses	8–12kbp ssRNA	7	Y	Y	Y	10^6–10^7
Adenovirus	36kbp dsDNA	8	N	N	N	10^{11}–10^{12}
Adeno-ass. virus	4.7kb ssDNA	4.5	Y	Y	N	10^6–10^8
Herpes simplex virus	150kbp dsDNA	25	N	Y	N	10^9–10^{10}

[a] Vector titre is given in transducing units/ml assayed on cultured cell lines. The titer given is for virus in medium harvested directly from packaging cells.

1.6.3 Targeting the Central Nervous System (CNS) is problematic

Access of drugs to CNS has always been a great challenge in pharmacology, due the presence of the blood-brain-barrier (BBB), a highly specialized structure that regulates the trafficking of molecules between blood and CNS parenchyma. Brain endothelial cells differ from endothelial cells in capillaries of other organs in two important ways. First, continuous tight junctions are present between the endothelial cells, which prevent transcapillary movement of polar molecules varying in size from proteins to ions. Second, there are no detectable transendothelial pathways. Thus, there is an absence of transcellular channels and fenestrations as well as a paucity of plasmalemmal and intracellular vesicles. As a result of these special anatomical features, the endothelial cells in brain provide a continuous cellular barrier between the blood and the interstitial fluid *(Siegel, 1999)*. This means that the CNS is not permeable to substances with low lipid solubility, thus high polar molecules that are essential for CNS survival, like glucose, amino acids, or vitamins, can pass the BBB only through receptor-mediated or carrier-mediated active transport.

For this reason, for a drug to gain access to the brain the molecule must possess high lipid-solubility (like almost all psychoactive drugs), or has to be able to interact with specific carriers or receptors on the surface of capillaries. A way to overcome the BBB may be direct administration in the CSF, through intrathecal injection into brain ventricles or in the subarachnoid space at lumbar level. Although this root of administration is sometimes used in the clinic, it represents an invasive technique that may be problematic when designing a treatment for progressive neurodegenerative disorders, like Alzheimer Disease, Parkinson Disease or ALS.

The use of viral vector-mediated approaches for treatment of neuronal disorders linked to genetic defects has gained great interest, because theoretically a single administration in the brain may determine longlasting expression of the transgene, ruling out the necessity for frequent administrations.

Alhough several authors have demonstrated that rLVs can transduce several cell-types within the CNS in vivo in rodents, including neurons, oligodendrocytes, astrocytes and adult neuronal stem cells *(Blomer et al., 1997; Jakobsson et al., 2003; Consiglio et al., 2004)*, the CNS still poses some particular challenges to gene therapy approaches. As already mentioned the BBB precludes the access of systemic molecules as large as a viral vector and the strong interconnection between different cell types in the nervous system could induce de-targeting of LVs, leading to infection of cell types other than those desired.

Interestingly, although there have been a number of studies on LVs delivery in the brain *(Naldini et al., 1996a; Baekelandt et al., 2002; Watson et al., 2002; Jakobsson et al., 2003)*, there is still a lack of information on experimental applications in the lumbar spinal cord. Enhancing knowledge in this area will be relevant for designing gene therapy approaches for motor neuron diseases, like Amyotrophic Lateral Sclerosis.

Motor neurons of spinal cord differ from other cell types in the CNS, as their cell body is inside spinal cord parenchyma, while axons project out, through the

peripheral nerves, to innervate muscles. Interestingly, some viruses, like Rabies Virus and Herpes Simplex Virus, take advantage of this feature to gain access to the nervous system: these viruses enter the nerve cell ending at the muscular junction or at skin level, respectively; then following entry into the axon, they can be retrogradely transported along microtubules to the neuronal cell body, within the CNS parenchyma *(Tsiang, 1979; Gillet et al., 1986; Whitely, 1996; Palmer et al., 2000)*. For these reasons several strategies have been developed to increase the efficiency and specificity of LVs in targeting CNS cells.

1.6.4 Strategies for broadening infectivity and increasing specificity.

Pseudotyping

One mechanism for expanding the cellular tropism of enveloped viruses is through the formation of phenotypically mixed particles (pseudotypes). This is a natural process that commonly occurs during viral assembly in cells infected with two or more enveloped viruses *(Zavada, 1982)*.

The first study for pseudotyping of HIV-1 vector particles dates back to 1990, with the work of Page and colleagues *(Page et al., 1990)*. These authors demonstrated that substituting native glycoproteins (GP) of HIV-1 with glycoproteins of Murine Leukemia Virus (MLV) led to production of recombinant viral particles that had lost tropism of wild-type HIV-1 and acquired that of MLV. Since then, several researchers have studied various combinations of viral pseudotypes (**Table 1.11**). One of the best known and most widely used is VSV-G. This glycoprotein derives from Vescicular Stomatitis Virus (a negative strand ssRNA virus, genus *Vesciculovirus*, family *Rhabdoviridae*). This pseudotype interacts with an unidentified ubiquitous cellular receptor, and uses phosphatidylserine in a postbinding step required for virus entry. This gives the vector a broad host-cell range, including infection of both neurons and glial cells

after injection into brain parenchyma *(Baekelandt et al., 2002)*. Moreover, VSV-G confers high vector particle stability, allowing concentration by ultracentrifugation. The most important technical drawback of VSV-G is that its constitutive expression is toxic for cells, thus raising problems in establishing packaging cell lines for high throughput production of lentiviral vectors. Moreover VSV-G pseudotypes are inactivated by human serum complement. Despite these problems, VSV-G-psedotyped lentiviral vectors have recently entered clinical application *(Manilla et al., 2005)*.

Of great interest for potential gene therapy approaches for neurodegenerative diseases are LVs pseudotyped with Rabies virus envelope. This virus belongs to the *Lyssavirus* genus, *Rhabdoviridae* family. Rabies glycoproteins are known to interact with neuronal cell adhesion molecule (NCAM1), p75 neurotrophin receptor (p75NTR) and nicotinic acetylcholine receptor (nAChR) *(Lafon, 2005)*. These receptors are present on the membrane of axonal terminals at the neuromuscular junctions; in fact peripheral muscles represent the main way through which the virus gains entrance to the CNS.

Of potential clinical importance for treatment of motor neuron diseases are EIAV-based vectors pseudotyped with Rabies glycoprotein. They have demonstrated to be able to target spinal cord motor neurons after delivery to peripheral muscle, in vivo, in rodent models of ALS *(Azzouz et al., 2004a)*.

Table 1.11. Tropism modification of lentiviral vectors by pseudotyping

Family	Genus	GP	Tropism	Reference
Rhabdoviridae	Vesciculovirus	VSVG	Pantropic	*(Naldini et al., 1996b)*
	Lyssavirus	RABIES	CNS (from peripheral muscles)	*(Azzouz et al., 2004b; Azzouz et al., 2004a)*
Arenaviridae	Arenavirus	LCMV	Pancreatic islet cells	*(Kobinger et al., 2004)*
Filoviridae	Filovirus	EBOLA	Airway epithelium Muscle/ myocytes	*(Kobinger et al., 2001)* *(MacKenzie et al., 2005)*
Togaviridae	Alphavirus	ROSS RIVER	Liver (hepatocytes + Kupffer cells)	*(Kang et al., 2002)*
Baculoviridae	Nucleopolyhedrovirus	GP64	Pantropic	*(Kumar et al., 2003)*

Tissue-specific promoters

In parallel with studies aimed at finding pseudotypes with increased specificity, most efforts to control vector expression have used transcriptional targeting by tissue-specific promoters. Usually lentiviral vectors carrying an expression cassette use strong ubiquitous promoters, like CMV. This is a 700bp sequence containing the cytomegalovirus immediate early promoter and enhancer. Lentiviral vectors containing the CMV promoter have been demonstrated to sustain long-term expression in rat brain *(Naldini et al., 1996a)*. However some studies showed that CMV is susceptible to transcriptional inactivation over time by methylation of cytosines in CpG dinucleotides *(Prosch et al., 1996)*. For these reasons other promoters have recently become more widely used in lentiviral vectors: EF1α (1.2Kb long) is the promoter of Elongation Factor alpha, an ubiquitously expressed housekeeping gene that plays a pivotal role in protein synthesis; hPGK (500bp) is the promoter of human Phosphoglycerate Kinase, an enzyme involved in glycolysis. It has been reported that EF1α and hPGK can sustain strong and stable expression of transgene in several cell types such as stem *cells (Hong et al., 2007)*, glial cells and neurons *(Deglon et al., 2000;*

Jakobsson et al., 2003). However, if the aim is to target a specific cell population, and avoid ectopic expression, the use of a cell-specific promoter may represent a better approach.

The rat neuron-specific enolase (rNSE) promoter (1.5Kb) is one of the most well characterized neuronal promoters. Delivery of lentiviral vectors carrying rNSE into rat brain resulted in 98% transduction of neurons, with absence of ectopic expression in glial cells. In contrast, the Glial Acidic Fibrillary Protein (GFAP) promoter (2.1Kb), was shown to direct expression specifically to astrocytes *(Jakobsson et al., 2003).*

However, several tissue-specific promoters comprise quite long sequences that span the 5' upstream region and sometimes some intronic sequences of the downstream gene. This poses great limitations for cloning into a lentiviral vector. As an example, the promoter of Neurofilament Heavy chain (NF-H) has been used with success for generation of transgenic animals with neuron-restricted expression. However the sequence is 8.5Kbp long and is not suitable for cloning in a lentivirus *(Hirasawa et al., 2001).* The promoter of Vescicular Acetyl-Choline Transporter (VAChT) has been used to target expression specifically in cholinergic neurons (including spinal cord motor neurons), but it is 6.4Kbp long *(Naciff et al., 1999).* On the other hand, when sufficiently short regulatory sequences are available, random integration of the vector into the host cell genome may lead to aberrant expression due to promoter and enhancer trapping.

For these reasons, efforts have been made to introduce further regulating sequences, like miRNA target sequences, to achieve de-targeting of transgene expression in undesired cell-types.

miRNA technology

miRNAs are endogenous small 21-23-nucleotide noncoding RNAs. Biogenesis of miRNA is initiated in the nucleus. miRNA genes are found in intergenic regions of the genome and in defined transcription units in both the sense and antisense orientations. They are transcribed by RNA polymerase II to form primary miRNA (pri-miRNA). These stem–loop pri-miRNAs are cropped to 70-nt pre-miRNAs by the Drosha–DGCR8 complex. Drosha is a nuclear RNase III that interacts with its cofactor, DGCR8, and produces RNA sequences that contain 5′ phosphate groups and 2-nt overhangs at their 3′ ends, starting from transcripts that contain a 5′-end cap structure and a polyA-tail sequence. After processing by Drosha, the pre-miRNAs are moved to the cytoplasm by a nuclear transport receptor complex. Once in the cytoplasm pre-miRNAs are processed by Dicer into ~22-nt mature miRNAs that are further unwound by an RNA helicase. Subsequently the antisense strand of so called miRNA/miRNA* duplex is assembled into an effector protein complex (miRNP). The miRNP then specifically interacts with the target mRNAs, generally at the 3'UTR, thus inhibiting translation *(Meister and Tuschl, 2004)* (**Figure 1.16**).

Many miRNAs have a distinct developmental and tissue-specific expression pattern, and they may play a pivotal role in defining cell identity. Based on this evidence, recent works by Brown and colleagues have demonstrated that microRNAs (miRNAs) may represent a new tool to control viral-vector mediated transgene expression *(Brown et al., 2006; Brown et al., 2007).* The authors introduced sequences targeted by cell-specific miRNAs into the genome of lentiviral vectors with the aim of preventing transgene expression in undesired cell lineages. Briefly, four tandem copies of a 23bp sequence with perfect complementarity to either mir-142-5p or mir-142-3p were inserted into the 3'-untranslated region of green fluorescent reporter gene inside a lentiviral vector. mir-142-5p and mir-142-3p were chosen because they are enriched in hematopoietic cell lineages. This strategy demonstrated that miRNA selection can

selectively de-target viral vector-mediated gene expression in hematopoietic cells in vivo.

This technological advancement is gaining great interest for the design of more selective lentiviral vectors, however studies to identify suitable miRNA sequences with tissue-specific expression are still ongoing

Figure 1.16. Overview of genesis and function of miRNA sequences

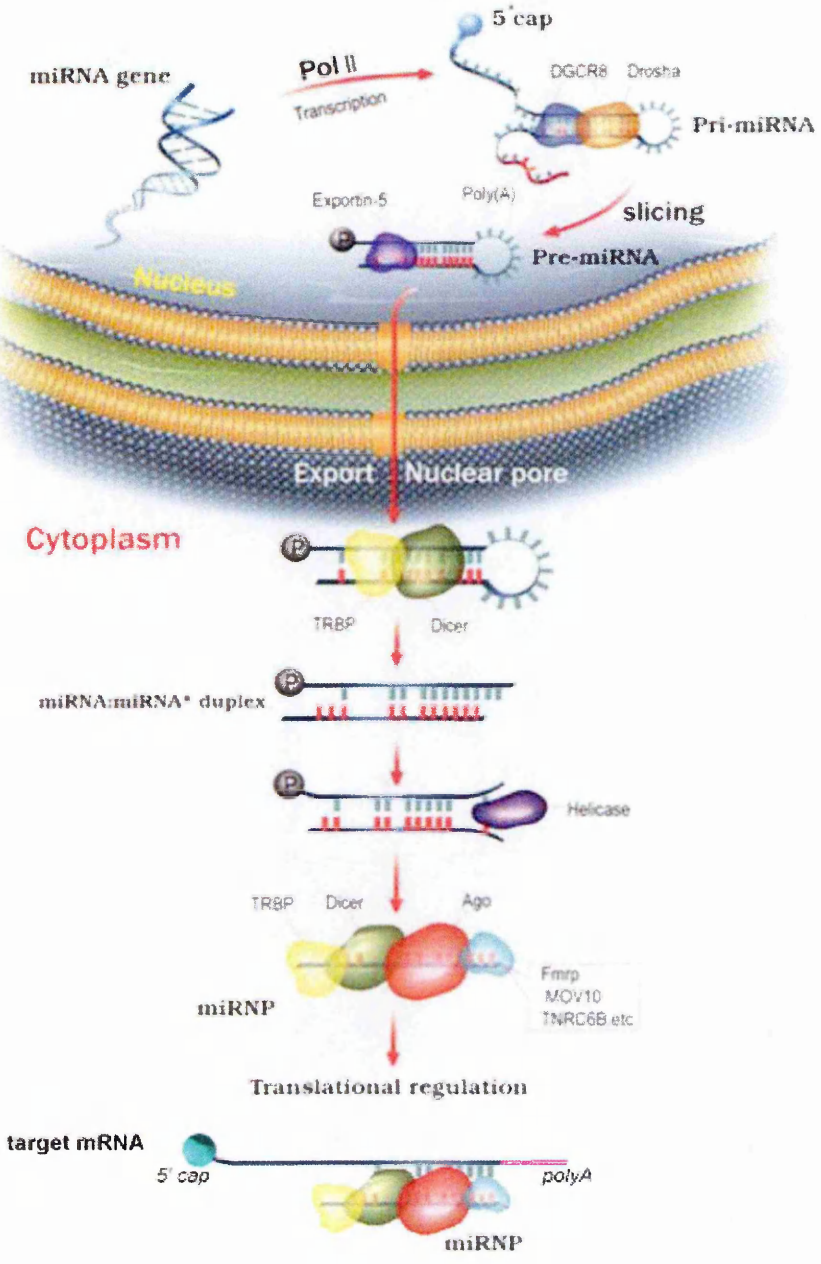

adapted from Chang et al., Hum Mol Gen 2009; 19(R1):R18-R26

1.7 HYPOTHESIS OF THE STUDY

The hypothesis of this study is that progressive loss of motor neurons seen in ALS is caused or is mediated by an upregulation of pro-degenerative p38MAPK and/or by insufficient activation of pro-survival Akt signalling pathways. Therefore, molecular inhibition of p38MAPK signalling or molecular activation of Akt could act to inhibit neuronal loss thereby modifying disease progression. In order to test this hypothesis we have developed lentiviral vectors to deliver siRNAs against p38MAPK and to deliver constitutive forms of Akt to a transgenic mouse model of ALS.

1.8 AIMS OF THE STUDY

- To test if selective activation of the Akt pro-survival pathway within motor neurons can effectively inhibit neurodegeneration and modify disease progression.
- To determine in vivo if a knock down of the p38MAPK pathway in glial cells and/or motor neurons in the SOD1G93A overexpressing mouse model of familial ALS influences the neurodegenerative process.

<u>These are specific issues pursued during the study:</u>

- Development of a lentiviral vector construct that allows selective expression of transgenes in motor neurons in vivo
- Induction of Akt pathway through expression of a mutant constitutively active isoform of Akt
- Intraspinal delivery of lentiviral vectors expressing constitutively active Akt in SOD1G93A mice, and analysis of the effect on disease progression and motor neuron survival
- Identification of candidate shRNA sequences targeting murine p38MAPK alpha

- In vitro validation of the potential neuroprotective effect of p38MAPK alpha downregulation
- Instraspinal delivery of lentiviral vectors expressing p38MAPK-targeted shRNA in SOD1G93A mice, and analysis of the effect on disease progression and motor neuron survival

CHAPTER 2

MATERIALS & METHODS

2.1 MATERIALS AND REAGENTS

2.1.1 Plasmids

- pAKT3: cDNA of human AKT3 gene, Transcript variant nr.2 (accession number NM_181690.1) fused at the N-terminal with HA-tag, and cloned in pCMV5. The plasmid was kindly provided by Dr. B. Hemmings, FMI, Switzerland.
- pMyr.AKT1: cDNA of human AKT1 gene (accession number NM_001014432) fused at the N-terminal with HA-tag a myristilation sequence, and cloned in pcDNA3.1-H+. The plasmid was kindly provided by Dr B. Hemmings, FMI, Switzerland.
- LV.NSE: lentiviral vector plasmid containing the rat Neuron Specific Enolase (rNSE) promoter and GFP as reporter gene. The plasmid was kindly provided by Dr. C. Lundberg, Lund University, Sweden.
- pHb9: plasmid containing 11 Kilobases of the 5' flanking region of Hb9 transcription factor. It was kindly provided by Dr. T. Jessell, Columbia University, USA.
- Bg.GFP: plasmid containing the β-globin minimal promoter and GFP as reporter gene. It was kindly provided by Dr. J. Johnson, UT Southwestern Medical Center, USA.

A map of the plasmid, with relevant features and restriction sites, is shown below.

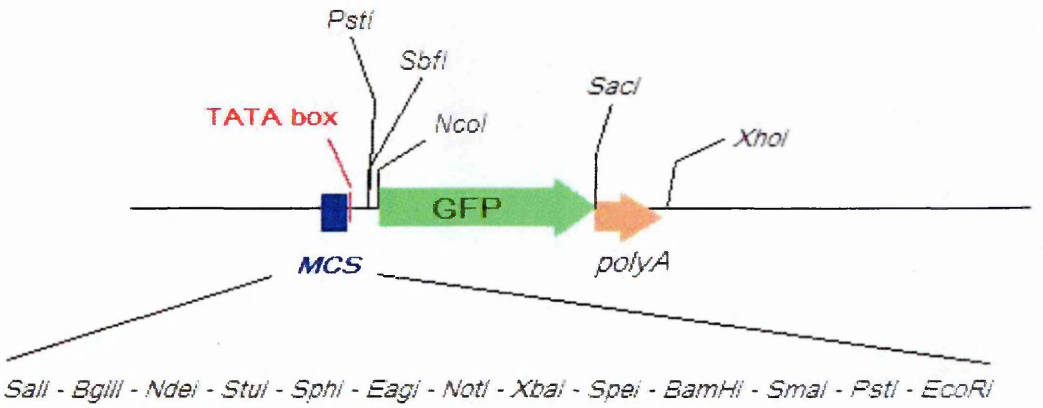

- pRabies-G: plasmid containing a sequence encoding for Rabies virus G glycoprotein (Rabies envelope). It was kindly provided by Dr. M. Sena-Estevez, Massachusetts General Hospital, USA.
- pMD2G: plasmid containing a sequence encoding for Vescicular Stomatitis Virus G glycoprotein (VSVG envelope). It was purchased from BD Biosciences (San Jose, California, USA).
- pCMVd8.74: adjuvant plasmid, carrying the genes encoding for viral capsid (gag) and reverse transcriptase (pol), under a REV-Responsive Element (RRE). It was provided by Trono Lab (Lausanne, Switzerland).
- pRSV.REV: adjuvant plasmid, carrying the gene encoding for REV transcription factor under Rous Sarcoma Virus (RSV) promoter. It was provided by Trono Lab.
- pLVTHM: lentiviral vector plasmid, containing GFP reporter gene under hEF1alpha ubiquitarious promoter. This plasmid contains also a cloning site for shRNAs (MluI-ClaI), under H1 RNA polymerase III promoter. It was provided by Trono Lab.

A map of the plasmid, with relevant features and restriction sites, is reported below.

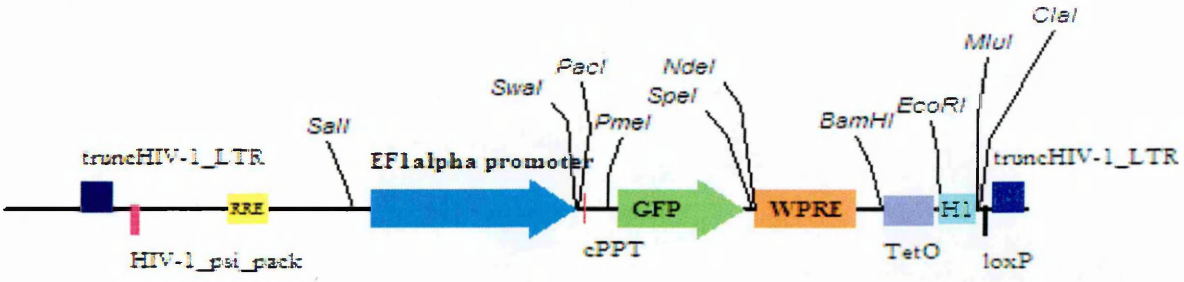

- pWPXLd: : lentiviral vector plasmid, containing GFP reporter gene under hEF1α ubiquitarious promoter. This plasmid also contains the post-transcriptional regulatory element of the Woodchuck hepatitis virus (WPRE) that enhances mRNA translation. It was purchased from Addgene Repository (Addgene Plasmid 12257).

A map of the plasmid, with relevant features and restriction recognition sites, is reported below.

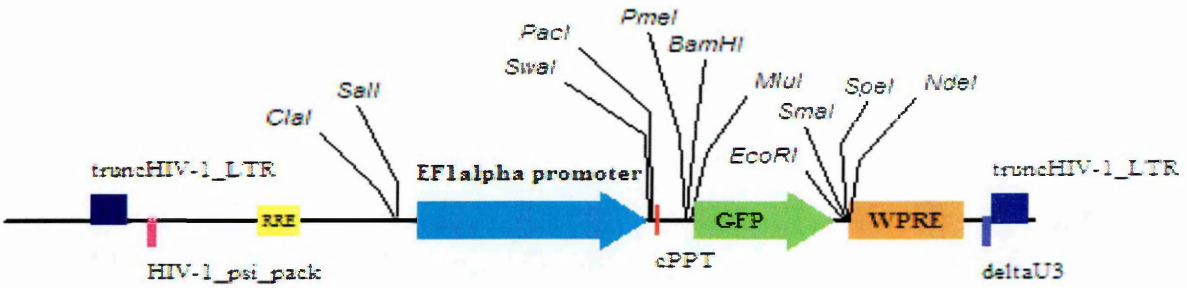

- pLKO.1: lentiviral vector plasmid, containing Puromycin resistance gene (Puro R) under hPGK ubiquitarious promoter. This plasmid contains also a cloning site for shRNAs, under U6 RNA polymerase III promoter. It was purchased from Sigma (St. Louis, Missouri, USA).

A map of the plasmid, with relevant features and restriction recognition sites, is reported here on the right side.

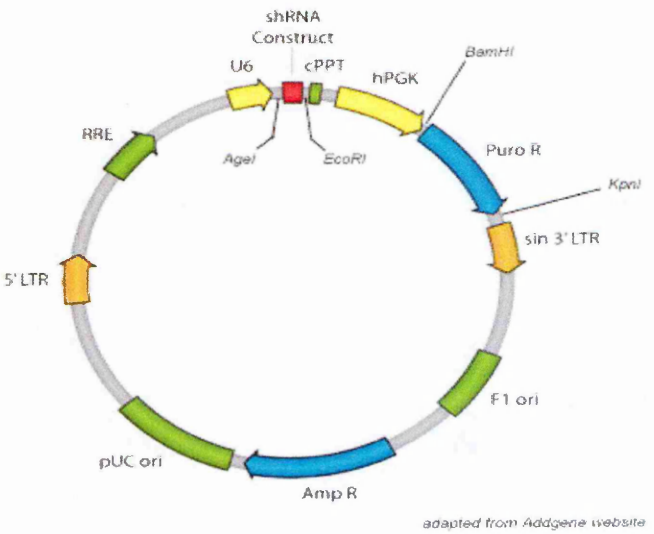

- TRC-shRNA: set of 5 different lentiviral vector plasmids, derived from pLKO.1, each containing a different candidate shRNA sequence targeting
- murine MAPK14. It was purchased from Open Biosystems (Huntsville,

- Alabama, USA).

Table 2.1. List of the different vectors produced and utilised in the project

Name	Original plasmid	Transgene		Reporter	
		Promoter	Gene	Promoter	Gene
WPX.NSE.GFP	WPXLd	//	//	rNSE	GFP
Bg.AB	Bg.GFP	//	//	Hb9.AB	GFP
Bg.1.6Kb	Bg.GFP	//	//	Hb9.1.6Kb	GFP
W.AB	WPXLd	//	//	Hb9.AB	GFP
W.1.6Kb	WPXLd	//	//	Hb9.1.6Kb	GFP
Myr.AKT3	pcDNA3.1	CMV	Myr.AKT3	//	HAtag *(fused to Myr.AKT3)*
WPX.Myr.AKT3	WPXLd	EF1alpha	Myr.AKT3	//	HAtag *(fused to Myr.AKT3)*
W.1.6.Myr.AKT3	WPXLd	Hb9.1.6Kb	Myr.AKT3	//	HAtag *(fused to Myr.AKT3)*
shRNA nr.7	pLKO.1	U6	shRNA nr.7	hPGK	GFP
shRNA nr.7*	pLVTHM	H1	shRNA nr.7*	EF1alpha	GFP

2.1.2 Antibodies

Actin. Mouse monoclonal antibody (Chemicon-Millipore, Billerica, Massachusetts, USA). It reacts with all six isoforms of vertebrate actin. *Working dilution for immunoblot: 1:5000.*

ChAT. Mouse monoclonal antibody (Chemicon-Millipore). It reacts with Choline Acetyl Transferase, an enzyme specifically present in Cholinergic neurons. *Working dilution for immunohistochemistry: 1:200*

CD11b. Rat polyclonal antibody (made in house). It detects the CD11b antigen also known as Mac-1 antigen, found on mouse macrophages, their precursors and granulocytes. *Working dilution for immunohistochemistry: 1:1000.*

CNPase Mouse monoclonal antibody (Chemicon-Millipore). It reacts specifically with 2', 3'-cyclic nucleotide 3'-phosphodiesterase (CNPase), an enzyme found almost exclusively in oligo-dendrocytes and Schwann cells. *Working dilution for immunohistochemistry: 1:400.*

ERK1,2. Mouse monoclonal antibody (Zymed-Invitrogen, Carlsbad, California, USA). It recognizes p42 and p44 isoforms of Extracellular regulated kinase. *Working dilution for immunoblot: 1:1000.*

GFAP. Mouse monoclonal antibody (Chemicon-Millipore). It reacts with Glial Fibrillar Acidic Protein, a cytoskeletal protein typically found in glial cells such as astrocytes. *Working dilution for immunohistochemistry: 1:2500.*

GFP. Rabbit polyclonal antibody (Molecular Probes-Invitrogen, Carlsbad, California, USA). It recognizes Green Fluorescent Protein and its mutant isoforms, specifically. *Working dilution for*

immunohistochemistry: 1:1500.

HA-tag. Mouse monoclonal antibody (Cell Signaling Technology, Danvers, Massachusetts, USA). It detects recombinant proteins containing the HA epitope tag. *Working dilution for immunohistochemistry: 1:100; for immunoblot:1:1000.*

JNK. Rabbit polyclonal antibody (Cell Signaling Technology, Danvers, Massachusetts, USA). It detects c-jun N-terminal kinase. *Working dilution for immunoblot:1:1000.*

PI3Kp85. Rabbit monoclonal antibody (Upstate-Millipore). It recognizes p85 subunit. This protein binds to activated (phosphorylated) protein-Tyr kinases, through its SH2 domain, and acts as an adapter, mediating the association of the p110 catalytic unit of PI3K to the plasma membrane. *Working dilution for immunoblot: 1:1000.*

p38 alpha. Rabbit polyclonal antibody (Cell Signaling Technology). It recognizes alpha isoform of p38 MAPK, specifically. *Working dilution for immunoblot: 1:1000.*

p38 tot Rabbit polyclonal antibody (Cell Signaling Technology). It recognizes all four isoforms of p38MAPK. *Working dilution for immunoblot: 1:1000.*

Phospho-Akt. Rabbit polyclonal antibody (Cell Signaling Technology). It detects Akt1 only when phosphorylated at serine 473, and Akt2 and Akt3 only when phosphorylated at equivalent sites. *Working dilution for immunoblot: 1:1000.* For immunohistochemistry experiments a rabbit monoclonal (IHC specific) antibody from the same company was used. *Working dilution: 1:500.*

Phospho-eIF2α. Rabbit polyclonal antibody (Cell Signaling Technology). It detects endogenous eIF2α only when phosphorylated at Ser^{51}, as a marker of induction of Interferon response. *Working dilution for immunoblot: 1:1000.*

Phospho-GSK3β. Rabbit polyclonal antibody (Cell Signaling Technology). It detects endogenous levels of GSK-3b only when phosphorylated at Ser^9, a specific target of activated Akt. *Working dilution for immunoblot: 1:1000.*

Phospho-JNK. Rabbit polyclonal antibody (Cell Signaling Technology). It detects endogenous levels of JNK only when phosphorylated at Thr^{183}/Tyr^{185}. *Working dilution for immunoblot: 1:1000.*

Phospho-p38. Rabbit monoclonal antibody (Cell Signaling Technology). It detects endogenous levels of p38 MAPK only when dually phosphorylated at Thr^{180} and Tyr^{182}. *Working dilution for immunoblot: 1:1000.*

Phospho-STAT1/2. Rabbit polyclonal antibody (Cell Signaling Technology). It detects phosphorylated tyrosine 701 of p91 Stat1 and also the p84 splice variant, as a marker of induction of Interferon response. *Working dilution for immunoblot: 1:1000.*

2.1.3 Reagents for molecular biology

Restriction Enzymes were purchased from New England Biolab (Ipswich, Massachusetts, USA).

T4 DNA Polymerase, T4 DNA Ligase, Thermosensitive Alkaline Phosphatase and Polynucleotide Kinase was purchased from Promega (Madison, WI, USA).

Pfx proof-reading DNA polymerase was purchased from Invitrogen.

DH5alpha bacteria were purchased from Invitrogen.

SC101 bacteria were purchased from Stratagene (Cedar Creek, Texas, USA). This strain, at variance with DH5alpha is dam-negative. It is used to produce plasmids when cutting with dam-sensitive restriction enzymes is required.

Kits for MINI- MIDI- and MAXI-preps, and kit for DNA-Clean up were purchased from Promega.

Kit for DNA gel-extraction was from Quiagen (Hilden, Germany).

All salts and solutions, where not specified, were from Sigma (St. Louis, Missouri, USA).

2.1.4 Cell lines

HEK293 (human endothelial kidney) cell line, *293T cell line* (a cell line derived from HEK293 cells by stable trasfection of Large T antigen) and *NIH3T3 murine fibroblast cell line* were obtained from Dr. Roberto Piva (CeRMS - Turin). The cell lines were obtained from Dr. Roberto Piva (CeRMS - Turin). Cells were plated in Dulbecco's Modified Medium, 10% FCS, 1% glutamine, 1% penicillin, 1% streptomycin and maintained at 37°C in a humidified 5% CO_2 incubator.

293T cells were used as packaging cell line for lentiviral vector production.

2.2 METHODS

2.2.1 LENTIVIRAL VECTOR PRODUCTION

High titre production of lentiviral vectors

Production of high titre viral vectors was performed by trasfection of 293T cells with 4 plasmids: pRSV-Rev and pCMVdR8.74 encoding gag/pol/rev proteins, pVSV-G for expression of VSV-G protein or pRabies for expression of Rabies G protein, and an appropriate transfer vector (pLVTHM, pWPXLd, or pLKO).

Briefly, 293T cells were plated at 70% confluence in Dulbecco's Modified Medium, 10% FCS, 1% glutamine, 1% penicillin, 1% streptomycin and maintained at 37°C in a humidified 5% CO2 incubator. Co-trasfection of the four plasmids was performed with Effectene kit (Quiagen) according to the manufacturer's instructions. After 16h the medium was replaced by fresh culture-medium containing 10mM Sodium Butyrate. Supernatants were harvested 24h and 48h post-transfection, filtered through a 0.45 micron filter

and stored at 4°C. New medium with 10mM Sodium Butyrate was added to the cells after the first harvesting. Concentrated viral stocks were produced by ultracentrifugation at 50,000g at 4°C for 2h. Viral pellets were resuspended in sterile PBS and then stored at -80°C until required.

End point dilution assay

This assay used HEK293 cells to measure the viral titre (Transfection Unit/mL) of each concentrated stock *(Blesch, 2004).* Briefly, cells were passaged and plated in 24 wells plates at a concentration of 50,000 cells/well, and then infected with 2 μL of serial ten-fold dilutions of each viral vector, in the presence of 8 μg/mL polybrene (Sigma). At 72h post-infection the wells infected with the highest dilution of virus and still containing cells expressing the reporter gene were taken into account. The titre was deduced by the number of positive cells measured in those wells, as assessed by visual counting at fluorescence microscope or by FACS.

2.2.2. G93A TRANSGENIC MOUSE MODEL OF ALS

Transgenic mice expressing about 20 copies of mutant human SOD1 with a Gly93Ala substitution (G93A mice) were originally obtained from Jackson Laboratories (B6SJL-TgNSOD-1-G93A-1Gur); the line is hemizygous for the transgene (Gurney et al., 1994). Male G93A mice were repeatedly backcrossed with non transgenic female C57BL/6 mice, obtaining transgenic mice on the homogeneous C57BL/6 genetic background. The animals used in the experiments are on the homogeneous 129SV genetic background. They have been generated in the laboratory by repeated backcross of G93A C57BL/6 males with non transgenic female 129SV mice.

These mice develop the first signs of neuropathology at the motor neuronal level around 4 weeks of age, while the first symptoms of muscular dysfunction appear

around 14 weeks of age, with progressive reduction in the extension reflex of the hind limbs, when the mice are raised by the tail. At about 15 weeks of age the mice show a progressive muscular weakness, revealed by the increasing difficulty in staying on a rotating bar. At 18 weeks of age the animals show hindlimb complete paralysis, and cannot recover if laid on one side.

Mitochondrial vacuolisation and swelling are among the earliest events observed at the histopathological level. Later, but still at the asymptomatic stage, G93A mice show signs of cytoskeletal disorganization in the motor neurons, with the accumulation of phosphorylated neurofilaments in the perykaria. Reactive gliosis, which involves activation of astrocytes and microglia, is detectable with the degeneration of motor neurons and becomes prominent at symptomatic stages, when the cell loss is remarkable *(Bendotti et al., 2001a; Ciavarro et al., 2003; Tortarolo et al., 2003).*

Procedures involving animals and their care were conducted in according to the institutional guidelines, that are in compliance with national (D.L. no. 116, G.U. suppl. 40, Feb. 18, 1992, Circolare No.8, G.U., 14 luglio 1994) and international laws and policies (EEC Council Directive 86/609, OJ L 358, 1 DEC.12, 1987; NIH guide for the Care and use of Laboratory Animals, U.S. National Research Council, 1996). The animals were housed under standard conditions (22 ± 1°C, 60% relative humidity, 12 hour light/dark schedule), 3-4 per cage, with free access to food (Altromin, MT, Rieper) and water.

Mouse genotyping

Genotyping was performed on tail biopsies collected from mice at weaning age. The samples were completly digested by overnight incubation at 55°C in Direct-PCR Lysis Buffer (Viagen Biotech, Los Angeles, California, USA) containing 0.1 µg/µl of Proteinase K (Promega). The following day they were incubated at 85°C for 30 minutes, to inactivate Proteinase K, and then stored at –20°C till the

screening.

PCR screening

50 ng of DNA from each animal were used as a substrate for qualitative PCR, in a mix containing 1X PCR buffer, GoTaq DNA Polymerase (0.25 U), deoxyNTPs (250 µM each), specific forward and reverse primers (0.5 µM each) in a final volume of 10 µl. All the reagents were purchased by Promega, except for primers that were synthesized by Invitrogen (Invitrogen).

The primer sequences and their annealing temperatures are reported below:

Gene	**Accession nr.**	**Primers**	**Sequence (5'-3')**	**Ta**
SOD1	NG_008689.1	Forward	CATCAGCCCTAATCCATCTGA	58°C
		Reverse	CGCGACTAACAATCAAAGTGA	58°C

The thermocycling profile used for amplification is reported below:

1. 94°C for 2 min (denaturation)
2. 94°C for 45 sec (denaturation)
3. 58°C for 45 sec (annealing)
4. 72°C for 1 min (amplification)

   Steps from 2 to 4

   repeated for 30 cycles
5. 72°C for 10 min (final amplification)

PCRs were performed in a MJ thermocycler (distributed by Bio-rad laboratories, Hercules, California, USA). Amplicons were resolved in 1% agarose gel, 2 µg/ml Ethidium bromide in Tris-Acetate-EDTA (40 mM Tris, 0.35% vol/vol acid acetic, 1 mM EDTA).

2.2.3 SURGICAL PROCEDURES FOR DELIVERY OF LENTIVIRAL VECTORS IN VIVO

Before delivery the concentrated viral stocks were thawed on ice and 4 μg/mL polybrene (Sigma) were added to the viral solution. The mix was then kept on ice during the whole procedure of administration.

All surgical procedures were performed under deep anesthesia by Equitensin (1% phenobarbitol/ 4% (vol/vol) chloral hydrate, 5 μL/g, ip). After surgery animals were kept on a warm pad for 30 minutes and then placed in separated cages for recovery.

Injection in peripheral muscles

Animals were first shaved in the regions of injection (i.e., gastrocnemius muscles). The viral solution was then administered through a 30 Gauge needle connected to a 10 μL Hamilton syringe and injected inside the muscle, according to the procedure already described *(Azzouz et al., 2004a)*.

Injection in the cerebral lateral ventriculi

Mice were placed in a stereotaxic frame (Kopf Instruments, Tujunga, California, USA). A midline incision was performed, and the skull was opened with a dental drill at two sites, 1.0 mm lateral to the bregma. A 30 Gauge needle was then inserted down to a depth of 2.0 mm under the dura. 5 μL/site of viral solution were then delivered with an infusion pump at a flow rate of 0.5 μL/min. The needle was left in place for an additional minute then gently withdrawn, and the skin was closed with metal clips.

Lumbar intrathecal administration

After shaving of the back at lumbar level, the junction between L_6 and sacral vertebrae was identified and a transverse cutaneous incision (1 cm) was performed at that level. A 30 gauge bevelled needle connected to a 10microL Hamilton syringe was then inserted between L_5 and L_6 spinous process as described *(Hylden and Wilcox, 1980)*, and outlined in **Figure 2.1**. The viral solution (5 μL) was injected in 1 min.

Figure 2.1. Scheme of the site of lumbar intrathecal injection

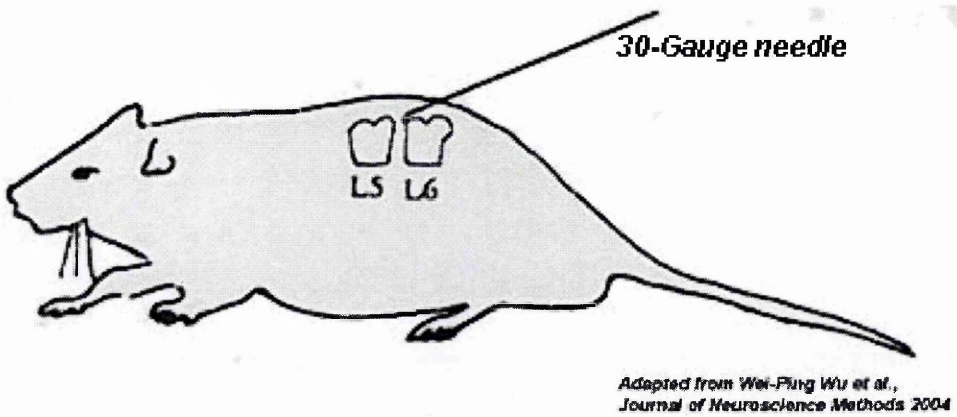

Schematic representation of intrathecal injection procedure. The needle was vertically positioned on the spinous process of L_6 vertebra, then inclined to 20°C, as referred to the plane of backbone, and finally inserted for 5 mm through the space between spinous and transverse processes of L_5 and L_6 vertebrae. Appearance of tail flick reflex during injection of the needle was considered as confirmation of proper procedure.

Injection into spinal cord parenchima after laminectomy

Animals back was shaved at dorsal level, and a cutaneous incision (3 cm) was performed to expose the backbone. T_{13} and L_1 vertebrae were identified, and exposed by separation of dorsal and intervertebral muscles. Animals were then placed on a Cunningham Spinal Cord Adaptor (Stoelting, Dublin, Ireland) mounted on a stereotaxic frame, and laminectomy of L_1 vertebra was done to uncover lumbar spinal cord at levels L_2-L_4 (**Figure 2.2**). Using a glass capillary (40±5 μm diameter) viral solution was injected bilaterally in two sites separated by 2 mm along the spinal cord (1.5 μL/site), with a flow rate of 0.2 μL/min.

Stereotaxic coordinates were referred to the midline of the dorsal horn (DH) of spinal cord; the needle was positioned at +/- 0.5 mm aside from the midline, then it was deepened into the parenchyma to 0.8 mm below the pia mater to reach the ventral horn (VH) where motor neurons are located; the injector was left in place for 1 min and then retracted for 0.2 mm before starting the delivery, as shown in **Figure 2.3**. After completion of the injection the needle was left in place for additional 2 min and then gently withdrawn. Dorsal muscles were then justaxposed by absorbable sutures, and skin sutured and disinfected.

Figure 2.2. Visualisation of the site of laminectomy

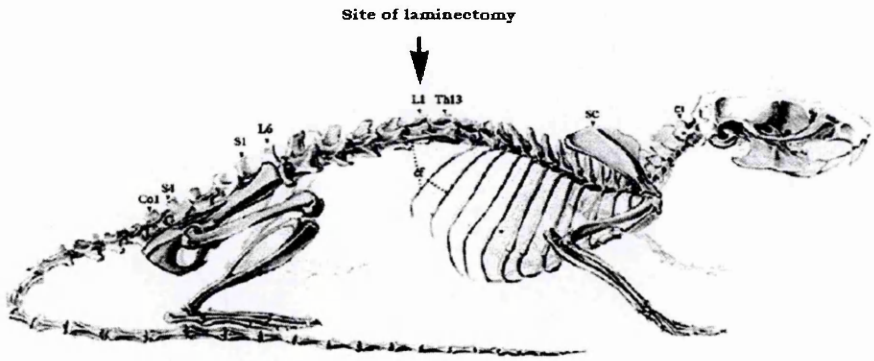

C1	1st cervical vertebra	SI	1st sacral vertebra
Sc	Scapula	S4	4th sacral vertebra
Th13	13th thoracic vertebra	Col	1st coccygeal vertebra
L6	6th lumbar vertebra	Cf	costae fluctuantes

Adapted from Cunningham Sp. Ad. operation manual

Figure 2.3. Scheme of the injection sites in spinal cord parenchima

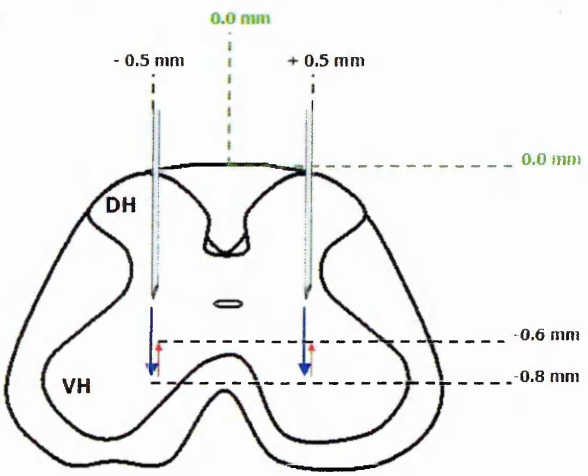

Visualisation of the spinal cord in the coronal plane. The stereotaxic coordinates used for injection are referred to the dorsal longitudinal midline, at level of pia mater. DH=dorsal horn, VH=ventral horn.

2.2.4 ANALYSIS OF MOTOR PERFORMANCE AND DISEASE PROGRESSION

At the age of 80 days, body weight was recorded and mice were tested for extension reflex and for motor performance (rotarod and grid tests) as described below. These tests were initially performed to monitor animal performance at the pre-symptomatic stage, before surgical operation, and to help animals to get used to post-surgery testing sessions.

Extension reflex

Animals were suspended by the tail, and adduction reflex was monitored for right and left hindlimb. A maximum of three points/limb were assigned in case of normal extension reflex; two to one point/limb were assigned for mild and strong deficits, respectively. Zero points were assigned when absence of reflex was observed.

Rotarod test

The test was performed using the accelerating Rotarod apparatus (7650 model, Ugo Basile). Once the animals were positioned on the rotating bar, testing commenced and the rotarod was accelerated at a constant rate of 4.2 rpm/min from 7 rpm to 28 rpm for a maximum of 5 min. The time (seconds) at which the animal fell from the rotarod was registered. Animals were given a maximum of three trials. Mice that managed to remain on the rod for the entire test duration were returned to the cage; their task was considered fully accomplished. Animals falling before 5 min were given 5 min rest and were then re-tested. The time of the best trial was registered and considered for the statistical analysis.

Grid test

Animals were posed on a horizontal grid and supported until they grabbed the

grid with both their fore and hind paws; the grid was then inverted so that the mice were allowed to hang upside down. Time spent hanging, before falling from the grid, was taken into account. Timing commenced as the grid was inverted and then stopped when the animal fell, for a maximum of 90 sec. Animals that fell before 90 sec repeated the trial, for a maximum of three trials, with at least 5 min of rest between each. The measures of the best performance were used for statistical analysis.

At the age of 84 days animals underwent surgical operation; laminectomy was performed (as already described in section 2.2.3) and viral vectors were injected in the spinal cord parenchyma. At the day after operation, animals were observed to check for motor deficits, due to accidental damage to spinal cord. Only healthy animals were kept for further analysis; unhealthy mice were sacrificed and not further considered in the analysis.

One week after operation, animals were re-tested for motor performances. Tests were then repeated twice a week until the end stage of the disease. Body weight was also recorded before each test session.

Mice at the end stage of the disease that were unable to right themselves within 30 sec after being placed on one side were euthanized by a high dose of anaesthetic and perfused for immunohistochemical analyses, or decapitated for collection of fresh tissues for western blot analysis. The age at death was recorded.

2.2.5 IMMUNOHISTOCHEMISTRY

Preparation of Tissue

Mice were anesthetized with Equithesin and transcardially perfused with 50 ml of phosphate buffered saline (PBS, phosphate buffer 0.01M, 0.9% NaCl) followed

by 50 ml of 4% paraformaldehyde solution in PBS. Brains and spinal cords were rapidly removed, post-fixed in fixative for 3 h, transferred to 20% sucrose solution in PBS overnight, then to 30% sucrose solution until they sank, and finally frozen in 2-methylbutane at −45°C and conserved at -80°C until required. Before freezing, spinal cord was divided in cervical, thoracic and lumbar segments and included in Tissue-tek OCT compound (Sakura, Zoeterwounde, The Netherlands).

Tissues were cut on a cryostat at -20°C to obtain sections of 30 µm. Brain was cut in the horizontal or coronal plane, while spinal cord was cut longitudinally or in the coronal plane. The lumbar level of the spinal cord was chosen for the experiments, because the hindlimbs of G93A mice are affected earlier and more severely compared to the forelimbs.

NISSL staining

This staining highlights the rough endoplasmic reticulum. It is used to view cell sizes and numbers in the nervous system.

For the staining procedure, sections were cut on cryostat at –20°C then mounted on gelatin-covered glass slides, and dried overnight at room temperature. The following day slides were dipped in water for 1 min, then in a graded series of ethanol (70%, 96% then absolute ethanol) and finally dipped in xylene. Following the xylene step the slides were dipped back to water and passed through the ethanol series in reverse sequence. After dipping in water for 1 min, slides were immersed into cresyl-violet 0.5% solution in water for 3 min, then washed 10 times in water, 10 times in 70% ethanol and dipped for 3 min in 3% acetic acid solution in ethanol. After 30 seconds slides were moved to 96% ethanol solution and then to absolute ethanol, and finally to xylene. Slides were finally coverslipped with DPX mounting medium (BDH, Poole Dorset, UK).

For some immunohistochemical experiments, with the aim of obtaining quantitative data, NISSL staining was performed on serial sections (1 every 10

sections, for a total of 24 sections for animal) from the spinal cord, starting from lumbar level L_2.

For colocalization experiments this procedure was substituted with incubation of free floating sections in Neuro Trace fluorescent NISSL stain (Molecular Probes-Invitrogen) at the appropriate wavelenght, dil.1:500 in PBS for 10 min.

Indirect immunofluorescence

Free-floating sections were treated for 1 h with a blocking solution composed of normal serum and Triton X-100 at the appropriate concentration in PBS. Subsequently, the sections were incubated overnight at 4°C with the primary antibody diluted in PBS containing normal serum and Triton X-100. Then, after three washes in PBS, samples were treated for 1 h with the appropriate secondary antibody conjugated to fluorochromes with various wavelengths (Alexa 488, 594 and 647, Molecular Probes-Invitrogen), diluted 1:500 in 1% normal serum 1% in PBS. Finally, sections were mounted on slides and coverslipped with a solution of Glycerol 50% in PBS. Control sections were incubated without the primary antibody.

Amplified immunofluorescence by streptavidin

Blocking was performed for 1 h at RT with normal serum and Triton X-100 at appropriate concentration in PBS. Subsequently, sections were rinsed and then incubated for 15 min at room temperature with Avidin Solution (Vector Labs, Peterborough, UK), then rinsed in PBS and incubated for 15 min at room temperature with Biotin Solution (Vector Labs) to block endogenous biotins. Samples were probed overnight at 4°C with the primary antibody, diluted in PBS containing normal serum and Triton X-100. The following day, after three washes in PBS, they were incubated with biotinylated secondary antibody (Vector Labs) at dil. 1:200 in 1% normal serum and PBS for 1 hour, then washed three times with PBS and finally incubated for 30 min with Streptavidin coniugated to

appropriate Alexa fluorochrome (Molecular Probes-Invitrogen). Subsequently, the sections were again washed with PBS and mounted on slides and coverslipped with a solution of Glycerol 50% in PBS. In each immunohistochemical experiment, some of the sections were processed without the primary antibody, in order to verify the specificity of the staining.

Amplified immunofluorescence by tyramide

Blocking was performed for 1 h at RT with normal serum and Triton X-100 at appropriate concentration in PBS. Subsequently, sections were rinsed and then incubated for 15 min at room temperature with 1% hydrogen peroxide to block endogenous peroxidases then rinsed in PBS. Samples were probed overnight at 4°C with the primary antibody, diluted in PBS containing normal serum and Triton X-100. The following day, after three washes in PBS, they were incubated with biotinylated secondary antibody (Vector Labs) at dil. 1:200 in 1% normal serum and PBS for 1 hour, then washed three times with PBS and incubated for 90 min in Blocking Reagent (Perkin Elmer, Waltham, Massachusetts, USA). Sections were incubated for 30 min in Streptavidin coniugated to horseradish peroxidase dil. 1:100 in Blocking Reagent. They were then washed three times in TNT (0.04% Tween in 0.1M Tris/Cl pH 7.6); finally reaction was developped by incubation for 8 min in Tyramide (Perkin Elmer) dil. 1:300 in Amplification Diluent (0.003% H_2O_2 in 0.1M Borate pH 8.5). Subsequently, the sections were again washed with PBS and mounted on slides and coverslipped with a solution of Glycerol 50% in PBS.

Staining of nuclei

Samples were incubated for 10 min in Hoescht 33258 dye (Polysciences Inc., Epperlheim, Germany) dil. 1:500 in PBS, then washed three times in PBS.

Image analysis

Fluorescence-labelled sections were analyzed under an Olympus Fluoview laser scanning confocal microscope, using three lasers: Ar with a 488 nm emission line to acquire Alexa 488 signal, He-Ne green laser with a 543 nm emission line to acquire Alexa 594 signal, He-Ne red laser with a 633 nm emission line to acquire Cy5 signal, and UV-Ar laser with a 351 nm emission line to acquire Hoescht staining. Analysis in double or triple staining was done by sequential scanning in order to avoid cross talk between the channels.

NISSL stained samples, prepared for quantitative analysis, were examined under an Olympus BX61 light microscope and images of the ventral spinal cord were collected with a camera, using AnaliSYS software (Soft Imaging Systems, ver. 3.2). Measures of area and number of cells with clear nucleus and nucleolus in the ventral horn spinal cord were performed using ImageJ (public domain software) on the calibrated images previously collected. Motor neurons were defined as cells with area higher than 250μm^2, similarly to already published studies *(Azzouz et al., 2000; Kaspar et al., 2003).*

2.2.6 PRIMARY CELL CULTURES

Preparation of primary cell cultures from mice embryos were performed by Dr Massimo Tortarolo, Dr Dario Lidonnici, Dr Gabriella Spaltro and Dr Cristina Daleno of the Lab. of Molecular Neurobiology, Mario Negri Inst., Milan. Neurons from rat pups were prepared by Dr Alessandra Sclip, Dr Alessio Colombo, and Dr Cristina Ploia, of the Lab. of Biology of Neurodegenerative Disorders, Unit of Cell Death and Neuroprotection Mechanisms, Mario Negri Inst., Milan.

Astrocytes

Cortical primary astrocyte cultures obtained from 15-16 day old mouse embryos (C57/BL6) were prepared in accordance with the protocol in use in the laboratory and previously described *(Tortarolo et al., 2004).*

Spinal neuronal-astrocytic co-culture

Primary spinal neurons were prepared from 14 to 15 day old mouse embryos (species). Spinal cords were isolated by dissection and the meninges removed. Spinal cords were then mechanically dissociated using a fire-polished glass Pasteur pipette in phosphate-buffered saline (PBS, Ca2+ and Mg2+ free) supplemented with glucose (33 mM). The cell suspension was layered onto a 4% BSA cushion, centrifuged at 1,000 rpm for 10 min, and the cells from the pellet were resuspended in culture medium composed of Neurobasal (Gibco) supplemented with 10% inactivated horse serum, 16.5 mM glucose, 1 ng/mL BDNF, 2 mM glutamine, 100 μg/mL streptomycin and 60 μg/mL penicillin. A mixture of hormones and salts composed of insulin (25 μg/mL), transferrin (100 μg/mL), putrescine (60 μM), progesterone (20 nM) and sodium selenate (30 nM) (all from Sigma) was also added to the culture medium. Cells were plated (one spinal cord/8 wells) positioned in each well of 48-well Nunc multiwell plates that had been previously coated with a confluent monolayer of astrocytes, to help neuronal health and survival. Cells were cultured at 37°C in a humidified atmosphere of 95% air and 5% CO_2 and used after 5-6 days in vitro.

Cortical neurons

Primary cortical neurons obtained from the brains of two-day old Sprague-Dawley rat pups, were prepared in accordance with the protocol used in the Unit of Cell Death and Neuroprotection Mechanisms as previously described *(Borsello et al., 2003).*

2.2.7 INFECTION OF CELL CULTURES

Infection of cell lines

For infection experiments NIH3T3 cells were passaged and plated in 6 wells plates at a concentration of 100,000 cells/well. Viral supernatants, each containing a different shRNA sequence, were administered to cells in the presence of 8 μg/mL polybrene (SIGMA) as adjuvant of infection. At 72 h post-infection cells were harvested for protein or RNA extraction, or used for subsequent analyses.

Infection of primary cell cultures

Astrocytes, in 6 well plates, were infected when they reached 60% confluence (about 7 days in culture). Viral vector ($6x10^6$ TU/well) was added to the culture medium. Medium was then replaced one day after infection, and then every 4 days until the end of the experiment. Infection of neuronal cultures was performed one day after plating with concentrated virus ($2x10^6$ TU/well), in the absence of AraC. One day after infection fresh medium was added to the cells; araC was added to a final concentration of 10mM to inhibit glial cell proliferation. Cells were tested at 3-4 days of culture.

2.2.8 TRANSFECTION OF CELL CULTURES

Transfection of cell lines

One day before transfection cells were passaged in 6 well plates at 50% confluence. The following day cells were transfected with purified DNA construct using Effectene trasfection reagent (Quiagen) according to the manufacturer's instructions. 0.5 μg and 1.0 μg of DNA were used for each construct, to assure maximal efficiency of expression. Medium was replaced 16 h after transfection,

then at 72 h post-transfection cells were fixed with 2% PFA in PBS, or pelleted and lysed for analysis of protein expression.

Transfection of primary cell cultures

Primary mouse spinal cord neurons were plated on a confluent monolayer of astrocytes in 48 well plates according to the protocol already described. One day after plating cells were transfected with purified DNA construct 0.3 μg/well using Effectene transfection reagent (Quiagen) according to the manufacturer's instructions. Medium was replaced 5h after transfection, then at 72h post-transfection cells were fixed with 2% PFA in PBS, or pelleted and lysed for analysis of protein expression.

2.2.9 SEMI-QUANTITATIVE PCR

RNA extraction

Total RNA was extracted using the Trizol reagent (Invitrogen), purified according to the manufacturers' instruction and resuspended in sterile water. RNA was quantified by spectrophotometer. Moreover, to check its quality, 2 μg of each sample were loaded in electrophoresis gel and 18S and 28S ribosomal bands were considered as indicators of RNA integrity.

Synthesis of cDNA

The cDNA used for semi-quantitative-PCR experiments was obtained by reverse transcription of total RNA with a Moloney murine leukaemia virus reverse transcriptase (MuLV RT) from Gene Amplification RNA PCR-core kit (Applied Biosystems). Oligo d(T)16 were used to allow retro-transcription of any messenger harbouring the polyA tail. Briefly, 2 μg of RNA from each sample were used as a substrate for cDNA synthesis in a mix containing 1X PCR Buffer, MuLV reverse transcriptase (2.5 U/μL), RNAse inhibitor (1U/μl), oligo dT (2.5 μM), and deoxyNTP (1 mM each) in a final volume of 40 μL. The mixture was incubated for

10 min at RT, then for 15 min at 42°C, for 5 min at 99°C, for 5 min at 4°C and then stored at –20°C until required.

PCR experiments

Semi-quantitative PCR was performed in a MJ thermocycler (distributed by Bio-rad laboratories). 120 ng of cDNA from each sample were used as a substrate for PCR reaction, in a mix containing 1X PCR buffer, GoTaq DNA Polymerase (0.25 U), deoxyNTPs (250 µM each), specific forward and reverse primers (0.5 µM each) in a final volume of 10 µL. All the reagents were purchased by Promega, except for primers that were synthesized by Invitrogen (Invitrogen).

Primers were designed to anneal on two different exons on the target sequence, in order to obtain a 500bp amplicon from cDNA, and a much larger fragment in case of amplification from contaminating genomic DNA.

The primer sequences and their annealing temperatures are reported below:

Gene	**Accession nr.**	**Primers**	**Sequence (5'-3')**	**Ta**
p38-alpha	NM 011951.2	Forward	CAGGAGAGGCCCACGTTCTAC	64°C
		Reverse	CATCATCAGTGTGCCGAGCCA	64°C
Actin	NM 007393.1	Forward	TGGATGACGATATCGCTGCG	58°C
		Reverse	ACAGAGTACTTGCGCTCAGG	58°C

Each sample was tested for the same gene in two or three different PCR reactions simultaneously. Each reaction differed from the others for number of cycles in the thermocycling profile.

The thermocycling profiles used for amplification in semi-quantitative PCR experiments are shown below:

Thermocycling profile	**Gene**	**Ta**	**Reaction**	**N**
1. 94°C for 2 min (denaturation) 2. 94°C for 45 sec (denaturation) 3. **Ta** for 45 sec (annealing) 4. 72°C for 1 min (amplification) Steps from 2 to 4 repeated for **N** cycles 5. 72°C for 7 min (final amplification)	p38-alpha	64°C	1st 2nd 3rd	24 26 28
	Actin	58°C	1st 2nd	16 18

2.2.10 DETECTION OF VIRAL GENOME INTAGRETED IN HOST CELLS

Extraction of genomic DNA

Cells were plated in 48wells plates. 3 days after infection medium was removed and cells were washed twice with PBS. Then cells were incubated 5 min with 100 µL/well of Lysis Buffer (composition described below). A little scraper was used to aid lysis. Lysates were then collected and incubated at 55°C for 2h, and then kept on ice. 30 µL of ice cold Protein Precipitation Solution (Promega) were added to each sample. After centrifugation at 13000 rpm for 20min the supernatants were collected, and then DNA was extracted by ethanol precipitation.

Composition of Lysis Buffer (amout/sample):

80uL Nuclei Lysis solution (Promega)

20uL 0.5M EDTA

4uL Proteinase K (Promega)

PCR experiments

PCR was performed in a MJ thermocycler (distributed by Bio-rad laboratories),

applying the protocol already described in section 2.2.2, with a different set of primers, listed below.

Gene	Accession nr. or reference	Primers	Sequence (5'-3')	Ta
GFP	*(Cormack et al., 1996)*	Forward	ACCACATGAAGCAGCACGACT	58°C
		Reverse	CTTGTACAGCTCGTCCATGC	58°C
AKT3	AF124141.1	Forward	GCTTACCCATACGATGTTCCAG	64°C
		Reverse	TTATTCTCGTCCACTTGCAGAGT	64°C

2.2.11 IMMUNOBLOTTING

Protein extraction from cell lines and tissues

Ice-cold Lysis Buffer (50 mM Tris/HCl pH 8, 150 mM NaCl, 5 mM EGTA pH 8, 1.5 mM MgCl2, 10% Glycerol, 1% Triton X-100, 50 mM NaF, 10 mM NaPP, 10 mM Na3VO4, 100 mg/mL PMSF, 20 mg/mL Leupeptin, 20 mg/mL Aprotinin) was added to cell pellets (50 µL/confluent 35mm dish) or to tissue samples (8 µL/mg of tissue). Cells were lysed by incubating on ice for 15 min, while tissues were homogenised by a teflon-on-glass homogeniser. Lysates were then cleared by centrifugation at 13,000 rpm for 15 min at 4°C. Supernatants were then collected and stored at –80°C until required.

Protein concentration of supernatants was measured by BCA protein assay (Pierce-Thermo Scientific, Rockford, Illinois, USA) according to the manufacturer's instructions.

Protein extraction from primary cell cultures

The same protocol described in the previous section was used with minor modifications. Briefly, medium was removed and cells were washed with PBS twice, then ice-cold lysis buffer was added in the wells (150 µL/well). The cell-plate was incubated 15 min on ice, aiding cell detachment and lysis by using a

scraper. Lysates from two wells treated in the same way were then collected and pooled, and then clarified as described in the previous paragraph.

SDS-poly-acrylamide gel elecrophoresis (SDS-PAGE)

Prior to electrophoresis, aliquots of homogenate were boiled in SDS sample buffer (1.2% SDS, 5% β-mercaptoethanol, 5% glycerol, 25.5 mM Tris/HCl pH6.8, 0.6% glycine) at 95°C for 5 min. Equal amounts of total protein (30 µg) were separated on 10% Tris-glycine polyacrylamide gels and electroblotted onto 0.2 µM nitrocellulose membranes, 90V for 2h using a BioRad mini-transfer system. To check for even protein loading and transfer, membranes were briefly immersed in Ponceau-S stain (0.2% Ponceau-S in 3% trichloro-acetic acid) and rinsed in water. Membranes were then placed between plastic sheets and scanned for later analysis.

Immunoblotting

Membranes were rinsed in PBS to remove Ponceau-S stain and immersed in blocking buffer (5% non-fat milk in TBS pH 7.4, 0.1% Tween). Membranes were then probed with the primary antibody diluted in BSA 3% in TBS/Tween, washed 4 times in TBST, and incubated with HRP-conjugated secondary antibody (Sigma) 1:2000 for 1h at RT. Membranes were washed 3 times in TBST for 5 min and the signal detected by enhanced chemioluminescence (ECL) using ECL reagent (GE HealthCare) for various exposure times to obtain signal within the linear range. Films were scanned on an Epson scanner and band intensities measured using Image J (public domain software). The obtained values were normalized to actin staining and expressed as percentage of the basal value registered in the control samples (i.e. not transgenic tissues). Mean values were used for statistical analysis by Student's t-test. The statistical analysis was done using Prism 4 for Windows, version 4.03.

2.2.12 PCR-CLONING EXPERIMENTS

The cDNA HA.AKT3 was PCR amplified using pAKT3 plasmid as template, a forward primer containing 39bp coding for a myristilation sequence, and a proofreading Pfx DNA polymerase.

The composition of PCR buffer and thermocycling profile are shown below; the sequences of forward and reverse primers are shown in the table.

PCR buffer:

1X	Pfx Amplification Buffer
0.3mM	dNTPs solution
1mM	$MgSO_4$
0.3microM	Forward primer
0.3microM	Reverse primer
Pfx DNA pol.	1 Unit

Water to final volume of 20 μL

Thermocycling profile:

1.	94°C for 5 min	(denaturation)
2.	94°C for 15 sec	(denaturation)
3.	60°C for 30 sec	(annealing)
4.	68°C for 2 min	(extension)
5.	Steps from 2 to 4 repeated for 29 cycles	
6.	4°C	

DNA template	Primers	Sequence (5'-3')	Ta
pAKT3 plasmid	Forward	GGGGTACCGCCGCCACC**ATGGGCTGCGTTTGCT CGTCGAATCCCGAGGACGACGCT**GCTTACCCATA CGATGTTCCAG *(the myristilation sequence is in bold; the nucleotides annealing to HA.AKT3 sequence are underlined)*	64°C
	Reverse	GGTCTAGATTATTCTCGTCCACTT-GCAGAGT *(the nucleotides annealing to AKT3 sequence are underlined)*	64°C

After the PCR reaction the DNA was cleaned using a PCR-clean up kit (Promega) and digested for 2h at 37°C with KpnI/XbaI restriction enzymes. The sample was then run on a preparative 0.8% agarose gel; the band corresponding to the amplified DNA was excised using a Quiquick gel-extraction kit from Quiagen and then religated into KpnI/XbaI site of pcDNA3.1H+ vector. The construct was finally sequence-verified by using T7 as sequencing primer.

2.2.13 DATA HANDLING AND STATISTICAL ANALYSIS

All the statistical analyses were performed using Prism 4 for Windows, version 4.03 (GraphPad Software Inc.).

In vitro experiments

Each experiment was repeated at least three times; in each experiment any condition was tested in duplicate or triplicate. For statistical analysis the mean values of three independent experiments were taken into account. The difference between groups was evaluated by one-way ANOVA followed by Tukey Kramer's *post hoc* test.

Semi-quantitative Reverse Transcription PCR

Three replicates for each experimental group were loaded on the same gel, in

alternate lanes, to correct for inter-gel variability. The ratio of the integrated optical densities for each gene tested versus actin of each sample was used as individual data for statistical analysis. The difference between groups was evaluated by one-way ANOVA followed by Tukey Kramer's *post hoc* test.

Western blot

Three to four replicates for each experimental group were loaded on the same gel, in alternate lanes, to correct for inter-gel variability. The ratio of the integrated optical densities for each protein tested versus actin of each sample was used as individual data for statistical analysis. The difference between groups was evaluated by one-way ANOVA followed by Tukey Kramer's *post hoc* test.

Treatments in vivo

It is known that during colony maintenance loss of gene copy numbers may occur *(Alexander et al., 2004)*. This determines relative milder disease progression in litters with lower copy number. In order to correct for this possible confounding effect, animals from the same litter were assigned to different experimental group and treated at the same time. Moreover sex can affect disease progression in G93A mice *(Heiman-Patterson et al., 2005)*; for this reason treatment was done only on female animals. The experiment was started when animals were 12 weeks old. Animals from the same litter were treated at the same time. At least 5 animals were assigned to each experimental group.

Behavioural tests

Analysis of motor performances and disease progression in treated animals was perfomed by a researcher blinded to the treatment. Analysis of neuromuscular impairment was done by two-way ANOVA for repeated measures followed by Bonferroni *post hoc* test for comparison between groups. Moreover the age of the animals when their performance, expressed as percentage of the respective best

trial, overcame a specific threshold was considered, as outlined below. The Log-rank test was used to compare probabilities in this case (End point analysis).

Measurement	Threshold levels considered for end point analysis		
Body weight	Drop of 5%	Drop of 10%	Drop of 15%
Extension reflex	Drop of 25%	Drop of 50%	Drop of 75%
Hanging time	Drop of 25%	Drop of 50%	Drop of 75%
Rota-rod	Drop of 25%	Drop of 50%	Drop of 75%

Survival

The survival time of the variously treated groups of mice was analyzed by the log-rank test.

Number of surviving motor neurons

The number of surviving motor neurons was evaluated by NISSL staining of 24 spinal cord sections of 30μm thickness, interspaced of 300μm, and collected between spinal cord level L_2 and spinal cord level L_4. The mean number of surviving neurons for each animal was then calculated. The mean of three-four animals for each experimental group was used in the analysis. The difference between groups was evaluated by one-way ANOVA followed by Tukey Kramer's *post hoc* test, and confirmed by Kruskal Wallis non-parametric test.

CHAPTER 3

DEVELOPMENT OF STRATEGIES FOR TARGETING MOUSE SPINAL CORD MOTOR NEURONS IN VIVO

As already mentioned in section 1.6.3 lentiviral vectors represent a powerful tool to drive expression of potential therapeutic genes or shRNAs in neurons or glial cells of CNS. It has already been demonstrated that VSVG-pseudotyped lentiviral vectors can efficiently infect cells of the striatum, hippocampus and thalamus in mouse brain, leading to longlasting expression of the transgene. Transduction of these brain areas is generally obtained by direct injection of the virus into the brain parenchyma, through stereotaxic surgery *(Watson et al., 2002)*. This methodological approach, though invasive, is not reported to induce relevant damage to the injected tissue, with the exception of a mild inflammatory reaction in the area immediately surrounding the injection site (often referred to as the needle tract) *(Abordo-Adesida et al., 2005)*. Nevertheless some drawbacks can be observed: a) the spread of the solution injected in the brain parenchyma is limited due to high density (high number of cells/area) of the tissue; b) the injected volume cannot be increased further than 1uL/injection site, since the brain may suffer for an increment of intracranic pressure as a consequence of excessive fluid in the parenchyma.

A similar approach has been recently adopted for delivery of viral vectors to spinal cord tissue. In this case a laminectomy of the vertebra covering the area of interest is necessary, to allow multiple injections in several adjacent segments of the spinal cord. A number of studies have described the use of this technique in the rat, mainly in models of spinal cord injury *(Zhao et al., 2003; Abdellatif et al., 2006; Hendriks et al., 2007)*. The first report of the use of this technique in mouse is from Guillot and colleagues *(Guillot et al., 2004)*. The authors performed intraspinal injection of β-Gal-expressing lentivector in two bilateral sites separated by 1.5 mm along the spinal cord, in 40-day-old mice. They reported a robust reporter gene expression in the neurons, with the signal widely distributed in the spinal cord parenchyma, and an absence of deterioration of functional motor behaviour in the animals. Moreover, they provided the first evidence that the procedure, though invasive, can be used for assessment of

potential therapeutic genes, such as GDNF, in the SOD1G93A mouse model of ALS. Interestingly, in a subsequent paper the same group delivered lentiviral vectors carrying a human SOD1-targeted shRNA in the spinal cord of presymptomatic SOD1G93A mice. This resulted in a substantial reduction of mutant SOD1 protein level in neurons and glia, with a delay in the onset and progression of the disease *(Raoul et al., 2005b)*. Since these studies demonstrated that an intraspinal delivery approach can be successfully used in SOD1G93A mice, we decided to use the same strategy to test the effect of new potentially therapeutic genes or shRNAs in the same model of ALS.

In the following sections the steps for development of lentiviral vectors suitable for in vivo delivery will be described.

3.1 Protocol for production of lentiviral vectors at high titre

Lentiviral vectors for in vivo delivery are usually produced at high titres, in the range of 10^8-10^9 TU/mL *(Guillot et al., 2004; Hendriks et al., 2007)*. This concentration is needed due to the fact that only small volumes of the viral solution can be injected. Moreover, further purification of viral vector-containing supernatants is necessary to remove cell debris and serum, thus reducing the probability of inducing detrimental inflammatory responses after injection in vivo *(Baekelandt et al., 2003)*.

For these reasons several modifications to the standard viral vector production protocols have been suggested; the most effective are listed below:

- enrichment of the culture medium with cholesterol-containing additives, to increase efficiency of budding of enveloped viruses *(Mitta et al., 2005)*, or with sodium butyrate, found to stimulate the activity of both HIV-1 LTR and CMV promoters in transfected plasmids *(Soneoka et al., 1995; White et al., 1995; Gasmi et al., 1999)*;
- scale up of the number of cell culture plates used for virus production, followed by ultracentrifugation (or ultrafiltration) of the supernatant

containing the viral vector, and resuspension of the pellet (or eluate) in a small amount of PBS *(Sena-Esteves et al., 2004).*

We started a collaboration with the laboratory of Molecular Oncology of the University of Turin which has established an efficient procedure for viral vector production *(Piva et al., 2006).* Minor modifications were introduced, that managed to further increase viral particle production: the number of 293T cell culture plates transfected at the same time was scaled up to 5, to increase the final amount of viral vector containing supernatants; culturing medium was supplemented with sodium butyrate; finally the virus was collected by ultracentrifugation and resuspended in a very small amount of PBS, leading to a final viral titre of $2.7x10^9$ TU/mL (Table 3.1). This concentration is in the range described by Raoul and co-workers for the delivery of VSV-G vectors in the spinal cord of SOD1G93A mice *(Raoul et al., 2005b).*

Table.3.1. High titre production of VSVG pseudotyped lentiviral vectors

Starting conditions	Plasmids	Amount of DNA (µg)
Envelope	pVSVG	0.60
Adjuvant	pCMV	1.00
Adjuvant	pREV	0.50
Transfer vector	pLVTHM	2.50

Trials	Additives	Fold concentration of supernatant	Titre (TU/mL)
1	//	100x	$2.0x10^6$
2	10mM NaButyrate	200x	$5.8x10^8$
3	10mM NaButyrate	400x	$2.7x10^9$

3.2 Direct injection into spinal cord parenchyma

In initial experiments high titre lentiviral vectors expressing a GFP reporter gene (see map of WPXLd vector in section 2.1.1) were injected into the spinal cord parenchyma of NTg mice, to verify the distribution of the virus and its efficiency of infection. As described in section 2.2.3, the virus was delivered at the L_3 and L_4 level of the spinal cord after laminectomy of L_1 vertebra. Two weeks after infection animals were sacrificed by perfusion and lumbar spinal cord was dissected. Serial coronal sections were cut starting from the spinal cord segment corresponding to T_{13} vertebra (24 section of 30µm thickness were collected, interspaced of 300µm). The specimens were then visualized under

epifluorescence microscope to qualitatively assess the extent of GFP expression. GFP positive cells were detected from L_2 to L_4 level, with maximal expression in the areas proximal to the injection sites (Figure 3.1). GFP was expressed in both neurons and glial cells (astrocytes and oligodendrocytes) of lumbar spinal cord as determined by immunohistochemistry (Figure 3.2).

3.3 Use of neuron-specific promoters in lentiviral vectors

Preliminary experiments confirmed that direct injection of high titre VSV-G pseudotyped lentivirus into spinal cord parenchyma guaranteed high efficiency of infection of several cell types. One of the aims of the project was to induce Akt pathway activation specifically in motor neurons. It has been demonstrated that reporter gene expression can be selectively restricted to neurons, including spinal cord motor neurons, by using promoters such as those for Choline Acetyl Transferase (ChAT) or neurofilament heavy chain (NF-H). However, these constructs are large (6.4Kb for ChAT and 8.5Kb for NF-H) and although they have been used to produce transgenic mice *(Naciff et al., 1999; Hirasawa et al., 2001)* they are not suitable for transfer in a lentiviral vector, as the resulting cassette would exceed the maximal cloning capacity. Therefore, as first approach we used a neuron-specific promoter of reduced length for replacement of the original ubiquitous EF1α promoter, in order to restrict transgene expression to neuronal cells.

3.3.1 Assessment of viral vectors carrying the rNSE promoter

A lentiviral vector construct containing the rat Neuron Specific Enolase promoter (rNSE) was first described by Jakobsson and colleagues *(Jakobsson et al., 2006).* They tested its efficiency of expression in vivo, in the rat brain, revealing strong longlasting expression in striatal neurons, with no ectopic expression in glial cells. Based on this evidence we decided to use the same promoter to obtain selective expression of our constructs in mouse spinal cord neurons. The

WPX.NSE.GFP vector was generated by subcloning of the ClaI/BamHI fragment derived from LV.NSE into the ClaI/SwaI site of pWPXLd (BamHI and SwaI sites destroyed). Transfection of these plasmids in vitro, in mixed neuron-astrocyte co-cultures, led to specific expression of the GFP reporter gene in neurons, with low ectopic expression in astrocytes (Figure 3.3). When the same cultures were infected with lentiviral vectors generated from this construct no signal corresponding to GFP was detected. To verify whether the lentiviruses were capable of infecting the cells, the same experiment was repeated and the genomic DNA was extracted from the culture 3 days later. The presence of GFP as a marker of integration of the viral DNA was confirmed by PCR (primer set listed in section 2.2.10). This comfirmed that the lentiviral vectors were functional (Figure 3.4), as we were able to detect the viral DNA integrated into the genome of the host cells, although transgene expression was still absent. To control that the lack of expression was not related to defects of the construct, we used it to infect rat cortical neurons, and we were able to detect GFP signal, though it was very faint (data not shown). Therefore, we tested the vector in vivo, in mice, to determine whether it displayed the same efficiency reported by Jackobsson in the rat brain, or whether it displayed the same failure to express as found in the murine cultures. Two weeks after injection of the vector in the spinal cord parenchyma of NTg mice, a fine expression of GFP reporter gene was detected in large neuronal cells of ventral horn spinal cord (Figure 3.5), as confirmed by co-localization of the signal with Neurotrace staining (arrow in A-C). However, expression could also be observed in some very small neurons localized in the ventral and in the dorsal area of spinal cord (asterisks in A-C, and D-F), as well as in some non-neuronal (probably glial) cells, localized in the gray and white matter (arrowheads in A-C). To overcome this expression in non-neuronal cells we decided to develop a motor neuron-specific construct, starting from the already described Hb9 promoter *(Arber et al., 1999)*.

3.3.2 Preparation of lentiviral vectors with motor neuron-restricted expression

Recently a 3.6Kb enhancer inside the 11Kb promoter of Hb9 has been identified. The 3.6Kb enhancer drives selective expression of reporter genes in spinal cord motor neurons in transgenic mice *(Nakano et al., 2005)*, and is sufficiently short to be suitable for cloning into a lentiviral vector. A NotI/SbfI fragment containing the 3.6Kb enhancer was cloned out of the original 11kb promoter of Hb9, and transferred into the NotI/BamHI site (BamHI site destroyed) of a plasmid containing the β-globin minimal promoter and GFP as reporter gene (Figure 3.6). Mixed neuronal-astrocyte co-cultures were transfected with Hb9_3.6Kb, in parallel with a plasmid with a non-specific promoter (CMV). Cell specificity of reporter gene expression was verified 3 days later. The Hb9 construct displayed selective expression in neuronal cells, with very low ectopic expression in the glial cells in contrast with the CMV promoter that resulted in transgene expression in both neurons and astrocytes (Figure 3.7).

In subsequent experiments we tried to sub-clone 3.6Kb enhancer into a lentiviral vector plasmid. A SalI/SbfI fragment (containing 3.6Kb enhancer and β-globin minimal promoter) was excised from Hb9_3.6Kb plasmid. The aim was to ligate this construct into the SalI/SwaI sites of pWPXLd, to substitute the constitutive EF1α promoter, after blunting of SbfI extremity. However, this was not possible, probably due to the high frequency of recombination when working with large inserts. Therefore, we tried to reduce the length of the promoter without affecting its specificity. Nakano and co-workers have described two short sequences (called "region A" and "region B") within the 3.6Kb enhancer of Hb9 (Figure 3.6), that are responsible for specificity of expression: region B is an enhancer that drives expression in motor neurons; whereas region A behaves as a repressor in not-neuronal cells *(Nakano et al., 2005)*. In initial experiments region A and region B were cloned by PCR and fused in a new 500bp promoter construct (Bg.AB) in collaboration with Mami Kurosaki and Mineko Terao from the Lab. of Molecular

Biology, Mario Negri Institute. Bg.AB was then transfected in mixed neuronal-astrocyte co-cultures. 3 days after transfection GFP reporter gene expression was detected in neurones (Figure 3.8), however strong ectopic expression was also observed in the surrounding astrocytes (Figure 3.9, A-D). As an alternative approach, we looked for cloning sites that helped to increase the distance between the regions A+B, and the β-globin minimal promoter, in a similar way to the pattern observed in the Hb9_3.6Kb construct. A single-cutting restriction site (NdeI) was found at 1.6Kb within the 3.6Kb enhancer. NdeI was used to sub-clone the resulting SalI/NdeI 1.6Kb fragment (containing regions A and B) before the β-globin minimal promoter in a new construct (Bg.1.6Kb). Bg.1.6Kb demonstrated the greatest selectivity for neurons after transfection in mixed neuronal-astrocyte cultures (Figure 3.9, E-H). The new promoter regions were subsequently excised from Bg.GFP plasmid by SalI/SbfI cut, and then successfully religated into the SalI/SwaI site of pWPXLd, after blunting of SbfI, to replace the EF1α promoter. The resulting W.AB and W.1.6Kb plasmids were used for the production of high titre lentiviral vectors, and administered in the spinal cord parenchyma of NTg mice. Two weeks after infection, animals were sacrificed and the lumbar spinal cord was sectioned, to verify the efficiency of infection and specificity of GFP reporter gene expression. W.AB resulted in expression of GFP in some large ventral horn neurons (Figure 3.10, arrow in D-F), although reporter gene expression was more frequently detected in smaller neurons (Figure 3.10, asterisks in D-F), and in glial cells throughout the gray and white matter, and in the dorsal horn (Figure 3.10 arrowheads in A-C). In contrast in animals treated with the W.1.6 vector specific expression of GFP reporter was only detected in large (Figure 3.11 arrowheads in A-C) and very large (Figure 3.11 arrows in A-C) neurons of the ventral horn spinal cord. Colocalization with ChAT staining confirmed that these cells were motor neurons. No ectopic expression in glial cells was observed.

Figure 3.1
Pattern of GFP reporter gene expression after injection in the spinal cord parenchyma

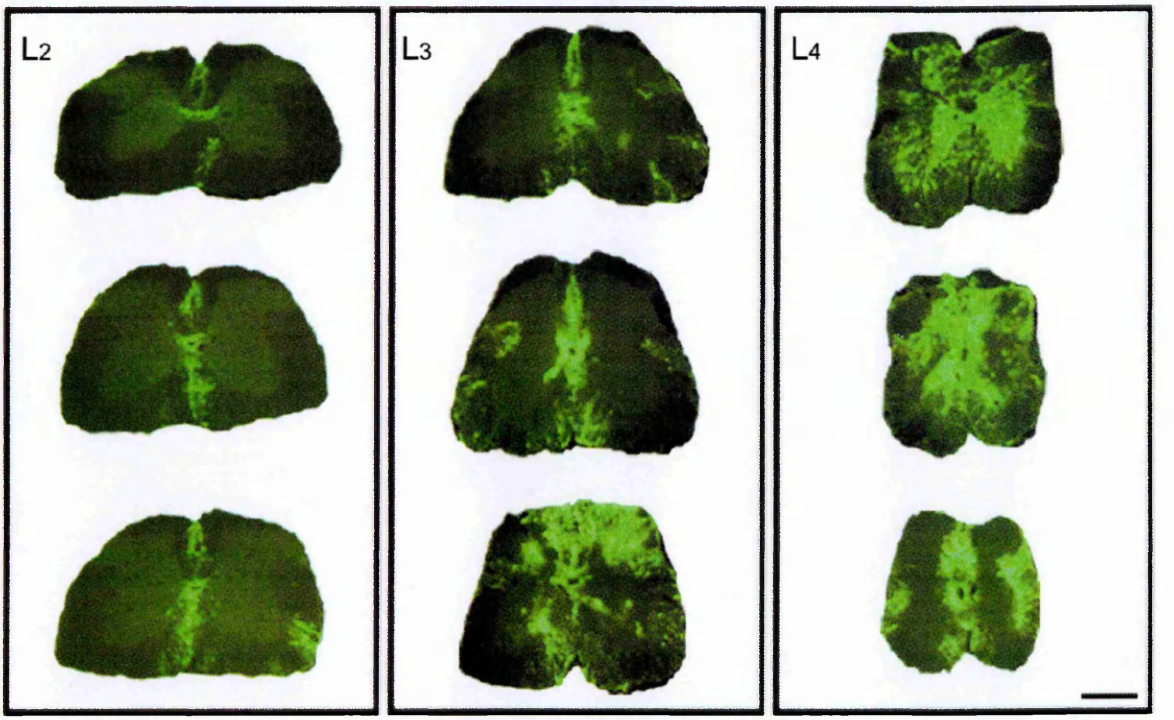

GFP reporter gene expression in spinal cord 2 weeks after injection of a lentiviral vector. From top to bottom, three subsequent serial sections, separated by 600µm, are shown for each of the levels L_2, L_3 and L_4. Scale bar = 200µm

Figure 3.2
Tropism of VSVG-pseudotyped lentiviral vector after delivery in the spinal cord parenchyma

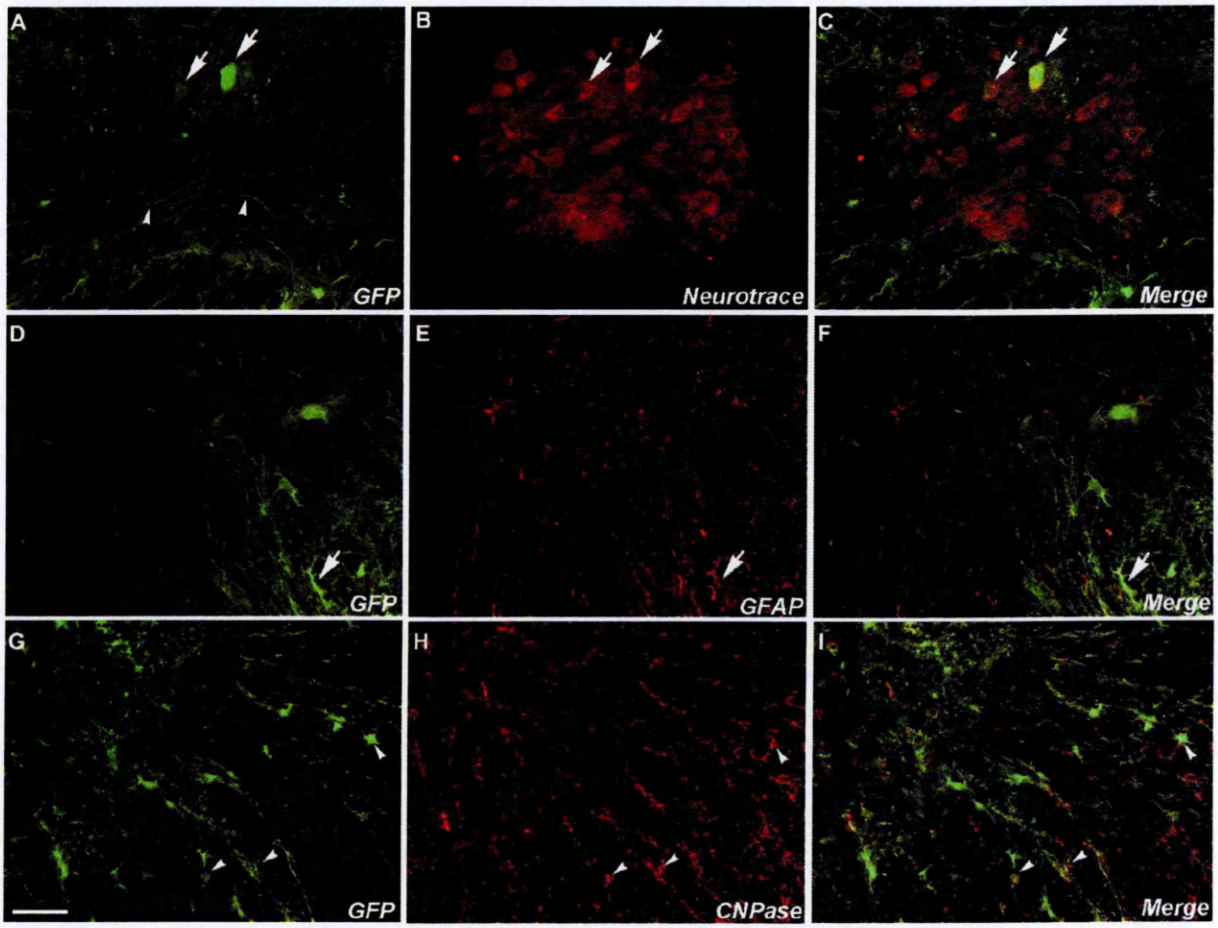

Laser scanning confocal microphotographs of GFP expression in lumbar spinal cord of mice, two weeks after injection. GFP expression in neurons, stained with Neurotrace fluorescent NISSL (arrows in A-C) and some neurites (arrowheads in A). GFP expression in astrocytes, confirmed by colocalization with a glial-specific intermediate filament, GFAP (arrows in D-F) and oligodendrocytes, confirmed by CNPase staining, which recognizes an oligodendrocyte-specific enzyme (arrowheads in G-I). Scale bar in G applies to A-I = 100μm

Figure 3.3.
Use of rNSE promoter leads to specific transgene expression in neurons, in vitro

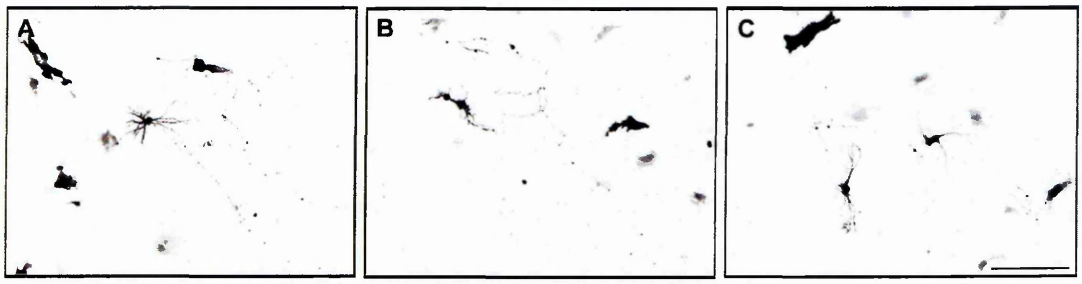

Representative photographs of reporter gene expression 3 days after transfection of mixed neuron/astrocyte co-cultures with rNSE promoter construct. Scale bar = 200μm

Figure 3.4.
Viral vectors carrying the rNSE promoter efficiently infect cells, in vitro

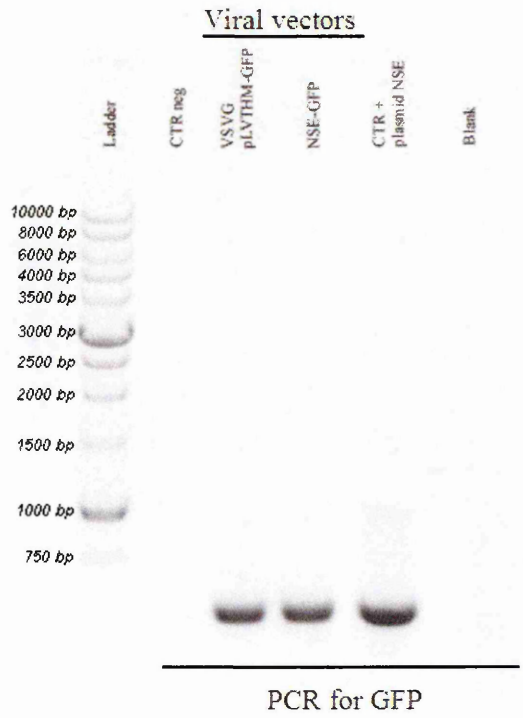

Representative PCR to assess the presence of the lentiviral vector genome in neuron/astrocyte co-cultures after infection with an empty vector expressing GFP (VSVG pLVTHM-GFP), or a vector expressing GFP under rNSE promoter (NSE-GFP). A positive signal is observed in the DNA samples from cultures infected with the viruses.

Figure 3.5.Viral vectors carrying rNSE promoter can infect cells in vivo, in the mouse

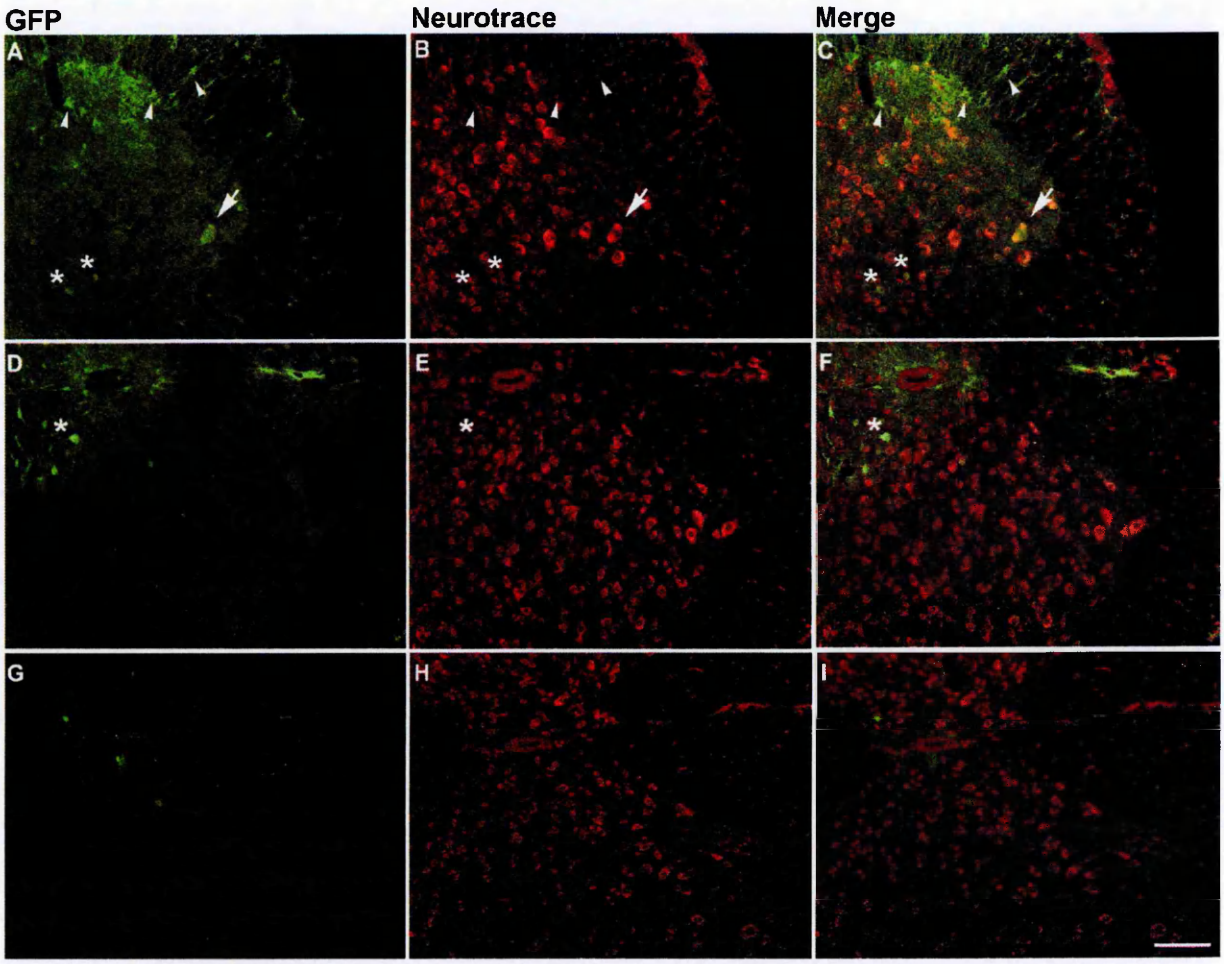

Laser scanning confocal photomicrographs of GFP expression in lumbar spinal cord of mice, two weeks after injection of a viral vector carrying rNSE promoter. Representative images of the different spinal cord levels are shown: L_2 (A-C), L_3 (D-F), L_4 (G-I). The construct is able to drive expression in large ventral horn spinal cord neurons (arrows in A-C), but also in small neurons of ventral (asterisks in A-C) and dorsal spinal cord (asterisks in D-F). Moreover ectopic expression can also be detected in some non-neuronal cells, probably glial cells (arrowheads in A-C). Scale bar = 100μm

Figure 3.6.

Scheme of 3.6Kb enhancer derived from original 11Kb Hb9 promoter

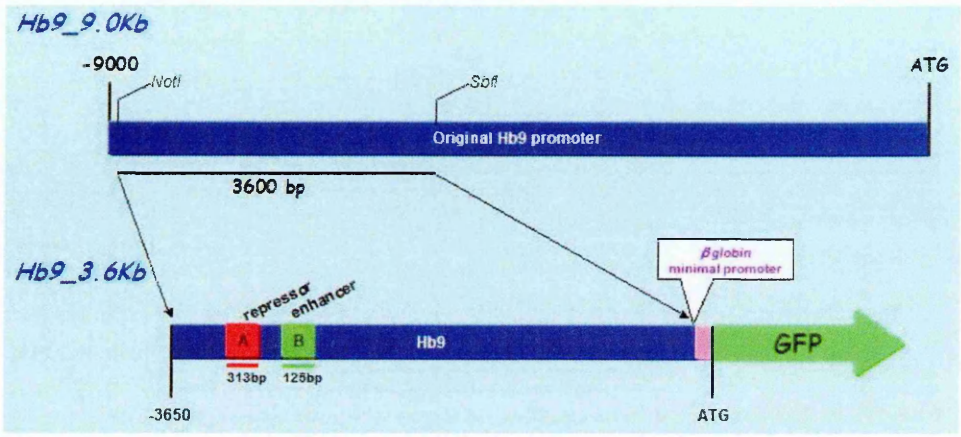

Figure 3.7

Hb9_3.6Kb-GFP can drive selective expression of transgene after transfection in vitro

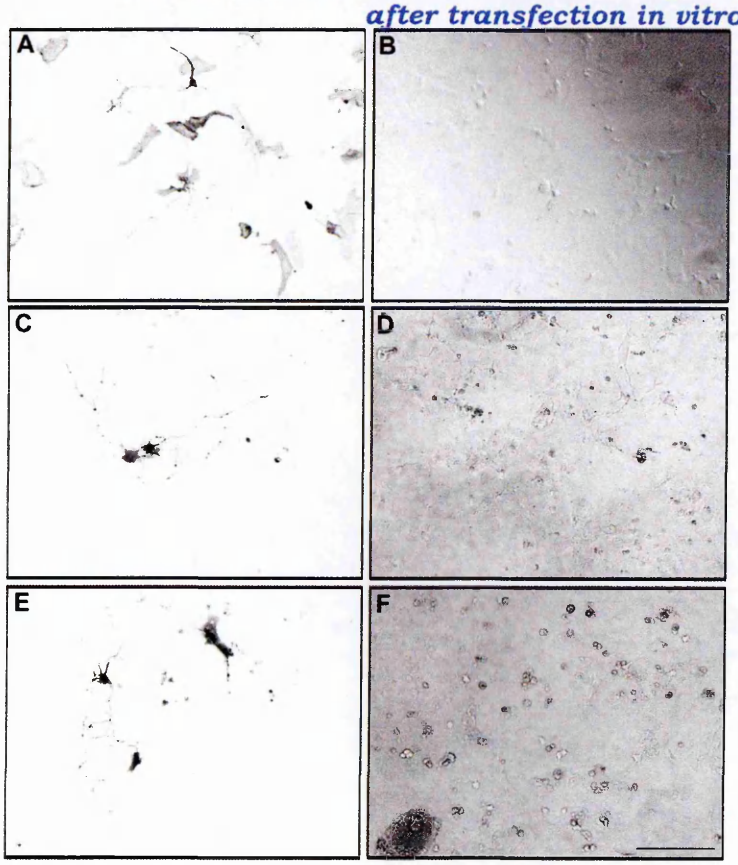

Representative photographs of reporter gene expression after transfection of mixed neuron/astrocyte co-cultures with the CMV ubiquitous promoter construct (A), or with Hb9_3.6Kb promoter contruct (C and E). B, D, F, light field picture of the culture shown in A, C, E. Scale bar = 200μm

Figure 3.8.
Scheme of the new constructs derived from 3.6Kb enhancer

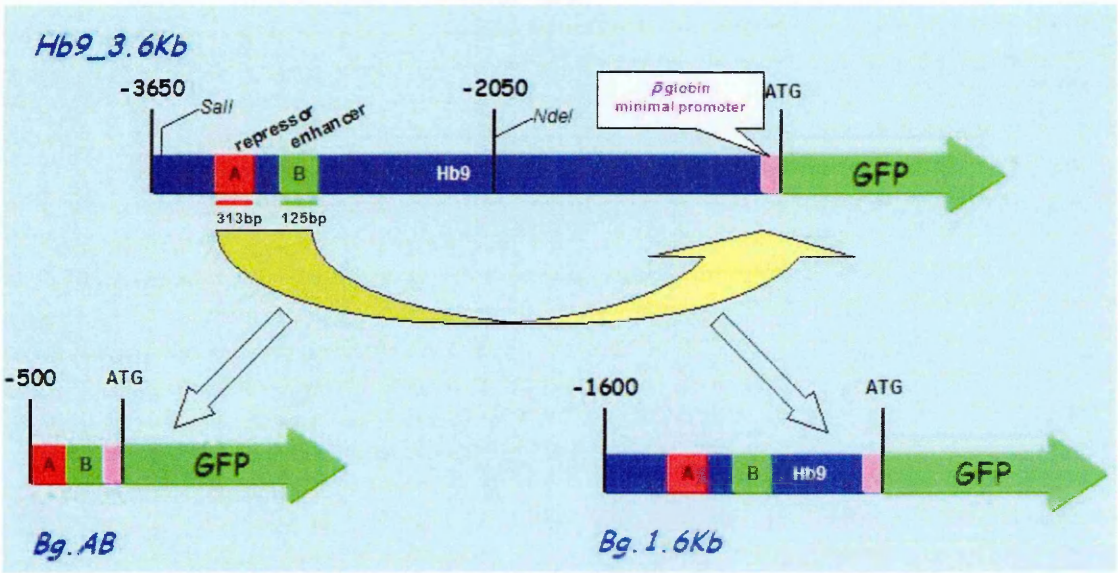

Figure 3.9.
Neuron specific expression of transgene after transfection of Bg.AB and Bg.1.6Kb constructs in mixed co-cultures

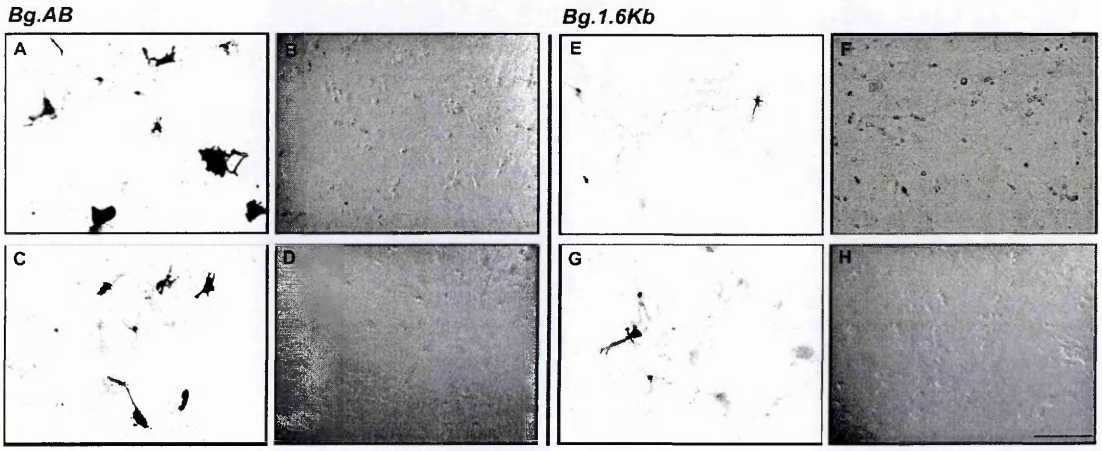

Representative photographs of reporter gene expression after transfection of mixed neuron/astrocyte co-cultures with the Bg.AB (A-D) or Bg.1.6Kb (E-H) neuron specific constructs. Bg.AB drives expression of GFP in neurons (arrows in A, C) as well as in astrocytes (arrowheads in A, C). In contrast, with Bg.1.6Kb the reporter gene is mainly localized in neuronal cells (arrows in E, G), with low ectopic expression in glial cells (arroheads in E, G). Scale bar = 200μm

Figure 3.10.

Viral vectors carrying the Hb9.AB promoter can infect motor neurons in vivo but lead to ectopic expression in non neuronal cells

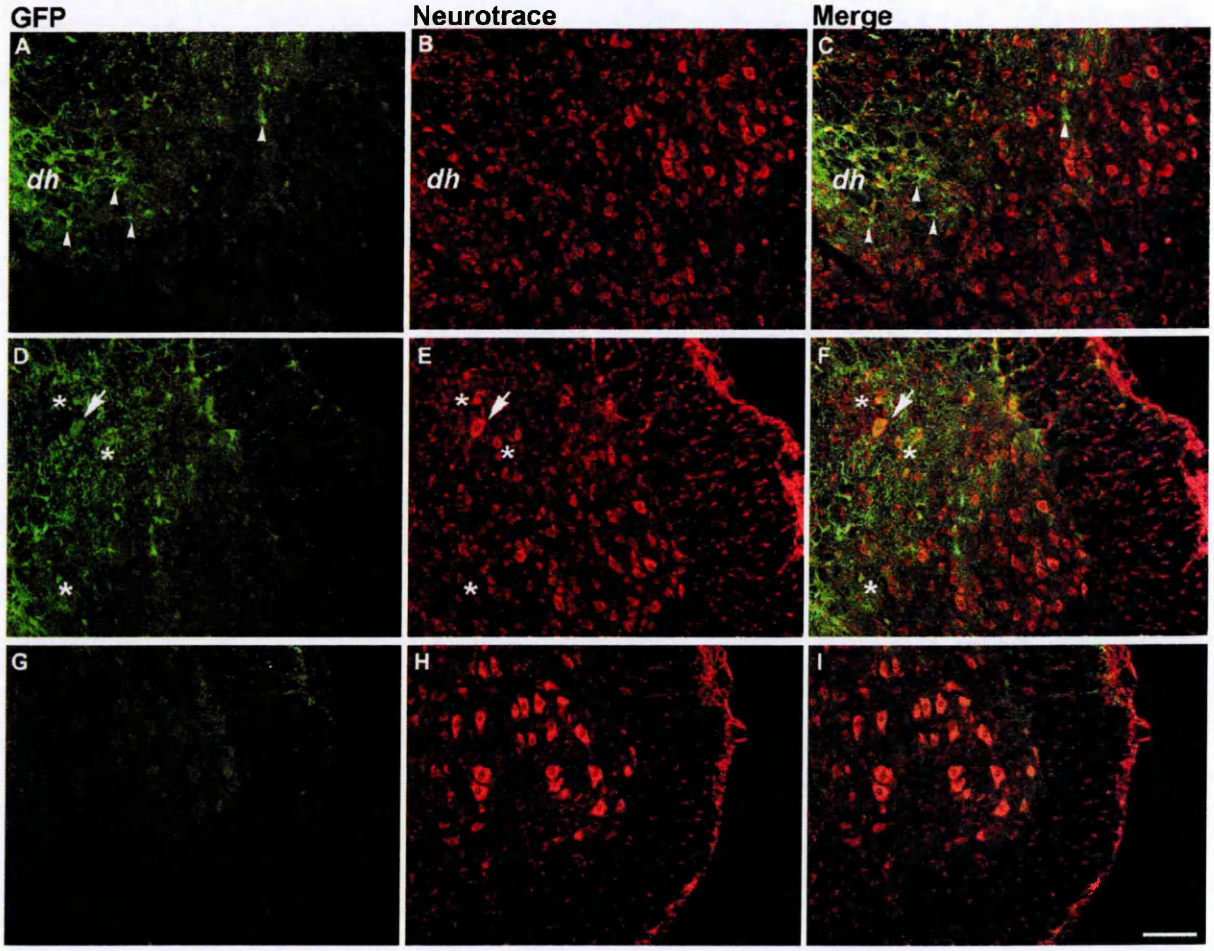

Laser scanning confocal photomicrographs of GFP expression in lumbar spinal cord of mice, two weeks after injection of a viral vector carrying the Hb9.AB promoter. Representative images of the different spinal cord levels are shown: L_2 (A-C), L_3 (D-F), L_4 (G-I). The construct is able to drive expression in ventral horn spinal cord large neurons (arrow in D-F), as well as in small neurons (asterisks in D-F). However there is prominent ectopic expression in non-neuronal cells throughout the spinal cord and in the dorsal horn (dh) (arrowheads in A-C). Scale bar = 100μm

Figure 3.11.

Viral vectors carrying the Hb9.1.6Kb promoter display higher specificity for ventral horn neurons in the spinal cord in vivo

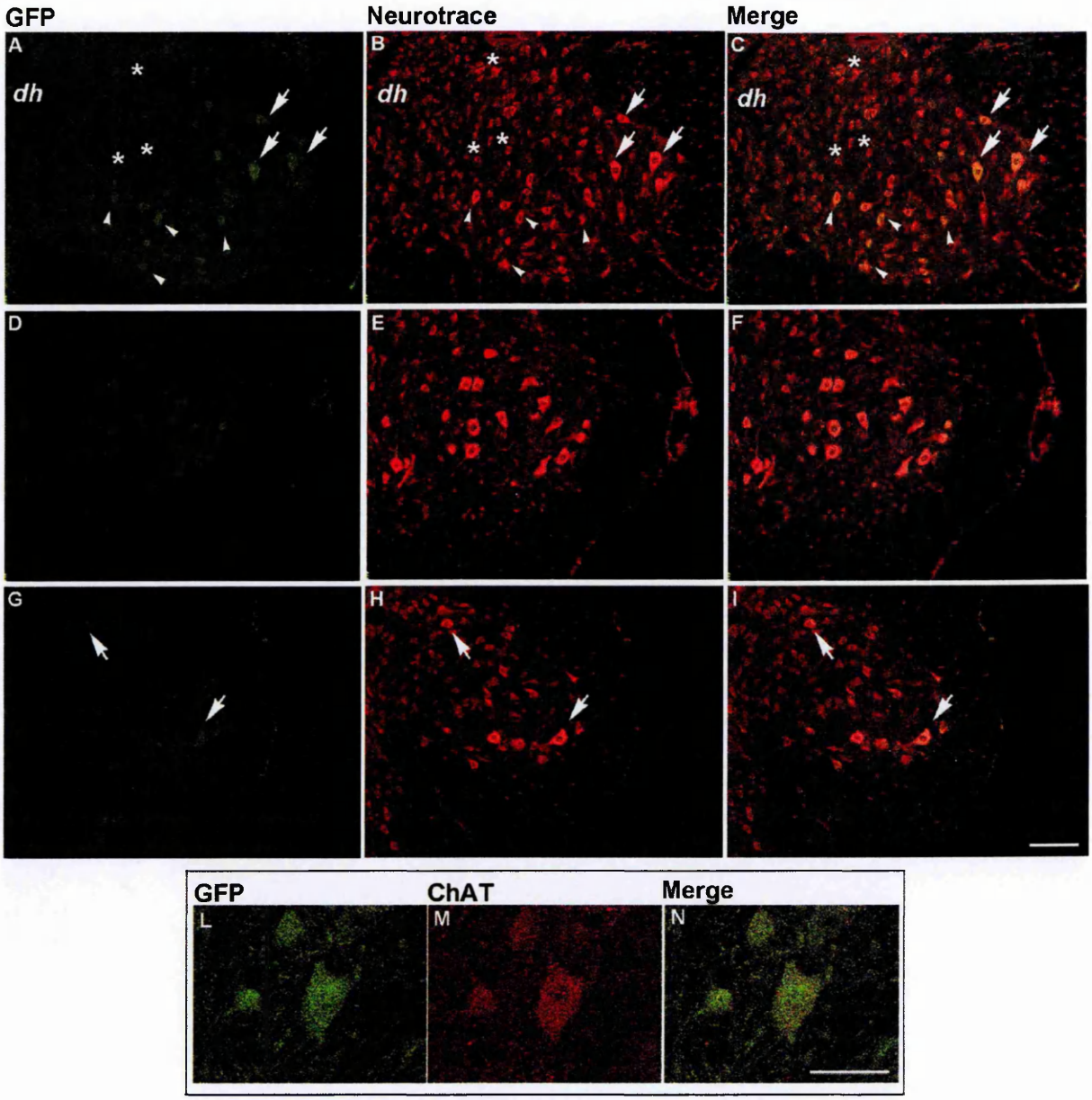

Laser scanning confocal photomicrographs of GFP expression in the lumbar spinal cord of mice, two weeks after injection of a viral vector carrying the Hb9.1.6Kb promoter. Representative images of the different spinal cord levels are shown: L_2 (A-C), L_3 (D-F), L_4 (G-I). The construct drives selective expression in ventral horn spinal cord neurons (arrowheads in A-C), as well as in some very large neurons (arrows in A-C, G-I). Little or no expression is detected in small neurons (asterisks in A-C), neither in non-neuronal cells nor in dorsal horn (dh). Large GFP positive neurons are motor neurons, as confirmed by colocalization with ChAT staining (L-N). Scale bar in I applies to A-H = 100μm; Scale bar in N applies to L, M = 50μm

3.4. Discussion

We have successfully designed and developed a lentiviral vector-based platform to target different spinal cord cell populations, in vivo, in the mouse.

Since a high titre vector preparation is needed for efficient delivery in vivo, we developed a protocol aimed at increasing viral particle production. According to previous reports *(Soneoka et al., 1995; Gasmi et al., 1999)*, we observed increased titre of VSVG lentivector using sodium butyrate in culture medium. This is probably due to increased transcription of our transfer vectors (plasmids pLVTHM or pWPXLd), since they contain a wild type 5' HIV-1 LTR sequence, whose activity is positively affected by sodium butyrate treatment *(White et al., 1995)*. Moreover, in our production procedure we transfected the pRSV.REV plasmid together with the standard two adjuvant plasmids (envelope and gag-pol). In our pRSV.REV plasmid the expression is under the control of RSV promoter, whose efficiency is known to be enhanced by sodium butyrate treatment *(Gorman et al., 1983)*. It is thus possible that sodium butyrate may also have exerted positive effects by enhanced expression of Rev. Rev is in fact necessary for translocation of the viral RNA genome from nucleus to the cytoplasm, where viral capsids are synthesized; it has been demonstrated that high expression of this adjuvant protein, from a separate plasmid, aids the packaging of full infective viral particles *(Dull et al., 1998)*. At variance with our results, in a recent study it has been shown that the use of sodium butyrate as an additive in culture medium does not improve the titre of VSVG-pseudotyped lentivectors *(Sena-Esteves et al., 2004)*. This discrepancy can be explained by the fact that in the work by Sena Estevez the transfer vector contained a 5'LTR fused to CMV, a modification that already enhances transcription of the transfer vector genome in a tat-independent manner *(Naviaux et al., 1996; Blesch, 2004)*. This may account for no further sensitivity to the effect of agents like sodium butyrate.

High titre lentiviral vectors, produced with our modified protocol, were delivered to NTg mice by direct intraspinal injection. Qualitative assessment of GFP reporter gene expression after two weeks confirmed the infection of neurons and glia, throughout the gray and white matter of the spinal cord. Neurons and oligodendrocytes were highly transduced, while GFP-positive astrocytes were detected to a lesser extent in general agreement with a previous study *(Guillot et al., 2004)*.

As second step in the vector development process, we successfully obtained neuron targeted gene expression in vivo. This was achieved by substitution of the ubiquitous EF1α promoter within the viral transfer vector, with neuron-specific regulatory sequences previously described in the literature.

The rat NSE promoter was initially tested, as its use in lenvitiral vectors had already been validated in rat brain *(Jakobsson et al., 2006)*. We found that lentivectors containing the rNSE promoter were not suitable for infection of murine neuronal-astrocyte co-cultures in vitro, and demonstrated that the lack of reporter gene expression was not due to a defect in the infectivity of the viral particles. In fact we were able to detect the presence of viral DNA integrated in the genome of infected cultures. Since expression of the reporter gene was detected only after infection of neuronal cultures obtained from rat, or after transient transfection of murine cultures with the rNSE transfer vector, we hypothesize that this promoter may be silenced after integration in the genome of murine cultures, in vitro. Nevertheless, intraspinal injection of rNSE viral vectors, in the mouse, demonstrated that this promoter is highly active in adult neurons, in vivo. In particular, we observed that in the mouse spinal cord reporter gene expression was localised mainly in small neuronal cells, and less frequently in large ventral horn motor neurons. Moreover, we also detected ectopic expression in non-neuronal cells.

It has been reported that NSE gene expression in neurons increases during development with differentiation of adult mature neurons *(Schmechel et al.,*

1980). Moreover constructs containing 1.8Kb of the NSE promoter sequence lead to specific expression in terminally differentiated neurons, and progressive accumulation of reporter gene during development in vivo, in the mouse *(Forss-Petter et al., 1990).* At variance with the study from Forss-Petter, we used a shorter promoter sequence *(Jakobsson et al., 2003),* so it can be hypothesized that some additional regulatory sequence is lacking, thus determining inefficient expression in mouse cultures in vitro, and reduced selectivity in vivo.

Due to this lack of specificity for the motor neuronal population, rNSE lenvitiral vectors were not developed further.

We provided evidence that enhancer sequences derived from the Hb9 promoter can be cloned in lentiviral vectors and are more selective for spinal cord motor neurons. Indeed, motor neuron specific expression of β-Gal has been already described in adult transgenic mice expressing LacZ gene under a 3.6Kb promoter construct derived from Hb9 promoter *(Nakano et al., 2005).* These authors also demonstrated that two short sequences (region A, of 313bp and region B, of 125bp) within this construct play a key role for the specific expression of the reporter gene. When these regulatory sequences were in close proximity to the open reading frame of the gene located downstream (construct W.AB), we found that expression occurred in neurons and glial cells, both in vitro and in vivo in mouse spinal cord. It is possible that this allocation of upstream regulatory sequences does not allow sufficient bending of DNA. This process is usually required for correct regulation of the initiation of transcription. In fact, in the original 3.6Kb construct, the A and B regions are more than 3Kb upstream of the transcription start site, so they may be considered as long-range regulatory sequences, similar to repressor sequences like REST, thyroid hormone receptors and the zinc-finger of NK-10 *(Thiel et al., 2001; Vilar and Saiz, 2005).* As confirmation of this hypothesis, we demonstrated that positioning the A and B regions 1.6Kb upstream of transcription starting site was sufficient to increase the specificity for neurons in vitro. This construct was successfully subcloned

into a lentiviral vector (W.1.6Kb), and proved to be motor-neuron specific after intraspinal injection in vivo in the mouse.

Overall these experiments highlight that lentiviruses carrying an Hb9 derived promoter can be regarded as powerful tool for motor neuron specific expression of a transgene in the spinal cord in vivo.

CHAPTER 4

INDUCTION OF THE AKT PATHWAY

As highlighted in section 1.3.7 there is emerging evidence that impairment of the PI3K/Akt signalling pathway may be involved in ALS. However the precise role played by Akt in the progressive pathology of ALS needs to be elucidated, as there are contradictory reports in the literature. Indeed, a reduction of PI3K and total Akt protein levels has been reported in homogenates and motor neurons from the spinal cord of asymptomatic SOD1G93A low-expressing mice, suggesting that a downregulation of the PI3K/Akt pathway may occur in ALS *(Warita et al., 2001)*. However, the same group has also reported increased nuclear staining for P-Akt in motor neurons in the same animal model *(Ilieva et al., 2003)*. In a more recent study P-Akt was found to be reduced in the spinal cord of SOD1G93A mice even at the presymptomatic stage, and these observations were confirmed in post-mortem tissues from human ALS patients *(Dewil et al., 2007b)*. In contrast, in our own studies we failed to observe changes in P-Akt in SOD1G93A mice during disease progression *(Peviani et al., 2007)* and levels were similar to controls, both at the pre-symptomatic stage and after symptom onset. The differences among these studies may be dependent on some methodological issues, such as the use of different anti-P-Akt antibodies, or a lack of uniformity between the protocols for tissue homogenisation and protein extraction. Moreover we detected P-Akt staining in some motor neurons showing perikarial accumulation of phosphorylated neurofilaments (a sign of degeneration), suggesting that death of these cells is probably not simply the consequence of a loss of Akt activation.

Nevertheless, since induction of Akt is part of a process that is normally activated to maintain the survival of neurons including motor neurons after an insult, for example an axotomy, it is conceivable that a reduction or no change in the levels of activated Akt may contribute to the incapacity of these cells to react to injury, thus leading to their death. Therefore, we hypothesised that the induction of P-Akt in motor neurons of SOD1G93A mice could help these cells to counteract the mechanisms leading to death, thus resulting in a delay in the pathology. In fact

delivery of IGF-I to SOD1G93A mice through motor neuron-targeted viral vectors *(Kaspar et al., 2003)*, or through intrathecal infusion *(Nagano et al., 2005)* partially reduced motor neuron loss and delayed disease progression and this effect was paralleled by increases of P-Akt in the spinal cord. Similarly, administration of a GDNF-expressing adenovirus in hindlimb muscles of the same animal model produced a sustained induction of P-Akt in the motor neurons of the spinal cord *(Manabe et al., 2002)*; moreover intracerebroventricular treatment of SOD1G93A rats with VEGF resulted in improvement of motor performance, prolonged survival and increased P-Akt levels in the spinal cord *(Storkebaum et al., 2005; Dewil et al., 2007b)*.

However, it is currently not clear whether the above effects, observed in ALS rodent models after treatment with IGF-I, VEGF and GDNF, may be dependent only on activation of the Akt pathway in motor neurons. In fact, several studies have shown that these growth factors can act also on other kinases, such as ERK and JNK *(Derijard et al., 1994; Sullivan et al., 2008)* and can influence the proliferation and survival of glial cells *(Mani et al., 2005; Chesik et al., 2008)*.

Therefore, we decided to develop a lentiviral-vector mediated, gene-based, approach aimed at inducing specific activation of the Akt pro-survival pathway in spinal cord motor neurons of SOD1G93A mice. In order to obtain sustained induction of the Akt pathway, we decided to use a mutant protein derived from the fusion of Akt, at the N-terminus, with a short 13 aminoacid sequence, a myristylation recognition site. As mentioned in section 1.5.4, this structural modification leads to constitutive membrane translocation of the kinase, thus determining continuous activation of the enzyme in a PI3K-independent manner. Moreover delivery of this gene through a lentiviral integrating vector is expected to provide longlasting transgene expression, helping to maintain increased levels of Akt phosphorylation during disease progression.

4.1 Generation of constitutively activated Akt constructs

It has been shown that Akt3, one of the three isoforms of Akt, displays specific neuroprotective properties in NSC34 cells, antagonizing mutant SOD1 toxicity specifically, whereas Akt1 appears to have a more generalized anti-apoptotic effect *(Kanekura et al., 2005)*. The same group provided further evidence for a role for Akt3 in neuroprotection with the identification of a novel Akt3-interacting protein, called BTBD10. Overexpression of BTBD10 in vitro inhibited PP2A activity, thus preventing Akt3 dephosphorylation, and leading to suppression of mutant SOD1 induced cell death *(Nawa et al., 2008)*. Therefore, we decided to develop a constitutively activated Akt3 mutant protein (Myr.Akt3) and to subclone it in a lentiviral vector containing a neuron specific promoter, to allow specific expression in spinal cord motor neurons in vivo.

In initial experiments, Myr.Akt3 was prepared by fusion of a myristylation sequence to the N-terminal of human HA.AKT3 (a fusion protein containing HAtag at its N-terminal), and its function tested in vitro, in comparison with Myr.AKT1, a similar fusion protein previously validated in the literature *(Andjelkovic et al., 1997)*. Briefly, the HA.AKT3 construct contained in plasmid pAKT3 was amplified by PCR, using the primer set and protocol described in section 2.2.12. The amplicon was then cut by KpnI and XbaI and ligated into plasmid pMyr.AKT1, after KpnI/XbaI excision of the Myr.AKT1 construct. Myr.AKT3 was first sequence verified, and then tested in parallel with a control empty vector and the pMyr.AKT1 plasmid, by transfection into HEK293 cells. Cells were lysed 3 days later, and proteins were extracted for western blot analysis (protocol described in section 2.2.11). Efficient induction of the Akt pathway was detected with both Myr.AKT1 and Myr.AKT3, as demonstrated by increased levels of Akt phosphorylated at Ser^{473}, and corresponding increase of GSK3β phosphorylated at Ser^{9} (a specific downstream target of Akt) (Figure 4.1).

Myr.AKT3 was subsequently excised from pcDNA3.1H+ by KpnI/XbaI cut and religated into PmeI/SpeI sites of pWPXLd lentiviral vector, after excision of GFP

(PmeI and SpeI sites destroyed). An initial batch of lentivirus was produced with the protocol described in section 2.2.1, using the new transfer vector (WPX.Myr.AKT3). 5 μL/well of concentrated virus (corresponding to $5,0x10^6$ TU) were added to primary mixed neuron-astrocytes co-cultures in 48 well plates, to test for infectivity and function of the new construct. A control GFP expressing viral vector (WPXLd) was tested in parallel. 3 days after infection DNA was extracted from 4 wells/condition (protocol described in section 2.2.10), and proteins were obtained from the remaining 2 wells (protocol described in section 2.2.11). PCR amplification of integrated viral DNA confirmed that WPX.Myr.Akt3 was fully infective (Figure 4.2,B) while western blot analysis of cell lysates demonstrated that Myr.Akt3 was functional, as increased levels of P-Akt were detected in cells infected with the new construct (Figure 4.2,C).

As a final step, the enhancer elements of Hb9, fused to β-globin minimal promoter, were excised from Hb9_1.6Kb plasmid (described in chapter 3) by SalI/SbfI digestion and then religated into SalI/SwaI sites of WPX.Myr.AKT3 (SbfI and SwaI sites destroyed), after excision of the EF1α ubiquitous promoter. The new W.1.6.Myr.AKT3 viral vector construct was then used to generate high titre viral vectors, for delivery in vivo.

4.2 Effect of induction of Akt pathway in vivo, in SOD1G93A mice

Lentiviral vectors W.1.6.Myr.AKT3 were intraspinally injected in 84day old SOD1G93A mice (n=7; Group E), following the protocol described in section 2.2.3. As control groups, SOD1G93A animals were injected with an empty vector expressing GFP (n = 6; Group B), and a further group of animals underwent laminectomy but did not receive an injection (n = 5; Group A). Motor performance and disease progression were analysed twice a week, as outlined in section 2.2.4. Treatment with Myr.Akt3 did not significantly alter the survival of SOD1G93A mice, as compared to the control groups (Figure 4.3)

We did not detect any difference between the three groups for the progression of body weight loss (Figure 4.4 A) or deficits of extention reflex (Figure 4.4 B) or rotarod performance (Figure 4.4 D). On the grid test, Myr.AKT3 treated mice showed a trend towards a better performance than control group A starting at 107 days of age, while from 118 days they showed a worst motor performance in respect to the group which received only EV (group B) on the same test (Figure 4.4, C). It is worth to note that disease progression in Group B was not significantly different from Group A, except for a tendency to a less steep decrease of motor performance on the grid test, starting from 111 days of age. However, despite the subtle differences observed in Myr.AKT3 treated group at the early phases of the pathology, the onset of disease (as assessed by endpoint analysis of performances) was not significantly delayed by the Myr.AKT3 treatment (Figure 4.5, A). The same results were obtained by comparison of the probability to reach more advanced stages of the disease (reduction of performance below 50% and 75% of the best performance) (Figure 4.5, B, C). However at the end stage, the hindlimbs of animals from Group A and B appeared completely paralysed, as expected with the severe loss of motor neurons at that phase of the pathology, whereas mice that received Myr.AKT3, still retained some movement of the digits.

To analyze the effects of Myr.AKT3 expression on motor neuronal survival, the spinal cords from animals at the age of sacrifice were collected, and then sectioned for NISSL staining. Neurons were classified according to their area. The mean number of motor neurons (with an area higher than 250μm^2) was considered in the analysis. Interestingly, the number of surviving cells in Myr.AKT3-treated group (16.53+/- 0.86 cells/hemisection) was significantly higher than the empty vector-treated Group B (12.67+/-1.06 cells/hemisection), and the control Group A (11,81+/-0.27 cells/hemisection)(Figure 4.6 A). To further confirm that the observed effect was due to Myr.AKT3, the expression of the transgene was visualized by immunohistochemistry, through staining of the

HAtag. In the spinal cord of animals injected with Myr.AKT3 lentivectors a clear expression of Myr.AKT3 could be detected in spinal cord motor neurons, as highlighted by colocalization of HAtag staining with MAP2 (Figure 4.7). HAtag was mainly localized at the submembrane and cytoplasmic level, with a weak signal detected in the nucleus. This is consistent with prevalent membrane targeting of the fusion protein, due to the presence of the myristylation sequence. Notably, infected motor neurons also displayed intense P-Akt immunoreactivity. This signal was only partially colocalised with HAtag, further supporting the evidence of a basal level of Akt phosphorylation in the motor neurons of SOD1G93A animals. Nevertheless, P-Akt immunoreactivity appeared to be higher in the motor neurons of Myr.AKT3 infected animals than in the control group, suggesting that expression of the transgene had indeed resulted in increased Akt activation (Figure 4.8).

Figure 4.1
Preparation of constitutively activated AKT constructs and validation in vitro

A.

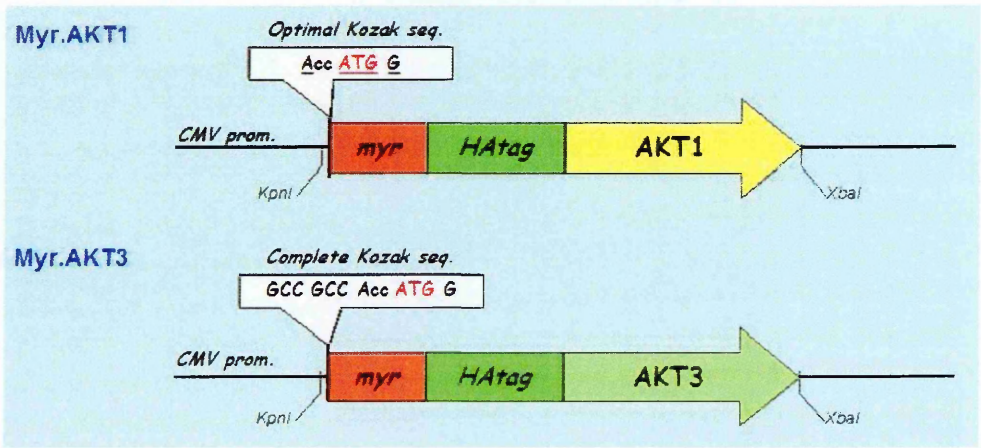

B.

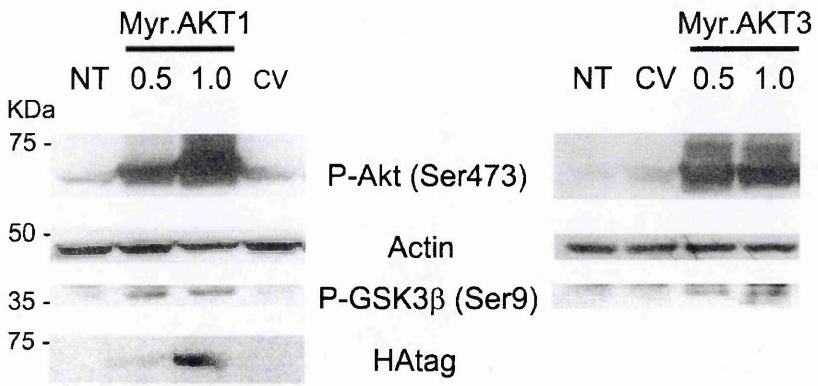

A. Schematic representation of relevant features contained in the sequence of Myr.AKT1 and Myr.AKT3 constructs. **B.** Representative immunoblots performed on HEK293 cell lysates after transfection with Myr.AKT1 or Myr.AKT3 (μg of DNA used for transfection are indicated), or with a control empty vector (CV), as compared to not-transfected (NT) condition. Strong increase of Akt phosphorylation was detected with Myr.AKT1 and Myr.AKT3 constructs. This is paralleled by increased phosphorylation of GSK3β at Ser^9, one of downstream targets of activated Akt.

Figure 4.2
Lentiviral vectors containing the Myr.AKT3 construct are fully infective and functional in vitro

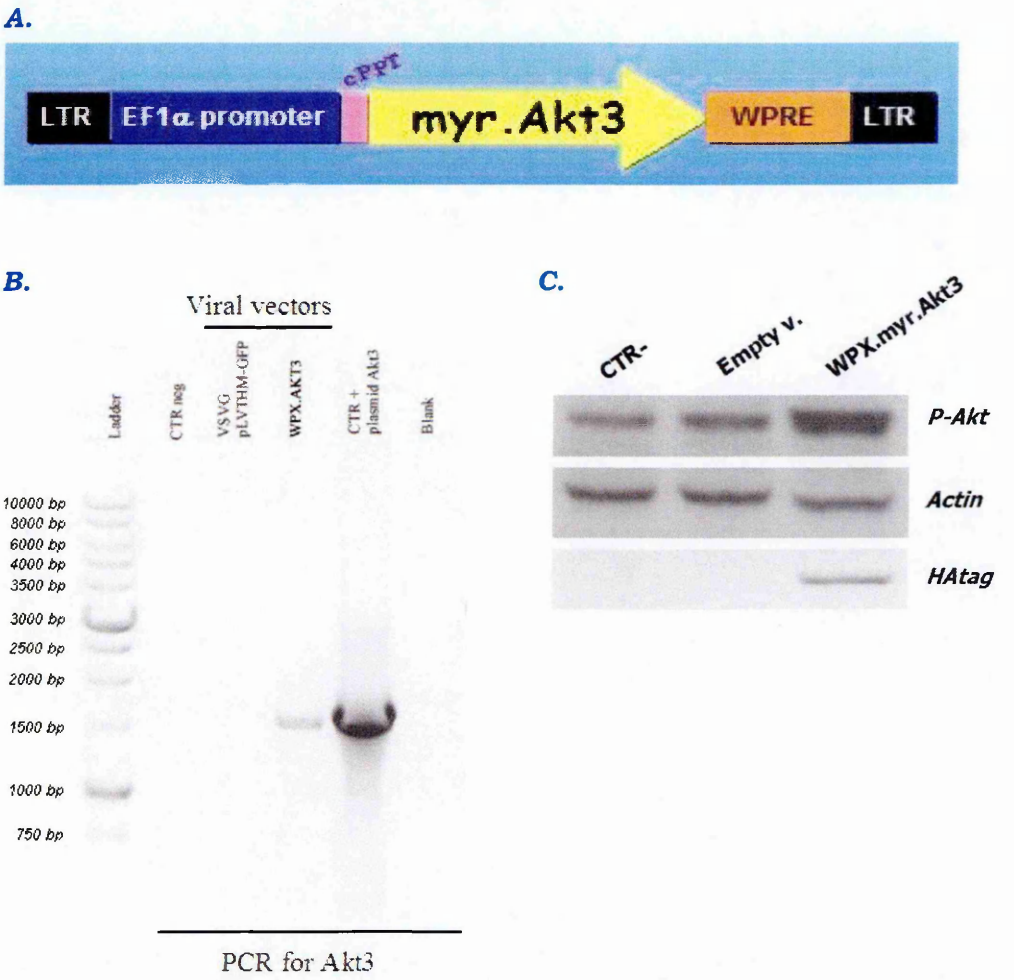

A. Schematic representation of the WPX.Myr.AKT3 lentiviral vector construct. **B.** Representative photographs of PCR reactions to confirm the presence of the lentiviral vector genome in neuron-astrocyte co-cultures after infection with an empty vector expressing GFP (VSVG pLVTHM-GFP), or a vector expressing Myr.AKT3 (WPX.AKT3). A positive signal was observed in the samples from cultures infected with the viruses. **C.** Representative immunoblots performed on lysates from the same cultures as in **A.** A clear increase of P-Akt was observed after infection with WPX.myr.AKT3 lentivector.

Figure 4.3
Treatment of SOD1G93A mice with W.1.6.Myr.AKT3 lentivector does not significantly modify survival

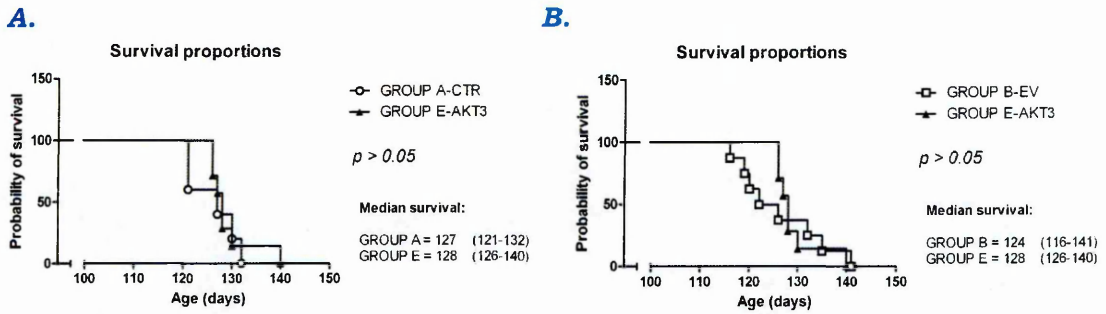

Comparison of survival curves for Group E (Myr.AKT3 treatment), and control Group A (Sham operated) (**A**), or control Group B (injection with Empty vector, EV) (**B**). Log-rank analysis of probabilities showed no significant difference.

Figure 4.4
Effect of Myr.AKT3 expression on disease progression in SOD1G93A mice

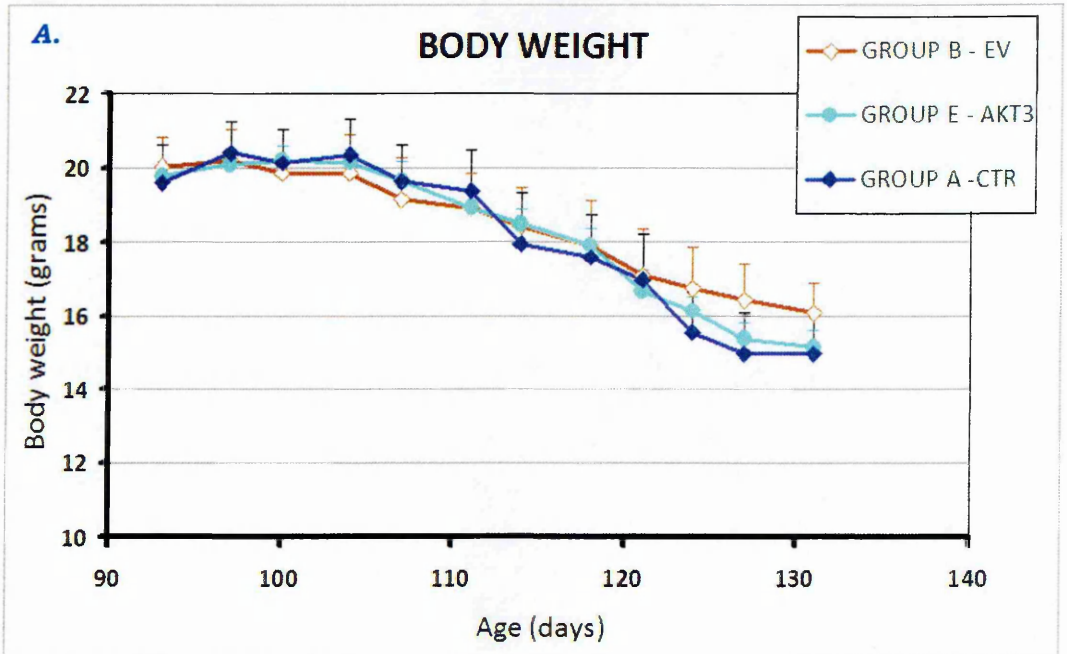

Two-way ANOVA for repeated measures
Group E vs Group A: *Fint* p=0.99
Group E vs Group B: *Fint* p=0.99
Group A vs Group B: *Fint* p=0.20

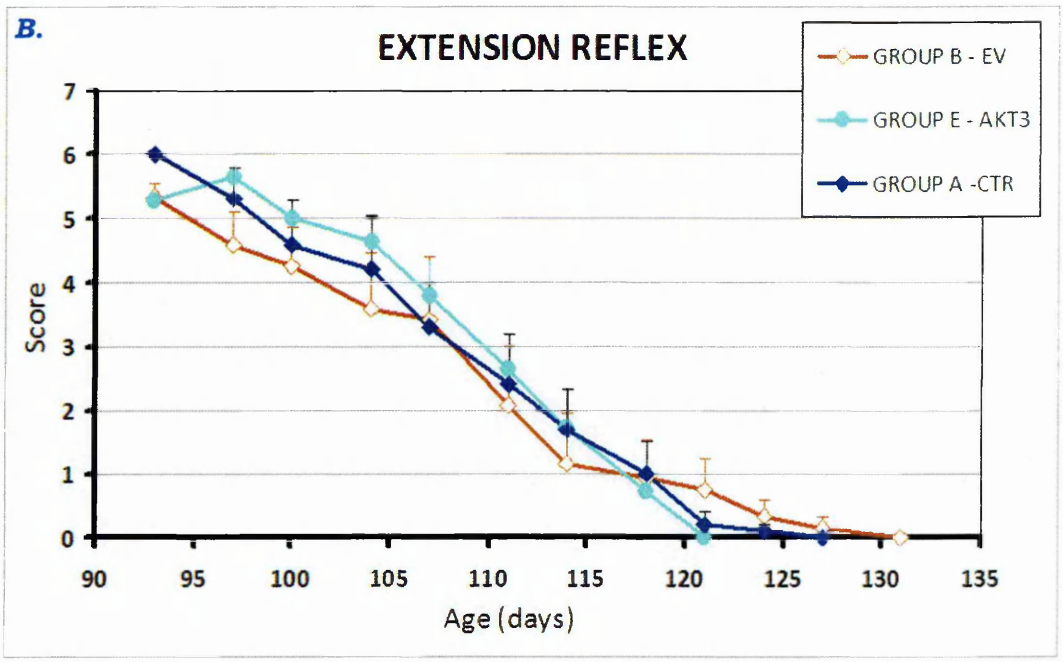

Two-way ANOVA for repeated measures
Group E vs Group A: *Fint* p=0.95
Group E vs Group B: *Fint* p=0.95
Group A vs Group B: *Fint* p=0.61

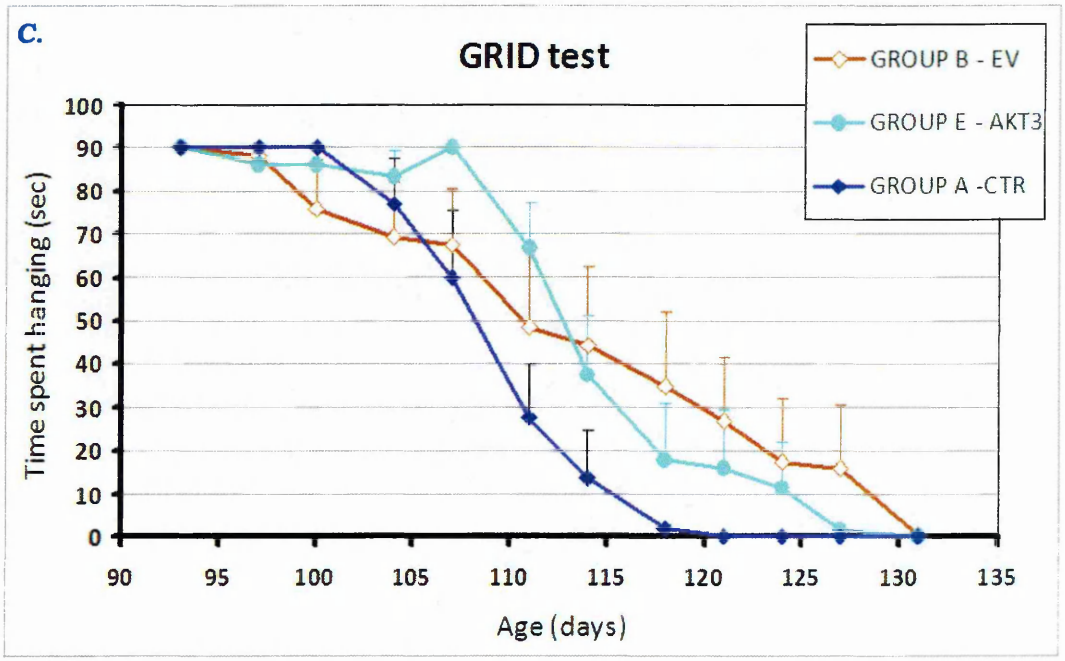

Two-way ANOVA for repeated measures
Group E vs Group A: *Fint* p=0.19
Group E vs Group B: *Fint* p=0.40
Group A vs Group B: *Fint* p=0.36

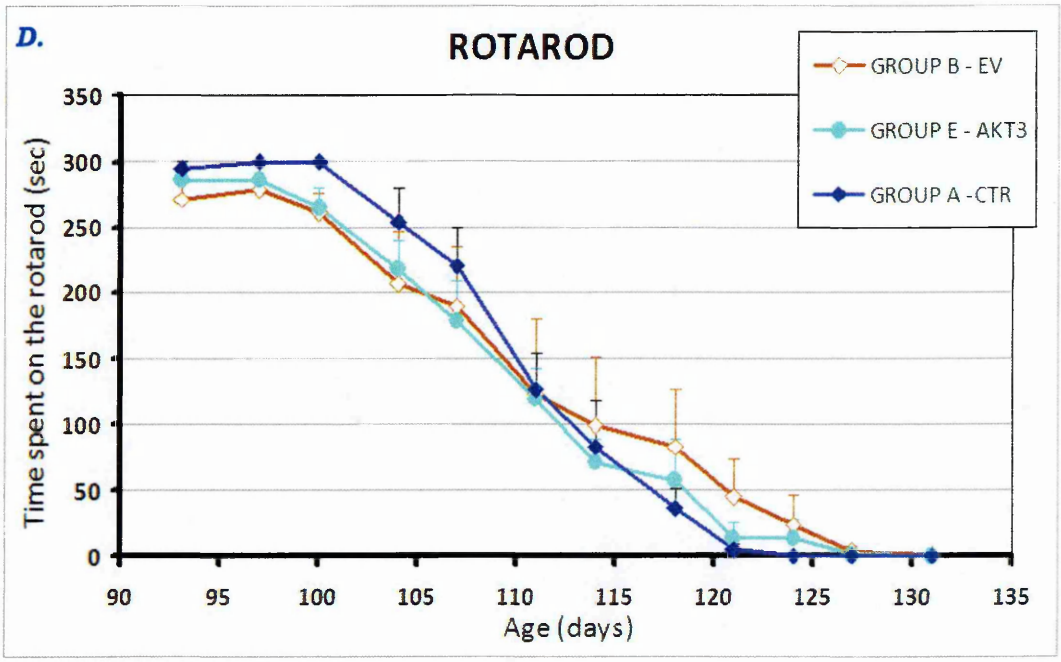

Two-way ANOVA for repeated measures
Group E vs Group A: *Fint* p=0.85
Group E vs Group B: *Fint* p=0.99
Group A vs Group B: *Fint* p=0.65

Body weight (**A**), extension reflex (**B**), and performance on grid test (**C**) and on rotarod (**D**) of Myr.AKT3 treated animals (Group E; n=7), compared to control sham operated mice (Group A; n=5) and to animals injected with empty vector (Group B; n=6). For grid test, Group B displayed a tendency to a less steep decrease of motor performances starting from 111 days of age. Group E shows a slightly better performance than control groups at 107 days of age, on the same test. However, statistical analysis by two-way ANOVA for repeated measures showed no significant effect for any group in any test.

Figure 4.5

End-point analysis of deficits in SOD1G93A mice after treatment with W.1.6.Myr.AKT3 or empty vector

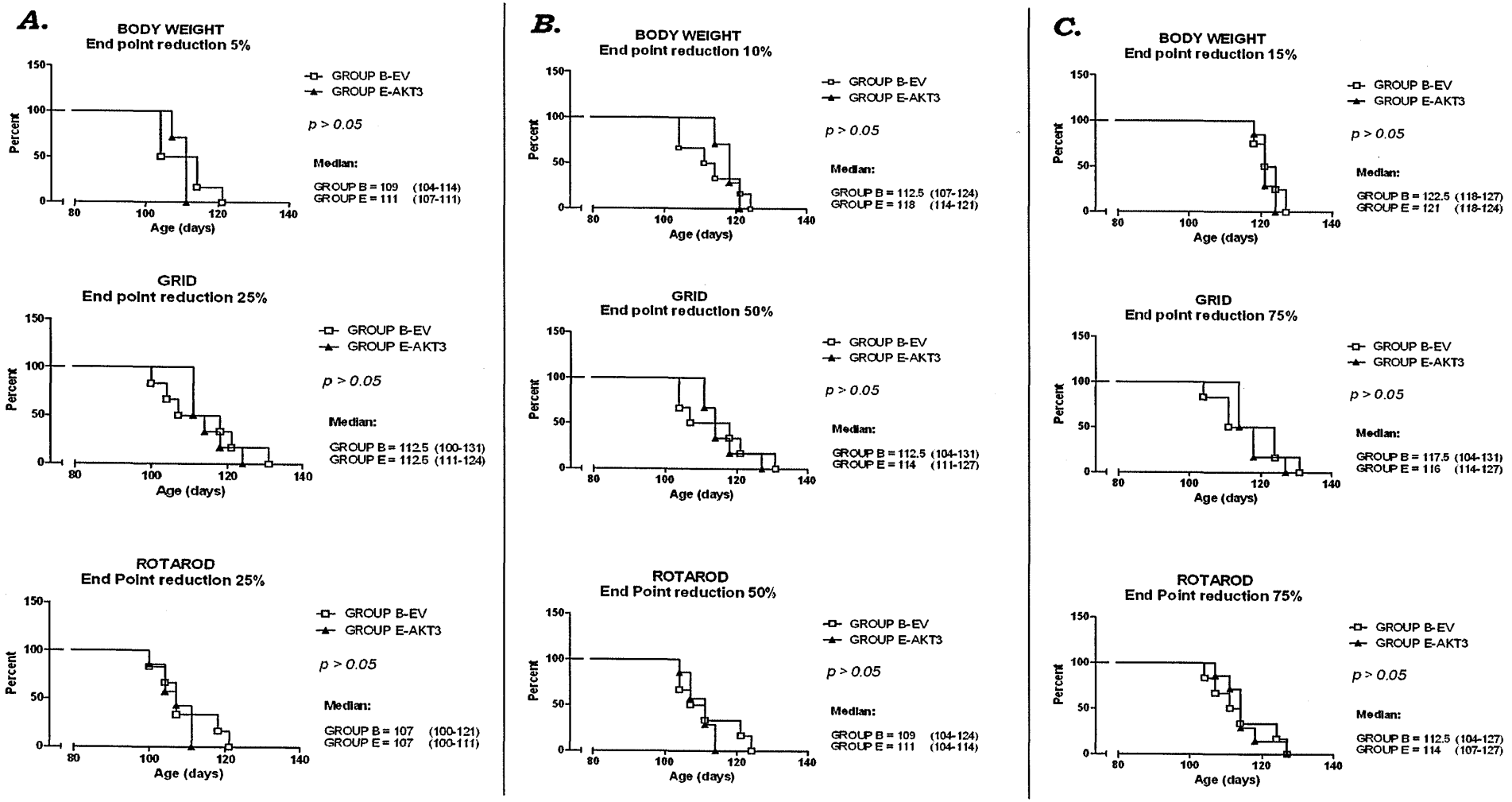

Probability to reach a specific reduction of body weight, or of motor performance on grid test and rotarod, for Myr.AKT3 treated animals (Group E; n=7), compared to animals injected with empty vector (Group B; n=6). **A.** Onset of motor deficits; **B.** Advanced stage of the disease, corresponding to a 50% drop of performances; **C.** Late stage of the pathology, corresponding to a 75% drop of motor performances. Log-rank analysis of probabilities showed no significant differences.

Figure 4.6
Expression of Myr.AKT3 increases motor neuron survival in SOD1G93A animals

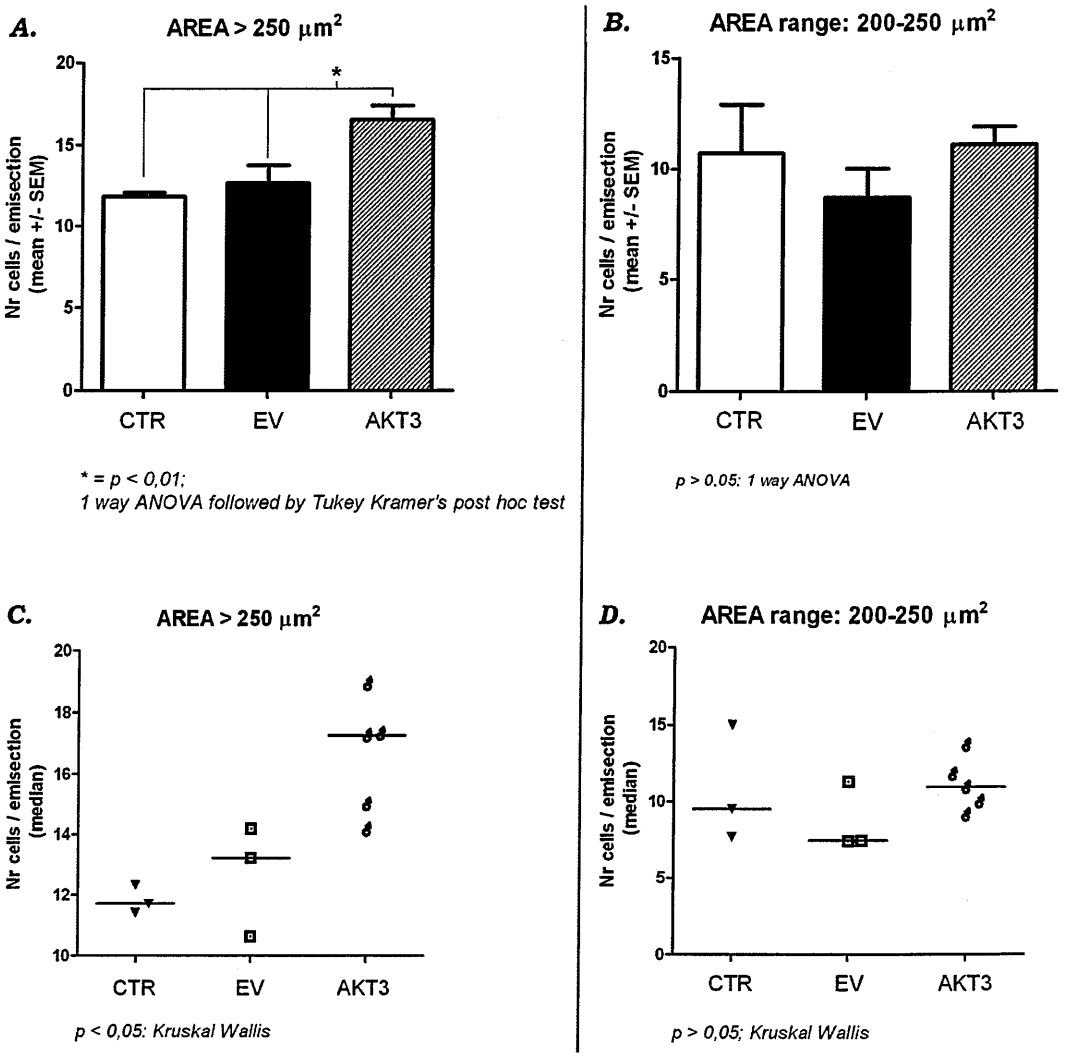

Evaluation of the number of surviving motor neurons in the lumbar spinal cord of SOD1G93A at the end stage of disease after treatment with Myr.AKT3 (AKT3; n=5), compared to animals that received injection of empty vector (EV; n=3) or sham operated mice (CTR; n=3). **A.** Mean number of surviving cells with area higher than 250μm² **B.** Number of surviving neurons with small area (range 200-250μm²), considered not to be motor neurons. In **C, D** the distribution of single data used in the analysis is represented. Statistical analysis was performed by 1 way ANOVA followed by Tukey Kramer's post hoc test. Results were confirmed with Kruskal Wallis non-parametric test for comparison of medians.

Figure 4.7

Intraspinal injection of W.1.6.Myr.AKT3 lentivector in SOD1G93A animals results in specific expression of the transgene in motor neurons

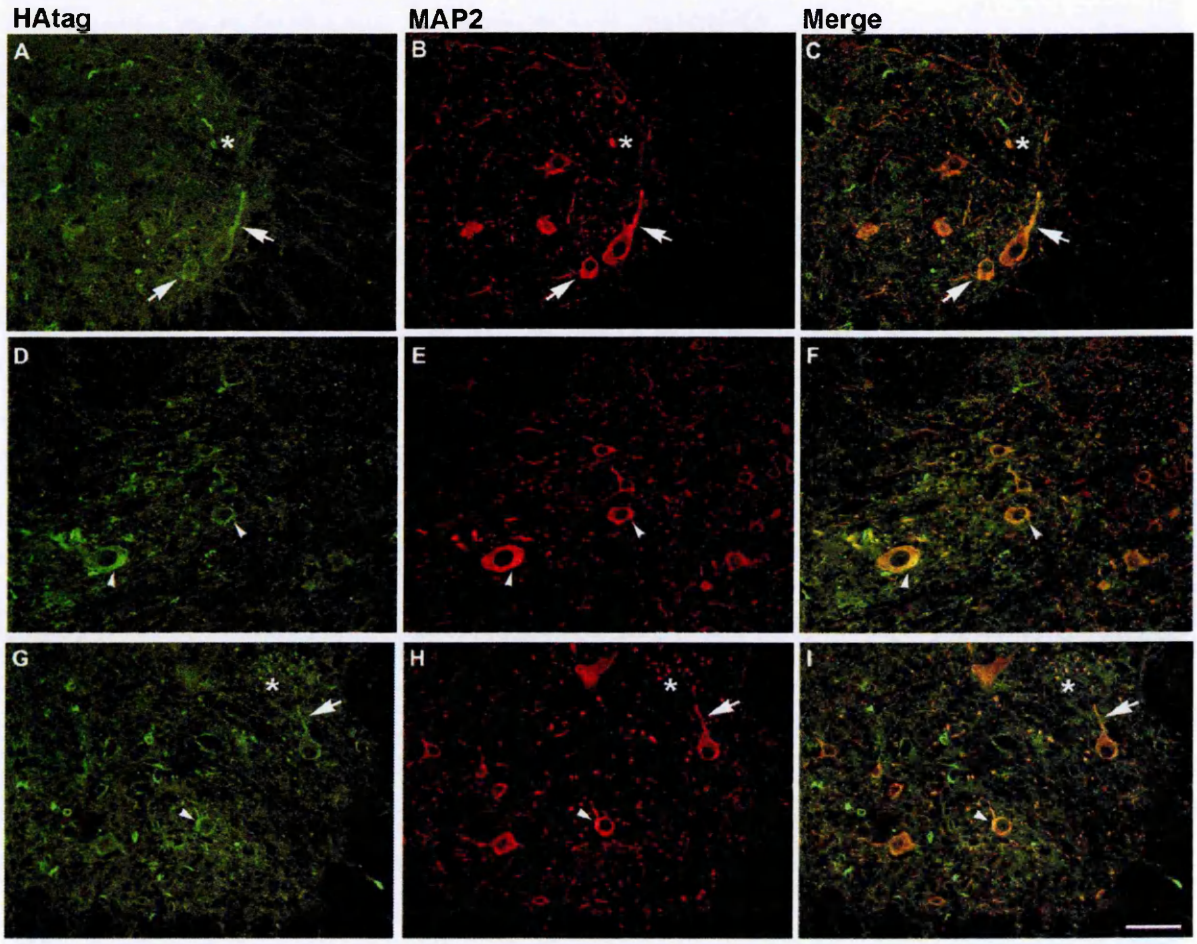

Representative confocal microscope microphotographs of HAtag (green) and MAP2 (red) immunostaining in lumbar spinal cord sections obtained from end stage SOD1G93A mice after treatment with Myr.AKT3 expressing lentivirus. Strong expression of the transgene is detected in motor neurons; the signal is mainly localized in the cytoplasm, extending to proximal neurites (arrows in A-C and G-I). In some cases HAtag was more intense in peripheral regions of the cytoplasm, probably indicating submembrane localization (arrowheads in D-I). Very faint or no signal was detected in the nucleus. In the grey matter some spot-like immunoreactivity for HAtag was also detected; colocalization of this signal with MAP2-positive spots suggests localization in transverse-sectioned neurites (asterisks in A-C, G-I). Scale bar= 50μm.

Figure 4.8

Myr.AKT3 expression results in increased P-Akt staining in motor neurons of SOD1G93A animals

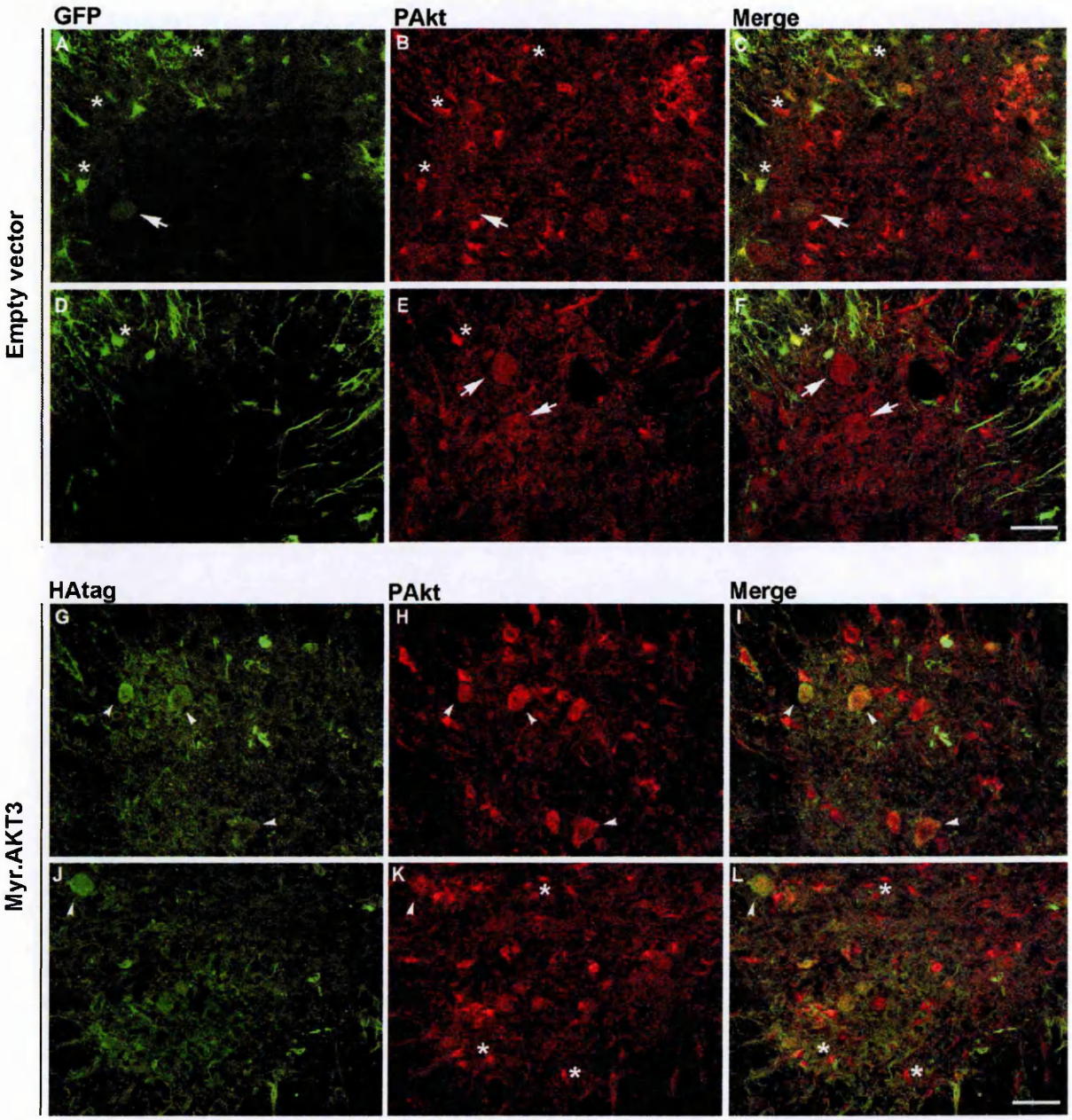

Laser scanning confocal microphotographs of PAkt (red) or HAtag (green) immunostainig in SOD1G93A animals treated with Myr.AKT3 expressing lentivirus (G-L), as compared to mice injected with empty GFP expressing lentivector (A-F). Strong spot-like PAkt immunoreactivity was detected throughout the grey matter in both treated groups, probably reflecting activation of the pathway in glial cells (asterisks in A-F and K-L). Motor neurons of animals injected with empty vector showed a faint PAkt staining (arrows in A-F); in contrast, intense immunoreactivity for PAkt was detected in motor neurons expressing Myr.AKT3 (arrowheads in G-L). Scale bars=50μm.

4.3 Discussion

We successfully produced a constitutively activated mutant form of AKT3. A 13aa myristylation sequence was added to the N-terminus of the cDNA of HA.AKT3, also containing an HAtag for tracking of the transgene. The new Myr.AKT3 construct displayed high efficiency of Akt phosphorylation after transfection in vitro, and caused increased phosphorylation of GSK3β at Ser^9, indicating that the protein expressed from the construct was functional in vivo. With the aim of specifically inducing the Akt pathway in motor neurons of SOD1G93A animals, we subcloned Myr.AKT3 in a lentiviral vector plasmid, and finally substituted the ubiquitous promoter with the Hb9_1.6Kb enhancer elements, previously described in chapter 3. The resulting lentivirus was then delivered by intraspinal injection in SOD1G93A mice at the pre-symptomatic stage. Our lentiviral vector-mediated approach resulted in specific sustained expression of the transgene in the lumbar spinal cord motor neurons, and strong increases in Akt phosphorylation, as assessed by immunohistochemistry. However, although the induction of Myr.AKT3 expression in SOD1G93A exerted a significant protection of motor neurons, this was not paralleled by an increased survival of the treated animals. The disease progression, in Myr.AKT3-treated mice, was comparable with sham operated animals or mice that received empty GFP expressing lentivector.

The lack of a clear beneficial effect on disease progression by Myr.Akt3 is in contrast with previous reports, that showed a protective effect of treatments with Akt-inducing growth factors, such as VEGF and IGF-I, both on neuron survival and disease progression *(Nagano et al., 2005; Storkebaum et al., 2005; Dewil et al., 2007b)*. Besides the possibility that protective mechanisms other than Akt pathway could have been activated by growth factors, another possible explanation is that we specifically targeted a subset of motor neurons, while in the studies from Storkebaum and Nagano the authors delivered the growth factors intrathecally. This may have produced a more widepread distribution of

VEGF or IGF-I. Although the authors only described effects on the neuronal cell population, this mode of administration may in fact have affected also other cell populations of the spinal cord such as the glial cells, possibly modifying their reactivity *(Nagano et al., 2005; Storkebaum et al., 2005).*

By histological analysis we reported a 41.6% increase of surviving motor neurons at the end stage of disease in the animals treated with Myr.AKT3. The effect we observed is in general agreement with reports of viral-vector mediated delivery of other pro-survival factors to motor neurons, such as bcl-2 or IGF-I (65.2% and 34% increase respectively) *(Azzouz et al., 2000; Kaspar et al., 2003).* However in these studies a delay of disease progression and an increase in survival was respectively reported. Akt induction might mirror the actions of bcl-2 as both are predicted to exert anti-apoptotic effects, due to inhibition of Bad and subsequent inhibition of cytochrome c release from the mitochondria. The main difference between the study with bcl-2 and our own approach is that intraspinal delivery of the bcl-2 expressing AAV, resulting in a protective phenotype, was performed in 5 weeks old SOD1G93A mice, largely before symptom onset *(Azzouz et al., 2000).* In contrast, we injected the mice at 12 weeks of age, just 2 weeks before symptoms appear. So it could be hypothesized that at the age we treated the mice some motor neurons may have already activated a specific pro-degenerative pathway that Myr.AKT3 expression was not able to counteract.

An important issue which is worth to underline from the present study, is the significant, although modest, reduction in spinal motor neurons loss evaluated at the end of the disease in spite of no beneficial effect on disease progression.

There is emerging evidence that ALS may display features of a distal axonopathy. In fact, distal axonal degeneration has been reported in the early stages of disease in SOD1G93A mice, before neuronal degeneration, and before onset of symptoms *(Fischer et al., 2004).* Moreover, in line with our results, some pre-clinical studies conducted on rodent models of ALS have reported a protection of motor neuronal cell bodies, but very little or no significant effect on disease

progression and survival, probably due to an insufficient protection of the peripheral axons *(Rouaux et al., 2007; Suzuki et al., 2007).* Nevertheless this does not explain why Myr.AKT3 expression in spinal cord motor neurons leads to preferential protection of the perikarion, while viral mediated delivery of VEGF or IGF-I, factors upstream of Akt pathway, also exerted an effect on phenotype and survival. The main difference with these studies is that we targeted motor neurons by intraspinal injection of a lentivector, while the authors of these studies infected the spinal cord by retrograde delivery of the virus after administration in peripheral muscles *(Kaspar et al., 2003; Azzouz et al., 2004a).* Through this strategy of delivery the authors obtained infection of a high number of motor neurons in different segments of the spinal cord, by simply injecting the virus in different muscular districts, while our intervention was limited only to a part of the lumbar spinal cord.

It has been shown that different subtypes of motor neuron can be identified, depending on the muscular region they innervate in the hindlimbs (fast-fatiguable, fast-fatigue-resistant and slow). Interestingly, in mouse models of ALS axons from fast fatiguable neurons are already affected at the presymptomatic stage, whereas axons from fast-fatigue resistant motor neurons become altered at symptom onset and axons of slow neurons remain resistant *(Pun et al., 2006).* Intraspinal injection leads to generalized infection of spinal cord motor neurons, probably transducing both healthy neurons and neurons that have already started the denervation process. Since Myr.AKT3 expression protects the motor neurons but has no or very little effect on motor performance, it is conceivable that Myr.AKT3 is not able to induce axon regrowth in cells that have become disconnected from the periphery, and that the level of Akt induction in cells still innervating the muscles is probably not sufficient to halt the denervation process. Since we detected Myr.AKT3 mainly at the plasma membrane or in the cytosol of the motor neurons, with only rare translocation to the nucleus, it is also possible that a specific nuclear function of activated Akt is required to

counteract the degenerative process. To better clarify these points another constitutively activated Akt construct could be tested by substitution of Ser^{473} and Thr^{308} with Asp. This is known to act as a permanently phosphorylated (activated) kinase, without the need for membrane translocation *(Alessi et al., 1996b)*.

Interestingly, it has been demonstrated that direct injection of a GDNF expressing viral-vector into the lumbar spinal cord could not prevent motor neuron loss and denervation while retrograde delivery of GDNF, through expression in peripheral muscles, was sufficient to maintain intact axonal projections to the periphery and protect motor neurons *(Wang et al., 2002; Guillot et al., 2004)*. An alternative approach deleted the pro-apoptotic gene Bax, resulting in a rescue of spinal cord motor neuron loss and a delay in, but not prevention of, neuromuscular denervation *(Gould et al., 2006)*.

Overall these data suggest that potential therapeutic interventions need to combine a protective effect on neuronal cell body with a preservation of the axonal projections to peripheral muscles. Our findings and other studies have highlighted that induction of the Akt pathway can be regarded as a potential strategy to sustain motor neuronal survival in the spinal cord, however further studies are needed to identify molecules that can intervene effectively in the pathological processes leading to peripheral denervation in ALS.

CHAPTER 5

USE OF RNA-INTERFERENCE

FOR TARGETING P38MAPK PATHWAY

5.1 RNAi, an introduction

One of the biggest recent breakthroughs in biology has been the discovery of RNA interference (RNAi). First described in plants, where it was known as post-transcriptional gene silencing, RNAi occurs also in a wide variety of eukaryotic organisms *(Tijsterman et al., 2002).* It is triggered by dsRNA precursors that vary in length and origin. These dsRNAs are rapidly processed into short RNA duplexes of 21 to 28 nucleotides in length, which then guide the recognition and ultimately the cleavage of complementary single-stranded RNAs, such as messenger RNAs or viral RNAs. RNA silencing mechanisms were first recognized as antiviral mechanisms that protect organisms from RNA viruses, or which prevent the random integration of transposable elements. In nature, dsRNA can in fact be produced by RNA-templated RNA polymerization (for example, from viruses) or by hybridization of overlapping transcripts (for example, from repetitive sequences such as transgene arrays or transposons). Such dsRNAs give rise to siRNAs, which generally guide mRNA degradation. The maturation of small RNAs is a stepwise process catalysed in the cytoplasm by a dsRNA-specific endonuclease, termed Dicer, which contains catalytic RNase III and dsRNA-binding domains. Processing of dsRNAs by Dicer yields RNA duplexes of about 21 nucleotides in length, which have 5'-phosphates and 2-nucleotide 3'- overhangs. Artificial introduction of long dsRNAs or siRNAs has been adopted as a tool to inactivate gene expression *(Meister and Tuschl, 2004).* Viral vectors, thanks to their high efficiency of infection both in cultured cells and in living organisms, represent a system frequently used to induce RNAi, allowing efficient downregulation of gene expression also in the CNS *(Van den Haute et al., 2003).* In this case, siRNAs derive from cleavage of a small-hairpin RNA, produced after transcription of a palyndromic sequence by RNA pol. III *(Snove and Rossi, 2006).*

5.2 RNAi as a tool to study the molecular mechanisms involved in ALS pathogenesis

The main technical advantage of RNAi is that it can be used to downregulate specific genes in vivo. This means that it is possible to interfere with specific pathways at a post-natal level; thing that would be very complicate if traditional knock-out technologies were applied. Recently, RNAi has been used to study the toxic properties of mutant SOD1 in ALS. In particular, siRNAs-mediated downregulation of the mutant protein in adult transgenic mice has been obtained, to verify whether the toxic events that occur early in the disease are reversible or whether they, once triggered, irreversibly lead to cell death even in the absence of mutant SOD1. In a work by Raoul and coworkers lentiviral vectors expressing a mutant SOD1-targeted shRNA were delivered in the spinal cord of 40 days old SOD1G93A mice. This determined a considerable delay of disease onset of 20 days; it also delayed the progression rate of motor deficits and ameliorated muscular strenght, though the effect on survival is not described *(Raoul et al., 2005b)*. Similarly, another group silenced mutant SOD1 by RNAi. In this case a lentiviral vector that can be retrogradely transported was injected in several peripheral muscles of 7 day old SOD1G93A mice. A remarkable delay of onset (by 115%) and increase of survival (by 77%) over control groups was reported *(Ralph et al., 2005)*. Recently, Wang and coworkers have administrated chemically modified siRNAs in vivo, in the same mouse model at symptom onset *(Wang et al., 2008)*. They observed a 6.5% extension of life span, thus providing evidence that chemically modified siRNAs can be delivered and are stable in vivo in transgenic mice, and that partial ablation of mutant SOD1 delays disease progression. However, since animals that received SOD1-targeted siRNAs still developed the disease and finally died, it is worthy considering that other proteins should be targeted to efficiently interfere with the disease progress.

Interestingly, RNAi-mediated downregulation of Fas signalling pathway has recently been tested in SOD1G93A mice *(Locatelli et al., 2007)*. The treatment,

initiated at 90 days of age, significantly improved motor performances and increased survival of 20 days, further supporting the evidence of an involvement of this pathway in motor neuronal degeneration in ALS *(Raoul et al., 2002; Raoul et al., 2005a; Raoul et al., 2006)*. p38MAPK is a key player of the signalling cascades activated upon exposure to stress stimuli, including Fas and cytokines. As already stated in section 1.4.3 we and other groups have provided evidence of an activation of p38MAPK pathway both in post mortem spinal cord specimens from human ALS patients and in mutant SOD1 mouse models. Progressive increase and activation of p38MAPK is associated with hyperphosphorylation and cytoplasmic accumulation of neurofilaments, a pathogenic hallmark of ALS *(Tortarolo et al., 2003; Bendotti et al., 2004; Holasek et al., 2005)*. A crosstalk between p38MAPK pathway and TNFα has been recently described in SOD1G93A mice, suggesting that this pathway may be a key player of the neuroinflammatory process involved in the degeneration of motor neurons in ALS *(Veglianese et al., 2006)*. Moreover, ASK1-p38MAPK pathway is also involved in ER-stress induced cell death *(Sekine et al., 2006)*. Interestingly upregulation of CHOP, an ER-stress induced pro-apoptotic protein, has been detected in sALS patients and ALS mouse models *(Ito et al., 2009)*, and crossbreeding of SOD1G93A mice with animals knockout for ASK1 was protective for motor neurons and determined a 25 days extension of survival *(Nishitoh et al., 2008)*. We hypothesized that p38MAPK may function as a critical molecule implicated in the triggering of several toxic responses in motor neurons and glial cells in ALS, so interfering with its activation may contribute to prolong life span by delaying the disease progression. In particular, since it has been observed that p38MAPK alpha is directly involved in neurofilaments phosphorylation in ALS *(Ackerley et al., 2004)*, this isoform may represent a potential therapeutic target. The availabe pharmacologic p38MAPK inhibitors have poor bioavailability to the CNS, and are not selective for one specific isoform (see section 1.4.4). Recently it has been demonstrated that Semapimod, a c-Raf inhibitor, delivered to

SOD1G93A mice starting from 70 days of age, effectively inhibited p38MAPK activation in the spinal cord, resulting in protection of motor neurons, though with a small effect on survival *(Dewil et al., 2007a)*. Since p38MAPK is not a selective target of Semapimod, the work by Dewil does not provide complete elucidation of the role played by this kinase in the pathologic process. For these reasons we decided to develop an RNAi-mediated approach with the aim to downregulate specifically p38MAPK alpha isoform in vivo, in the spinal cord of a mouse model of ALS.

5.3 Screening of p38MAPK-targeted shRNA candidate sequences

In the course of identifying more active and more specific siRNA duplexes to guide mRNA cleavage, it has been noticed that the sequence composition of the siRNA duplex has an impact on the ratio of 'sense' (same sequence as the target gene) and 'antisense' (complementary to the target gene) siRNAs entering the RISC complex. Effective siRNAs show reduced thermodynamic stability at the 5'-end of the antisense siRNA relative to the 3'- end within the duplex *(Dykxhoorn et al., 2003; Cheng and Chang, 2007)*.

To our knowledge, there are no shRNA sequences already validated for targeting murine p38MAPK alpha, in the literature. For this reason we initially chose a set of five already described shRNAs targeting the human protein, numbered 1 to 5 (Table 5.1). According to the rules described above we mutated these sequences to obtain perfect matching with murine p38MAPK alpha without loosing the potential to induce RNAi. Some of the sequences were 29nts long, at variance with the commonly used 19nts oligomers. The design of these 29nts sequences has been done according to the description of Siolas et al., that demonstrated that 29-mers can be more effective than 19-mers in the triggering of RNAi *(Siolas et al., 2005)*. In order to easily detect a shRNA sequence effective in murine p38MAPK-alpha downregulation, lentiviruses each carrying one of these sequences were used to infect NIH3T3 cell line (as described in section 2.2.7).

p38MAPK alpha protein and mRNA levels were analysed 3 days after infection by western blotting and RT-PCR respectively. Since none of the first five candidate shRNAs proved to be effective in downregulating p38MAPK alpha, we moved to another set of 5 shRNAs (numbered 6 to 7 in Table 5.1), cloned in pLKO.1 plasmids. The puromicine resistance, in these plasmids, was excised by BamHI/KpnI cut and substituted with GFP reporter gene. Lentiviral vectors, each containing one of these candidates, were used to infect NIH3T3 cell line in the same experimental setting as before.

Table 5.1. List of candidate shRNA sequences targeting murine p38MAPK alpha

Seq ID	Nr ntds	Target sequence (5'→3') BLAST on p38MAPK alpha sequence	Reference article/ designed by...	Notes
1	19	CCCCAGAGATCATGCTGAA 865	*(Siolas et al., 2005)9}5)*	The authors designed shRNas for human p38MAPK. Some of these sequences have been chosen and modified to adapt to murine p38MAPK gene.
2	29	ACCGTTTCAGTCCATCATTCACGCCAAAA 467		
3	19	CCGAAGATGAACTTCGCAAAT 1092	Seq. 1092, designed by the Broad Institute	//
4	19	CCAACAATTCTGCTCTGGTTA 3168	Seq. TRC55223, designed by the Broad Institute	//
5	19	CCTCTTGTTGAAAGATTCCTT 1463	Seq.TRC23119, designed by "The RNAi Consortium"	//
6	19	CCTGACCTATGATGAAGTCAT 1313	Seq. TRC23122, designed by "The RNAi Consortium"	Purchased from Open Biosystem
7	19	GCTGAATTGGATGCACTATAA 878	Seq. TRC23123, designed by "The RNAi Consortium"	Purchased from Open Biosystem
8	19	CTCAGAGTCTGCAAGAAACTA 1049	Seq. TRC55224, designed by "The RNAi Consortium"	Purchased from Open Biosystem
9	19	GTCTGCAAGAAACTACATTCA 1055	Seq. TRC55225, designed by "The RNAi Consortium"	Purchased from Open Biosystem
10	19	CGAGGGCTGAAGTATATACAT 702	Seq. TRC55227, designed by "The RNAi Consortium"	Purchased from Open Biosystem

Three days after infection we detected by western blot a 80% reduction of p38MAPK alpha with sequence nr.7. This effect was not due to generalized reduction of protein synthesis, since seq.nr.7 downregulated p38MAPK alpha

isoform without any influence on the levels of other proteins, like PI3Kp85, or ERK and without inducing interferone response, as demonstrated by lack of increase of P-STAT and P-eIF2α (Figure 5.1, A). RT-PCR preformed on RNA extracted from the same cultures confirmed that sequence nr.7 was able to reduce the mRNA of p38MAPK alpha by 45% rate (Figure 5.1, B). To provide a complete validation of the RNAi effect, three point mutations were introduced into sequence nr.7 with the aim to dysrupt the matching with the mRNA of murine p38MAPK alpha (Figure 5.2). Lentiviral vectors containing the new sequence, named shRNA nr.7*, were used to infect primary murine astrocyte cultures under basal non-stimulated conditions, in parallel with shRNA nr.7 and a GFP expressing empty vector. Lysates extracted from these cultures at three days post infection showed a 70% reduction of p38MAPK alpha in shRNA nr.7 infected cells by western blotting, and no changes of the protein levels with shRNA nr.7*, as predicted (Figure 5.3).

5.4 shRNA nr.7 selectively inhibits TNFα induced p38MAPK phosphorylation

TNFα signaling has been strongly implicated in ALS, and p38MAPK is one of the key mediators of the effects induced by cytokine stimulation, such as in the regulation of transcription of several pro-degenerative genes including nitric-oxide synthase, TNFα, TNFα receptors, and IL-1. In addition, TNFα exposure in cultured astrocytes produces a strong activation of p38MAPK and the other stress-induced kinases, JNK and ERK *(Da Silva and Silva, 1997)*. To further validate the activity and specificity of shRNA nr.7, we decided to study the effect of TNFα exposure in cells following p38MAPK downregulation. In particular we investigated whether shRNA nr.7 knockdown was sufficient to maintain low levels of p38MAPK phosphorylation upon cytokine-stimulation and also whether this may influence the activation of JNK kinase which shares common upstream activators with p38MAPK, such as ASK1 *(Mielke and Herdegen, 2000)*. Murine

astrocyte cultures were infected with lentiviruses expressing shRNA nr.7, shRNA nr.7* or an empty GFP expressing vector (as described in section 2.2.7) in triplicate, or left untreated as a negative control. After three days (when sufficient downregulation of p38MAPK by shRNA nr.7 is expected) the medium was replaced with fresh medium containing 100ng/mL TNFα and then incubated for 15min or 60min at 37°C. The concentration of TNFα and times of exposure were chosen according to previously published reports *(Da Silva and Silva, 1997)*, and from our own preliminary observations, showing that a short time of exposure (15min) to TNFα was sufficient to stimulate p38MAPK phosphorylation, whereas a longer time of exposure (60min) was needed to stimulate JNK phosphorylation (data not shown). Exposure to TNFα for 15min caused a 5-fold increase of p38MAPK phosphorylation in non-infected astrocytes compared with basal levels. A similar increase in p38MAPK phosphorylation was also detected in cells infected with shRNA nr.7*. In contrast, in cells infected with shRNA nr.7 the levels of p38MAPK phosphorylation remained very low following exposure to TNFα (Figure 5.4 A, B). However exposure to TNFα for 60min was sufficient to induce a clear and robust 2-fold increase in phosphorylated JNK (Figure 5.4 C, D) both in shRNA nr.7* and shRNA nr.7 infected cells, over non-stimulated control cultures. This effect was significant only for astrocytes infected with shRNA nr.7. Expression of p38MAPK-targeted shRNA did not modify the levels of total JNK (Figure 5.4 C, E).

5.5 shRNA nr.7 protects cultured neurons against colchicine induced toxicity

Colchicine is a microtubule dysrupting agent that induces apoptosis in several cell types, including neurons. This paradigm of cell toxicity can be used to mimick the alterations of cytoskeleton observed in many neurodegenerative diseases, including Alzheimer's disease and ALS *(Bonfoco et al., 1995; Williamson and Cleveland, 1999; Ackerley et al., 2004)*. A recent paper revealed that p38MAPK and JNK pathways are involved in the apoptotic process induced by colchicine in rat cortical neurons *(Yang et al., 2007)*. In particular, the authors showed that pharmacologic inhibition of p38MAPK or JNK was able to reduce neuronal loss after treatment with colchicine. This effect was synergistic if p38MAPK and JNK were both inhibited at the same time. We used the same experimental paradigm to test whether the shRNA targeting p38MAPK exerted a similar protective effect. Primary rat cortical neurons, obtained from the brains of two-day old rat pups, were prepared in collaboration with the Unit of Cell death and Neuroprotection Mechanisms of Mario Negri Institute, in accordance with the protocol described in section 2.2.6. In initial experiments neurons at day 1 after plating were infected by lentiviruses expressing p38MAPK-targeted shRNA nr.7, or with empty GFP expressing vector, or left untreated as negative control. At day 6, cells were lysed and proteins extracted. Analysis by western blot demonstrated that shRNA nr.7 retained the ability to downregulate p38MAPK alpha also in rat-derived cells, without activation of proteins of the Interferon response, such as P-eIF1α (Figure 5.5 A). Subsequently neurons at day 1 after plating were infected by lentiviruses expressing shRNA nr.7, or shRNA nr.7*, or left not infected as negative control. At day 6, cells were challenged by exposure to colchicine 1μM for 24h according to the procedure already described by Yang *(Yang et al., 2007)*. The rate of cell mortality in this case was measured by LDH assay (Roche, Basel, Switzerland). In uninfected neurons, colchicine determined a 2.6-fold increase of LDH release as compared to untreated cells. Infection with shRNA nr.7 reduced

colchicine-induced neuronal death (as measured by LDH release) by 40%, as compared to uninfected colchicine-treated neurons whereas shRNA nr.7* was completely ineffective (Figure 5.5 B).

5.6 Effect of p38MAPK downregulation in vivo, in SOD1G93A mice

Based on the data obtained in the in vitro studies, lentiviral vectors containing a GFP-expressing empty vector, or shRNA nr.7* or shRNA nr.7 were delivered by intraspinal injection in animals at the presymptomatic stage (84 days). In order to allow direct comparison of the effect of each sequence, lentivectors expressing shRNA nr.7 or shRNA nr.7* were administered in the right side of the spinal cord, whereas a GFP-expressing empty vector was delivered in the contralateral side. The surgical procedure was as described in section 2.2.3 with minor modifications (outlined in Figure 5.6 B). To further monitor possible effects induced by the intraspinal injection of lentivectors, a GFP-expressing empty-vector was administered monolaterally in the spinal cord of a separate group of SOD1G93A and NTg animals, and the contralateral side was left untreated (sham operated), as outlined in Figure 5.6 A. Three animals were treated for each experimental group. Mice were sacrificed 16 days after injection, and the spinal cord was collected and sectioned for NISSL staining and counting of surviving motor neurons. The ratio between the number of cells in the treated versus control side of spinal cord was calculated, and used for comparison between groups. Interestingly, when we analyzed the effect of GFP-expressing empty vector alone, while we did not detect any difference between injected and sham-operated side in NTg animals, in SOD1G93A mice we noticed a slight, although not significant, decrease of surviving neurons in the injected side. (Figure 5.7 A). To better elucidate this result, we re-calculated the comparison after subgrouping the surviving neurons according to the spinal cord level in which they were located (the areas surrounding the injected sides, L_3 and L_4 segment of spinal cord, were considered) (Figure 5.7 B). At level L_3 there were no significant

differences between right and left side in NTg and in SOD1G93A animals. In contrast, at level L_4 we detected a significant reduction of the number of motor neurons in the empty vector-injected side of SOD1G93A animals, suggesting that in transgenic animals these cells may be susceptible to the trauma generated by an injection in the parenchyma. Despite this effect, in SOD1G93A animals we detected a tendency to protection (1.6-fold increase) of motor neurons (area higher than 250μm^2) in the side of spinal cord injected with shRNA nr.7, versus the contralateral empty vector-injected side, as compared to the treatment with shRNA nr.7*, that was completely ineffective (Figure 5.8 A). This was furtherly confirmed when the surviving neurons were subgrouped according to the spinal cord level (Figure 5.8 B). No significant difference was observed for neurons of small areas, in the range 200-250μm^2 (data not shown).

In order to evaluate the effect of p38MAPK alpha downregulation on disease progression, a new experiment was set up in which high titre lentiviral vectors expressing shRNA nr.7 were intraspinally injected in 84day old SOD1G93A mice (n=7; Group C), as described in section 2.2.3.4. As control groups, SOD1G93A animals were injected with a vector expressing shRNA nr.7* (n = 5; Group D). Moreover, since these experiments were conducted in parallel with those described in section 4.2, Group A (n =5 ; animals that underwent laminectomy but did not receive an injection) was used as a further control for Group C and Group D. Motor performance and disease progression were analysed twice a week, as outlined in section 2.2.4.

Surprisingly, the median survival of animals treated with shRNA nr.7 (Group C) was 8 days shorter than the control Group A, and 6.5 days shorter than control Group D. Although this difference was small, it is statistically significant. The survival of animals that received shRNA nr.7* was not different from sham operated animals (Figure 5.9).

Animals from all groups displayed a gradual and comparable gain of body weight at 93 and 97 days of age, probably due to post-operative recovery. However,

starting from 100 days, control groups A and D displayed a comparable progressive loss of body weight, whereas in Group C a steeper decrease was observed (Figure 5.10, A) although this difference was not significant, by 2-way ANOVA analysis for repeated measures. However, when the cumulative probability to reach a 5%, 10% or 15% drop in body weight was analysed, the trend for Group C to lose body weight before Group A (Figure 5.11 A) or Group D (Figure 5.12 A) became significant.

The treatment with shRNA nr.7 also accelerated the progression of motor deficits. Extension reflex test highlighted a tendency of Group C to already show a deficit at 93 and 97 days, as compared to control groups. This trend became statistically significant from day 100 to day 111 versus both control groups. The performance of Group D was not significantly different from Group A, although from day 104 the progression of deficits appeared slightly worse than the sham operated animals (Figure 5.10, B). The grid test confirmed that motor deficits in Group C were measurable from day 97, as compared to control groups. This became significant at day 104 and 107 (Figure 5.10, C). Similarly, Group C displayed a significantly impaired rotarod performance starting at day 97 until end stage, as compared with control groups (Figure 5.10 D). The progression of motor deficits in the animals treated with shRNA nr.7* (Group D) was comparable with Group A in both tests. These observations were confirmed by analysis of the cumulative probability to reach a 25%, 50% or 75% drop of performance on the grid (Figure 5.11 B and 5.12 B) and on the rotarod (Figure 5.11 C and 5.12 C).

In order to verify whether the phenotype in shRNA nr.7-treated animals was linked with increased loss of motor neurons, the spinal cords from mice that reached end stage of disease were collected, and sectioned for NISSL staining. The mean number of motor neurons (with an area higher than 250μm^2) was considered in the analysis. The number of surviving cells in shRNA nr.7-treated group (8.03+/-0.89 cells/hemisection) was lower than shRNA nr.7*-treated

Group D (10.04+/-0.99 cells/hemisection) or Group A (11.81+/-0.27 cells/hemisection) although this difference was statistically significant only versus Group A. In fact the number of surviving neurons in Group D was slightly lower than Group A (Figure 5.13 A). Curiously, for Group C we noticed an interesting, though not significant, decrease of neurons with an area between 200 and 250 μm^2 (6.71 +/- 0.77 cells/hemisection), as compared to control Group A (10.74 +/- 2.18 cells/hemisection) or Group D (10.37 +/- 1.20 cells/hemisection) (Figure 5.13 B). Based on this evidence we decided to subgroup the surviving neurons, counted in each group, according to the spinal cord level in which they were located (from L_2 to L_4) (Figure 5.14). In level L_2 the number of cells with an area higher than 250μm^2 was not significantly different between groups, however Group D displayed a slight reduction of cells as compared to Group C and control Group A. In level L_3 a loss of cells could be observed for Group C as compared to Group D, which in turn showed a slight increase compared to Group A. In level L_4 both Group C and Group D showed a smaller number of cells as compared to Group A; this difference was significant only for Group C (Figure 5.14 A). When the number of small neurons (area 200-250 μm^2) was evaluated, no differences were detected between groups at level L_2. However, Group C displayed a modest decrease of cells at level L_3, as compared to the other groups; this trend was maintained and became significant at level L_4 (Figure 5.14 B). Overall these data suggest that the phenotype observed after treatment with shRNA nr.7 may be in part explained by the moderate but significant decrease of motor neurons observed in these mice at the end stage of the pathology. In particular, from the analysis of the different spinal cord segments it appears that delivery of shRNA nr.7 produced a greater loss of neurons in the areas surrounding the sites of injection (level L_3 and L_4). This was not simply due to the trauma induced by the intraspinal injection, because in animals treated with shRNA nr.7*-expressing lentivirus the number of motor neurons at least at level L_3 was comparable with the sham operated group.

It is known that glial reactivity plays a critical role during disease progression in ALS *(Boillee et al., 2006a; Boillee et al., 2006b)*; moreover prominent activation of p38MAPK has been described in astrocytes and reactive microglia in SOD1G93A mice, suggesting that this pathway is crucial for induction of neuroinflammation in ALS *(Tortarolo et al., 2003; Wengenack et al., 2004)*. Since shRNA-expressing lentiviruses are expected to infect both neurons and glial cells, we decided to verify whether p38MAPK downregulation altered glial reactivity in shRNA nr.7-treated mice. In order to do this, we performed immunohistochemistry for markers of astrocytosis (GFAP) and microgliosis (CD11b) on spinal cord sections from animals that reached end stage of the disease.

Animals injected with shRNA nr.7* displayed classical reactive astrocytosis, similar to that observed in untreated SOD1G93A mice at the end stage of the disease, characterized by hypertrophic astrocytes scattered throughout the gray and white matter of the spinal cord. The morphology of these cells was not altered by expression of shRNA nr.7* (arrowheads in Figure 5.15 A-C and D-F). In contrast, animals that received shRNA nr.7 displayed strong immunoreactivity for GFAP in the areas surrounding the injection sites (Figure 5.15 H). The morphology of astrocytes in these areas was altered, with filamentous-like structures protrudring throughout the spinal cord parenchyma. Interestingly we observed that these structures were rarely co-localized with the GFP reporter gene signal (asterisks in Figure 5.15 G-I). Moreover, in these regions we observed some very small GFAP negative GFP-expressing cells (arrowheads in Figure 5.15 G-I), and some larger round GFP-positive cells (arrows in Figure 5.15 G-I). In contrast, astrocytosis appeared normal in infected areas that were far from the injection sites (Figure 5.15 J-L). Interestingly, some motor neurons infected with lentivirus expressing shRNA nr.7 could still be detected in these regions at the end stage of disease, as confirmed by GFP staining (arrows in Figure 5.15 J-L and M-O). The immunohistochemistry for CD11b revealed an intense microgliosis in animals treated with shRNA nr.7*, as expected in mice at the end stage of the

disease. The expression of shRNA nr.7* in these cells apparently did not alter their morphology (arrowheads in Figure 5.16 A-C and E-G), whereas in animals treated with shRNA nr.7 the infected microglial cells often appeared larger and rounder in the regions surrounding the sites of injection (arrowheads in Figure 5.16 I-K) as well as in the areas located far from them (arrowheads in Figure 5.16 M-O). In particular, in the spinal cord near the site of injection high microglial reactivity appeared, with round GFP-positive microglial cells scattered throughout the parenchyma. Interestingly, Hoescht nuclear staining highlighted an increase of cells in these areas. Many of these cells appeared organized in clusters, often localized in areas not expressing shRNA nr.7 (GFP negative) as shown by asterisks in Figure 5.16 O-P. We also detected some surviving motor neurons expressing shRNA nr.7 (arrows in Figure 5.16 I, K). Since these motor neurons are still present at the end stage of the disease, we hypothesized that the reduction of neurons evidenced by NISSL staining probably was not the consequence of a direct toxic effect of p38MAPK downregulation in these cells.

Figure 5.1
Screening of candidate shRNA sequences targeting p38MAPK alpha, in vitro

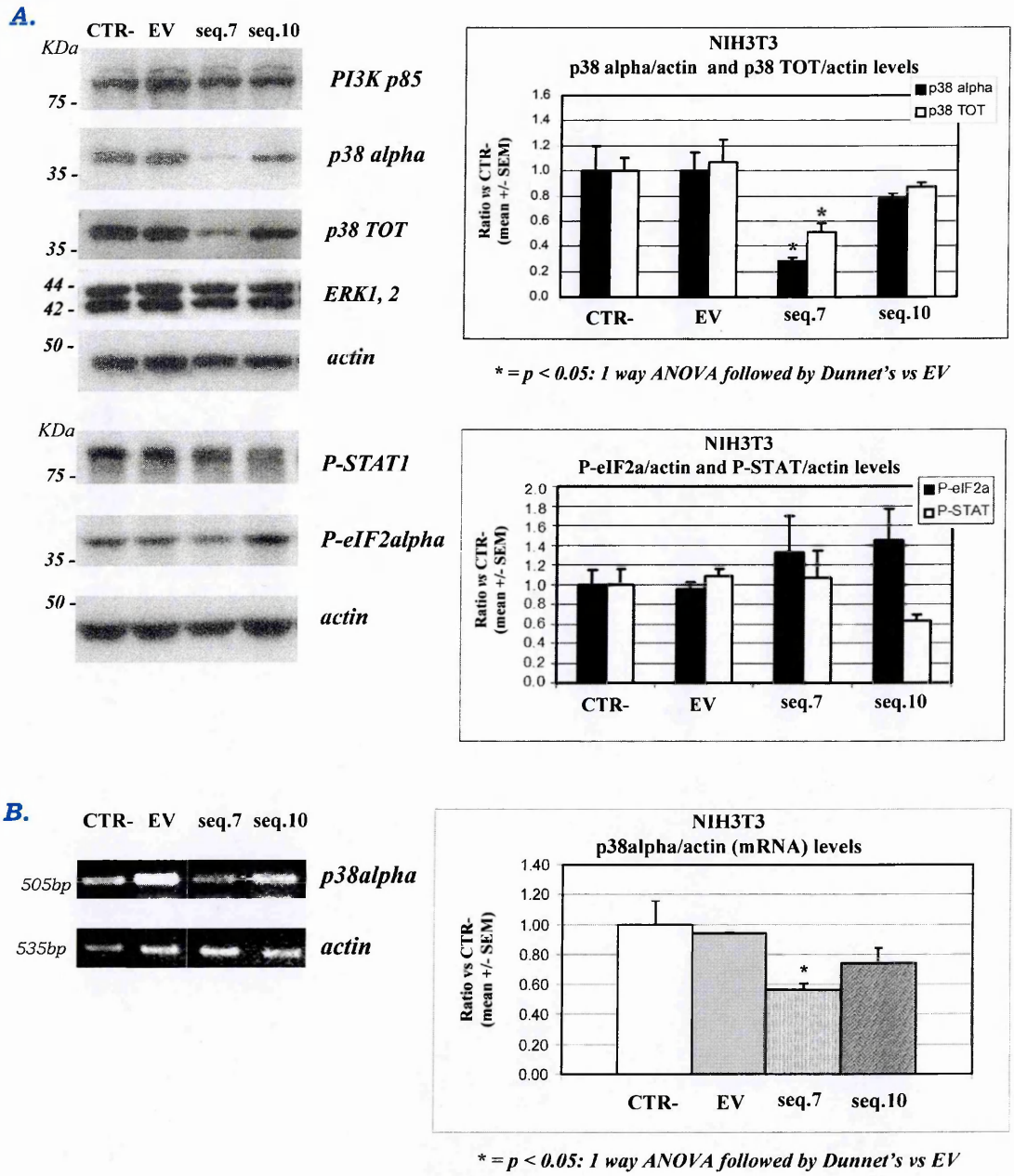

A. Representative immunoblots, and quantification, of p38MAPK alpha, P-STAT and P-eIF2α protein levels in lysates from NIH3T3 obtained 3 days after infection with candidate shRNA sequences targeting p38MAPK. Seq. 7 downregulated p38MAPK alpha by 80%, without inducing activation of anti-viral response, as confirmed by lack of increase of P-STAT and P-eIF2a (n=3). **B.** Quantification of p38MAPK alpha mRNA levels, by RT-PCR, in extracts from NIH3T3 cells infected as described in A. Seq. 7 is able to decrease the mRNA of p38MAPK alpha by 45% (n=3).

Figure 5.2
Schematic representation of shRNA nr.7 sequence*

Sequence shRNA nr.7 **(5′→ 3′):** gctgaattggatgcactataa **Sequence shRNA nr.7*** **(5′→ 3′):** gctgaactggatgcattacaa

Sequence of shRNA nr.7 and shRNA nr.7*. The 3 mutated nucleotides introduced into shRNA nr.7 to obtain shRNA nr.7* are highlighted in yellow. These mutations have been chosen according to the mRNA sequence of human p38MAPK alpha.

Figure 5.3
Test of the selected shRNA sequences on primary cultured mouse astrocytes

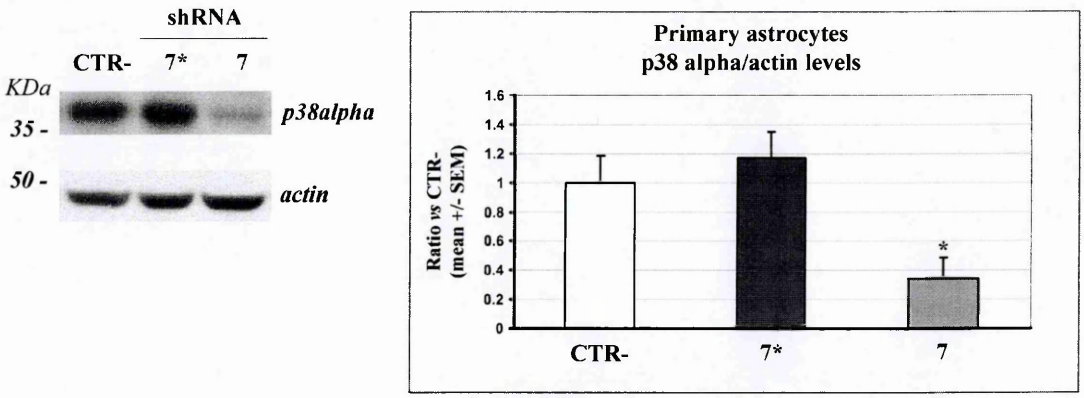

** = p < 0.05: 1 way ANOVA followed by Dunnet's vs CTR-*

Representative immunoblots, and quantification, of p38MAPK alpha protein levels in lysates from astrocytes obtained 3 days after infection with shRNA nr.7 or shRNA nr.7*. Seq. 7 retains the ability to downregulate p38MAPK alpha (by 70%), whereas the mutations introduced in shRNA nr.7* completely abolish this effect (n=3).

Figure 5.4
TNFα-mediated induction of p38MAPK and JNK in murine astrocyte cultures; effect of shRNA nr.7

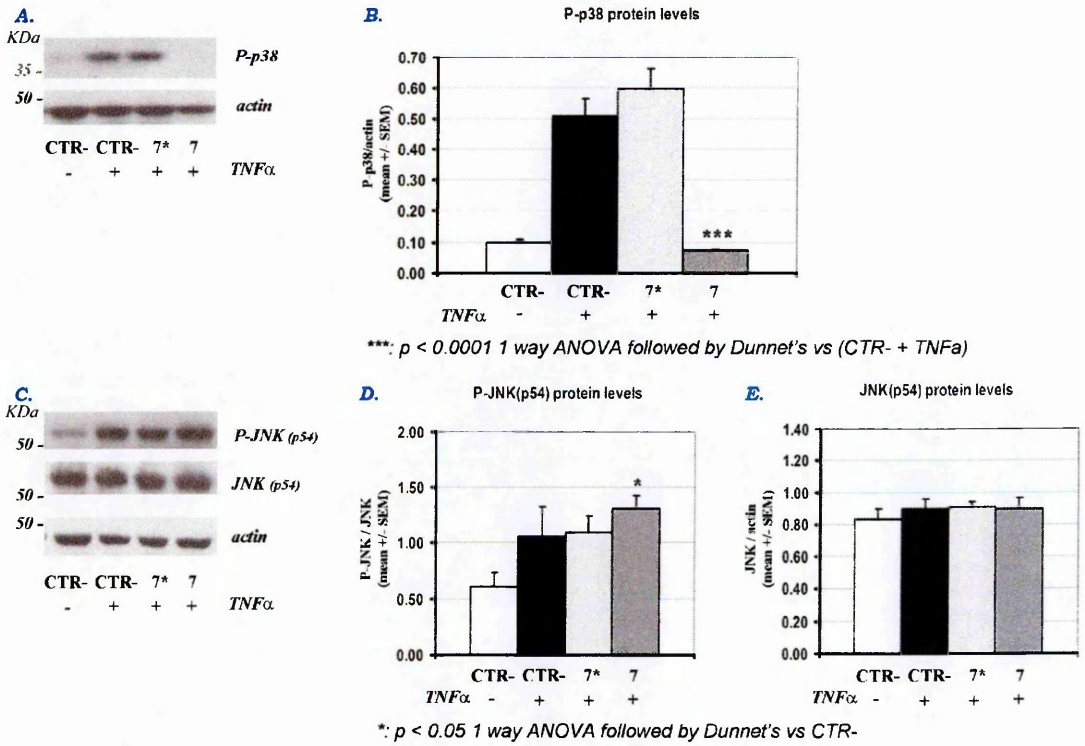

TNFα-mediated induction of p38MAPK and JNK in murine primary astrocyte cultures. **A.** Representative immunoblots for P-p38 in lysates obtained after exposure to TNFα 100ng/mL for 15'. Cytokine-stimulation leads to strong increase of P-p38 in uninfected cultures or in cells infected with shRNA nr.7*. P-p38 are maintained at low basal levels in cultures infected with shRNA nr.7. In **B** the quantification of P-p38/actin ratio for each band shown in A is represented (n=3). **C.** Representative immunoblots for P-JNK in lysates obtained after exposure to TNFα 100ng/mL for 60'. This stimulation leads to a 2-fold increase of P-JNK in not infected cultures, in cells infected with shRNA nr.7*, as well as in cultures infected with shRNA nr.7. Seq. 7 does not modify the levels of total JNK in these cultures. In **D** and **E** the quantification of P-JNK/JNK ratio and of JNK/actin ratio for each band shown in C are represented (n=3).

Figure 5.5
Test of shRNA nr.7 on rat neuronal cultures

A.

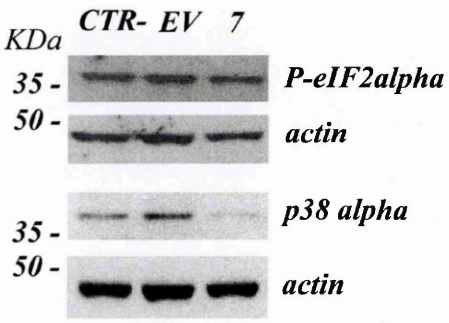

B.

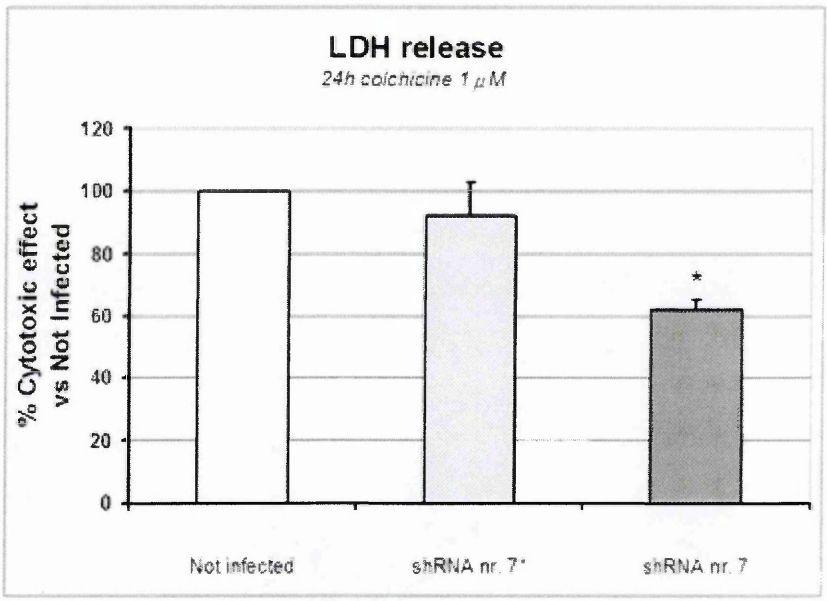

** = p < 0.05; Student's t-test vs shRNA nr.7**

A. Representative immunoblots for p38MAPK and P-eIF2alpha in lysates obtained from rat primary cortical neurons 3 days after infection with candidate shRNA nr.7 or control empty vector (EV). Seq.7 retained the ability to downregulated p38MAPK alpha without inducing anti-viral response (no increase of P-eIF2alpha). **B.** Induction of cell death in rat cortical neurons through exposure to 1µM colchicine for 24h. Expression of shRNA nr.7 reduces the death of neurons by 40%, as assessed by LDH release assay, as compared to cells infected with shRNA nr.7* or treated uninfected neurons (each column represent the mean +/- SEM of four independent experiments). Colchicine-induced LDH release in uninfected cells was increased 2.6-fold as compared to untreated uninfected neurons.

Figure 5.6
Test of shRNA nr.7-mediated effects at short term: schematic representation of the injection in the spinal cord

A. ***B.***

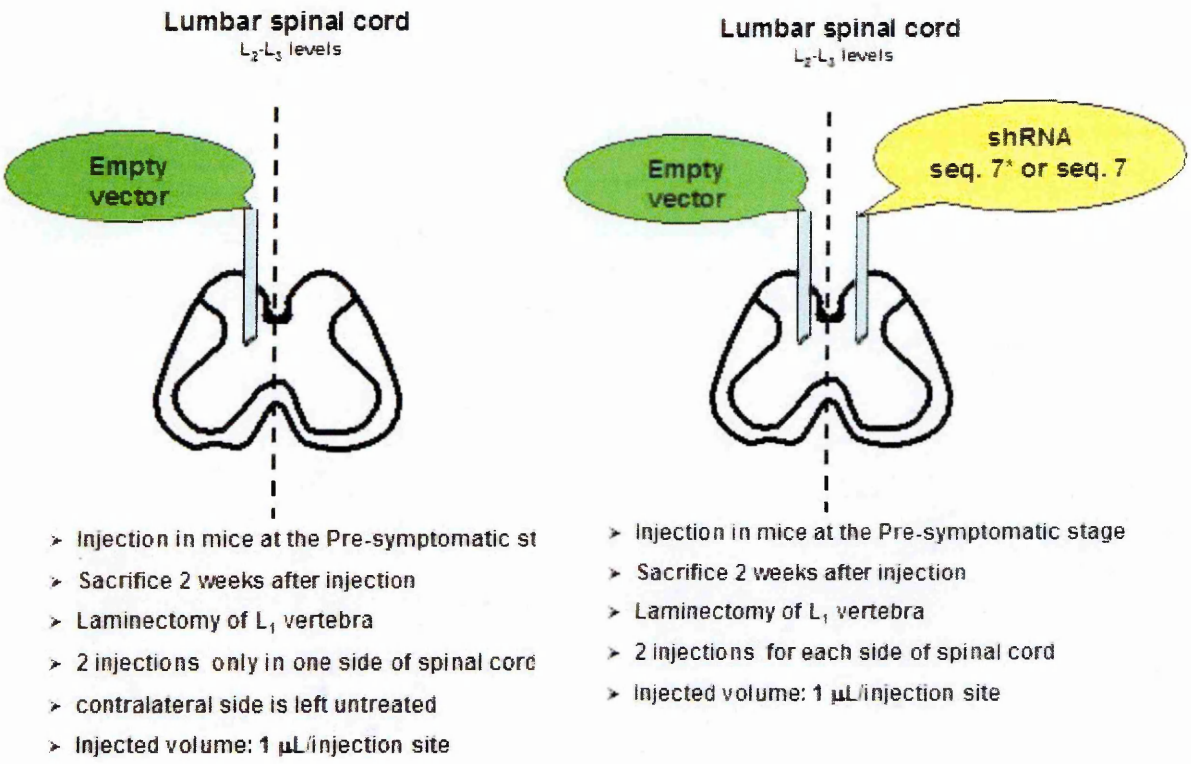

A. Monolateral delivery of GFP-expressing vector in NTg or presymptomatic SOD1G93A mice, to evaluate possible effects induced by lentiviral vector delivery. **B.** Scheme of the injection procedure of viral vectors in the lumbar spinal cord of SOD1G93A pre-symptomatic mice, for testing of short-term effect of shRNA nr.7 expression on motor neuron survival. Empty vector was injected in the left side of spinal cord, while shRNA nr.7* or shRNA nr.7 expressing lentivirus were delivered in the contralateral side.

Figure 5.7
Higher susceptibility of SOD1G93A motor neurons to intraspinal injection of an empty viral vector

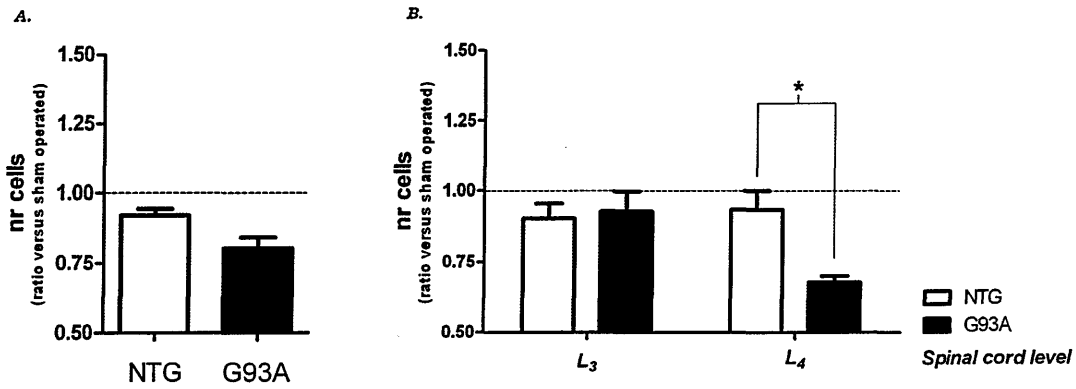

p > 0.05; Student's t-test

** = p < 0.05; 2 way ANOVA followed by Bonferroni's post hoc test*

Fint significative

Evaluation of the number of surviving motor neurons in NTg or SOD1G93A animals 16 days after treatment with empty lentiviral vector, as compared to sham operated contralateral side. N=3 for each experimental group. **A.** Mean number of surviving cells with area higher than 250μm²; the ratio between empty vector-injected side versus sham is shown. Statistical analysis was performed by Student's unpaired t-test. **B.** Mean number of surviving cells with area higher than 250μm², subgrouped depending on the spinal cord segment in which they are localized (L_3 or L_4). Statistical analysis was performed by 2 way ANOVA followed by Bonferroni's post hoc test.

Figure 5.8
Protection of motor neurons in the spinal cord side injected with shRNA nr.7

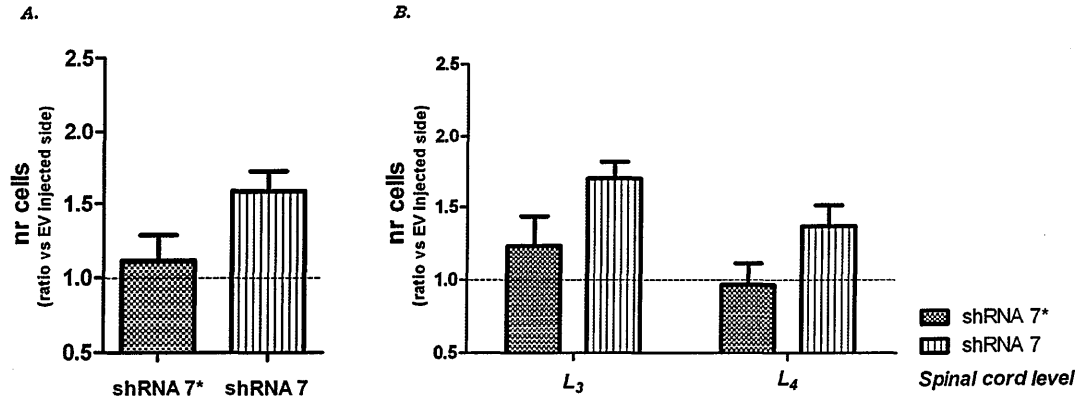

p > 0.05; Student's t-test

p > 0.05; 2 way ANOVA

Evaluation of the number of surviving motor neurons in SOD1G93A animals 16 days after treatment with shRNA nr.7 or shRNA nr.7*, as compared to empty-vector (EV) injected contralateral side. N=3 for each experimental group. **A.** Mean number of surviving cells with area higher than 250μm²; the ratio between shRNA-treated versus EV-injected side is shown. Statistical analysis was performed by Student's unpaired t-test. **B.** Mean number of surviving cells with area higher than 250μm², subgrouped depending on the spinal cord segment in which they are localized (L_3 or L_4). Statistical analysis was performed by 2 way ANOVA followed by Bonferroni's post hoc test.

Figure 5.9

Treatment of SOD1G93A mice with lentivectors expressing shRNA nr.7 significantly reduces life span

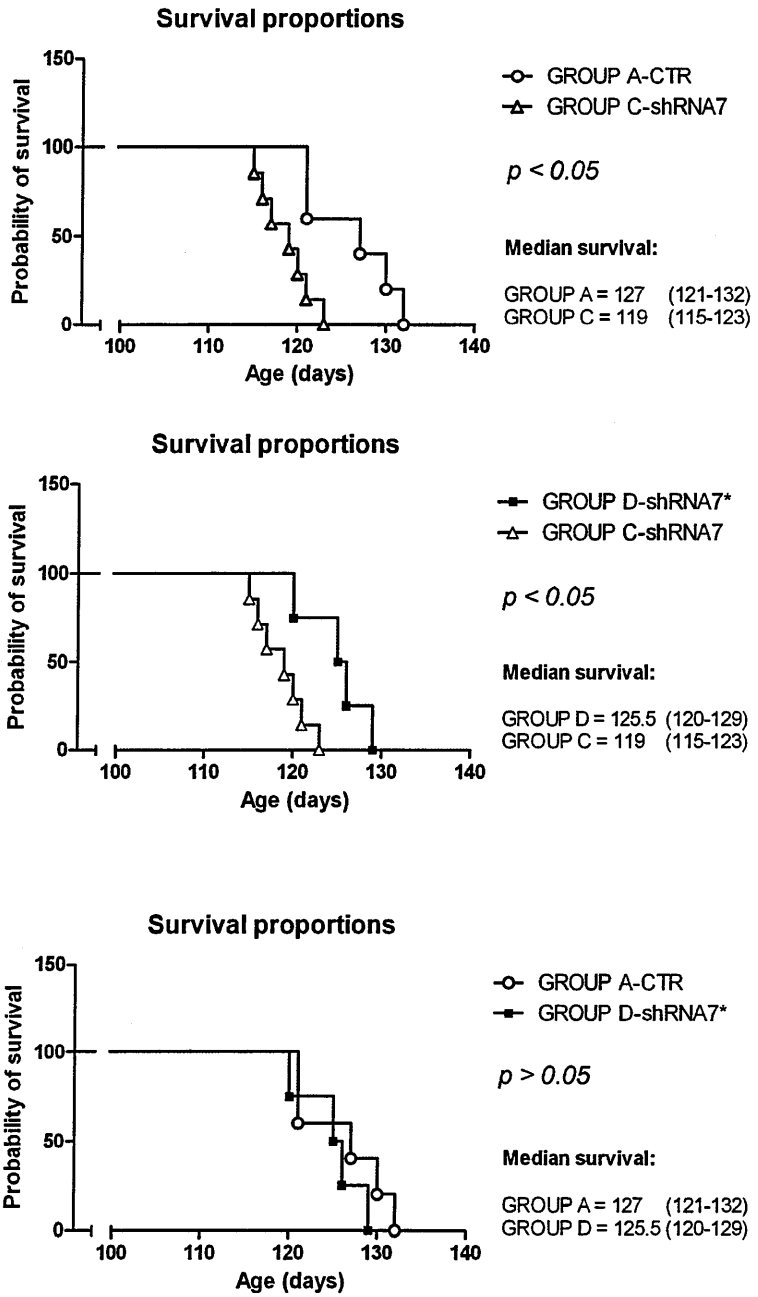

Comparison of survival curves for Group C (shRNA nr.7 treatment) versus control Group A (Sham operated) (**A**), or control Group C versus control Group D(shRNA nr.7* treatment) (**B**), and Group D versus Group A. Log-rank analysis of probabilities showed a significant shortening of survival in Group C, as compared to Group A or Group D. No significant difference was observed between Group D and Group A.

Figure 5.10
Effect of shRNA nr.7n on disease progression in SOD1G93A mice

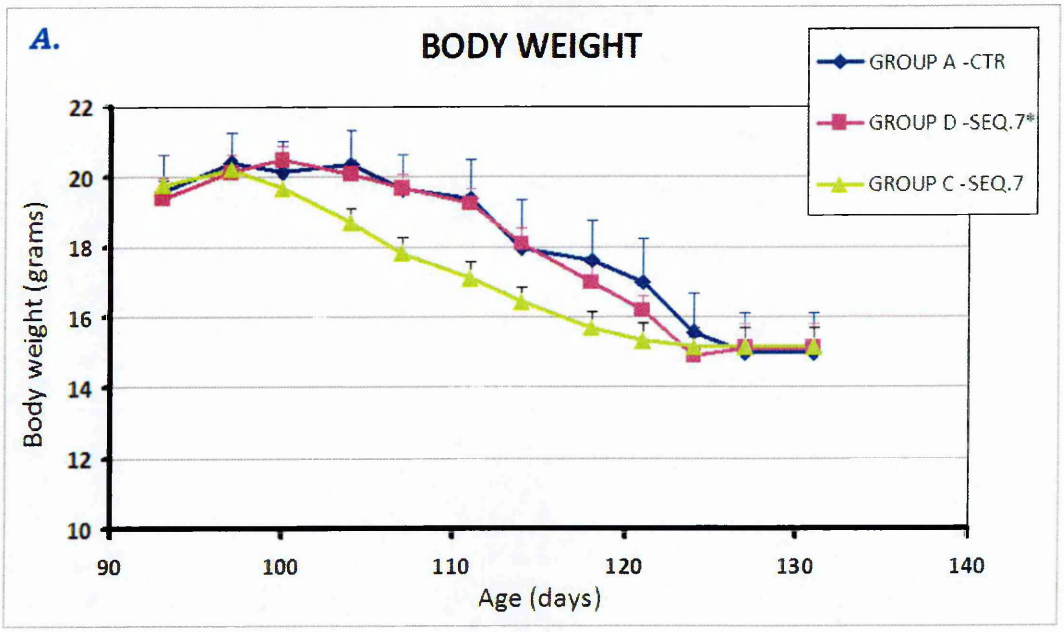

2-way ANOVA for repeeated measures:
Group C vs Group D: *Fint* p=0.09
Group C vs Group A: *Fint* p=0.09

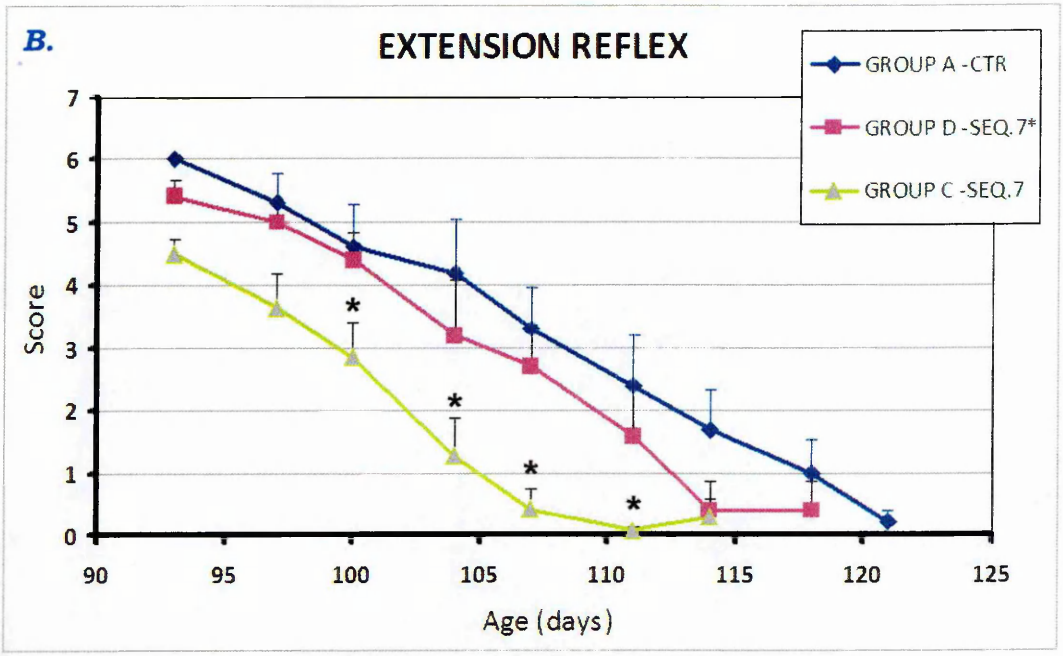

2-way ANOVA for repeated measures:
Group C vs Group D: *Fint* p=0.0042
Group C vs Group A: *Fint* p=0.003

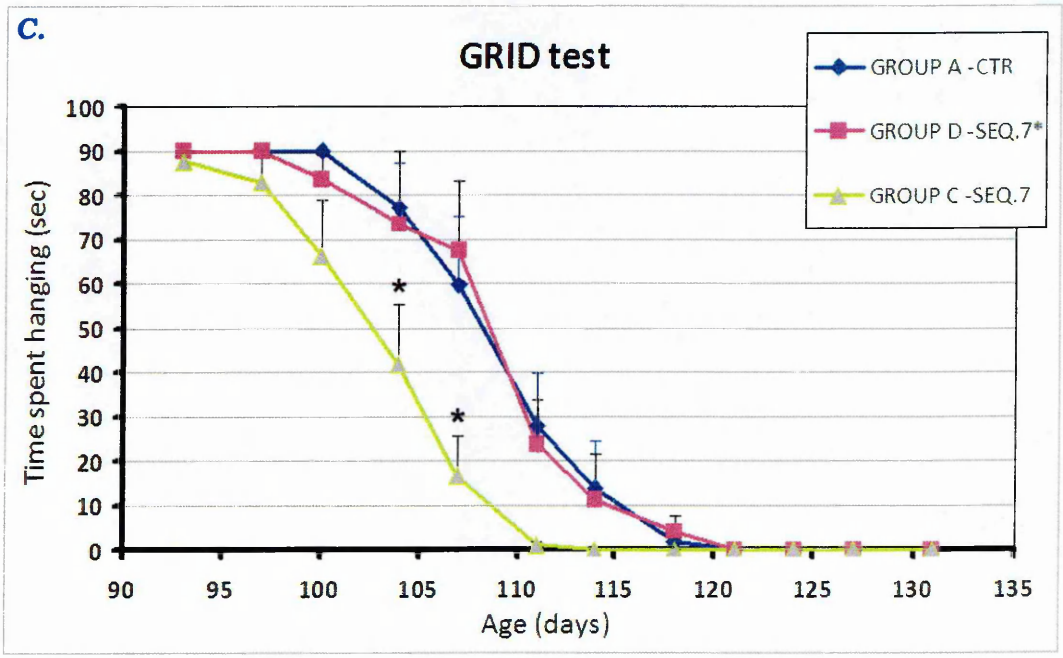

2-way ANOVA for repeated measures:
Group C vs Group D: *Fint* p=0.0068
Group C vs Group A: *Fint* p=0.0048

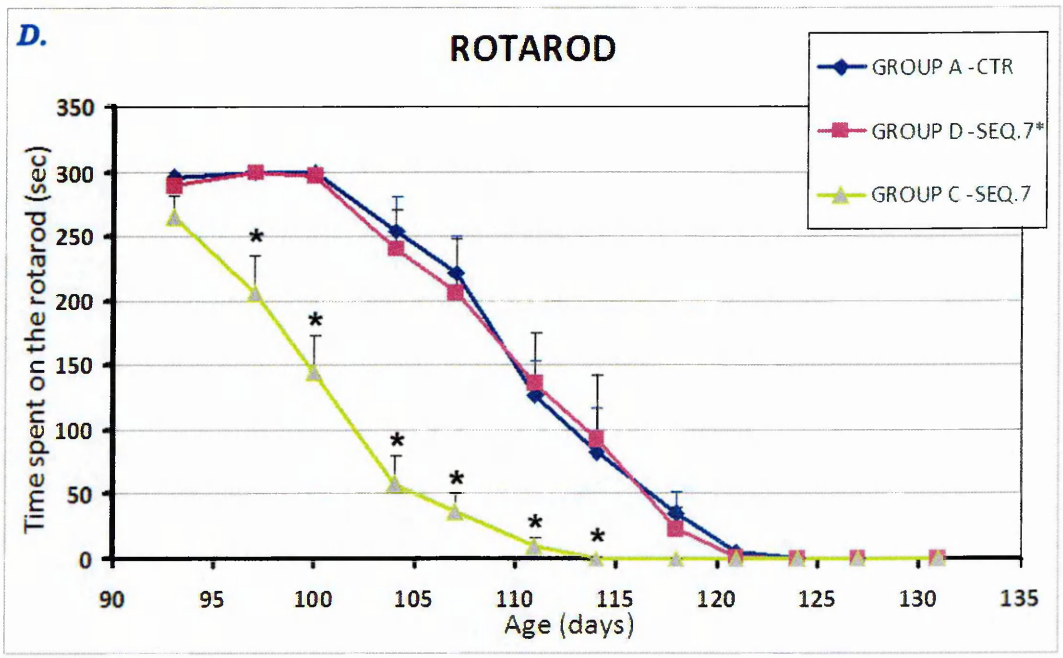

2-way ANOVA for repeated measures:
Group C vs Group D: *Fint* p<0.0001
Group C vs Group A: *Fint* p<0.0001

Body weight (**A**), extension reflex (**B**), and performance on grid test (**C**) and on rotarod (**D**) of animals treated with shRNA nr.7 (Group C; n=7), compared to control sham operated mice (Group A; n=5) and to animals treated with shRNA nr.7* (Group D; n=5). No difference in the disease progression was observed between animals of Group D and Group A for all measures. In Group C a steeper descrease of body weight was observed starting from 100 days, in contrast to the control groups A and D. Group C displayed a tendency to have a lower extension reflex score already at 93 and 97 days, as compared to control groups. From day 100 to day 111 this deficit became statistically significant versus both control groups. The grid test highlighted an anticipation of motor deficits for Group C from day 97 till end stage of the disease. The performance of Group C resulted significantly lower than the control groups at 104 and 107 days of age. Similarly, the rotarod test evidences a significantly worse performance for Group C from day 97 till end stage of disease, in contrast with control groups. Comparison of the progression of deficits between groups was done by two-way ANOVA for repeated measures followed by Student's t-test at each time point in case of significant interaction (the results of the statistical analysis are shown under each graph).

Figure 5.11

End-point analysis of deficits in SOD1G93A mice after treatment with shRNA nr.7; comparison with sham operated group

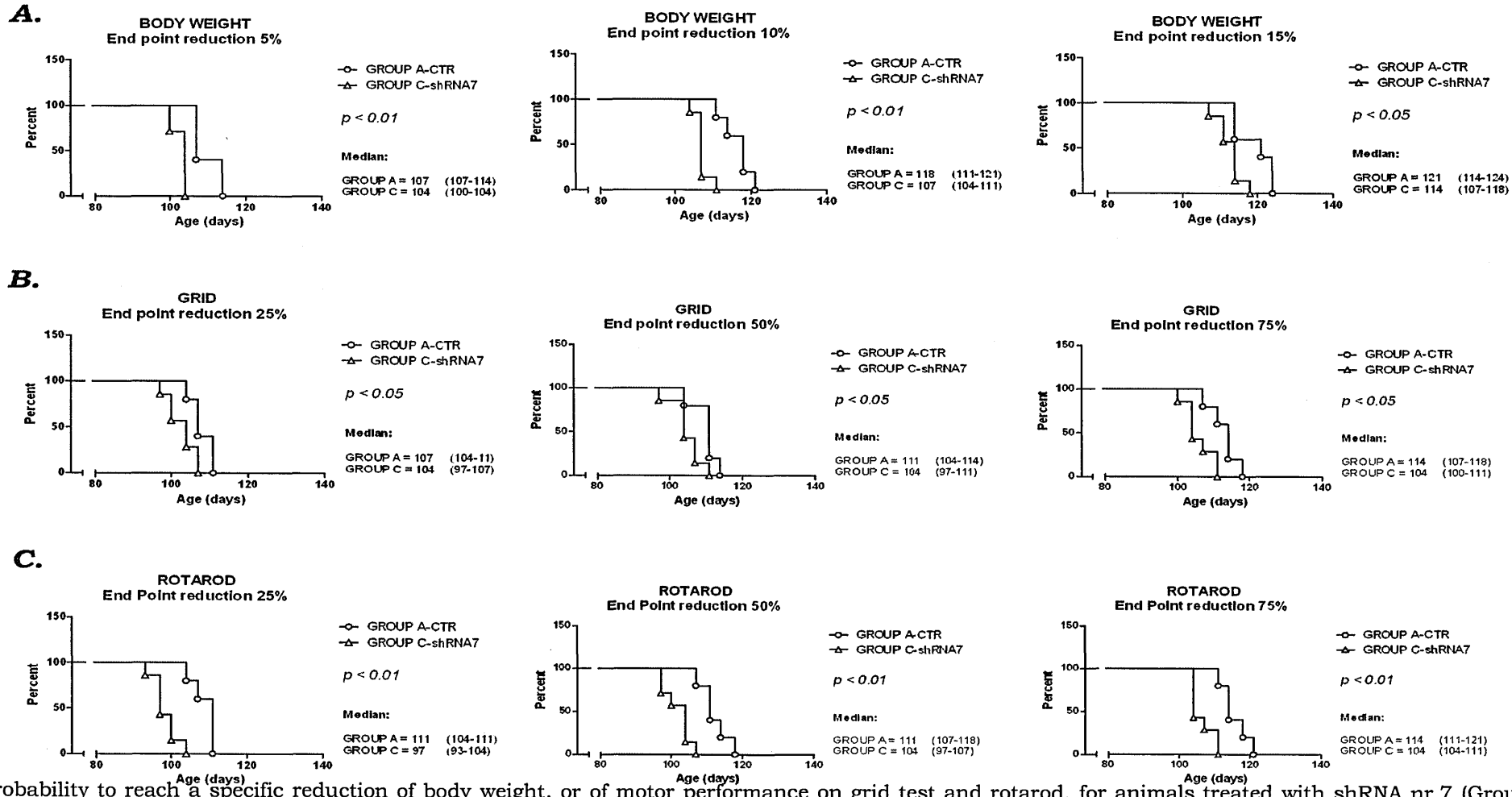

Probability to reach a specific reduction of body weight, or of motor performance on grid test and rotarod, for animals treated with shRNA nr.7 (Group C; n=7), compared to sham operated animals (Group A; n=5). A. Progressive reduction of body weight (5% drop, 10% drop or 15% drop); B. Progression of motor deficits on the grid (25% drop, corresponding to onset of disease; 50% drop corresponding to advanced stage of the disease; 75% drop corresponding to a late stage of the disease); C. Progression of motor deficits on the rotarod (25% drop, 50% drop, 75% drop, corresponding to onset, advanced stage and late stage of the disease, respectively). Log-rank analysis of probabilities showed significant acceleration of deficits for Group C, as compared to Group A at all end points.

Figure 5.12

End-point analysis of deficits in SOD1G93A mice after treatment with shRNA nr.7; comparison with shRNA nr.7* treated group

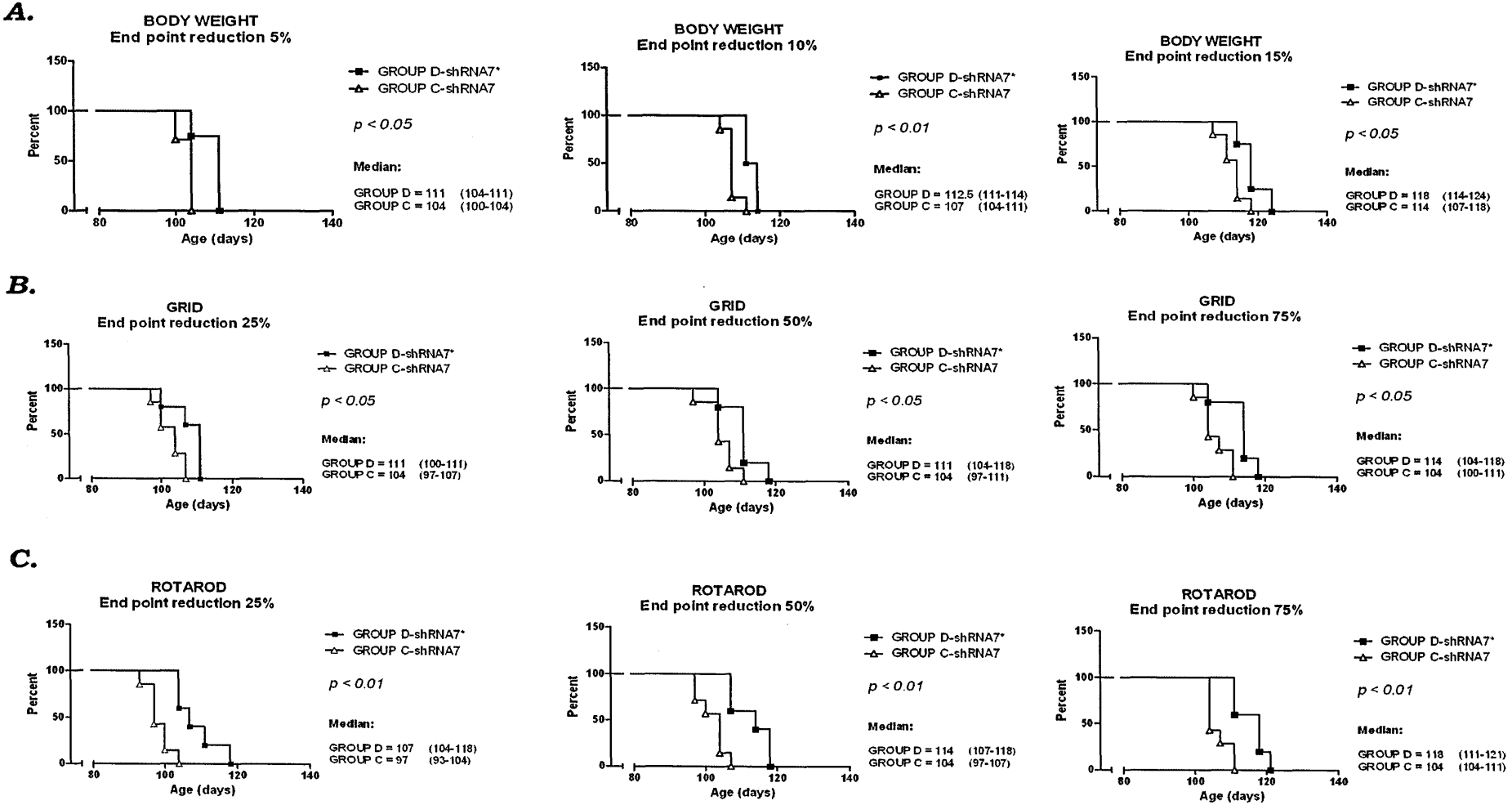

Probability to reach a specific reduction of body weight, or of motor performance on grid test and rotarod, for animals treated with shRNA nr.7 (Group C; n=7), compared to animals treated with shRNA nr.7* (Group D; n=5). **A.** Progressive reduction of body weight (5% drop, 10% drop or 15% drop); **B.** Progression of motor deficits on the grid (25% drop, corresponding to onset of disease; 50% drop corresponding to advanced stage of the disease; 75% drop corresponding to a late stage of the disease); **C.** Progression of motor deficits on the rotarod (25% drop, 50% drop, 75% drop, corresponding to onset, advanced stage and late stage of the disease, respectively). Log-rank analysis of probabilities showed significant acceleration of deficits for Group C, as compared to Group A at all end points.

Figure 5.13

Expression of shRNA nr.7 causes a mild decrease of motor neuron survival in SOD1G93A animals

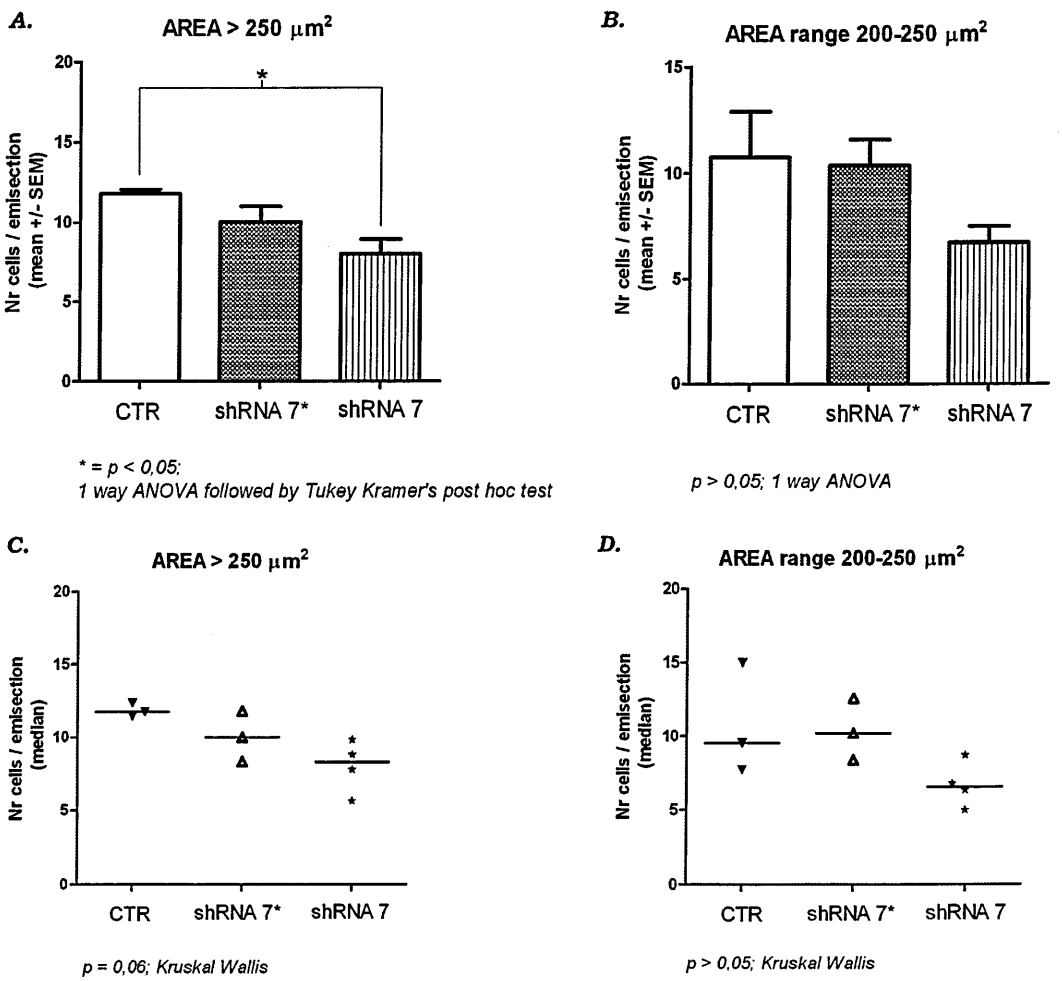

Evaluation of the number of surviving motor neurons in the lumbar spinal cord of SOD1G93A at the end stage of disease after treatment with shRNA nr.7 (shRNA 7; n=4), compared to animals treated with shRNA nr.7* (shRNA 7*; n=3) or sham operated mice (CTR; n=3). **A.** Mean number of surviving cells with area higher than 250μm²; **B.** Number of surviving neurons with small area (range 200-250μm²), considered not to be motor neurons. In **C, D** the distribution of single data used in the analysis is represented. Statistical analysis was performed by 1 way ANOVA followed by Tukey Kramer's post hoc test. Results confirmed with Kruskal Wallis non-parametric test for comparison of medians.

Figure 5.14
Analysis of motor neuron survival in treated SOD1G93A mice at different spinal cord levels

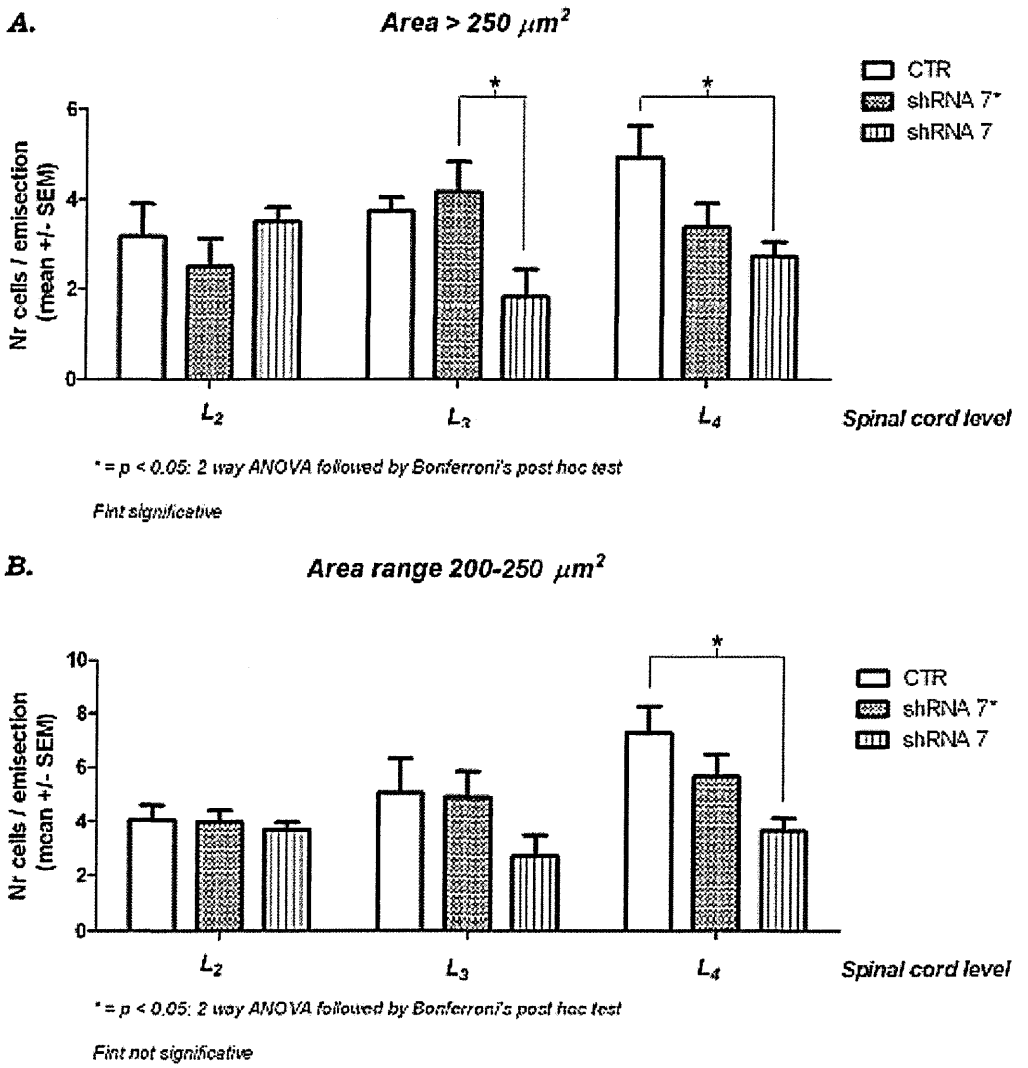

Evaluation of the number of surviving motor neurons in different lumbar spinal cord segments (L_2-L_4) at the end stage of disease after treatment with shRNA nr.7 (shRNA 7; n=4), compared to treatment with shRNA nr.7* (shRNA 7*; n=3) or sham operated mice (CTR; n=3). **A.** Mean number of surviving cells with area higher than 250μm²; **B.** Number of surviving neurons with small area (range 200-250μm²). Statistical analysis was performed by 2 way ANOVA followed by Bonferroni's post hoc test (no significant interaction was observed between the treatment and the spinal cord level).

Figure 5.15
Effect of shRNA nr.7 expression on reactive astrocytosis in SOD1G93A mice

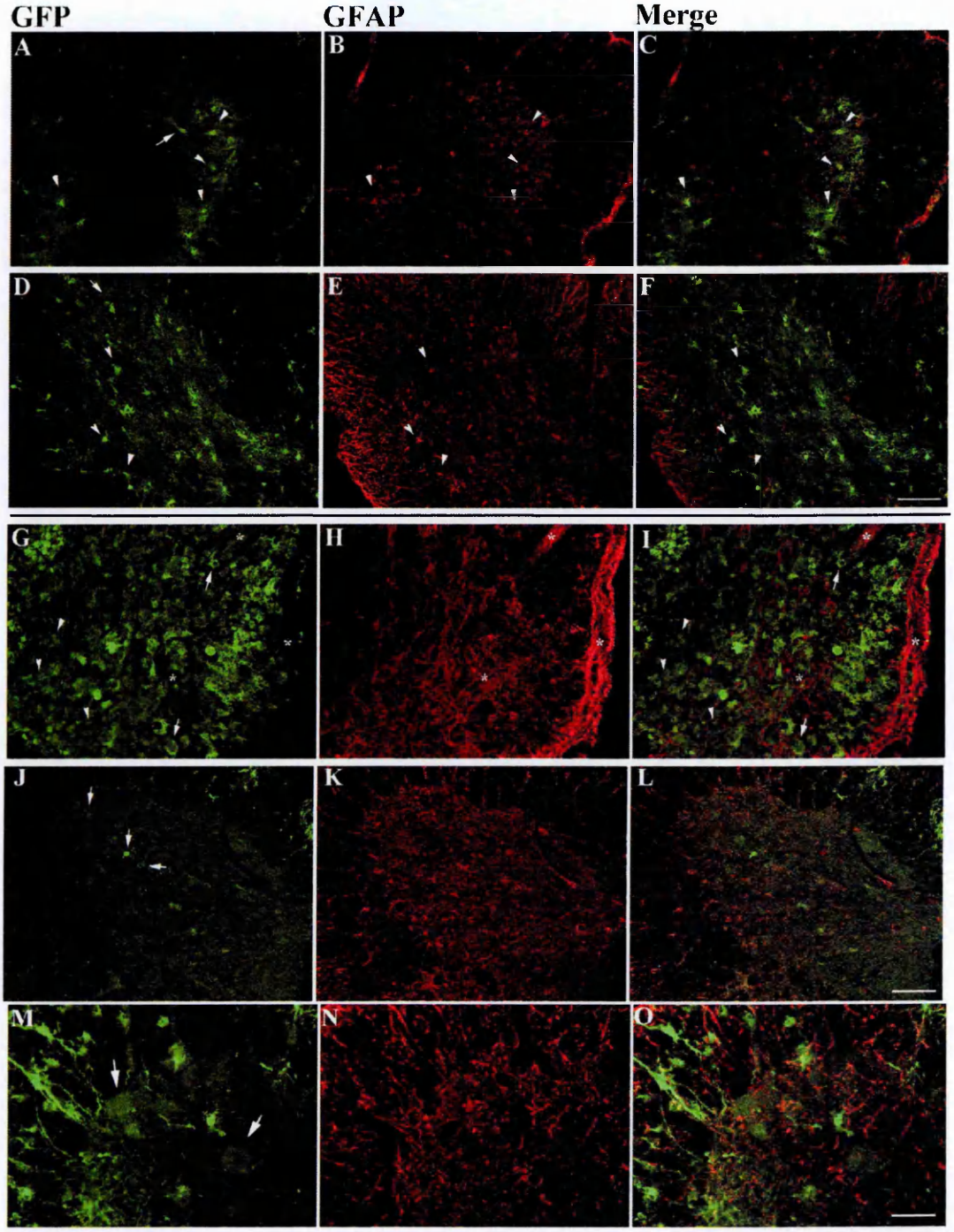

Representative confocal microscope microphotographs of GFP (green) and GFAP (red) immunostainings in lumbar spinal cord sections obtained from end stage SOD1G93A mice after treatment with lentiviruses expressing shRNA nr.7* (**A-F**) or shRNA nr.7 (**G-O**). In animals treated with shRNA nr.7* GFP signal is detected in astrocytes (arrowheads in **A-F**) and surviving neurons (arrow in **A**). Astrocytes are hypertrophic, as expected at this stage of the disease. Expression of shRNA nr.7* does not modify astrocytes morphology. In animals treated with shRNA nr.7 some infected motor neurons can be detected (arrows in **J** and **M**). Astrocyte morphology appears normal (**K** and **L**) except in areas surrounding the sites of injection (**H**). In these regions GFAP staining appears filamentous and highly intense, and rarely colocalized with GFP signal (asterisks in **G-I**). Several GFP-expressing cells of very small area are also detected (arrowheads in **G, I**), moreover some larger round-shaped cells appear (arrow in **G,I**). Scale bar in F applies to A-E = 100μm; scale bar in L applies to G-K = 100μm; scale bar in O applies to M, N = 50μm.

Figure 5.16
Effect of shRNA nr.7 expression on reactive microgliosis in SOD1G93A mice

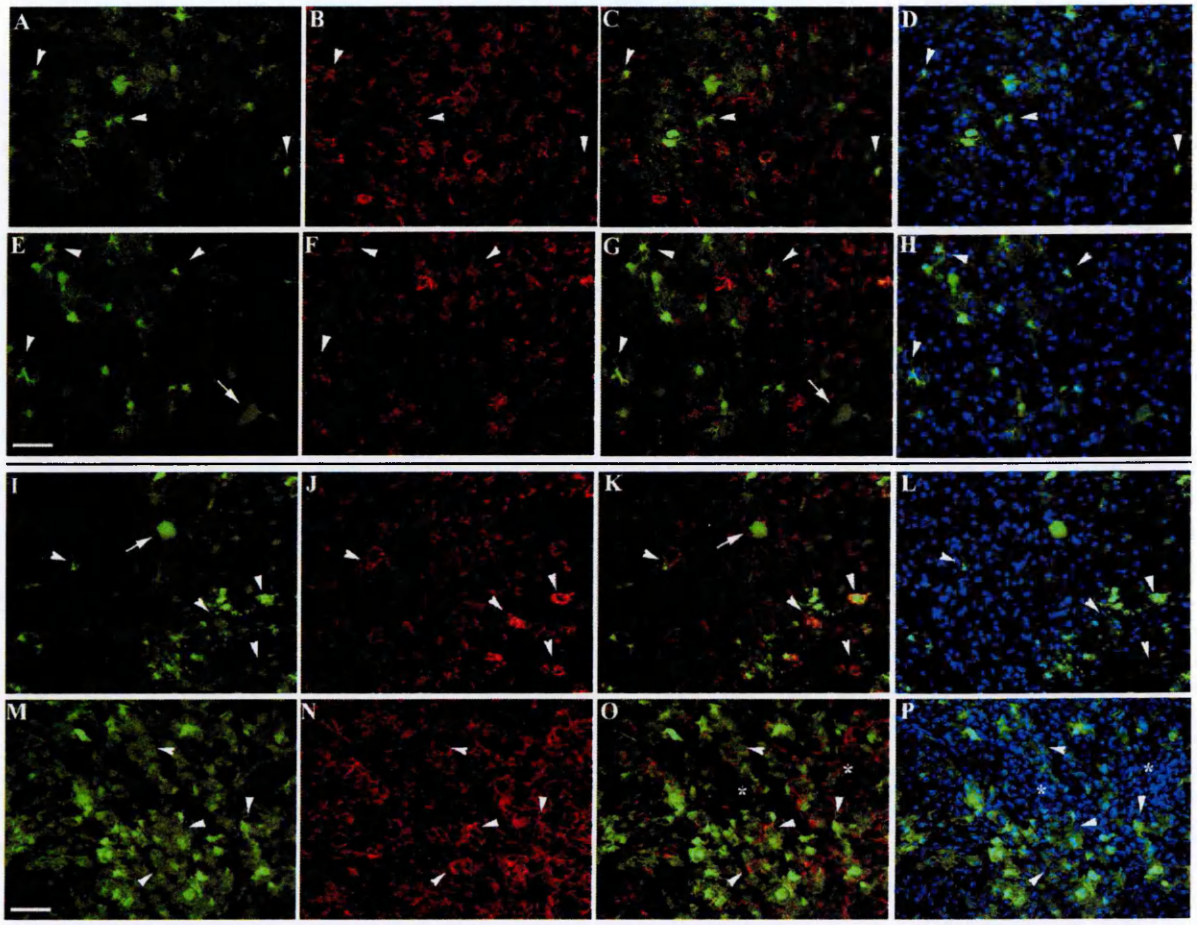

Representative confocal microscope microphotographs of GFP native signal (green), CD11b (red) and Hoescht nuclear (blue) immunostainings in lumbar spinal cord sections obtained from end stage SOD1G93A mice after treatment with lentiviruses expressing shRNA nr.7* (**A-H**) or shRNA nr.7 (**I-P**). In animals treated with shRNA nr.7* GFP signal is detected in several microglial cells (arrowheads in **A-H**) and surviving neurons (arrows in **E, G**). The microglia has a classical stellate morphology, as expected for the reactive microgliosis already described at this stage of the disease. Expression of shRNA nr.7* does not modify this morphology. In animals treated with shRNA nr.7 some infected motor neurons can be detected (arrows in **I** and **K**). The infected microglial cells display a round-shaped amoeboid-like morphology both far (arrowheads in **I-L**) and near the injection site (arrowheads in **M-P**). In the regions surrounding the injection site a strong immunoreactivity for CD11b is detected, with almost all infected microglial cells displaying a round-shaped morphology. In these areas an increase of cells is also detected, as evidenced by nuclear staining (**P**). Some of these cells are organized in clusters (asterisks in **O, P**), rarely colocalizing with GFP signal. Scale bars = 50μm.

5.7 Discussion

We have identified a shRNA sequence (shRNA nr.7) that efficiently targets murine p38MAPK alpha. Lentiviral vectors carrying this sequence induced up to an 80% reduction in p38MAPK alpha protein levels in cultured cells. TNFα strongly activates p38MAPK *(Da Silva and Silva, 1997)* but the levels of phosphorylated p38MAPK were strongly inhibited by shRNA nr.7, even in the presence of TNFα. Importantly, the levels of JNK, a closely related MAP kinase family member, were unaltered by shRNA nr.7 indicating selectivity of action for this sequence. However, upon TNFα stimulation in primary astrocytes, the phosphorylation state of this kinase was slightly higher in shRNA nr.7-treated cells, as compared to control groups, suggesting that reduction of p38MAPK may induce a shift to increased activation of JNK. Furthermore, shRNA nr.7 induced p38MAPK downregulation in rat neuronal cultures partially protected against colchicine induced cell death, confirming findings with conventional p38MAPK inhibitors *(Yang et al., 2007)*. Exposure to colchicine is a paradigm of cell death in vitro caused by cytoskeletal dysorganization, a pathological hallmark that is found also in dying motor neurons in vivo, in ALS. In particular, perikarial accumulation of phosphorylated neurofilaments has been described in the motor neurons of ALS patients and in mouse models, and has been associated with activation of p38MAPK alpha. Therefore, to further dissect the role played by this kinase in vivo, we delivered lentiviral vectors expressing p38MAPK-targeted shRNA to presymptomatic SOD1G93A mice and assessed neuronal survival 16 days later. Interestingly, we highlighted a tendency of protection of motor neurons in the areas that were infected by lentiviruses expressing shRNA nr.7. However, when we evaluated the effect of p38MAPK alpha downregulation on disease progression, in a separate experiment, surprisingly we observed an acceleration in motor deficits and a decreased life span in animals that received shRNA nr.7. In line with this effect, histological analysis performed at the end stage of disease revealed a modest but significant increase of the motor neuron

loss in the spinal cord segments corresponding to the sites of injection. However, infected motor neurons could still be detected at the end stage of the disease suggesting that p38MAPK downregulation might have protected these cells. This may support the general hypothesis that inhibition of p38MAPK in motor neurons may be protective. However, it does not explain why the disease is exacerbated by the prolonged downregulation of p38MAPK. Treatment of SOD1G93A mice with non specific pharmacological p38MAPK inhibitors has resulted in increased survival of motor neurons, although with a very small effect on disease progression and life span *(Dewil et al., 2007a)*. The protective effects of p38MAPK inhibition on motor neurons may be due to reduced microglial activation *(Dewil et al., 2007a)*, or by direct anti-apoptotic effects *(Raoul et al., 2002; Raoul et al., 2005a)*. A further mechanism of protection may be prevention of cytoskeletal disorganization, although we have no direct evidence for this. However, in contrast to previous work *(Dewil et al., 2007a)*, we observed a clear worsening of symptoms in animals treated with shRNA nr.7, as compared to control groups. Analysis of astrogliosis reactivity in these mice did not reveal substantial morphological alterations of the infected astrocytes, as compared to control groups. However in the areas surrounding the injection sites a strong GFAP immunoreactivity (with filamentous shape) could be detected. Since this anomalous staining rarely colocalized with GFP it can be deduced that it is not a direct consequence of shRNA nr.7 expression in astrocytes. On the other hand, expression of shRNA nr.7 in microglial cells induced interesting alterations in their morphology: the cells lost their typical stellate structure and became rounded. This effect appeared more prominent in the regions proximal to the injection sites, where maximal expression of GFP reporter gene was detected. Curiously, in these areas, and only in animals injected with shRNA nr.7, we detected a strong increase of cells, as determined by Hoescht nuclear staining. These cells were often organized in clusters, and were rarely positive for CD11b staining or for GFP. It can be excluded that these cells may have invaded the

parenchyma from the peripheral circulation during or immediately after administration of the lentiviral vector. The intraspinal injection procedure is quite invasive and causes some bleeding after preparative laminectomy, and the injection may cause some additional trauma, probably recruiting some neutrophils, and lymphocytes *(Schnell et al., 1999)*. Nevertheless, we used lentiviruses pseudotyped with VSVG, that gives broad tropism, so it can be hypothesized that if those cells migrated in the tissue during the injection, they should have been infected by the virus. Since we observed the opposite effect (high number of non-infected cells), it is conceivable that the effect we observed is in some way linked to p38MAPK downregulation. Reactive microglia are capable of releasing several molecules, including cytokines and chemokines *(Koistinaho and Koistinaho, 2002)*. We observed an anomalous morphology for reactive microglia in animals treated with shRNA nr.7, so it can be hypothesized that alterations in the microglial cells may have influenced the reactivity of other cell types. Although we cannot prove this, it is interesting to note that similar morphological alterations are detected in NG2-positive reactive microglial cells after spinal cord injury *(Leskovar et al., 2000; Hendriks et al., 2007)*. It has been recently demonstrated that in spinal cord injury activated microglial cells and macrophages may cause retraction of damaged axons, thus creating a cellular barrier to potential regeneration in the CNS (Horn et al., 2008). In ALS it has been suggested that reactive microgliosis may contribute to the worsening of motor deficits, since reduced induction of microgliosis correlates with delayed progression of disease *(Kriz et al., 2002; Van Den Bosch et al., 2002; Clement et al., 2003)*. Indeed, it has also been reported that, depending on the stimuli acting on the microglial cells, this population can also exert a neuroprotective function, for instance by releasing growth factors *(Beers et al., 2008; Chiu et al., 2008)*. This suggests that modulation of the responses induced in microglial cells critically influences neuronal survival. In a recent paper SOD1G37R mice were treated with M-CSF with the aim of inducing a neuroprotective microglial cell

phenotype, but surprisingly the result was an acceleration of disease progression and reduced survival *(Gowing et al., 2009)*. In line with our results, the authors describe altered microglial cells with amoeboid-like morphology in the spinal cord of symptomatic mice treated with M-CSF, suggesting that M-CSF may have induced a macrophage-like neurotoxic phenotype. Interestingly the number of surviving motor neurons was not significantly different in MCF-treated group, as compared to control, however an increased denervation of peripheral muscles was reported.

Overall our results indicate that p38MAPK downregulation in motor neurons is potentially neuroprotective, since we reported substantial preservation of motor neurons shortly after delivery of lentiviruses expressing shRNA nr.7, and we could detect infected motor neurons still surviving at the end stage of the pathology. However, this effect is apparently offset by the abnormal activation of microglial cells (evidenced by the altered morphology) which may lead to more rapid worsening of the disease. To better dissect the role of p38MAPK pathway, and with the aim of potentiating the therapeutic potential of its inhibition in motor neurons, alternative strategies may be suggested: 1) specific expression of shRNA nr.7 in motor neurons may be obtained by administration of Rabies pseudotyped lentiviruses (or similar viral vectors capable of retrograde transport) in peripheral muscles 2) intraspinal delivery of a lentiviral vector containing a dominant negative mutant of p38MAPK *(Ludwig et al., 1998)*, expressed under Hb9.1.6 motor neuron specific promoter (described in chapter 3). Specific inhibition of the p38MAPK pathway in motor neurons, obtained through these approaches, may then protect this cell type without the risk of inducing aberrant activation of microglial cells.

An additional observation made during p38MAPK downregulation experiments in vivo, was that the spinal cord of SOD1G93A mice appeared to be highly susceptible to the intraspinal injection procedure. In fact we detected a slight increase of motor neuronal loss in L_4 segment of the spinal cord, in the site that

received the injection of an empty vector as opposed to the contralateral sham operated side. This damage is probably not sufficient to cause a significant alteration in the pathology as motor performance analysis of animals injected with an emtpy vector or shRNA nr.7* showed very similar motor deficits to those displayed by sham operated animals. This effect of the injection procedure on motor neuron survival may be explained by the fact that the spinal cord is more susceptible to trauma than other CNS regions, like brain. This feature has been associated with increased induction of inflammatory responses in the spinal cord *(Schnell et al., 1999)*; although it is evident that the injection of a small capillary is not comparable to the damage caused by the classical paradigms of spinal cord trauma, transient induction of glial reactivity has been reported for intraspinal delivery of lentiviral vectors *(Abdellatif et al., 2006)*. If this is normally well tolerated, it is conceivable that in SOD1G93A animals, where glial cells and motor neurons suffer from the toxic effects induced by mutant SOD1, a higher susceptibility may be expected. Based on this evidence, caution should be taken when considering the strategies for delivery to the spinal cord of SOD1G93A animals; probably, where possible, a procedure that is less invasive than intraspinal injection would be preferred.

CHAPTER 6

DEVELOPMENT OF NON-INVASIVE APPROACHES FOR DELIVERY OF VIRAL VECTORS TO SPINAL CORD MOTOR NEURONS

In chapter 5 we reported a mild increase of motor neuronal degeneration in the spinal cord segment L_4 of SOD1G93A animals, two weeks after injection of a GFP expressing lentiviral vector. This happened specifically in transgenic animals, probably reflecting a higher sensitivity of mutant SOD1G93A expressing motor neurons to the trauma caused by the injection, or to some component of the viral vector preparation (as already discussed in the previous session). Assessment of motor performances of treated animals didn't show substantial deficits, as compared to mice that underwent laminectomy without receiving any injection. However, despite the effect on motor neurons may be considered not detrimental for the pathology, this may still represent a limitation for further development of any gene-therapy approach in human ALS patients. Since the disease is multifocal and progressive, several motor neurons in different spinal cord districts should be targeted in order to obtain a significant effect on the pathology. For this reason, direct delivery in spinal cord parenchyma of a putative therapeutic viral vector would necessary require a high number of multiple injections, thus increasing the probability to cause adverse effects due to invasiveness of the procedure.

Since the main advantage of lentiviral vectors is their ability to drive longlasting transgene expression in vivo, they still gain great interest for treatment of chronic pathologies, like ALS, because a single administration may be sufficient to obtain the desired therapeutic effect over time. We then decided to further develop this viral vector system by testing two potential less-invasive delivery approaches, in parallel:

- delivery of VSVG pseudotyped viral vectors in the cerebrospinal fluid;
- use of Rabies-G pseudotyping to allow retrograde transduction of spinal cord motor neurons after injection in peripheral muscles.

6.1 Delivery in cerebrospinal fluid

Administration of potential therapeutic drugs in the cerebrospinal fluid is often described as a strategy to increase CNS bioavailability for drugs that usually do not cross the blood-brain barrier. These compounds are administered in the cerebral lateral ventricles through stereotaxic injection, since CSF potentially represents a good carrier for the wide distribution of molecules through the whole CNS. This delivery approach has already been used successfully in SOD1G93A mice, demonstrating a protective effect of compounds such as cyclosporin, or Fas-targeted siRNAs *(Karlsson et al., 2004; Locatelli et al., 2007)*. Since the delay of disease progression, observed after intrathecal delivery of these drugs, is paralleled by reduced loss of motor neurons in the lumbar spinal cord, it can be hypothesized that this way of administration allows targeting of the cells localized in the spinal cord. On the other side, administration in the subarachnoid space at lumbar level can represent a valid alternative to obtain increased delivery to the motor neurons within the spinal cord. In fact, it has already been shown that intrathecal (IT) administration of drugs to lumbar spinal cord can help in obtaining a high concentration of the molecules at the lumbar level *(Hylden and Wilcox, 1980; Bellasio et al., 2003)*. In addition treatment of SOD1G93A mice with IGF-I or TAT-BcL-XL fusion protein, delivered intrathecally at lumbar level, significantly slowed the disease progression and reduced motor neuron loss *(Nagano et al., 2005; Ohta et al., 2008)*.

Therefore, we tested the efficiency of VSVG pseudotyped lentiviral vectors to infect spinal cord cells after intrathecal delivery in NTg mice.

6.1.1 Injection in cerebral lateral ventricles (ICV delivery)

GFP expressing viral vectors were injected in the two lateral ventricles (5μL/injection site), according to the procedure described in section 2.2.3. At one and four weeks post-injection animals were sacrificed by intracardial perfusion;

then brain and lumbar spinal cord were dissected and sectioned to visualize GFP signal.

As shown in Figure 6.1, through ICV delivery it was not possible to highlight infection of cells within brain or spinal cord parenchyma. GFP signal was localized only in choroid plexus and ependymal cells of the lateral, third and fourth ventricles, with rare diffusion into the spinal cord. A few GFP positive cells were observed inside the spinal cord canal (arrow in Figure 6.1) or at the emergence of spinal nerves (data not shown). This pattern of distribution was maintained between 1 and 4 weeks post-injection. Due to the low efficiency of the viral vectors for infection of lumbar spinal cord cells, this delivery approach was not further developed, and administration at lumbar level was considered potentially more efficient.

6.1.2 Injection in subarachnoid space of spinal cord at lumbar level (ITL delivery)

This procedure of administration was designed according to Hylden and collegues *(Hylden and Wilcox, 1980)* and through helpful assistance of Dr Elisa Nicolussi and Rosalia Bertorelli of Schering Plough Italia. Initial testing was done by injecting 5µL of a 2% Trypan-blue dye solution in the subarachnoid space of lumbar spinal cord, according to the procedure outlined in section 2.2.3. Animals were sacrificed immediately after administration and backbone was dissected out and post-fixed in paraformaldheyde for 24h before spinal cord extraction. A fine blue staining was observed on the surface of lumbar spinal cord (Figure 6.2), confirming that the procedure had been appropriately set up. With the same procedure VSVG vectors were delivered to NTg mice, and GFP reporter gene expression was assessed two weeks after injection. VSVG vector administered through this route spread widely along the lumbar spinal cord (from sacral to L_1 portion). However though several GFP positive cells were found in the meninges

and in the outer regions of white matter, the virus did not penetrate in the spinal cord parenchyma (Figure 6.3).

Several authors have demonstrated that the induction of hyperosmolality in blood can help to increase dissemination of adeno-associated viral vectors into brain parenchyma after injection into CSF *(Fu et al., 2003; Burger et al., 2005)*. For this reason we decided to test this approach to try to increase lentiviral vector distribution.

6.1.3 Effect of mannitol-induced BBB disruption on viral vector bioavailability after ITL delivery

Systemic mannitol-induced hyperosmolality is a well established technique used to induce disruption of the blood-brain barrier (BBB) in vivo. This procedure determines shrinkage of the tight junctions between the endothelial cells that compose the BBB in vivo, thus allowing polar molecules to easily pass from blood into cerebral parenchyma. Similarly, an increase of permeability of the barrier between CSF and CNS tissue has also been reported after mannitol treatment *(Ghodsi et al., 1999)*. However the effect of hyperosmolality on the BBB at spinal cord level, in the mouse, has not been described. In some studies BBB impermeable substances, like horseradish peroxidase, Evans Blue dye or C^{14}-sucrose, have been delivered intravenously in the mice. The extent of BBB opening is generally visualized by leakage of the staining for these substances in the brain parenchyma. In a first set of experiments we defined a protocol for induction of BBB disruption in the mouse, and verified it in vivo. The procedure was set up as already described with minor modifications *(Ghodsi et al., 1999)*. Briefly, we performed a single intra-peritoneal injection of mannitol (0.03mL/g of a 25% mannitol solution in 0.1M phosphate buffer) 10 min prior to intravenous delivery of 200µL Evans Blue (2% solution in 0.1M phosphate buffer). 20 minutes later animals were sacrificed by intracardial perfusion of PBS, then the backbone

was dissected and post-fixed in paraformaldheyde solution for 24h before spinal cord extraction. Tissues were then criopreserved and cut, for visualization of Evans Blue staining under epifluorescence microscope. This dye is normally not fluorescent; however after delivery in the blood flow it binds to serum albumin, determining a red fluorescent signal after green light illumination. As it can be noticed from Figure 6.4, the spinal cord parenchima (A) and the central canal (inset in A) of saline treated animals appears dark, with only some discrete puncta positively marked with Evans Blue dye signal. This probably reflect the presence of albumin-bound dye in CNS capillaries. Upon mannitol injection, a clear increase of red fluorescent signal can be observed in the boundaries of the capillaries, as it can be deduced by the morphology of the staining. Moreover a diffuse increase of fluorescence can be detected in the parenchyma of spinal cord and in the central canal (inset in B), probably reflecting the extravasation of albumin-bound Evans Blue.

Since intraperitoneal injection of mannitol demonstrated to be sufficient for induction of transient BBB dysruption, as evidenced by Evan Blue dye extravasation, this protocol was used to increase penetration of VSVG-pseudotyped viral vectors in spinal cord parenchyma, after administration in the subarachnoid space of lumbar spinal cord. Surprisingly, the GFP reporter gene expression in the spinal cord was similar between the mice treated or untreated with mannitol two weeks after viral vector delivery, and it was only found at the meningeal level. No GFP-expressing cells were detected in white and grey matter of spinal cord.

6.2 Rabies-G pseudotyping

Rabies virus is an RNA based, enveloped neurotropic virus. It usually infects humans through the saliva of infected domestic or wild animals *(Leung et al., 2007)*. This virus gains access to the CNS by entering in peripheral nerve terminals, located in muscles. This is probably mediated by interaction of Rabies

envelope proteins with the alpha subunit of acetil-choline nicotinic receptors or other surface proteins like NCAM or CD56, or p75NTR *(Lafon, 2005)*. After entering in the synaptic terminals, retrograde transport along axons delivers the viral particles to the motor neuronal cell bodies when viral genome is released, allowing synthesis of new viruses and transynaptic spreading of the infection to upstream CNS areas *(Ugolini, 2008)*. Pseudotyping of lentiviral vectors with Rabies-G protein is gaining increased interest for developing of innovative gene therapy approaches, as it has been demonstrated that this modification allows retrograde transport of lentivectors from peripheral muscular districts, along axons, to motor neuronal cell bodies in rodents *(Mazarakis et al., 2001; Wong et al., 2004)*. The main advantages of this strategy are: a) selective targeting of spinal cord motor neurons, thanks to the natural neuronal tropism conferred by the pseudotype; b) dispensability of cell-specific promoters, and specific targeting of shRNA sequences to the motor neurons (H1 and U6 RNApol III promoters are regulatory sequences needed for induction of RNAi, that would lead to ubiquitarious expression if the virus is not targeted to specifc cell types); c) this therapeutic approach may be more easily translated into clinic, since it is definitively less invasive than intraspinal injection; moreover multiple spinal cord segments may potentially be targeted by simply injecting the virus in the corresponding muscular districts.

Interestingly, by using this gene-therapy approach, Azzouz and co-workers have reported one of the most strong effects ever obtained in SOD1G93A mice with a conventional therapeutic treatment *(Carri et al., 2006)*. The authors prepared a VEGF expressing Rabies-G lentivector and delivered it in different muscles of SOD1G93A mice before symptom onset, at three weeks of age. This determined a delay of onset of 28 days, and a slow disease progression, with significant increase of survival of 30% over the empty-vector treated animals. The effect observed on the disease phenotype was paralleled by increased expression of VEGF in spinal cord, and increase of 44% of surviving motor neurons at the end

stage of the disease. Remarkably, this effect was retained also when the vector was administrated at symptom onset, suggesting that this strategy may be promising for treatment of ALS patiens *(Azzouz et al., 2004a)*. We decided to adopt a similar approach to modify the tropism of our lentiviral vectors.

6.2.1 Set up of a protocol for production of Rabies-G lentiviral vectors at high titre

Mazarakis and co-workers described the use of a viral titre in the range of $6x10^8$-$3x10^9$ TU/mL *(Mazarakis et al., 2001)*. Initial production of Rabies pseudotyped lentivectors, performed following the protocol already set up in section 3.1 for VSVG, lead to a titre lower than that described in the literature (Table 6.1 - Trial 1). To improve viral particle production the original protocol was modified in subsequent steps: increase of the amount of envelope plasmid (with the aim to facilitate packaging of viral particles) and progressive increase of the fold concentration of the virus-containing supernatants after ultracentrifugation. As outlined in Table 6.1 - Trial 5, the modified protocol lead to a final titre of $3.1x10^8$ TU/mL, that was considered sufficiently high for in vivo delivery.

Table.6.1. High titre production of Rabies pseudotyped lentiviral vectors

Starting conditions	Plasmids	Amount of DNA (µg)
Envelope	pRabies	0.60
Adjuvant	pCMV	1.00
Adjuvant	pREV	0.50
Transfer vector	pLVTHM	2.50

Trials	Amount of pRabies transfected (µg)	Additives	Fold concentration of supernatant	Titre (TU/mL)
1	0.60	//	100x	$8.4x10^6$
2	2.50	10mM NaButyrate	100x	$9.5x10^6$
3	1.25	10mM NaButyrate	100x	$1.4x10^7$
4	0.83	10mM NaButyrate	100x	$2.1x10^7$
5	0.83	10mM NaButyrate	200x	$3.1x10^8$

6.2.2 Delivery of Rabies-G pseudotyped vectors in peripheral muscles

Rabies pseudotyped GFP-espressing lentivectors were administered to gastrocnemius muscles in 10 weeks-old NTg mice. 3-4 weeks post-injection animals were sacrificed by intracardial perfusion and lumbar spinal cord sections were analysed for reporter gene expression. GFP positive cells have never been observed in the spinal cord of mice injected in the gastrocnemius region. The signal was totally absent also from the muscles (data not shown). To verify that the injection procedure was correct, a separate group of animals received injection of FluoroGold (a retrograde tracer that becomes fluorescent upon UV illumination) in right gastrocnemius, following the same protocol used for viral vector delivery. The level of spinal cord expected to be stained by the FluroGold was highilighted by concomitant injection of DiI in the contralateral sciatic nerve. DiI is a lipophilic dye that passively propagate in membrane compartments in living animals as well as fixed tissue specimens. It becomes fluorescent upon green light illumination. 5 days after injection of Fluorogold and DiI, remarkable positivity for Fluorogold was detected in the cell bodies of spinal cord motor neurons ipsilateral to the injected gastrocnemius (Figure 6.5). This result is consistent with the literature *(Sagot et al., 1998; Haenggeli and Kato, 2002)*, and further confirms that inefficiency of Rabies lentivectors was not due to wrong delivery procedures. In order to verify the extent of retrograde infectivity of Rabies lentivectors in the CNS in our condition, we decided to deliver this lentivirus in the striatum of NTg mice and to examine its expression in the cells projecting to the striatum (i.e cortex, substantia nigra). One μL of a low titre batch of Rabies (titre $0.8x10^8$ TU/mL) was administered in 5 min according to the procedure described in section 2.2.3.2, with an appropriate set of stereotaxic coordinates: +2.0mm laterality, +0.5mm antero-posteriority, -4.0mm dorso-ventrality referred to Bregma. Two weeks after infections animals were sacrificed by perfusion, and brains serially sectioned to visualize GFP reporter gene

expression. The signal was observed in the striatum, as expected, moreover we could detect some positive cells in the cortex, in an area that was far from the needle tract (Figure 6.6). Since neurons of the cortex are known to project to the striatum, this result confirmed that Rabies lentivirus can be retrogradely transported after administration in brain parenchima.

Figure 6.1.
Pattern of GFP reporter gene expression in CNS after ICV delivery

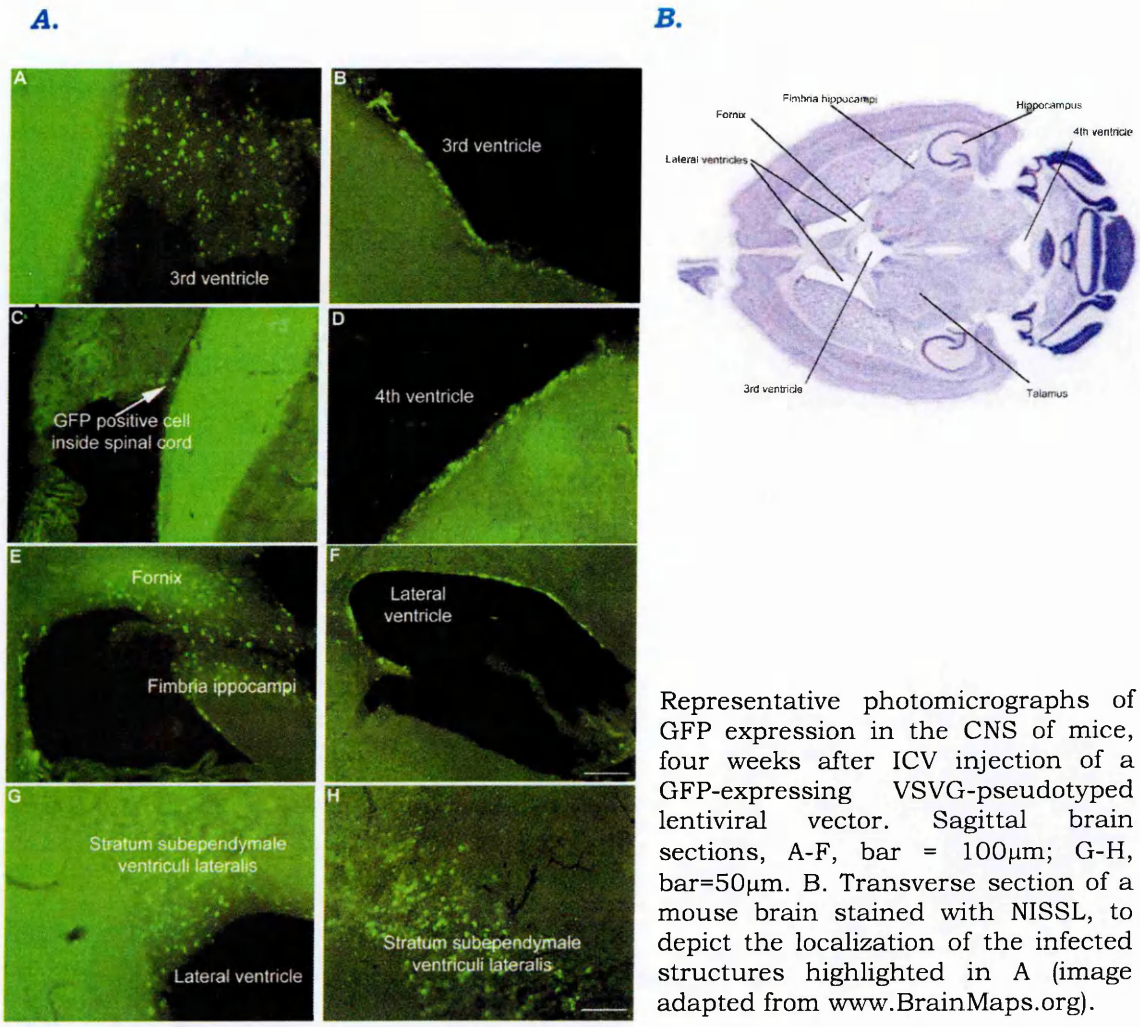

Representative photomicrographs of GFP expression in the CNS of mice, four weeks after ICV injection of a GFP-expressing VSVG-pseudotyped lentiviral vector. Sagittal brain sections, A-F, bar = 100μm; G-H, bar=50μm. B. Transverse section of a mouse brain stained with NISSL, to depict the localization of the infected structures highlighted in A (image adapted from www.BrainMaps.org).

Figure 6.2.
Trypan-blue dye dystribution after IT delivery at lumbar level

Representative photographs of spinal cords from mice injected with Trypan-blue dye in the subarachnoid space at lumbar level. Animals were sacrificed immediately after injection, then spinal cords extracted and post-fixed in 4% phosphate-buffered paraformaldehyde. Clear blue staining of the lumbar part of spinal cord can be observed.

Figure 6.3.
GFP expression in spinal cord
after IT delivery of lentivectors at lumbar level

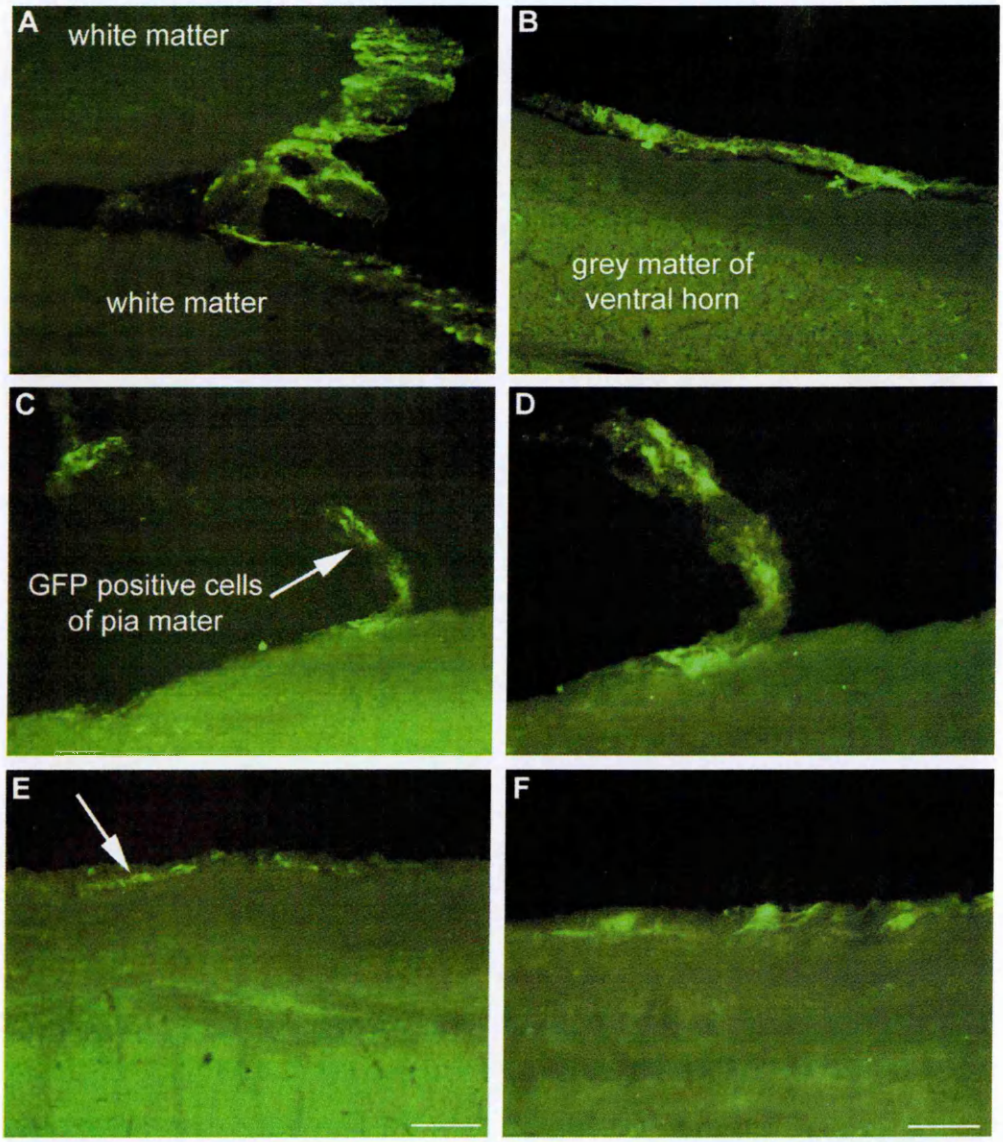

Representative photomicrographs of GFP expression in the lumbar spinal cord of mice one week after IT injection of a GFP-expressing VSVG-pseudotyped lentiviral vector. Spinal cords have been sectioned following longitudinal direction. A-C,E, bar = 100μm; D,F, bar =50um.

Figure 6.4.
Evan Blue dye distribution after IV delivery and concomitant BBB dysruption

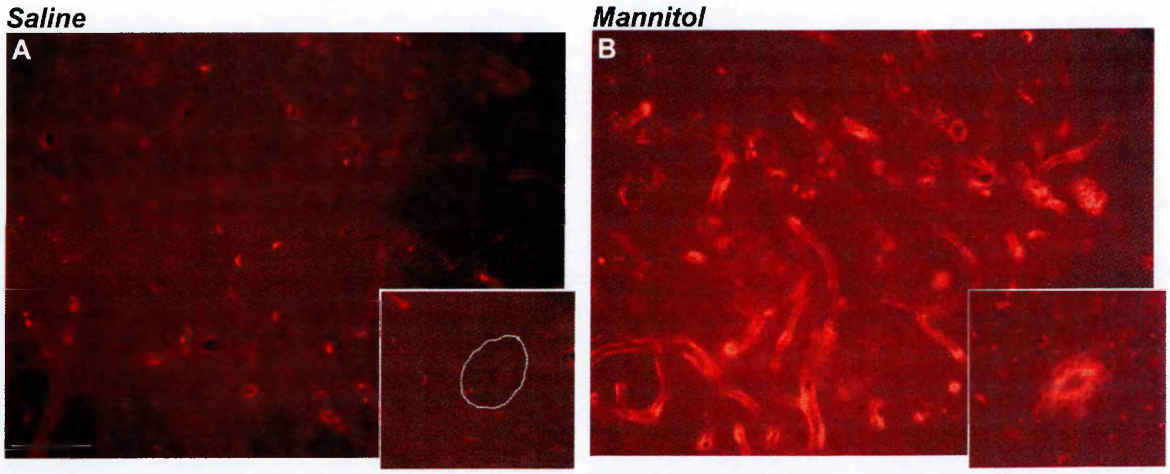

Representative photomicrographs of fluorescence emitted by Evan Blue dye in the ventral horn of lumbar spinal cord of mice after IP injection of saline (A) or a 25% solution of mannitol (B). Insets in A and B show a detail of the fluorescence detected in the central canal of spinal cord. Bar =50μm.

Figure 6.5.
Efficient trasduction of spinal cord motor neurons after delivery of Fluorogold in pripheral muscles

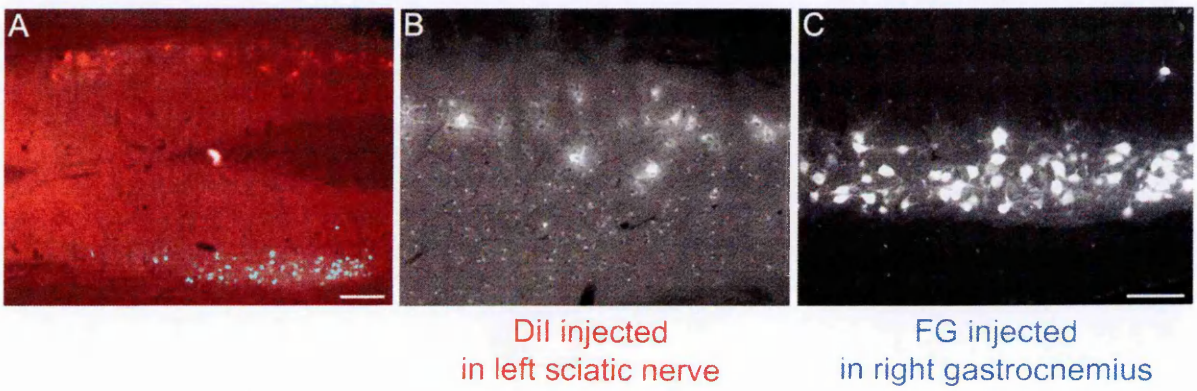

Representative photomicrographs of fluorescence emitted by Fluorgold (blue signal in A) or DiI dye (red signal in A) in the lumbar spinal cord of mice 5 days after injection in gastrocnemius or sciatic nerve, respectively. Remarkable labelling of motor neurons can be detected in the side of spinal cord contralateral to DiI staining (A) and ipsilateral to the side of injection in the muscles (C). Bar in A=200μm; bar in C applies to B=100μm.

Figure 6.6.

Rabies lentivector can retrogradelly infect neuronal cells after delivery in brain parenchima

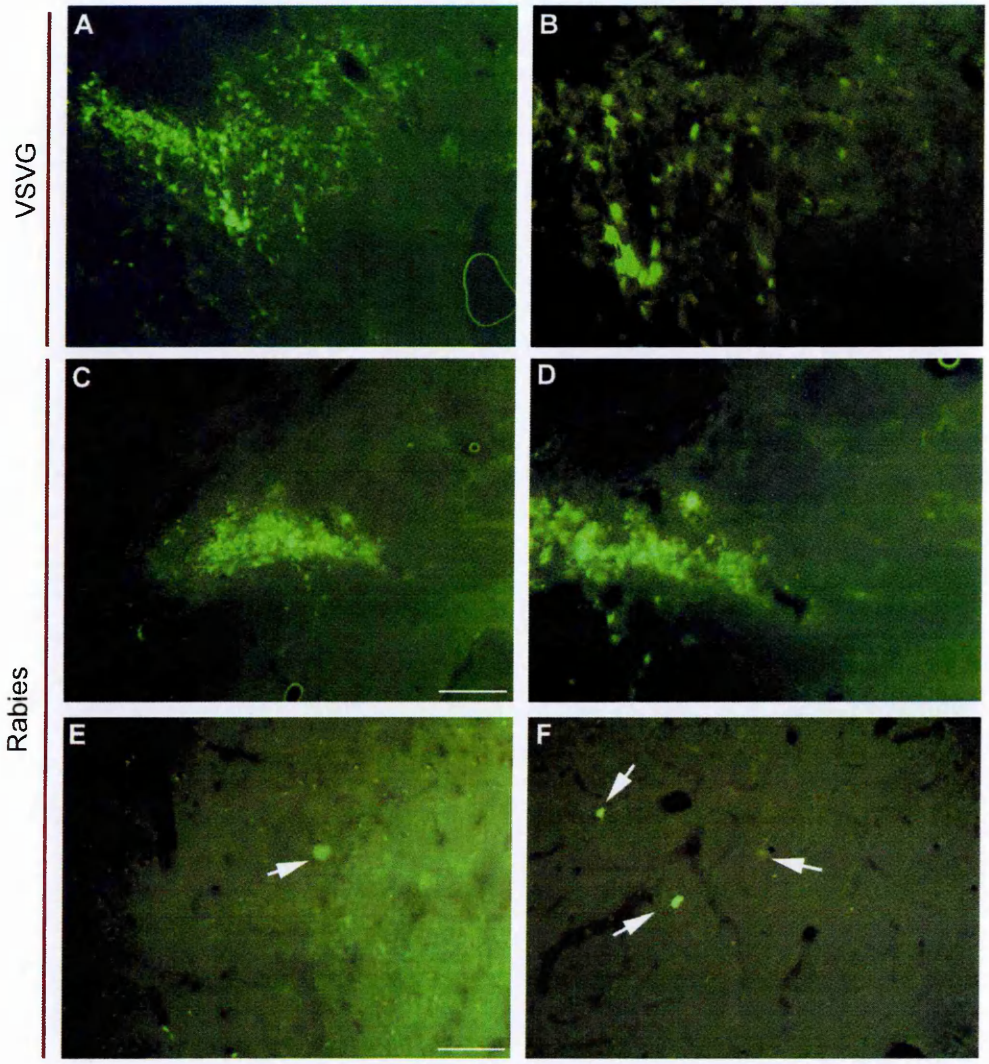

Representative photomicrographs of GFP expression in the brain of mice one week after injection of a GFP-expressing VSVG- or Rabies- lentiviral vectors in the striatum. Reporter signal is detectable in the area of injection (A-D); the expression is more prominent with VSVG vector than with Rabies. GFP positive signal could be detected in cortical neurons only in the side injected with Rabies lentivector (arrows in E, F). Bar in C applies also to A =100μm; bar in E applies to B, D and F=50μm.

6.3 Discussion

We tested different strategies for obtaining good transduction of motor neurons in SOD1G93A animals using non-invasive delivery of viral vectors to the spinal cord in order to avoid the risk to induce injection-dependent neuronal sufference. Although administration into the cerebrospinal fluid may be regarded as a potential good approach of delivery, we demonstrated that injection of lentivectors ICV or in the subarachnoid space at lumbar level is not suitable for infection of parenchymal cells of nervous system. Injection in the cerebral lateral ventricles mainly leads to transduction of cells in the ependymal layers and choroid plexus of brain ventricles, with little diffusion in the central canal of spinal cord. Similarly, when we administered the lentivectors in the subarachnoid space at lumbar level, we observed infection only at meningeal level. This pattern of expression may depend on the hydrodynamics of CSF flux. In fact in normal conditions CSF tends to flow away from CNS parenchyma as it is produced by choroid plexus and circulates in ventricles and in the subarachnoid space, and then it is reabsorbed into blood at venous sinuses. So although the flux of this fluid allows the distribution of the viral particles in the cavities of the CNS, it may represent an obstacle to diffusion in the parenchyma. Another possibility is that the thick structure of ependyma may entrap the viral particles, reducing the probability of further diffusion. In this case is worth to notice that transduced ependymal cells might represent a reservoire for production and release of potential therapeutic molecules, such as growth factors. After infection with viruses expressing these secretable proteins, the cells of ependyma may in fact perpetually produce and release them into the cerebrospinal fluid, allowing a widespread diffusion into several CNS areas.

There are few examples of positive results using ICV injection of engineerised viral vectors. ICV administration of leptin-expressing adenoassociated viral vectors (AAV) has been proposed as a substitutive of insuline administration to treat hyperglycemia and hyperphagia. In fact a single injection of the vector was

able to maintain increased hypothalamic levels of leptin, rescued the mortality, and normalized body weight and blood glycemia in a mouse model of hyperglycemia. These effects were maintained for all duration of observation (52 weeks) *(Kojima et al., 2009)*. Similarly a substitutive-therapy approach has been tested for a mouse model of Mucopolysaccharidosis VII. This is a lysosomal storage disease caused by a deficiency of β-glucuronidase enzyme. Ghodsi and co-workers injected an AAV carrying the gene for β-glucuronidase in cerebral ventricles of β-glucuronidase deficient mice. Interestingly they reported a correction of the disease in the subependymal region, grey matter of the brain and also in distant cortex areas, providing evidence that this approach is useful for widespread distribution of a protein in the CNS *(Ghodsi et al., 1999)*. This therapeutic strategy may be beneficial also for ALS. Intrathecal administration of IGF in SOD1G93A mice, through microosmotic pumps, has in fact determined a significant improvement of motor performance, retarded the onset of disease, and extended survival *(Nagano et al., 2005)*.

In order to enhance spreading of the viral particles in the parenchyma we explored the possibility to dysrupt the blood-brain-barrier through mannitol systemic administration. Delivery of hypertonic solutions in blood circulation is a widely accepted technique that is clinically used to reduce brain hydrodinamic pressure secondary to traumatic injuries *(Jantzen, 2007)*. In fact, due to blood hyperosmolality, water drains out of brain back into blood capillaries. Interestingly, it has been noticed that during this phenomenon CSF flux is reversed, so that liquids pour from subarachnoidal space into the parenchyma *(Milhorat et al., 1970; Donato et al., 1994)*. This strategy has been successfully used also to enhance spreading of adenoassociated viral vector (AAV) particles in the brain *(Fu et al., 2003; Burger et al., 2005)*. We tested the same procedure for lentiviral vectors delivered in the subarachnoid space at lumbar level but we didn't report any modification of the pattern of infection, as compared to saline

treated animals. Lentiviral particles have dimensions in the range of 80-100nm, largely bigger than adenoassociated viral particles (20-25nm). The smaller dimension of AAV may facilitate the spreading through the meningeal cell layer. Alternatively, meninges may display surface receptors not recognised by AAV, reducing the probability for the viral particles to infect these cells. Testing with other viral vector types, with different particle dimensions or tropism (like Adenovirus or Herpes virus) may help elucidating this point.

Targeting of spinal cord motor neurons from the periphery represents a very intriguing strategy. We investigated this possibility in the mouse by delivering Rabies-pseudotyped HIV-1 based lentiviral vectors in gastrocnemius muscles. Despite we set up a correct delivery procedure, as confirmed by experiments with Fluorogold dye, we did never manage to obtain infection of the motor neurons with our viral vector system. This is in contrast with what described by Wong and Azzouz in different works *(Azzouz et al., 2004a; Wong et al., 2004)*. Referring to the papers from this group we observed that the authors used a viral preparation with a concentration in the range $6x10^8$-$3x10^9$ TU/mL. We had to go through several trials to efficiently increase the titre of our Rabies pseudotyped-vector particles, ending with a concentration slightly slower than desired ($3.8x10^8$ TU/mL). This may explain our result, since in the case of AAV it has been demonstrated that titre is crucial for infection of motor neurons after peripheral delivery *(Kaspar et al., 2003)*. However Kaspar described a progressive reduction of infectivity moving from $1x10^{10}$ to $4x10^9$ viral particles (0.4 log drop in the concentration). The titre of our vector is just 0.3 log lower than the concentration used by Mazarakis' group for delivery in the mouse *(Wong et al., 2004)*, so probably other factors may have contributed to determine the inefficiency of our Rabies lentivectors. Interestingly the strain of Rabies used for pseudotyping is reported to modify viral infectivity in the brain *(Yan et al., 2002)*. We verified that our glycoprotein derives from SAD B19 Rabies strain *(Conzelmann et al., 1990)*, while Mazarakis' group used ERA- and CVS- pseudotyped non-primate (EIAV)

lentivectors. The SAD B19 and CVS are reported to be closely related *(Wu et al., 2007)* however in our system another variable has been introduced: the strain of our transfer vector was HIV-1 instead of EIAV. We tested whether this may affect infectivity by administration in the brain, and could demonstrate that the vectors we used are capable of retrograde transport to the cortex if delivered in the striatum; this observation was confirmed by other groups using different Rabies strain (RV-G) *(Kato et al., 2007)*. In a paper from Mentis and co-workers the authors described fine infection of muscle fibres and spinal cord motor neurons after administration of a HIV-based Rabies pseudotyped vector (strains CVS-N2c and –B2c) in the gastrocnemius of mice *(Mentis et al., 2006)*. Alhough we used a titre lower than Mentis, we never detected infection of muscle fibers. Overall these observations suggest that substitution of the Rabies strain with another already validated glycoprotein or further increase in titre may be necessary to achieve motor neuron infection in our model system.

CHAPTER 7

GENERAL DISCUSSION

AND CONCLUSIONS

7.1 GENERAL DISCUSSION

The aim of the work presented in this thesis was to develop a lentiviral vector-based platform to specifically target, in vivo, intracellular molecular pathways critically involved in ALS.

Numerous signalling pathways have been found to be altered in ALS, but we focussed our studies on p38MAPK and Akt. p38MAPK is a stress activated protein kinase and is considered to be a key molecule involved in the activation of several pro-degenerative pathways in ALS, including cytokine-induced neuroinflammation and cytoskeletal alterations *(Bendotti et al., 2005)*. On the other hand Akt is a lipid activated protein kinase that mediates many of the pro-survival activities of trophic factors such as IGF1 and VEGF exhibiting protective effect on motor neurons in ALS models *(Nagano et al., 2005; Storkebaum et al., 2005; Dewil et al., 2007b)*. We decided to develop approaches to target these pathways separately and specifically. We did this in order to gain a better understanding of their overall relevance to ALS pathology and also as a first pre-clincal step in the assessment of their therapeutic potential.

Induction of Akt was obtained by preparation of a myristylated mutant that anchors Akt at the membrane and results in a constitutively active kinase in vivo. Of the three known Akt isoforms, Akt3 was chosen because this isoform is predominately expressed in the CNS *(Easton et al., 2005)*. Furthermore, a myristylated mutant construct of Akt3 had already been used to demonstrate its neuroprotective function in a cell culture model expressing mutant SOD1 *(Kanekura et al., 2005)* which gave us confidence that this approach could work. To restrict the expression of this construct to motor neurons, we prepared a promoter derived from Hb9 upstream regulatory sequences, and demonstrated for the first time that it can be packaged into lentiviral vectors and act specifically in vivo. Treatment of SOD1G93A mice with motor neuron-restricted

membrane-targeted myr.Akt3 construct resulted in a modest protection of motor neurons, with no significant effects on disease progression or survival. Therefore, we suggest that combining this approach with additional strategies also targeting the peripheral compartment may be a more promising strategy. For example, it has been shown that deletion of Nogo-A expression in the muscles of SOD1G86R mice reduces the denervation of peripheral muscles and increases survival *(Jokic et al., 2006)*. Moreover, expression of a locally acting isoform of insulin-like growth factor 1 in muscular regions of SOD1-mutant mice helps maintain the integrity of the neuromuscular junctions, thus delaying motor neuron death and extending survival *(Dobrowolny et al., 2005)*. In a recent report pleiotrophin has been proposed as a new candidate neurotrophic factor for motor neuron disease, since it improved peripheral axonal regeneration in animal models of acute nerve injuries *(Mi et al., 2007)*. Increased expression of this factor in peripheral muscles or Schwann cells may aid the reinnervation of motor plaques or favour axonal sprouting. It has been recently suggested that selective increase of superoxide dismutase activity in Schwann cells of ALS mouse models may help these cells to detoxify reactive oxygen species (ROS) generated by macrophage invasion of peripheral nerves, during axonal retraction *(Lobsiger et al., 2009)*. Preserving or increasing this ROS-scavenging activity could be useful in order to maintain the production and release of trophic factors by Schwann cells, thus providing support to motor neuronal axons affected by the disease. The availability of promoters and viral vectors specific for muscles *(Richard et al., 2008; Towne et al., 2008)*, astrocytes *(Jakobsson et al., 2003)*, Schwann cells *(Feltri et al., 2002; Scherer et al., 2005)*, microglia *(He et al., 2006)*, and motor neurons (our study) represent powerful tools to rapidly test new cell specific therapeutic strategies for ALS.

For targetting the p38MAPK pathway in SOD1G93A mice we used an RNAi-based approach that resulted in a rather complicated picture. In fact, we observed that

downregulation of p38MAPK alpha can protect motor neurons in vitro and in SOD1G93A mice at the early stages of the pathology, while unexpectedly we found that this approach is not able to sustain neuronal survival during disease progression, eventually resulting in worsening of symptoms and shortening of life span. We think that this late effect is due to the hyperactivation of detrimental microglial cells which is in line with recent results *(Gowing et al., 2009)*. However this aspect needs to be further carachterized.

Two of the four p38MAPK isoforms, p38MAPKalpha and p38MAPKbeta, are known to be expressed in the spinal cord. Although some studies have indicated differential roles for these two isoforms in the induction of hyperalgesia and neuropathic pain after acute nerve or spinal cord injuries *(Svensson et al., 2005)*, there is still surprisingly little known of their function in chronic neurodegenerative diseases like ALS. The only available data suggests the involvement of p38MAPK alpha in the process of perikarial accumulation of phosphorylated neurofilaments in the motor neurons of both ALS patients and ALS mouse models *(Ackerley et al., 2004)*. Therefore, to further dissect the role played by p38MAPK alpha in ALS, we decided to selectively downregulate it in SOD1G93A mice using small interference RNA. The shRNA sequence selected for use in our study was extensively validated by: 1) specific reduction of mRNA and protein levels of mouse p38MAPKalpha in cell cultures; 2) absence of the RNAi knockdown effect following the introduction of three point mutations into the candidate shRNA sequence, disrupting the recognition of the target mRNA 3) partial neuroprotective effect of p38MAPKalpha-targeted shRNAs against colchicine-induced cell death, in primary cortical neurons. The protection observed in primary neurons is consistent with previously reported protection against colchicine using pharmacological p38MAPK inhibitors *(Yang et al., 2007)*. The authors went on to suggest a functional interplay between p38MAPK and JNK in the death process although it is worth noting that a number of studies have excluded the involvement of JNK activation in the degeneration of motor

neurons in ALS, both in patients and mouse models *(Migheli et al., 1997; Holasek et al., 2005; Veglianese et al., 2006)*. However, our results do lend further support to the hypothesis that specific targeting of p38MAPK alpha might prevent or inhibit motor neuron loss in ALS. Interestingly, we did detect a partial protection of motor neurons by p38MAPK alpha-targeted shRNA 16 days after treatment, although at the end stage of the disease this effect was not maintained, and additionally an increased death of small ventral horn neurons was reported. In contrast, others have reported that semapimod, an anti-inflammatory drug that inhibits c-Raf activation and reduces p38MAPK activation, offered significant protection to motor neuronal cell bodies in the spinal cord of SOD1G93A mice at the end stage of disease, although with little effect on the behavioural phenotype *(Dewil et al., 2007a)*. On the other hand, minocycline, a second generation tetracycline with anti-inflammatory and anti-apoptotic properties, decreased the levels of activated p38MAPK and microglial reactivity in the spinal cord of SOD1G37R mice resulting in a slower disease progression and increased survival *(Kriz et al., 2002; Zhu et al., 2002)*. Minocycline and semapimod are non-selective inhibitors of p38MAPK and certainly do not discriminate between p38MAPK isoforms. It is possible, therefore, that the protection observed with these drugs is unrelated to p38MAPK inhibition or that the lack of isoform selectivity results in a greater overall efficacy. Indeed, since ventral horn neurons, including motor neurons, express both p38MAPK alpha and p38MAPK beta it is possible that our strategy, aimed at specific downregulation of alpha isoform, does not provide sufficient inhibition of p38MAPK signalling due to the residual activity provided by the beta isoform. It is in fact quite conceivable that upstream stressful stimuli may shift their signalling preference to the induction of the non-targeted p38MAPK beta isoform in the absence of p38MAPK alpha expression. A study on adult mouse brain has highlighted that p38MAPK alpha is preferentially localized to the cytoplasm and nucleus of neurons, while p38MAPK beta is mainly concentrated in the nucleus

of neurons and in microglial cells *(Lee et al., 2000)*. A similar cellular localization of these isoforms has also been reported in rat spinal cord, although at the subcellular level the staining for p38MAPK beta in neurons appeared to be mainly cytoplasmic in this tissue *(Svensson et al., 2005)*. This evidence suggests that the two isoforms may have distinct functional roles in neurons. Due to technical problems with immunohistochemistry for p38MAPK alpha and beta we were unable to dissect this issue during our study, however we believe that further analyses are needed to better dissect the role played by p38MAPK beta in motor neurons, in ALS.

Furthermore, we also observed substantial alterations in the morphology of microglia at the end stage of disease, in animals that were treated with p38MAPK alpha-targeted shRNA. This was quite unexpected, since the main isoform expressed in microglia is p38MAPK beta *(Svensson et al., 2005)*. It has been reported that under pathological conditions, such as following transient global brain ischemia, p38MAPK alpha isoform is specifically upregulated in microglia, whereas p38MAPK beta is mainly increased in astrocytes *(Piao et al., 2002)*. Reactive microglia cells contribute to neuropathic pain *(Mika et al., 2009)* and microglia expressing mutant SOD1 drive neurotoxicity, as compared to wild type microglia *(Beers et al., 2006; Boillee et al., 2006b; Xiao et al., 2007)* thus modulation of microglia could be regarded as a potential therapeutic strategy. However, there is also increasing evidence that activation of microglia might also be beneficial, both in models of acute injury *(Neumann et al., 2006a; Lalancette-Hebert et al., 2007)*, and in ALS *(Beers et al., 2008; Chiu et al., 2008)*. So instead of aiming at complete inhibition of microglial activation, maintenance of immune system function and microglial reactivity might be preferable and manipulating p38MAPK signalling might be one way achieving this. CD11b immunoreactivity progressively increases in the spinal cord of mutant-SOD1 mice during disease, and detects different microglial cell subgroups: mature microglia, macrophages and Gr1+ myeloid precursor cells. Gowing and collegues selectively removed the

myeloid population of spinal cord from mutant-SOD1 expressing mice, demonstrating that elimination of proliferating microglia apparently has no effect on neurodegeneration in SOD1G93A mice *(Gowing et al., 2008)*. In a subsequent study the same group demonstrated that treatment of SOD1G37R mice with M-CSF resulted in induction of a neurotoxic phenotype in the microglia, leading to acceleration of the disease *(Gowing et al., 2009)*. Similarly, LPS-induced stimulation of innate immunity accelerates the disease in SOD1G37R mice, leading to exacerbation of resident microglial reactivity and neuronal death *(Nguyen et al., 2004)*. This suggests that a further clarification of the dynamics of microglial reactivity during the progression of ALS is needed . The design of more selective tools, aimed at targeting only the potential neurotoxic microglial sub-populations, may be a more effective way of counteracting the pathological process. Indeed, induction of p38MAPK in microglia regulates the transcription of inflammatory genes, such as IL-1 and TNFα, which are associated with a reactive phenotype. Interestingly, the macrophage lineage appears to be sensitive to p38MAPK alpha inhibition. Deletion of p38MAPK alpha in macrophages in vitro inhibits cellular activation after LPS stimulation and reduces the release of pro-inflammatory cytokines such as TNFα, IL-12 and IL-18 *(Kang et al., 2008)*; deficiency of p38MAPK alpha increases macrophagic susceptibility to ER-stress, promoting cell death *(Seimon et al., 2009)*. Our study suggests that expression of p38MAPK-targeted shRNA in microglial cells results in a more neurotoxic phenotype. This may result from the loss of a subgroup of potentially neuroprotective microglia, or could be due to hyper-activation of p38MAPK beta. Alternatively, since JNK has been found activated in microglial cells at the end stage of the disease, it is possible that p38MAPK alpha downregulation leads to further induction of JNK-pathway. Specific targeting of p38MAPK beta or JNK in microglia will be needed in order to clarify whether these proteins are responsible for the toxic properties exerted by this cell population in ALS.

In parallel with experiments aimed at targeting Akt and p38MAPK pathway, we also conducted an extensive characterization of the pattern of infectivity of VSVG-pseudotyped lentiviral vectors in the lumbar spinal cord of mice, and provided evidence that this approach allows transduction of the main cell types present in this tissue, namely astrocytes, oligodendrocytes, microglial cells and neurons, including motor neurons. We found that administration of a GFP-expressing control vector, with this approach, did not significantly influence the progression of pathology in SOD1G93A mice. However, from histological studies, we detected a modest loss of motor neurons at the site of injection. This suggests that SOD1G93A motor neurons are probably more susceptible to the trauma generated by invasive surgery of the spinal cord. This issue is in line with a study by Azzouz and co-workers *(Azzouz et al., 2000)*, in which the authors reported an increased, though not significant, loss of motor neurons in the areas surrounding the most caudal injection site, for SOD1G93A mice injected with GFP-expressing rAAV or PBS, as compared to untreated animals. Other groups that applied the same technique for the delivery of viral vectors or cells, did not describe this effect, mainly because they did not analyze motor neurons survival in animals that received control vector as compared to sham operated mice *(Willing et al., 2001; Guillot et al., 2004; Raoul et al., 2005b; Franz et al., 2009)*. So, particular caution needs to be considered in the use of intraspinal delivery which has been proposed as a tool for administration of potential therapeutic compounds, including stem cells, in ALS patients. Other possible delivery strategies need to be developed. For example, retrograde transport to motor neuronal cell bodies following administration in peripheral muscles, appears to be an intriguing alternative. Although this approach was unsuccessful in our study, probably due to insufficient increase of viral vector titre or pseudotyping with a wrong Rabies strain, evidence from the literature suggests that the technique is feasible *(Mazarakis et al., 2001; Mentis et al., 2006)*. In addition to

testing other possible modes of delivery, alternative vector systems, such as AAV, are also worthy of consideration *(Kaspar et al., 2003)*. Interestingly, it has been recently demonstrated that efficient transduction of spinal cord motor neurons can be obtained by injection of AAVs into the peripheral nerves *(Federici and Boulis, 2006; Wu et al., 2009)*. This new approach appears to offer the advantage of increasing the probability of transduction of CNS motor neurons using lower doses of virus.

7.2. CONCLUSIONS

This thesis has provided extensive demonstration of the suitability of viral vector-mediated approaches for fine dissection, in vivo, of the molecular mechanisms involved in ALS. Numerous studies conducted both on human ALS patients and in animal models of ALS have contributed to our understanding of some of the pathological mechanisms involved in the disease. However, finding a truly effective therapy is still challenging. A reason for the lack of success to date is that it has been very difficult to identify the appropriate molecular targets. We have concentrated on p38MAPK and Akt signalling pathways, two of the molecular mechanisms known to be altered in ALS, and whose specific roles in the disease process have not yet been completely elucidated. Using a gene-based strategy we have demonstrated that preservation of motor neuronal perikaria in the spinal cord, through activation of Akt3, is not sufficient to prevent or retard the progression of motor deficits, suggesting that targeting of the peripheral compartment might be a more successful approach. Moreover, we have evidenced that downregulation of p38MAPK alpha is protective for motor neurons, but we found that expression of p38MAPK-targeted shRNA in the spinal cord is eventually detrimental, probably due to induction of microglia with a more neurotoxic phenotype. We believe that RNAi-mediated cell-specific downregulation of p38MAPK alpha and p38MAPK beta, or targeting of JNK, will

clarify the differential roles played by these kinases in microglia and neurons in ALS.

Overall it is anticipated that these studies may help in the identification of new potential therapeutic targets for this devastating disease.

BIBLIOGRAPHY

Abdellatif AA, Pelt JL, Benton RL, Howard RM, Tsoulfas P, Ping P, Xu XM, Whittemore SR (2006) Gene delivery to the spinal cord: comparison between lentiviral, adenoviral, and retroviral vector delivery systems. J Neurosci Res 84:553-567.

Abordo-Adesida E, Follenzi A, Barcia C, Sciascia S, Castro MG, Naldini L, Lowenstein PR (2005) Stability of lentiviral vector-mediated transgene expression in the brain in the presence of systemic antivector immune responses. Hum Gene Ther 16:741-751.

Abrahams S, Leigh PN, Goldstein LH (2005) Cognitive change in ALS: a prospective study. Neurology 64:1222-1226.

Ackerley S, Grierson AJ, Banner S, Perkinton MS, Brownlees J, Byers HL, Ward M, Thornhill P, Hussain K, Waby JS, Anderton BH, Cooper JD, Dingwall C, Leigh PN, Shaw CE, Miller CC (2004) p38alpha stress-activated protein kinase phosphorylates neurofilaments and is associated with neurofilament pathology in amyotrophic lateral sclerosis. Mol Cell Neurosci 26:354-364.

Adams JL, Boehm JC, Kassis S, Gorycki PD, Webb EF, Hall R, Sorenson M, Lee JC, Ayrton A, Griswold DE, Gallagher TF (1998) Pyrimidinylimidazole inhibitors of CSBP/p38 kinase demonstrating decreased inhibition of hepatic cytochrome P450 enzymes. Bioorg Med Chem Lett 8:3111-3116.

Adams RH, Porras A, Alonso G, Jones M, Vintersten K, Panelli S, Valladares A, Perez L, Klein R, Nebreda AR (2000) Essential role of p38alpha MAP kinase in placental but not embryonic cardiovascular development. Mol Cell 6:109-116.

Aebischer P, Schluep M, Deglon N, Joseph JM, Hirt L, Heyd B, Goddard M, Hammang JP, Zurn AD, Kato AC, Regli F, Baetge EE (1996a) Intrathecal delivery of CNTF using encapsulated genetically modified xenogeneic cells in amyotrophic lateral sclerosis patients. Nat Med 2:696-699.

Aebischer P, Pochon NA, Heyd B, Deglon N, Joseph JM, Zurn AD, Baetge EE, Hammang JP, Goddard M, Lysaght M, Kaplan F, Kato AC, Schluep M, Hirt L, Regli F, Porchet F, De Tribolet N (1996b) Gene therapy for amyotrophic lateral sclerosis (ALS) using a polymer encapsulated xenogenic cell line engineered to secrete hCNTF. Hum Gene Ther 7:851-860.

Aggarwal S, Cudkowicz M (2008) ALS drug development: reflections from the past and a way forward. Neurotherapeutics 5:516-527.

Aksoy H, Dean G, Elian M, Deng HX, Deng G, Juneja T, Storey E, McKinlay Gardner RJ, Jacob RL, Laing NG, Siddique T (2003) A4T mutation in the SOD1 gene causing familial amyotrophic lateral sclerosis. Neuroepidemiology 22:235-238.

Alessi DR, Caudwell FB, Andjelkovic M, Hemmings BA, Cohen P (1996a) Molecular basis for the substrate specificity of protein kinase B; comparison with MAPKAP kinase-1 and p70 S6 kinase. FEBS Lett 399:333-338.

Alessi DR, Andjelkovic M, Caudwell B, Cron P, Morrice N, Cohen P, Hemmings BA (1996b) Mechanism of activation of protein kinase B by insulin and IGF-1. Embo J 15:6541-6551.

Alexander GM, Erwin KL, Byers N, Deitch JS, Augelli BJ, Blankenhorn EP, Heiman-Patterson TD (2004) Effect of transgene copy number on survival in the G93A SOD1 transgenic mouse model of ALS. Brain Res Mol Brain Res 130:7-15.

Alexianu ME, Ho BK, Mohamed AH, La Bella V, Smith RG, Appel SH (1994) The role of calcium-binding proteins in selective motoneuron vulnerability in amyotrophic lateral sclerosis. Ann Neurol 36:846-858.

Altomare DA, Testa JR (2005) Perturbations of the AKT signaling pathway in human cancer. Oncogene 24:7455-7464.

Andersen PM, Nilsson P, Ala-Hurula V, Keranen ML, Tarvainen I, Haltia T, Nilsson L, Binzer M, Forsgren L, Marklund SL (1995) Amyotrophic lateral sclerosis associated with homozygosity for an Asp90Ala mutation in CuZn-superoxide dismutase. Nat Genet 10:61-66.

Andersen PM, Sims KB, Xin WW, Kiely R, O'Neill G, Ravits J, Pioro E, Harati Y, Brower RD, Levine JS, Heinicke HU, Seltzer W, Boss M, Brown RH, Jr. (2003) Sixteen novel mutations in the Cu/Zn superoxide dismutase gene in amyotrophic lateral sclerosis: a decade of discoveries, defects and disputes. Amyotroph Lateral Scler Other Motor Neuron Disord 4:62-73.

Andjelkovic M, Alessi DR, Meier R, Fernandez A, Lamb NJ, Frech M, Cron P, Cohen P, Lucocq JM, Hemmings BA (1997) Role of translocation in the activation and function of protein kinase B. J Biol Chem 272:31515-31524.

Andrus PK, Fleck TJ, Gurney ME, Hall ED (1998) Protein oxidative damage in a transgenic mouse model of familial amyotrophic lateral sclerosis. J Neurochem 71:2041-2048.

Aoki M, Kato S, Nagai M, Itoyama Y (2005) Development of a rat model of amyotrophic lateral sclerosis expressing a human SOD1 transgene. Neuropathology 25:365-370.

Aoki M, Batista O, Bellacosa A, Tsichlis P, Vogt PK (1998) The akt kinase: molecular determinants of oncogenicity. Proc Natl Acad Sci U S A 95:14950-14955.

Aouadi M, Laurent K, Prot M, Le Marchand-Brustel Y, Binetruy B, Bost F (2006) Inhibition of p38MAPK increases adipogenesis from embryonic to adult stages. Diabetes 55:281-289.

Arai T, Hasegawa M, Akiyama H, Ikeda K, Nonaka T, Mori H, Mann D, Tsuchiya K, Yoshida M, Hashizume Y, Oda T (2006) TDP-43 is a component of ubiquitin-positive tau-negative inclusions in frontotemporal lobar degeneration and amyotrophic lateral sclerosis. Biochem Biophys Res Commun 351:602-611.

Arber S, Han B, Mendelsohn M, Smith M, Jessell TM, Sockanathan S (1999) Requirement for the homeobox gene Hb9 in the consolidation of motor neuron identity. Neuron 23:659-674.

Arisato T, Okubo R, Arata H, Abe K, Fukada K, Sakoda S, Shimizu A, Qin XH, Izumo S, Osame M, Nakagawa M (2003) Clinical and pathological studies of familial amyotrophic lateral sclerosis (FALS) with SOD1 H46R mutation in large Japanese families. Acta Neuropathol 106:561-568.

Avossa D, Rosato-Siri MD, Mazzarol F, Ballerini L (2003) Spinal circuits formation: a study of developmentally regulated markers in organotypic cultures of embryonic mouse spinal cord. Neuroscience 122:391-405.

Avossa D, Grandolfo M, Mazzarol F, Zatta M, Ballerini L (2006) Early signs of motoneuron vulnerability in a disease model system: Characterization of transverse slice cultures of spinal cord isolated from embryonic ALS mice. Neuroscience 138:1179-1194.

Azzouz M, Hottinger A, Paterna JC, Zurn AD, Aebischer P, Bueler H (2000) Increased motoneuron survival and improved neuromuscular function in transgenic ALS mice after intraspinal injection of an adeno-associated virus encoding Bcl-2. Hum Mol Genet 9:803-811.

Azzouz M, Ralph GS, Storkebaum E, Walmsley LE, Mitrophanous KA, Kingsman SM, Carmeliet P, Mazarakis ND (2004a) VEGF delivery with retrogradely transported lentivector prolongs survival in a mouse ALS model. Nature 429:413-417.

Azzouz M, Le T, Ralph GS, Walmsley L, Monani UR, Lee DC, Wilkes F, Mitrophanous KA, Kingsman SM, Burghes AH, Mazarakis ND (2004b) Lentivector-mediated SMN replacement in a mouse model of spinal muscular atrophy. J Clin Invest 114:1726-1731.

Bacher M, Dodel R, Aljabari B, Keyvani K, Marambaud P, Kayed R, Glabe C, Goertz N, Hoppmann A, Sachser N, Klotsche J, Schnell S, Lewejohann L, Al-Abed Y (2008) CNI-1493 inhibits Abeta production, plaque formation, and cognitive deterioration in an animal model of Alzheimer's disease. J Exp Med 205:1593-1599.

Badger AM, Bradbeer JN, Votta B, Lee JC, Adams JL, Griswold DE (1996) Pharmacological profile of SB 203580, a selective inhibitor of cytokine suppressive binding protein/p38 kinase, in animal models of arthritis, bone resorption, endotoxin shock and immune function. J Pharmacol Exp Ther 279:1453-1461.

Baekelandt V, Eggermont K, Michiels M, Nuttin B, Debyser Z (2003) Optimized lentiviral vector production and purification procedure prevents immune response after transduction of mouse brain. Gene Ther 10:1933-1940.

Baekelandt V, Claeys A, Eggermont K, Lauwers E, De Strooper B, Nuttin B, Debyser Z (2002) Characterization of lentiviral vector-mediated gene transfer in adult mouse brain. Hum Gene Ther 13:841-853.

Bagrodia S, Derijard B, Davis RJ, Cerione RA (1995) Cdc42 and PAK-mediated signaling leads to Jun kinase and p38 mitogen-activated protein kinase activation. J Biol Chem 270:27995-27998.

Barboric M, Peterlin BM (2005) A new paradigm in eukaryotic biology: HIV Tat and the control of transcriptional elongation. PLoS Biol 3:e76.

Barnett SF, Defeo-Jones D, Fu S, Hancock PJ, Haskell KM, Jones RE, Kahana JA, Kral AM, Leander K, Lee LL, Malinowski J, McAvoy EM, Nahas DD, Robinson RG, Huber HE (2005) Identification and characterization of pleckstrin-homology-domain-dependent and isoenzyme-specific Akt inhibitors. Biochem J 385:399-408.

Beal MF, Palomo T, Kostrzewa RM, Archer T (2000) Neuroprotective and neurorestorative strategies for neuronal injury. Neurotox Res 2:71-84.

Beal MF, Ferrante RJ, Browne SE, Matthews RT, Kowall NW, Brown RH, Jr. (1997) Increased 3-nitrotyrosine in both sporadic and familial amyotrophic lateral sclerosis. Ann Neurol 42:644-654.

Beardmore VA, Hinton HJ, Eftychi C, Apostolaki M, Armaka M, Darragh J, McIlrath J, Carr JM, Armit LJ, Clacher C, Malone L, Kollias G, Arthur JS (2005) Generation and characterization of p38beta (MAPK11) gene-targeted mice. Mol Cell Biol 25:10454-10464.

Beaulieu JM, Nguyen MD, Julien JP (1999) Late onset of motor neurons in mice overexpressing wild-type peripherin. J Cell Biol 147:531-544.

Beckman JS, Carson M, Smith CD, Koppenol WH (1993) ALS, SOD and peroxynitrite. Nature 364:584.

Beers DR, Henkel JS, Zhao W, Wang J, Appel SH (2008) CD4+ T cells support glial neuroprotection, slow disease progression, and modify glial morphology in an animal model of inherited ALS. Proc Natl Acad Sci U S A 105:15558-15563.

Beers DR, Henkel JS, Xiao Q, Zhao W, Wang J, Yen AA, Siklos L, McKercher SR, Appel SH (2006) Wild-type microglia extend survival in PU.1 knockout mice with familial amyotrophic lateral sclerosis. Proc Natl Acad Sci U S A 103:16021-16026.

Bellacosa A, Testa JR, Staal SP, Tsichlis PN (1991) A retroviral oncogene, akt, encoding a serine-threonine kinase containing an SH2-like region. Science 254:274-277.

Bellasio S, Nicolussi E, Bertorelli R, Reggiani A (2003) Melanocortin receptor agonists and antagonists modulate nociceptive sensitivity in the mouse formalin test. Eur J Pharmacol 482:127-132.

Belsh JM (1999) Diagnostic challenges in ALS. Neurology 53:S26-30; discussion S35-26.

Bendotti C, Carri MT (2004) Lessons from models of SOD1-linked familial ALS. Trends Mol Med 10:393-400.

Bendotti C, Atzori C, Piva R, Tortarolo M, Strong MJ, DeBiasi S, Migheli A (2004) Activated p38MAPK is a novel component of the intracellular inclusions found in human amyotrophic lateral sclerosis and mutant SOD1 transgenic mice. J Neuropathol Exp Neurol 63:113-119.

Bendotti C, Calvaresi N, Chiveri L, Prelle A, Moggio M, Braga M, Silani V, De Biasi S (2001a) Early vacuolization and mitochondrial damage in motor neurons of FALS mice are not associated with apoptosis or with changes in cytochrome oxidase histochemical reactivity. J Neurol Sci 191:25-33.

Bendotti C, Tortarolo M, Suchak SK, Calvaresi N, Carvelli L, Bastone A, Rizzi M, Rattray M, Mennini T (2001b) Transgenic SOD1 G93A mice develop reduced GLT-1 in spinal cord without alterations in cerebrospinal fluid glutamate levels. J Neurochem 79:737-746.

Bendotti C, Bao Cutrona M, Cheroni C, Grignaschi G, Lo Coco D, Peviani M, Tortarolo M, Veglianese P, Zennaro E (2005) Inter- and intracellular signaling in amyotrophic lateral sclerosis: role of p38 mitogen-activated protein kinase. Neurodegener Dis 2:128-134.

Bianchi M, Ulrich P, Bloom O, Meistrell M, 3rd, Zimmerman GA, Schmidtmayerova H, Bukrinsky M, Donnelley T, Bucala R, Sherry B, et al. (1995) An inhibitor of macrophage arginine transport and nitric oxide production (CNI-1493) prevents acute inflammation and endotoxin lethality. Mol Med 1:254-266.

Bilsland LG, Nirmalananthan N, Yip J, Greensmith L, Duchen MR (2008) Expression of mutant SOD1 in astrocytes induces functional deficits in motoneuron mitochondria. J Neurochem 107:1271-1283.

Blair IP, Bennett CL, Abel A, Rabin BA, Griffin JW, Fischbeck KH, Cornblath DR, Chance PF (2000) A gene for autosomal dominant juvenile amyotrophic lateral sclerosis (ALS4) localizes to a 500-kb interval on chromosome 9q34. Neurogenetics 3:1-6.

Blesch A (2004) Lentiviral and MLV based retroviral vectors for ex vivo and in vivo gene transfer. Methods 33:164-172.

Blomer U, Naldini L, Kafri T, Trono D, Verma IM, Gage FH (1997) Highly efficient and sustained gene transfer in adult neurons with a lentivirus vector. J Virol 71:6641-6649.

Boehm JC, Smietana JM, Sorenson ME, Garigipati RS, Gallagher TF, Sheldrake PL, Bradbeer J, Badger AM, Laydon JT, Lee JC, Hillegass LM, Griswold DE, Breton JJ, Chabot-Fletcher MC, Adams JL (1996) 1-substituted 4-aryl-5-pyridinylimidazoles: a new class of cytokine suppressive drugs with low 5-lipoxygenase and cyclooxygenase inhibitory potency. J Med Chem 39:3929-3937.

Boillee S, Vande Velde C, Cleveland DW (2006a) ALS: a disease of motor neurons and their nonneuronal neighbors. Neuron 52:39-59.

Boillee S, Yamanaka K, Lobsiger CS, Copeland NG, Jenkins NA, Kassiotis G, Kollias G, Cleveland DW (2006b) Onset and progression in inherited ALS determined by motor neurons and microglia. Science 312:1389-1392.

Bolos J (2005) Structure-activity relationships of p38 mitogen-activated protein kinase inhibitors. Mini Rev Med Chem 5:857-868.

Bolshakov VY, Carboni L, Cobb MH, Siegelbaum SA, Belardetti F (2000) Dual MAP kinase pathways mediate opposing forms of long-term plasticity at CA3-CA1 synapses. Nat Neurosci 3:1107-1112.

Bommel H, Xie G, Rossoll W, Wiese S, Jablonka S, Boehm T, Sendtner M (2002) Missense mutation in the tubulin-specific chaperone E (Tbce) gene in the mouse mutant progressive motor neuronopathy, a model of human motoneuron disease. J Cell Biol 159:563-569.

Bonetto V, Nardo G, Pozzi S, Mantovani S, Garbelli S, Marinou K, Basso M, Mora G, Bendotti C (2009) Nitroproteomics of peripheral blood mononuclear cells from patients and a rat model of ALS. Antioxid Redox Signal.

Bonfoco E, Ceccatelli S, Manzo L, Nicotera P (1995) Colchicine induces apoptosis in cerebellar granule cells. Exp Cell Res 218:189-200.

Borchelt DR, Wong PC, Becher MW, Pardo CA, Lee MK, Xu ZS, Thinakaran G, Jenkins NA, Copeland NG, Sisodia SS, Cleveland DW, Price DL, Hoffman PN (1998) Axonal transport of mutant superoxide dismutase 1 and focal axonal abnormalities in the proximal axons of transgenic mice. Neurobiol Dis 5:27-35.

Borsello T, Clarke PG, Hirt L, Vercelli A, Repici M, Schorderet DF, Bogousslavsky J, Bonny C (2003) A peptide inhibitor of c-Jun N-terminal kinase protects against excitotoxicity and cerebral ischemia. Nat Med 9:1180-1186.

Borthwick GM, Johnson MA, Ince PG, Shaw PJ, Turnbull DM (1999) Mitochondrial enzyme activity in amyotrophic lateral sclerosis: implications for the role of mitochondria in neuronal cell death. Ann Neurol 46:787-790.

Bosch A, Perret E, Desmaris N, Trono D, Heard JM (2000) Reversal of pathology in the entire brain of mucopolysaccharidosis type VII mice after lentivirus-mediated gene transfer. Hum Gene Ther 11:1139-1150.

Brancho D, Tanaka N, Jaeschke A, Ventura JJ, Kelkar N, Tanaka Y, Kyuuma M, Takeshita T, Flavell RA, Davis RJ (2003) Mechanism of p38 MAP kinase activation in vivo. Genes Dev 17:1969-1978.

Brazil DP, Yang ZZ, Hemmings BA (2004) Advances in protein kinase B signalling: AKTion on multiple fronts. Trends Biochem Sci 29:233-242.

Brodbeck D, Cron P, Hemmings BA (1999) A human protein kinase Bgamma with regulatory phosphorylation sites in the activation loop and in the C-terminal hydrophobic domain. J Biol Chem 274:9133-9136.

Bronson RT, Lake BD, Cook S, Taylor S, Davisson MT (1993) Motor neuron degeneration of mice is a model of neuronal ceroid lipofuscinosis (Batten's disease). Ann Neurol 33:381-385.

Brooks AI, Stein CS, Hughes SM, Heth J, McCray PM, Jr., Sauter SL, Johnston JC, Cory-Slechta DA, Federoff HJ, Davidson BL (2002) Functional correction of established central nervous system deficits in an animal model of lysosomal storage disease with feline immunodeficiency virus-based vectors. Proc Natl Acad Sci U S A 99:6216-6221.

Brooks BR, Miller RG, Swash M, Munsat TL (2000) El Escorial revisited: revised criteria for the diagnosis of amyotrophic lateral sclerosis. Amyotroph Lateral Scler Other Motor Neuron Disord 1:293-299.

Brown BD, Venneri MA, Zingale A, Sergi Sergi L, Naldini L (2006) Endogenous microRNA regulation suppresses transgene expression in hematopoietic lineages and enables stable gene transfer. Nat Med 12:585-591.

Brown BD, Gentner B, Cantore A, Colleoni S, Amendola M, Zingale A, Baccarini A, Lazzari G, Galli C, Naldini L (2007) Endogenous microRNA can be broadly exploited to regulate transgene expression according to tissue, lineage and differentiation state. Nat Biotechnol 25:1457-1467.

Brown SD, Balling R (2001) Systematic approaches to mouse mutagenesis. Curr Opin Genet Dev 11:268-273.

Browne SE, Bowling AC, Baik MJ, Gurney M, Brown RH, Jr., Beal MF (1998) Metabolic dysfunction in familial, but not sporadic, amyotrophic lateral sclerosis. J Neurochem 71:281-287.

Bruijn LI, Beal MF, Becher MW, Schulz JB, Wong PC, Price DL, Cleveland DW (1997a) Elevated free nitrotyrosine levels, but not protein-bound nitrotyrosine or hydroxyl radicals, throughout amyotrophic lateral sclerosis (ALS)-like disease implicate tyrosine nitration as an aberrant in vivo property of one familial ALS-linked superoxide dismutase 1 mutant. Proc Natl Acad Sci U S A 94:7606-7611.

Bruijn LI, Houseweart MK, Kato S, Anderson KL, Anderson SD, Ohama E, Reaume AG, Scott RW, Cleveland DW (1998) Aggregation and motor neuron toxicity of an ALS-linked SOD1 mutant independent from wild-type SOD1. Science 281:1851-1854.

Bruijn LI, Becher MW, Lee MK, Anderson KL, Jenkins NA, Copeland NG, Sisodia SS, Rothstein JD, Borchelt DR, Price DL, Cleveland DW (1997b) ALS-linked SOD1 mutant G85R mediates damage to astrocytes and promotes rapidly progressive disease with SOD1-containing inclusions. Neuron 18:327-338.

Brunet A, Datta SR, Greenberg ME (2001) Transcription-dependent and -independent control of neuronal survival by the PI3K-Akt signaling pathway. Curr Opin Neurobiol 11:297-305.

Brunialti AL, Poirier C, Schmalbruch H, Guenet JL (1995) The mouse mutation progressive motor neuronopathy (pmn) maps to chromosome 13. Genomics 29:131-135.

Bu X, Huang P, Qi Z, Zhang N, Han S, Fang L, Li J (2007) Cell type-specific activation of p38 MAPK in the brain regions of hypoxic preconditioned mice. Neurochem Int 51:459-466.

Buratti E, Baralle FE (2001) Characterization and functional implications of the RNA binding properties of nuclear factor TDP-43, a novel splicing regulator of CFTR exon 9. J Biol Chem 276:36337-36343.

Buratti E, Baralle FE (2008) Multiple roles of TDP-43 in gene expression, splicing regulation, and human disease. Front Biosci 13:867-878.

Buratti E, Brindisi A, Pagani F, Baralle FE (2004) Nuclear factor TDP-43 binds to the polymorphic TG repeats in CFTR intron 8 and causes skipping of exon 9: a functional link with disease penetrance. Am J Hum Genet 74:1322-1325.

Burger C, Nguyen FN, Deng J, Mandel RJ (2005) Systemic mannitol-induced hyperosmolality amplifies rAAV2-mediated striatal transduction to a greater extent than local co-infusion. Mol Ther 11:327-331.

Bush AI (2002) Is ALS caused by an altered oxidative activity of mutant superoxide dismutase? Nat Neurosci 5:919; author reply 919-920.

Butler MP, O'Connor JJ, Moynagh PN (2004) Dissection of tumor-necrosis factor-alpha inhibition of long-term potentiation (LTP) reveals a p38 mitogen-activated protein kinase-dependent mechanism which maps to early-but not late-phase LTP. Neuroscience 124:319-326.

Cai H, Lin X, Xie C, Laird FM, Lai C, Wen H, Chiang HC, Shim H, Farah MH, Hoke A, Price DL, Wong PC (2005) Loss of ALS2 function is insufficient to trigger motor neuron degeneration in knock-out mice but predisposes neurons to oxidative stress. J Neurosci 25:7567-7574.

Calleja V, Laguerre M, Larijani B (2009) 3-D structure and dynamics of protein kinase B-new mechanism for the allosteric regulation of an AGC kinase. J Chem Biol 2:11-25.

Carri MT, Grignaschi G, Bendotti C (2006) Targets in ALS: designing multidrug therapies. Trends Pharmacol Sci 27:267-273.

Carri MT, Ferri A, Battistoni A, Famhy L, Gabbianelli R, Poccia F, Rotilio G (1997) Expression of a Cu,Zn superoxide dismutase typical of familial amyotrophic lateral sclerosis induces mitochondrial alteration and increase of cytosolic Ca2+ concentration in transfected neuroblastoma SH-SY5Y cells. FEBS Lett 414:365-368.

Carriedo SG, Yin HZ, Weiss JH (1996) Motor neurons are selectively vulnerable to AMPA/kainate receptor-mediated injury in vitro. J Neurosci 16:4069-4079.
Carroll RC, Beattie EC, von Zastrow M, Malenka RC (2001) Role of AMPA receptor endocytosis in synaptic plasticity. Nat Rev Neurosci 2:315-324.
Castillo SS, Brognard J, Petukhov PA, Zhang C, Tsurutani J, Granville CA, Li M, Jung M, West KA, Gills JG, Kozikowski AP, Dennis PA (2004) Preferential inhibition of Akt and killing of Akt-dependent cancer cells by rationally designed phosphatidylinositol ether lipid analogues. Cancer Res 64:2782-2792.
Cavalli V, Kujala P, Klumperman J, Goldstein LS (2005) Sunday Driver links axonal transport to damage signaling. J Cell Biol 168:775-787.
Cavalli V, Vilbois F, Corti M, Marcote MJ, Tamura K, Karin M, Arkinstall S, Gruenberg J (2001) The stress-induced MAP kinase p38 regulates endocytic trafficking via the GDI:Rab5 complex. Mol Cell 7:421-432.
Chambers DM, Peters J, Abbott CM (1998) The lethal mutation of the mouse wasted (wst) is a deletion that abolishes expression of a tissue-specific isoform of translation elongation factor 1alpha, encoded by the Eef1a2 gene. Proc Natl Acad Sci U S A 95:4463-4468.
Chaudhary LR, Hruska KA (2003) Inhibition of cell survival signal protein kinase B/Akt by curcumin in human prostate cancer cells. J Cell Biochem 89:1-5.
Chen W, Saeed M, Mao H, Siddique N, Dellefave L, Hung WY, Deng HX, Sufit RL, Heller SL, Haines JL, Pericak-Vance M, Siddique T (2006) Lack of association of VEGF promoter polymorphisms with sporadic ALS. Neurology 67:508-510.
Chen WS, Xu PZ, Gottlob K, Chen ML, Sokol K, Shiyanova T, Roninson I, Weng W, Suzuki R, Tobe K, Kadowaki T, Hay N (2001) Growth retardation and increased apoptosis in mice with homozygous disruption of the Akt1 gene. Genes Dev 15:2203-2208.
Chen Y, Yee D, Dains K, Chatterjee A, Cavalcoli J, Schneider E, Om J, Woychik RP, Magnuson T (2000) Genotype-based screen for ENU-induced mutations in mouse embryonic stem cells. Nat Genet 24:314-317.
Chen YZ, Bennett CL, Huynh HM, Blair IP, Puls I, Irobi J, Dierick I, Abel A, Kennerson ML, Rabin BA, Nicholson GA, Auer-Grumbach M, Wagner K, De Jonghe P, Griffin JW, Fischbeck KH, Timmerman V, Cornblath DR, Chance PF (2004) DNA/RNA helicase gene mutations in a form of juvenile amyotrophic lateral sclerosis (ALS4). Am J Hum Genet 74:1128-1135.
Cheng TL, Chang WT (2007) Construction of simple and efficient DNA vector-based short hairpin RNA expression systems for specific gene silencing in mammalian cells. Methods Mol Biol 408:223-241.
Chesik D, De Keyser J, Wilczak N (2008) Insulin-like growth factor system regulates oligodendroglial cell behavior: therapeutic potential in CNS. J Mol Neurosci 35:81-90.
Cheung PC, Campbell DG, Nebreda AR, Cohen P (2003) Feedback control of the protein kinase TAK1 by SAPK2a/p38alpha. Embo J 22:5793-5805.
Chinni SR, Sarkar FH (2002) Akt inactivation is a key event in indole-3-carbinol-induced apoptosis in PC-3 cells. Clin Cancer Res 8:1228-1236.
Chiu IM, Chen A, Zheng Y, Kosaras B, Tsiftsoglou SA, Vartanian TK, Brown RH, Jr., Carroll MC (2008) T lymphocytes potentiate endogenous neuroprotective inflammation in a mouse model of ALS. Proc Natl Acad Sci U S A 105:17913-17918.
Cho H, Thorvaldsen JL, Chu Q, Feng F, Birnbaum MJ (2001) Akt1/PKBalpha is required for normal growth but dispensable for maintenance of glucose homeostasis in mice. J Biol Chem 276:38349-38352.
Choi WS, Chun SY, Markelonis GJ, Oh TH, Oh YJ (2001) Overexpression of calbindin-D28K induces neurite outgrowth in dopaminergic neuronal cells via activation of p38 MAPK. Biochem Biophys Res Commun 287:656-661.
Chou SM (1992) Immunohistochemical and ultrastructural classification of peripheral neuropathies with onion-bulbs. Clin Neuropathol 11:109-114.
Chow CY, Zhang Y, Dowling JJ, Jin N, Adamska M, Shiga K, Szigeti K, Shy ME, Li J, Zhang X, Lupski JR, Weisman LS, Meisler MH (2007) Mutation of FIG4 causes neurodegeneration in the pale tremor mouse and patients with CMT4J. Nature 448:68-72.
Chow CY, Landers JE, Bergren SK, Sapp PC, Grant AE, Jones JM, Everett L, Lenk GM, McKenna-Yasek DM, Weisman LS, Figlewicz D, Brown RH, Meisler MH (2009)

Deleterious variants of FIG4, a phosphoinositide phosphatase, in patients with ALS. Am J Hum Genet 84:85-88.
Chun KH, Kosmeder JW, 2nd, Sun S, Pezzuto JM, Lotan R, Hong WK, Lee HY (2003) Effects of deguelin on the phosphatidylinositol 3-kinase/Akt pathway and apoptosis in premalignant human bronchial epithelial cells. J Natl Cancer Inst 95:291-302.
Chung J, Yang H, de Beus MD, Ryu CY, Cho K, Colon W (2003) Cu/Zn superoxide dismutase can form pore-like structures. Biochem Biophys Res Commun 312:873-876.
Ciavarro GL, Calvaresi N, Botturi A, Bendotti C, Andreoni G, Pedotti A (2003) The densitometric physical fractionator for counting neuronal populations: application to a mouse model of familial amyotrophic lateral sclerosis. J Neurosci Methods 129:61-71.
Clement AM, Nguyen MD, Roberts EA, Garcia ML, Boillee S, Rule M, McMahon AP, Doucette W, Siwek D, Ferrante RJ, Brown RH, Jr., Julien JP, Goldstein LS, Cleveland DW (2003) Wild-type nonneuronal cells extend survival of SOD1 mutant motor neurons in ALS mice. Science 302:113-117.
Cleveland DW, Rothstein JD (2001) From Charcot to Lou Gehrig: deciphering selective motor neuron death in ALS. Nat Rev Neurosci 2:806-819.
Coffer PJ, Woodgett JR (1991) Molecular cloning and characterisation of a novel putative protein-serine kinase related to the cAMP-dependent and protein kinase C families. Eur J Biochem 201:475-481.
Coffin (1992) Structure and classification of retroviruses. In: The retroviridae (Levy JA, ed), pp 19-49: Plenum Press, New York.
Coffin (1996) Retroviridae and their replication. In: Virology (al. BNFe, ed), p 1767 1848: Raven Press, New York.
Coffin JMH, Stephen H.; Varmus, Harold E. (1997) Retroviruses: Plainview (NY): Cold Spring Harbor Laboratory Press.
Consiglio A, Gritti A, Dolcetta D, Follenzi A, Bordignon C, Gage FH, Vescovi AL, Naldini L (2004) Robust in vivo gene transfer into adult mammalian neural stem cells by lentiviral vectors. Proc Natl Acad Sci U S A 101:14835-14840.
Conus NM, Hannan KM, Cristiano BE, Hemmings BA, Pearson RB (2002) Direct identification of tyrosine 474 as a regulatory phosphorylation site for the Akt protein kinase. J Biol Chem 277:38021-38028.
Conzelmann KK, Cox JH, Schneider LG, Thiel HJ (1990) Molecular cloning and complete nucleotide sequence of the attenuated rabies virus SAD B19. Virology 175:485-499.
Cook SA, Johnson KR, Bronson RT, Davisson MT (1995) Neuromuscular degeneration (nmd): a mutation on mouse chromosome 19 that causes motor neuron degeneration. Mamm Genome 6:187-191.
Corbo M, Hays AP (1992) Peripherin and neurofilament protein coexist in spinal spheroids of motor neuron disease. J Neuropathol Exp Neurol 51:531-537.
Corcia P, Mayeux-Portas V, Khoris J, de Toffol B, Autret A, Muh JP, Camu W, Andres C (2002) Abnormal SMN1 gene copy number is a susceptibility factor for amyotrophic lateral sclerosis. Ann Neurol 51:243-246.
Corcia P, Camu W, Halimi JM, Vourc'h P, Antar C, Vedrine S, Giraudeau B, de Toffol B, Andres CR (2006) SMN1 gene, but not SMN2, is a risk factor for sporadic ALS. Neurology 67:1147-1150.
Cormack BP, Valdivia RH, Falkow S (1996) FACS-optimized mutants of the green fluorescent protein (GFP). Gene 173:33-38.
Corrado L, Battistini S, Penco S, Bergamaschi L, Testa L, Ricci C, Giannini F, Greco G, Patrosso MC, Pileggi S, Causarano R, Mazzini L, Momigliano-Richiardi P, D'Alfonso S (2007) Variations in the coding and regulatory sequences of the angiogenin (ANG) gene are not associated to ALS (amyotrophic lateral sclerosis) in the Italian population. J Neurol Sci 258:123-127.
Cote F, Collard JF, Julien JP (1993) Progressive neuronopathy in transgenic mice expressing the human neurofilament heavy gene: a mouse model of amyotrophic lateral sclerosis. Cell 73:35-46.
Couillard-Despres S, Meier J, Julien JP (2000) Extra axonal neurofilaments do not exacerbate disease caused by mutant Cu,Zn superoxide dismutase. Neurobiol Dis 7:462-470.

Couillard-Despres S, Zhu Q, Wong PC, Price DL, Cleveland DW, Julien JP (1998) Protective effect of neurofilament heavy gene overexpression in motor neuron disease induced by mutant superoxide dismutase. Proc Natl Acad Sci U S A 95:9626-9630.

Cox GA, Mahaffey CL, Frankel WN (1998) Identification of the mouse neuromuscular degeneration gene and mapping of a second site suppressor allele. Neuron 21:1327-1337.

Cox LE, Ferraiuolo L, Goodall EF, Heath PR, Higginbottom A, Mortiboys H, Hollinger HC, Hartley JA, Brockington A, Burness CE, Morrison KE, Wharton SB, Grierson AJ, Ince PG, Kirby J, Shaw PJ Mutations in CHMP2B in lower motor neuron predominant amyotrophic lateral sclerosis (ALS). PLoS One 5:e9872.

Cuenda A, Cohen P (1999) Stress-activated protein kinase-2/p38 and a rapamycin-sensitive pathway are required for C2C12 myogenesis. J Biol Chem 274:4341-4346.

Cuenda A, Rousseau S (2007) p38 MAP-kinases pathway regulation, function and role in human diseases. Biochim Biophys Acta 1773:1358-1375.

Culbert AA, Skaper SD, Howlett DR, Evans NA, Facci L, Soden PE, Seymour ZM, Guillot F, Gaestel M, Richardson JC (2006) MAPK-activated protein kinase 2 deficiency in microglia inhibits pro-inflammatory mediator release and resultant neurotoxicity. Relevance to neuroinflammation in a transgenic mouse model of Alzheimer disease. J Biol Chem 281:23658-23667.

Cullen BR (2009) Viral RNAs: lessons from the enemy. Cell 136:592-597.

Curran MA, Kaiser SM, Achacoso PL, Nolan GP (2000) Efficient transduction of nondividing cells by optimized feline immunodeficiency virus vectors. Mol Ther 1:31-38.

Da Silva DM, Silva EM (1997) [The family and the smoking habits of adolescents]. Servir 45:137-147.

Dal Canto MC, Gurney ME (1994) Development of central nervous system pathology in a murine transgenic model of human amyotrophic lateral sclerosis. Am J Pathol 145:1271-1279.

Datta SR, Brunet A, Greenberg ME (1999) Cellular survival: a play in three Akts. Genes Dev 13:2905-2927.

Davidson SM, Morange M (2000) Hsp25 and the p38 MAPK pathway are involved in differentiation of cardiomyocytes. Dev Biol 218:146-160.

De Vos KJ, Grierson AJ, Ackerley S, Miller CC (2008) Role of axonal transport in neurodegenerative diseases. Annu Rev Neurosci 31:151-173.

DeFeo-Jones D, Barnett SF, Fu S, Hancock PJ, Haskell KM, Leander KR, McAvoy E, Robinson RG, Duggan ME, Lindsley CW, Zhao Z, Huber HE, Jones RE (2005) Tumor cell sensitization to apoptotic stimuli by selective inhibition of specific Akt/PKB family members. Mol Cancer Ther 4:271-279.

Deglon N, Tseng JL, Bensadoun JC, Zurn AD, Arsenijevic Y, Pereira de Almeida L, Zufferey R, Trono D, Aebischer P (2000) Self-inactivating lentiviral vectors with enhanced transgene expression as potential gene transfer system in Parkinson's disease. Hum Gene Ther 11:179-190.

Del Bo R, Ghezzi S, Scarlato M, Albani D, Galimberti D, Lucca U, Tettamanti M, Scarpini E, Forloni G, Bresolin N, Comi GP (2008) Role of VEGF gene variability in longevity: a lesson from the Italian population. Neurobiol Aging 29:1917-1922.

Deng HX, Shi Y, Furukawa Y, Zhai H, Fu R, Liu E, Gorrie GH, Khan MS, Hung WY, Bigio EH, Lukas T, Dal Canto MC, O'Halloran TV, Siddique T (2006) Conversion to the amyotrophic lateral sclerosis phenotype is associated with intermolecular linked insoluble aggregates of SOD1 in mitochondria. Proc Natl Acad Sci U S A 103:7142-7147.

Derijard B, Hibi M, Wu IH, Barrett T, Su B, Deng T, Karin M, Davis RJ (1994) JNK1: a protein kinase stimulated by UV light and Ha-Ras that binds and phosphorylates the c-Jun activation domain. Cell 76:1025-1037.

Dewil M, dela Cruz VF, Van Den Bosch L, Robberecht W (2007a) Inhibition of p38 mitogen activated protein kinase activation and mutant SOD1(G93A)-induced motor neuron death. Neurobiol Dis 26:332-341.

Dewil M, Lambrechts D, Sciot R, Shaw PJ, Ince PG, Robberecht W, Van den Bosch L (2007b) Vascular endothelial growth factor counteracts the loss of phospho-Akt preceding motor neurone degeneration in amyotrophic lateral sclerosis. Neuropathol Appl Neurobiol 33:499-509.

Di Giorgio FP, Carrasco MA, Siao MC, Maniatis T, Eggan K (2007) Non-cell autonomous effect of glia on motor neurons in an embryonic stem cell-based ALS model. Nat Neurosci 10:608-614.

Doble A, Kennel P (2000) Animal models of amyotrophic lateral sclerosis. Amyotroph Lateral Scler Other Motor Neuron Disord 1:301-312.

Dobrowolny G, Giacinti C, Pelosi L, Nicoletti C, Winn N, Barberi L, Molinaro M, Rosenthal N, Musaro A (2005) Muscle expression of a local Igf-1 isoform protects motor neurons in an ALS mouse model. J Cell Biol 168:193-199.

Dobrowolny G, Aucello M, Rizzuto E, Beccafico S, Mammucari C, Boncompagni S, Belia S, Wannenes F, Nicoletti C, Del Prete Z, Rosenthal N, Molinaro M, Protasi F, Fano G, Sandri M, Musaro A (2008) Skeletal muscle is a primary target of SOD1G93A-mediated toxicity. Cell Metab 8:425-436.

Donato T, Shapira Y, Artru A, Powers K (1994) Effect of mannitol on cerebrospinal fluid dynamics and brain tissue edema. Anesth Analg 78:58-66.

Donello JE, Loeb JE, Hope TJ (1998) Woodchuck hepatitis virus contains a tripartite posttranscriptional regulatory element. J Virol 72:5085-5092.

Dubois M, Lalonde R, Julien JP, Strazielle C (2005) Mice with the deleted neurofilament of low-molecular-weight (Nefl) gene: 1. Effects on regional brain metabolism. J Neurosci Res 80:741-750.

Dull T, Zufferey R, Kelly M, Mandel RJ, Nguyen M, Trono D, Naldini L (1998) A third-generation lentivirus vector with a conditional packaging system. J Virol 72:8463-8471.

Durham HD, Roy J, Dong L, Figlewicz DA (1997) Aggregation of mutant Cu/Zn superoxide dismutase proteins in a culture model of ALS. J Neuropathol Exp Neurol 56:523-530.

Dykxhoorn DM, Novina CD, Sharp PA (2003) Killing the messenger: short RNAs that silence gene expression. Nat Rev Mol Cell Biol 4:457-467.

Easton RM, Cho H, Roovers K, Shineman DW, Mizrahi M, Forman MS, Lee VM, Szabolcs M, de Jong R, Oltersdorf T, Ludwig T, Efstratiadis A, Birnbaum MJ (2005) Role for Akt3/protein kinase Bgamma in attainment of normal brain size. Mol Cell Biol 25:1869-1878.

Ebneth A, Godemann R, Stamer K, Illenberger S, Trinczek B, Mandelkow E (1998) Overexpression of tau protein inhibits kinesin-dependent trafficking of vesicles, mitochondria, and endoplasmic reticulum: implications for Alzheimer's disease. J Cell Biol 143:777-794.

Eckert RL, Efimova T, Balasubramanian S, Crish JF, Bone F, Dashti S (2003) p38 Mitogen-activated protein kinases on the body surface--a function for p38 delta. J Invest Dermatol 120:823-828.

Efimova T, Broome AM, Eckert RL (2003) A regulatory role for p38 delta MAPK in keratinocyte differentiation. Evidence for p38 delta-ERK1/2 complex formation. J Biol Chem 278:34277-34285.

Eisen A, Calne D (1992) Amyotrophic lateral sclerosis, Parkinson's disease and Alzheimer's disease: phylogenetic disorders of the human neocortex sharing many characteristics. Can J Neurol Sci 19:117-123.

Estevez AG, Crow JP, Sampson JB, Reiter C, Zhuang Y, Richardson GJ, Tarpey MM, Barbeito L, Beckman JS (1999) Induction of nitric oxide-dependent apoptosis in motor neurons by zinc-deficient superoxide dismutase. Science 286:2498-2500.

Federici T, Boulis NM (2006) Gene-based treatment of motor neuron diseases. Muscle Nerve 33:302-323.

Feltri ML, Graus Porta D, Previtali SC, Nodari A, Migliavacca B, Cassetti A, Littlewood-Evans A, Reichardt LF, Messing A, Quattrini A, Mueller U, Wrabetz L (2002) Conditional disruption of beta 1 integrin in Schwann cells impedes interactions with axons. J Cell Biol 156:199-209.

Feng J, Park J, Cron P, Hess D, Hemmings BA (2004) Identification of a PKB/Akt hydrophobic motif Ser-473 kinase as DNA-dependent protein kinase. J Biol Chem 279:41189-41196.

Ferrante RJ, Browne SE, Shinobu LA, Bowling AC, Baik MJ, MacGarvey U, Kowall NW, Brown RH, Jr., Beal MF (1997) Evidence of increased oxidative damage in both sporadic and familial amyotrophic lateral sclerosis. J Neurochem 69:2064-2074.

Ferrer I, Gomez-Isla T, Puig B, Freixes M, Ribe E, Dalfo E, Avila J (2005) Current advances on different kinases involved in tau phosphorylation, and implications in Alzheimer's disease and tauopathies. Curr Alzheimer Res 2:3-18.

Ferri A, Nencini M, Casciati A, Cozzolino M, Angelini DF, Longone P, Spalloni A, Rotilio G, Carri MT (2004) Cell death in amyotrophic lateral sclerosis: interplay between neuronal and glial cells. Faseb J 18:1261-1263.

Fischer LR, Culver DG, Tennant P, Davis AA, Wang M, Castellano-Sanchez A, Khan J, Polak MA, Glass JD (2004) Amyotrophic lateral sclerosis is a distal axonopathy: evidence in mice and man. Exp Neurol 185:232-240.

Follenzi A, Ailles LE, Bakovic S, Geuna M, Naldini L (2000) Gene transfer by lentiviral vectors is limited by nuclear translocation and rescued by HIV-1 pol sequences. Nat Genet 25:217-222.

Forss-Petter S, Danielson PE, Catsicas S, Battenberg E, Price J, Nerenberg M, Sutcliffe JG (1990) Transgenic mice expressing beta-galactosidase in mature neurons under neuron-specific enolase promoter control. Neuron 5:187-197.

Franz CK, Federici T, Yang J, Backus C, Oh SS, Teng Q, Carlton E, Bishop KM, Gasmi M, Bartus RT, Feldman EL, Boulis NM (2009) Intraspinal cord delivery of IGF-I mediated by adeno-associated virus 2 is neuroprotective in a rat model of familial ALS. Neurobiol Dis 33:473-481.

Fu H, Muenzer J, Samulski RJ, Breese G, Sifford J, Zeng X, McCarty DM (2003) Self-complementary adeno-associated virus serotype 2 vector: global distribution and broad dispersion of AAV-mediated transgene expression in mouse brain. Mol Ther 8:911-917.

Fujita Y, Okamoto K (2005) Golgi apparatus of the motor neurons in patients with amyotrophic lateral sclerosis and in mice models of amyotrophic lateral sclerosis. Neuropathology 25:388-394.

Gallo KA, Johnson GL (2002) Mixed-lineage kinase control of JNK and p38 MAPK pathways. Nat Rev Mol Cell Biol 3:663-672.

Gao T, Furnari F, Newton AC (2005) PHLPP: a phosphatase that directly dephosphorylates Akt, promotes apoptosis, and suppresses tumor growth. Mol Cell 18:13-24.

Gao X, Wang H, Sairenji T (2004) Inhibition of Epstein-Barr virus (EBV) reactivation by short interfering RNAs targeting p38 mitogen-activated protein kinase or c-myc in EBV-positive epithelial cells. J Virol 78:11798-11806.

Gasmi M, Glynn J, Jin MJ, Jolly DJ, Yee JK, Chen ST (1999) Requirements for efficient production and transduction of human immunodeficiency virus type 1-based vectors. J Virol 73:1828-1834.

Ghodsi A, Stein C, Derksen T, Martins I, Anderson RD, Davidson BL (1999) Systemic hyperosmolality improves beta-glucuronidase distribution and pathology in murine MPS VII brain following intraventricular gene transfer. Exp Neurol 160:109-116.

Gillet JP, Derer P, Tsiang H (1986) Axonal transport of rabies virus in the central nervous system of the rat. J Neuropathol Exp Neurol 45:619-634.

Gills JJ, Dennis PA (2004) The development of phosphatidylinositol ether lipid analogues as inhibitors of the serine/threonine kinase, Akt. Expert Opin Investig Drugs 13:787-797.

Gong YH, Parsadanian AS, Andreeva A, Snider WD, Elliott JL (2000) Restricted expression of G86R Cu/Zn superoxide dismutase in astrocytes results in astrocytosis but does not cause motoneuron degeneration. J Neurosci 20:660-665.

Gorman CM, Howard BH, Reeves R (1983) Expression of recombinant plasmids in mammalian cells is enhanced by sodium butyrate. Nucleic Acids Res 11:7631-7648.

Gould TW, Buss RR, Vinsant S, Prevette D, Sun W, Knudson CM, Milligan CE, Oppenheim RW (2006) Complete dissociation of motor neuron death from motor dysfunction by Bax deletion in a mouse model of ALS. J Neurosci 26:8774-8786.

Gowing G, Lalancette-Hebert M, Audet JN, Dequen F, Julien JP (2009) Macrophage colony stimulating factor (M-CSF) exacerbates ALS disease in a mouse model through altered responses of microglia expressing mutant superoxide dismutase. Exp Neurol.

Gowing G, Philips T, Van Wijmeersch B, Audet JN, Dewil M, Van Den Bosch L, Billiau AD, Robberecht W, Julien JP (2008) Ablation of proliferating microglia does not affect motor neuron degeneration in amyotrophic lateral sclerosis caused by mutant superoxide dismutase. J Neurosci 28:10234-10244.

Greenway MJ, Alexander MD, Ennis S, Traynor BJ, Corr B, Frost E, Green A, Hardiman O (2004) A novel candidate region for ALS on chromosome 14q11.2. Neurology 63:1936-1938.

Greenway MJ, Andersen PM, Russ C, Ennis S, Cashman S, Donaghy C, Patterson V, Swingler R, Kieran D, Prehn J, Morrison KE, Green A, Acharya KR, Brown RH, Jr., Hardiman O (2006) ANG mutations segregate with familial and 'sporadic' amyotrophic lateral sclerosis. Nat Genet 38:411-413.

Griffin RJ, Moloney A, Kelliher M, Johnston JA, Ravid R, Dockery P, O'Connor R, O'Neill C (2005) Activation of Akt/PKB, increased phosphorylation of Akt substrates and loss and altered distribution of Akt and PTEN are features of Alzheimer's disease pathology. J Neurochem 93:105-117.

Gros-Louis F, Laurent S, Lopes AA, Khoris J, Meininger V, Camu W, Rouleau GA (2003) Absence of mutations in the hypoxia response element of VEGF in ALS. Muscle Nerve 28:774-775.

Gros-Louis F, Lariviere R, Gowing G, Laurent S, Camu W, Bouchard JP, Meininger V, Rouleau GA, Julien JP (2004) A frameshift deletion in peripherin gene associated with amyotrophic lateral sclerosis. J Biol Chem 279:45951-45956.

Guillot S, Azzouz M, Deglon N, Zurn A, Aebischer P (2004) Local GDNF expression mediated by lentiviral vector protects facial nerve motoneurons but not spinal motoneurons in SOD1(G93A) transgenic mice. Neurobiol Dis 16:139-149.

Gurney ME, Pu H, Chiu AY, Dal Canto MC, Polchow CY, Alexander DD, Caliendo J, Hentati A, Kwon YW, Deng HX, et al. (1994) Motor neuron degeneration in mice that express a human Cu,Zn superoxide dismutase mutation. Science 264:1772-1775.

Hadano S, Benn SC, Kakuta S, Otomo A, Sudo K, Kunita R, Suzuki-Utsunomiya K, Mizumura H, Shefner JM, Cox GA, Iwakura Y, Brown RH, Jr., Ikeda JE (2006) Mice deficient in the Rab5 guanine nucleotide exchange factor ALS2/alsin exhibit age-dependent neurological deficits and altered endosome trafficking. Hum Mol Genet 15:233-250.

Hadano S, Hand CK, Osuga H, Yanagisawa Y, Otomo A, Devon RS, Miyamoto N, Showguchi-Miyata J, Okada Y, Singaraja R, Figlewicz DA, Kwiatkowski T, Hosler BA, Sagie T, Skaug J, Nasir J, Brown RH, Jr., Scherer SW, Rouleau GA, Hayden MR, Ikeda JE (2001) A gene encoding a putative GTPase regulator is mutated in familial amyotrophic lateral sclerosis 2. Nat Genet 29:166-173.

Haenggeli C, Kato AC (2002) Rapid and reproducible methods using fluorogold for labelling a subpopulation of cervical motoneurons: application in the wobbler mouse. J Neurosci Methods 116:119-124.

Hafezparast M, Ahmad-Annuar A, Hummerich H, Shah P, Ford M, Baker C, Bowen S, Martin JE, Fisher EM (2003a) Paradigms for the identification of new genes in motor neuron degeneration. Amyotroph Lateral Scler Other Motor Neuron Disord 4:249-257.

Hafezparast M, Klocke R, Ruhrberg C, Marquardt A, Ahmad-Annuar A, Bowen S, Lalli G, Witherden AS, Hummerich H, Nicholson S, Morgan PJ, Oozageer R, Priestley JV, Averill S, King VR, Ball S, Peters J, Toda T, Yamamoto A, Hiraoka Y, Augustin M, Korthaus D, Wattler S, Wabnitz P, Dickneite C, Lampel S, Boehme F, Peraus G, Popp A, Rudelius M, Schlegel J, Fuchs H, Hrabe de Angelis M, Schiavo G, Shima DT, Russ AP, Stumm G, Martin JE, Fisher EM (2003b) Mutations in dynein link motor neuron degeneration to defects in retrograde transport. Science 300:808-812.

Hall ED, Oostveen JA, Gurney ME (1998) Relationship of microglial and astrocytic activation to disease onset and progression in a transgenic model of familial ALS. Glia 23:249-256.

Hammer RP, Jr., Tomiyasu U, Scheibel AB (1979) Degeneration of the human Betz cell due to amyotrophic lateral sclerosis. Exp Neurol 63:336-346.

Han J, Lee JD, Bibbs L, Ulevitch RJ (1994) A MAP kinase targeted by endotoxin and hyperosmolarity in mammalian cells. Science 265:808-811.

Hand CK, Khoris J, Salachas F, Gros-Louis F, Lopes AA, Mayeux-Portas V, Brewer CG, Brown RH, Jr., Meininger V, Camu W, Rouleau GA (2002) A novel locus for familial amyotrophic lateral sclerosis, on chromosome 18q. Am J Hum Genet 70:251-256.

Hanz S, Fainzilber M (2006) Retrograde signaling in injured nerve--the axon reaction revisited. J Neurochem 99:13-19.

Hart MN, Cancilla PA, Frommes S, Hirano A (1977) Anterior horn cell degeneration and Bunina-type inclusions associated with dementia. Acta Neuropathol 38:225-228.
Hayward C, Colville S, Swingler RJ, Brock DJ (1999) Molecular genetic analysis of the APEX nuclease gene in amyotrophic lateral sclerosis. Neurology 52:1899-1901.
He W, Qiang M, Ma W, Valente AJ, Quinones MP, Wang W, Reddick RL, Xiao Q, Ahuja SS, Clark RA, Freeman GL, Li S (2006) Development of a synthetic promoter for macrophage gene therapy. Hum Gene Ther 17:949-959.
Heiman-Patterson TD, Deitch JS, Blankenhorn EP, Erwin KL, Perreault MJ, Alexander BK, Byers N, Toman I, Alexander GM (2005) Background and gender effects on survival in the TgN(SOD1-G93A)1Gur mouse model of ALS. J Neurol Sci 236:1-7.
Hendriks WT, Eggers R, Verhaagen J, Boer GJ (2007) Gene transfer to the spinal cord neural scar with lentiviral vectors: predominant transgene expression in astrocytes but not in meningeal cells. J Neurosci Res 85:3041-3052.
Henshall DC, Araki T, Schindler CK, Lan JQ, Tiekoter KL, Taki W, Simon RP (2002) Activation of Bcl-2-associated death protein and counter-response of Akt within cell populations during seizure-induced neuronal death. J Neurosci 22:8458-8465.
Hensley K, Floyd RA, Gordon B, Mou S, Pye QN, Stewart C, West M, Williamson K (2002) Temporal patterns of cytokine and apoptosis-related gene expression in spinal cords of the G93A-SOD1 mouse model of amyotrophic lateral sclerosis. J Neurochem 82:365-374.
Hentati A, Ouahchi K, Pericak-Vance MA, Nijhawan D, Ahmad A, Yang Y, Rimmler J, Hung W, Schlotter B, Ahmed A, Ben Hamida M, Hentati F, Siddique T (1998) Linkage of a commoner form of recessive amyotrophic lateral sclerosis to chromosome 15q15-q22 markers. Neurogenetics 2:55-60.
Hervias I, Beal MF, Manfredi G (2006) Mitochondrial dysfunction and amyotrophic lateral sclerosis. Muscle Nerve 33:598-608.
Higgins CM, Jung C, Ding H, Xu Z (2002) Mutant Cu, Zn superoxide dismutase that causes motoneuron degeneration is present in mitochondria in the CNS. J Neurosci 22:RC215.
Hirano A, Nakano I, Kurland LT, Mulder DW, Holley PW, Saccomanno G (1984) Fine structural study of neurofibrillary changes in a family with amyotrophic lateral sclerosis. J Neuropathol Exp Neurol 43:471-480.
Hirasawa M, Cho A, Sreenath T, Sauer B, Julien JP, Kulkarni AB (2001) Neuron-specific expression of Cre recombinase during the late phase of brain development. Neurosci Res 40:125-132.
Hirose Y, Katayama M, Stokoe D, Haas-Kogan DA, Berger MS, Pieper RO (2003) The p38 mitogen-activated protein kinase pathway links the DNA mismatch repair system to the G2 checkpoint and to resistance to chemotherapeutic DNA-methylating agents. Mol Cell Biol 23:8306-8315.
Hishikawa N, Niwa J, Doyu M, Ito T, Ishigaki S, Hashizume Y, Sobue G (2003) Dorfin localizes to the ubiquitylated inclusions in Parkinson's disease, dementia with Lewy bodies, multiple system atrophy, and amyotrophic lateral sclerosis. Am J Pathol 163:609-619.
Holasek SS, Wengenack TM, Kandimalla KK, Montano C, Gregor DM, Curran GL, Poduslo JF (2005) Activation of the stress-activated MAP kinase, p38, but not JNK in cortical motor neurons during early presymptomatic stages of amyotrophic lateral sclerosis in transgenic mice. Brain Res 1045:185-198.
Hommes D, van den Blink B, Plasse T, Bartelsman J, Xu C, Macpherson B, Tytgat G, Peppelenbosch M, Van Deventer S (2002) Inhibition of stress-activated MAP kinases induces clinical improvement in moderate to severe Crohn's disease. Gastroenterology 122:7-14.
Hong M, Lee VM (1997) Insulin and insulin-like growth factor-1 regulate tau phosphorylation in cultured human neurons. J Biol Chem 272:19547-19553.
Hong S, Hwang DY, Yoon S, Isacson O, Ramezani A, Hawley RG, Kim KS (2007) Functional analysis of various promoters in lentiviral vectors at different stages of in vitro differentiation of mouse embryonic stem cells. Mol Ther 15:1630-1639.
Horn KP, Busch SA, Hawthorne AL, van Rooijen N, Silver J (2008) Another barrier to regeneration in the CNS: activated macrophages induce extensive retraction of dystrophic axons through direct physical interactions. J Neurosci 28:9330-9341.
Hosler BA, Siddique T, Sapp PC, Sailor W, Huang MC, Hossain A, Daube JR, Nance M, Fan C, Kaplan J, Hung WY, McKenna-Yasek D, Haines JL, Pericak-Vance MA,

Horvitz HR, Brown RH, Jr. (2000) Linkage of familial amyotrophic lateral sclerosis with frontotemporal dementia to chromosome 9q21-q22. Jama 284:1664-1669.
Houde M, Laprise P, Jean D, Blais M, Asselin C, Rivard N (2001) Intestinal epithelial cell differentiation involves activation of p38 mitogen-activated protein kinase that regulates the homeobox transcription factor CDX2. J Biol Chem 276:21885-21894.
Howard MO, Schwartz LW, Newton JF, Qualls CW, Jr., Yodis LA, Ventre JR (1991) Comparative biochemical and morphometric changes associated with induction of the hepatic mixed function oxidase system in the rat. Toxicol Pathol 19:115-122.
Howland DS, Liu J, She Y, Goad B, Maragakis NJ, Kim B, Erickson J, Kulik J, DeVito L, Psaltis G, DeGennaro LJ, Cleveland DW, Rothstein JD (2002) Focal loss of the glutamate transporter EAAT2 in a transgenic rat model of SOD1 mutant-mediated amyotrophic lateral sclerosis (ALS). Proc Natl Acad Sci U S A 99:1604-1609.
Huang H, Ryu J, Ha J, Chang EJ, Kim HJ, Kim HM, Kitamura T, Lee ZH, Kim HH (2006) Osteoclast differentiation requires TAK1 and MKK6 for NFATc1 induction and NF-kappaB transactivation by RANKL. Cell Death Differ 13:1879-1891.
Hudson AJ (1981) Amyotrophic lateral sclerosis and its association with dementia, parkinsonism and other neurological disorders: a review. Brain 104:217-247.
Humbert S, Bryson EA, Cordelieres FP, Connors NC, Datta SR, Finkbeiner S, Greenberg ME, Saudou F (2002) The IGF-1/Akt pathway is neuroprotective in Huntington's disease and involves Huntingtin phosphorylation by Akt. Dev Cell 2:831-837.
Hylden JL, Wilcox GL (1980) Intrathecal morphine in mice: a new technique. Eur J Pharmacol 67:313-316.
Ichijo H, Nishida E, Irie K, ten Dijke P, Saitoh M, Moriguchi T, Takagi M, Matsumoto K, Miyazono K, Gotoh Y (1997) Induction of apoptosis by ASK1, a mammalian MAPKKK that activates SAPK/JNK and p38 signaling pathways. Science 275:90-94.
Ikeda Y, Collins MK, Radcliffe PA, Mitrophanous KA, Takeuchi Y (2002) Gene transduction efficiency in cells of different species by HIV and EIAV vectors. Gene Ther 9:932-938.
Ilieva H, Nagano I, Murakami T, Shiote M, Shoji M, Abe K (2003) Sustained induction of survival p-AKT and p-ERK signals after transient hypoxia in mice spinal cord with G93A mutant human SOD1 protein. J Neurol Sci 215:57-62.
Ince (2000) Neuropathology, RHJ Brown Edition. London.
Ishihara T, Hong M, Zhang B, Nakagawa Y, Lee MK, Trojanowski JQ, Lee VM (1999) Age-dependent emergence and progression of a tauopathy in transgenic mice overexpressing the shortest human tau isoform. Neuron 24:751-762.
Ito Y, Sakagami H, Kondo H (1996) Enhanced gene expression for phosphatidylinositol 3-kinase in the hypoglossal motoneurons following axonal crush. Brain Res Mol Brain Res 37:329-332.
Ito Y, Yamada M, Tanaka H, Aida K, Tsuruma K, Shimazawa M, Hozumi I, Inuzuka T, Takahashi H, Hara H (2009) Involvement of CHOP, an ER-stress apoptotic mediator, in both human sporadic ALS and ALS model mice. Neurobiol Dis.
Jaarsma D, Teuling E, Haasdijk ED, De Zeeuw CI, Hoogenraad CC (2008) Neuron-specific expression of mutant superoxide dismutase is sufficient to induce amyotrophic lateral sclerosis in transgenic mice. J Neurosci 28:2075-2088.
Jaarsma D, Rognoni F, van Duijn W, Verspaget HW, Haasdijk ED, Holstege JC (2001) CuZn superoxide dismutase (SOD1) accumulates in vacuolated mitochondria in transgenic mice expressing amyotrophic lateral sclerosis-linked SOD1 mutations. Acta Neuropathol 102:293-305.
Jaarsma D, Haasdijk ED, Grashorn JA, Hawkins R, van Duijn W, Verspaget HW, London J, Holstege JC (2000) Human Cu/Zn superoxide dismutase (SOD1) overexpression in mice causes mitochondrial vacuolization, axonal degeneration, and premature motoneuron death and accelerates motoneuron disease in mice expressing a familial amyotrophic lateral sclerosis mutant SOD1. Neurobiol Dis 7:623-643.
Jakobsson J, Ericson C, Jansson M, Bjork E, Lundberg C (2003) Targeted transgene expression in rat brain using lentiviral vectors. J Neurosci Res 73:876-885.
Jakobsson J, Nielsen TT, Staflin K, Georgievska B, Lundberg C (2006) Efficient transduction of neurons using Ross River glycoprotein-pseudotyped lentiviral vectors. Gene Ther 13:966-973.

Jantzen JP (2007) Prevention and treatment of intracranial hypertension. Best Pract Res Clin Anaesthesiol 21:517-538.
Jellinger KA (2008) Neuropathological aspects of Alzheimer disease, Parkinson disease and frontotemporal dementia. Neurodegener Dis 5:118-121.
Jiang Y, Gram H, Zhao M, New L, Gu J, Feng L, Di Padova F, Ulevitch RJ, Han J (1997) Characterization of the structure and function of the fourth member of p38 group mitogen-activated protein kinases, p38delta. J Biol Chem 272:30122-30128.
Jiang ZY, Zhou QL, Coleman KA, Chouinard M, Boese Q, Czech MP (2003) Insulin signaling through Akt/protein kinase B analyzed by small interfering RNA-mediated gene silencing. Proc Natl Acad Sci U S A 100:7569-7574.
Jin KL, Mao XO, Nagayama T, Goldsmith PC, Greenberg DA (2000) Induction of vascular endothelial growth factor receptors and phosphatidylinositol 3'-kinase/Akt signaling by global cerebral ischemia in the rat. Neuroscience 100:713-717.
Johnson-Farley NN, Patel K, Kim D, Cowen DS (2007) Interaction of FGF-2 with IGF-1 and BDNF in stimulating Akt, ERK, and neuronal survival in hippocampal cultures. Brain Res 1154:40-49.
Johnston JA, Illing ME, Kopito RR (2002) Cytoplasmic dynein/dynactin mediates the assembly of aggresomes. Cell Motil Cytoskeleton 53:26-38.
Johnston JA, Dalton MJ, Gurney ME, Kopito RR (2000) Formation of high molecular weight complexes of mutant Cu, Zn-superoxide dismutase in a mouse model for familial amyotrophic lateral sclerosis. Proc Natl Acad Sci U S A 97:12571-12576.
Jokic N, Gonzalez de Aguilar JL, Dimou L, Lin S, Fergani A, Ruegg MA, Schwab ME, Dupuis L, Loeffler JP (2006) The neurite outgrowth inhibitor Nogo-A promotes denervation in an amyotrophic lateral sclerosis model. EMBO Rep 7:1162-1167.
Jones PF, Jakubowicz T, Pitossi FJ, Maurer F, Hemmings BA (1991) Molecular cloning and identification of a serine/threonine protein kinase of the second-messenger subfamily. Proc Natl Acad Sci U S A 88:4171-4175.
Jung C, Higgins CM, Xu Z (2002) Mitochondrial electron transport chain complex dysfunction in a transgenic mouse model for amyotrophic lateral sclerosis. J Neurochem 83:535-545.
Kanekura K, Hashimoto Y, Niikura T, Aiso S, Matsuoka M, Nishimoto I (2004) Alsin, the product of ALS2 gene, suppresses SOD1 mutant neurotoxicity through RhoGEF domain by interacting with SOD1 mutants. J Biol Chem 279:19247-19256.
Kanekura K, Hashimoto Y, Kita Y, Sasabe J, Aiso S, Nishimoto I, Matsuoka M (2005) A Rac1/phosphatidylinositol 3-kinase/Akt3 anti-apoptotic pathway, triggered by AlsinLF, the product of the ALS2 gene, antagonizes Cu/Zn-superoxide dismutase (SOD1) mutant-induced motoneuronal cell death. J Biol Chem 280:4532-4543.
Kang Y, Stein CS, Heth JA, Sinn PL, Penisten AK, Staber PD, Ratliff KL, Shen H, Barker CK, Martins I, Sharkey CM, Sanders DA, McCray PB, Jr., Davidson BL (2002) In vivo gene transfer using a nonprimate lentiviral vector pseudotyped with Ross River Virus glycoproteins. J Virol 76:9378-9388.
Kao SY, Calman AF, Luciw PA, Peterlin BM (1987) Anti-termination of transcription within the long terminal repeat of HIV-1 by tat gene product. Nature 330:489-493.
Karlsson J, Fong KS, Hansson MJ, Elmer E, Csiszar K, Keep MF (2004) Life span extension and reduced neuronal death after weekly intraventricular cyclosporin injections in the G93A transgenic mouse model of amyotrophic lateral sclerosis. J Neurosurg 101:128-137.
Kaspar BK, Llado J, Sherkat N, Rothstein JD, Gage FH (2003) Retrograde viral delivery of IGF-1 prolongs survival in a mouse ALS model. Science 301:839-842.
Kato S, Saito M, Hirano A, Ohama E (1999) Recent advances in research on neuropathological aspects of familial amyotrophic lateral sclerosis with superoxide dismutase 1 gene mutations: neuronal Lewy body-like hyaline inclusions and astrocytic hyaline inclusions. Histol Histopathol 14:973-989.
Kato S, Inoue K, Kobayashi K, Yasoshima Y, Miyachi S, Inoue S, Hanawa H, Shimada T, Takada M (2007) Efficient gene transfer via retrograde transport in rodent and primate brains using a human immunodeficiency virus type 1-based vector pseudotyped with rabies virus glycoprotein. Hum Gene Ther 18:1141-1151.
Katome T, Obata T, Matsushima R, Masuyama N, Cantley LC, Gotoh Y, Kishi K, Shiota H, Ebina Y (2003) Use of RNA interference-mediated gene silencing and adenoviral overexpression to elucidate the roles of AKT/protein kinase B isoforms in insulin actions. J Biol Chem 278:28312-28323.

Kawahara Y, Ito K, Sun H, Aizawa H, Kanazawa I, Kwak S (2004) Glutamate receptors: RNA editing and death of motor neurons. Nature 427:801.
Kawamata T, Akiyama H, Yamada T, McGeer PL (1992) Immunologic reactions in amyotrophic lateral sclerosis brain and spinal cord tissue. Am J Pathol 140:691-707.
Kennel PF, Finiels F, Revah F, Mallet J (1996) Neuromuscular function impairment is not caused by motor neurone loss in FALS mice: an electromyographic study. Neuroreport 7:1427-1431.
Kew J, Leigh N (1992) Dementia with motor neurone disease. Baillieres Clin Neurol 1:611-626.
Keyse SM (2000) Protein phosphatases and the regulation of mitogen-activated protein kinase signalling. Curr Opin Cell Biol 12:186-192.
Kholodenko BN (2002) MAP kinase cascade signaling and endocytic trafficking: a marriage of convenience? Trends Cell Biol 12:173-177.
Kholodenko BN (2006) Cell-signalling dynamics in time and space. Nat Rev Mol Cell Biol 7:165-176.
Kiaei M, Petri S, Kipiani K, Gardian G, Choi DK, Chen J, Calingasan NY, Schafer P, Muller GW, Stewart C, Hensley K, Beal MF (2006) Thalidomide and lenalidomide extend survival in a transgenic mouse model of amyotrophic lateral sclerosis. J Neurosci 26:2467-2473.
Kieran D, Hafezparast M, Bohnert S, Dick JR, Martin J, Schiavo G, Fisher EM, Greensmith L (2005) A mutation in dynein rescues axonal transport defects and extends the life span of ALS mice. J Cell Biol 169:561-567.
Kiernan JA, Hudson AJ (1991) Changes in sizes of cortical and lower motor neurons in amyotrophic lateral sclerosis. Brain 114 (Pt 2):843-853.
Kilani M, Micallef J, Soubrouillard C, Rey-Lardiller D, Demattei C, Dib M, Philippot P, Ceccaldi M, Pouget J, Blin O (2004) A longitudinal study of the evolution of cognitive function and affective state in patients with amyotrophic lateral sclerosis. Amyotroph Lateral Scler Other Motor Neuron Disord 5:46-54.
Kim AH, Khursigara G, Sun X, Franke TF, Chao MV (2001) Akt phosphorylates and negatively regulates apoptosis signal-regulating kinase 1. Mol Cell Biol 21:893-901.
Kim AH, Yano H, Cho H, Meyer D, Monks B, Margolis B, Birnbaum MJ, Chao MV (2002) Akt1 regulates a JNK scaffold during excitotoxic apoptosis. Neuron 35:697-709.
Kim HP, Wang X, Nakao A, Kim SI, Murase N, Choi ME, Ryter SW, Choi AM (2005) Caveolin-1 expression by means of p38beta mitogen-activated protein kinase mediates the antiproliferative effect of carbon monoxide. Proc Natl Acad Sci U S A 102:11319-11324.
Kim VN, Mitrophanous K, Kingsman SM, Kingsman AJ (1998) Minimal requirement for a lentivirus vector based on human immunodeficiency virus type 1. J Virol 72:811-816.
Klivenyi P, Ferrante RJ, Matthews RT, Bogdanov MB, Klein AM, Andreassen OA, Mueller G, Wermer M, Kaddurah-Daouk R, Beal MF (1999) Neuroprotective effects of creatine in a transgenic animal model of amyotrophic lateral sclerosis. Nat Med 5:347-350.
Kobinger GP, Weiner DJ, Yu QC, Wilson JM (2001) Filovirus-pseudotyped lentiviral vector can efficiently and stably transduce airway epithelia in vivo. Nat Biotechnol 19:225-230.
Kobinger GP, Deng S, Louboutin JP, Vatamaniuk M, Matschinsky F, Markmann JF, Raper SE, Wilson JM (2004) Transduction of human islets with pseudotyped lentiviral vectors. Hum Gene Ther 15:211-219.
Koistinaho M, Koistinaho J (2002) Role of p38 and p44/42 mitogen-activated protein kinases in microglia. Glia 40:175-183.
Kojima S, Asakawa A, Amitani H, Sakoguchi T, Ueno N, Inui A, Kalra SP (2009) Central leptin gene therapy, a substitute for insulin therapy to ameliorate hyperglycemia and hyperphagia, and promote survival in insulin-deficient diabetic mice. Peptides 30:962-966.
Kolde G, Bachus R, Ludolph AC (1996) Skin involvement in amyotrophic lateral sclerosis. Lancet 347:1226-1227.
Komori T, Morikawa Y, Tamura S, Doi A, Nanjo K, Senba E (2005) Subcellular localization of glucose transporter 4 in the hypothalamic arcuate nucleus of ob/ob mice under basal conditions. Brain Res 1049:34-42.

Kong J, Xu Z (2000) Overexpression of neurofilament subunit NF-L and NF-H extends survival of a mouse model for amyotrophic lateral sclerosis. Neurosci Lett 281:72-74.

Kontoyiannis D, Pasparakis M, Pizarro TT, Cominelli F, Kollias G (1999) Impaired on/off regulation of TNF biosynthesis in mice lacking TNF AU-rich elements: implications for joint and gut-associated immunopathologies. Immunity 10:387-398.

Kordower JH, Emborg ME, Bloch J, Ma SY, Chu Y, Leventhal L, McBride J, Chen EY, Palfi S, Roitberg BZ, Brown WD, Holden JE, Pyzalski R, Taylor MD, Carvey P, Ling Z, Trono D, Hantraye P, Deglon N, Aebischer P (2000) Neurodegeneration prevented by lentiviral vector delivery of GDNF in primate models of Parkinson's disease. Science 290:767-773.

Kosuge Y, Sekikawa-Nishida K, Negi H, Ishige K, Ito Y (2009) Characterization of chronic glutamate-mediated motor neuron toxicity in organotypic spinal cord culture prepared from ALS model mice. Neurosci Lett 454:165-169.

Kriz J, Nguyen MD, Julien JP (2002) Minocycline slows disease progression in a mouse model of amyotrophic lateral sclerosis. Neurobiol Dis 10:268-278.

Kriz J, Meier J, Julien JP, Padjen AL (2000) Altered ionic conductances in axons of transgenic mouse expressing the human neurofilament heavy gene: A mouse model of amyotrophic lateral sclerosis. Exp Neurol 163:414-421.

Kumar CC, Madison V (2005) AKT crystal structure and AKT-specific inhibitors. Oncogene 24:7493-7501.

Kumar M, Bradow BP, Zimmerberg J (2003) Large-scale production of pseudotyped lentiviral vectors using baculovirus GP64. Hum Gene Ther 14:67-77.

Kunkel MT, Ni Q, Tsien RY, Zhang J, Newton AC (2005) Spatio-temporal dynamics of protein kinase B/Akt signaling revealed by a genetically encoded fluorescent reporter. J Biol Chem 280:5581-5587.

Kurland LT, Molgaard CA (1982) Guamanian ALS: hereditary or acquired? Adv Neurol 36:165-171.

Kwiatkowski TJ, Jr., Bosco DA, Leclerc AL, Tamrazian E, Vanderburg CR, Russ C, Davis A, Gilchrist J, Kasarskis EJ, Munsat T, Valdmanis P, Rouleau GA, Hosler BA, Cortelli P, de Jong PJ, Yoshinaga Y, Haines JL, Pericak-Vance MA, Yan J, Ticozzi N, Siddique T, McKenna-Yasek D, Sapp PC, Horvitz HR, Landers JE, Brown RH, Jr. (2009) Mutations in the FUS/TLS gene on chromosome 16 cause familial amyotrophic lateral sclerosis. Science 323:1205-1208.

Kyriakis JM, Avruch J (2001) Mammalian mitogen-activated protein kinase signal transduction pathways activated by stress and inflammation. Physiol Rev 81:807-869.

Lafon M (2005) Rabies virus receptors. J Neurovirol 11:82-87.

Lagier-Tourenne C, Cleveland DW (2009) Rethinking ALS: the FUS about TDP-43. Cell 136:1001-1004.

Lai C, Xie C, McCormack SG, Chiang HC, Michalak MK, Lin X, Chandran J, Shim H, Shimoji M, Cookson MR, Huganir RL, Rothstein JD, Price DL, Wong PC, Martin LJ, Zhu JJ, Cai H (2006) Amyotrophic lateral sclerosis 2-deficiency leads to neuronal degeneration in amyotrophic lateral sclerosis through altered AMPA receptor trafficking. J Neurosci 26:11798-11806.

Lalancette-Hebert M, Gowing G, Simard A, Weng YC, Kriz J (2007) Selective ablation of proliferating microglial cells exacerbates ischemic injury in the brain. J Neurosci 27:2596-2605.

Lambrechts D, Storkebaum E, Morimoto M, Del-Favero J, Desmet F, Marklund SL, Wyns S, Thijs V, Andersson J, van Marion I, Al-Chalabi A, Bornes S, Musson R, Hansen V, Beckman L, Adolfsson R, Pall HS, Prats H, Vermeire S, Rutgeerts P, Katayama S, Awata T, Leigh N, Lang-Lazdunski L, Dewerchin M, Shaw C, Moons L, Vlietinck R, Morrison KE, Robberecht W, Van Broeckhoven C, Collen D, Andersen PM, Carmeliet P (2003) VEGF is a modifier of amyotrophic lateral sclerosis in mice and humans and protects motoneurons against ischemic death. Nat Genet 34:383-394.

LaMonte BH, Wallace KE, Holloway BA, Shelly SS, Ascano J, Tokito M, Van Winkle T, Howland DS, Holzbaur EL (2002) Disruption of dynein/dynactin inhibits axonal transport in motor neurons causing late-onset progressive degeneration. Neuron 34:715-727.

Landers JE, Melki J, Meininger V, Glass JD, van den Berg LH, van Es MA, Sapp PC, van Vught PW, McKenna-Yasek DM, Blauw HM, Cho TJ, Polak M, Shi L, Wills AM, Broom WJ, Ticozzi N, Silani V, Ozoguz A, Rodriguez-Leyva I, Veldink JH, Ivinson AJ, Saris CG, Hosler BA, Barnes-Nessa A, Couture N, Wokke JH, Kwiatkowski TJ, Jr., Ophoff RA, Cronin S, Hardiman O, Diekstra FP, Leigh PN, Shaw CE, Simpson CL, Hansen VK, Powell JF, Corcia P, Salachas F, Heath S, Galan P, Georges F, Horvitz HR, Lathrop M, Purcell S, Al-Chalabi A, Brown RH, Jr. (2009) Reduced expression of the Kinesin-Associated Protein 3 (KIFAP3) gene increases survival in sporadic amyotrophic lateral sclerosis. Proc Natl Acad Sci U S A 106:9004-9009.

Lariviere RC, Beaulieu JM, Nguyen MD, Julien JP (2003) Peripherin is not a contributing factor to motor neuron disease in a mouse model of amyotrophic lateral sclerosis caused by mutant superoxide dismutase. Neurobiol Dis 13:158-166.

Lechner C, Zahalka MA, Giot JF, Moller NP, Ullrich A (1996) ERK6, a mitogen-activated protein kinase involved in C2C12 myoblast differentiation. Proc Natl Acad Sci U S A 93:4355-4359.

Lee HK, Kumar P, Fu Q, Rosen KM, Querfurth HW (2009) The insulin/Akt signaling pathway is targeted by intracellular beta-amyloid. Mol Biol Cell 20:1533-1544.

Lee JC, Griswold DE, Votta B, Hanna N (1988) Inhibition of monocyte IL-1 production by the anti-inflammatory compound, SK&F 86002. Int J Immunopharmacol 10:835-843.

Lee JC, Badger AM, Griswold DE, Dunnington D, Truneh A, Votta B, White JR, Young PR, Bender PE (1993) Bicyclic imidazoles as a novel class of cytokine biosynthesis inhibitors. Ann N Y Acad Sci 696:149-170.

Lee JC, Laydon JT, McDonnell PC, Gallagher TF, Kumar S, Green D, McNulty D, Blumenthal MJ, Heys JR, Landvatter SW, et al. (1994a) A protein kinase involved in the regulation of inflammatory cytokine biosynthesis. Nature 372:739-746.

Lee MK, Marszalek JR, Cleveland DW (1994b) A mutant neurofilament subunit causes massive, selective motor neuron death: implications for the pathogenesis of human motor neuron disease. Neuron 13:975-988.

Lee SH, Park J, Che Y, Han PL, Lee JK (2000) Constitutive activity and differential localization of p38alpha and p38beta MAPKs in adult mouse brain. J Neurosci Res 60:623-631.

Leger B, Vergani L, Soraru G, Hespel P, Derave W, Gobelet C, D'Ascenzio C, Angelini C, Russell AP (2006) Human skeletal muscle atrophy in amyotrophic lateral sclerosis reveals a reduction in Akt and an increase in atrogin-1. Faseb J 20:583-585.

Leigh PN, Dodson A, Swash M, Brion JP, Anderton BH (1989) Cytoskeletal abnormalities in motor neuron disease. An immunocytochemical study. Brain 112 (Pt 2):521-535.

Leskovar A, Moriarty LJ, Turek JJ, Schoenlein IA, Borgens RB (2000) The macrophage in acute neural injury: changes in cell numbers over time and levels of cytokine production in mammalian central and peripheral nervous systems. J Exp Biol 203:1783-1795.

Leung AK, Davies HD, Hon KL (2007) Rabies: epidemiology, pathogenesis, and prophylaxis. Adv Ther 24:1340-1347.

Leung CL, He CZ, Kaufmann P, Chin SS, Naini A, Liem RK, Mitsumoto H, Hays AP (2004) A pathogenic peripherin gene mutation in a patient with amyotrophic lateral sclerosis. Brain Pathol 14:290-296.

Li B, Xu W, Luo C, Gozal D, Liu R (2003) VEGF-induced activation of the PI3-K/Akt pathway reduces mutant SOD1-mediated motor neuron cell death. Brain Res Mol Brain Res 111:155-164.

Li J, Miller EJ, Ninomiya-Tsuji J, Russell RR, 3rd, Young LH (2005) AMP-activated protein kinase activates p38 mitogen-activated protein kinase by increasing recruitment of p38 MAPK to TAB1 in the ischemic heart. Circ Res 97:872-879.

Ligon LA, LaMonte BH, Wallace KE, Weber N, Kalb RG, Holzbaur EL (2005) Mutant superoxide dismutase disrupts cytoplasmic dynein in motor neurons. Neuroreport 16:533-536.

Lindberg MJ, Tibell L, Oliveberg M (2002) Common denominator of Cu/Zn superoxide dismutase mutants associated with amyotrophic lateral sclerosis: decreased stability of the apo state. Proc Natl Acad Sci U S A 99:16607-16612.

Lindberg MJ, Bystrom R, Boknas N, Andersen PM, Oliveberg M (2005) Systematically perturbed folding patterns of amyotrophic lateral sclerosis (ALS)-associated SOD1 mutants. Proc Natl Acad Sci U S A 102:9754-9759.

Litman P, Ohne O, Ben-Yaakov S, Shemesh-Darvish L, Yechezkel T, Salitra Y, Rubnov S, Cohen I, Senderowitz H, Kidron D, Livnah O, Levitzki A, Livnah N (2007) A novel substrate mimetic inhibitor of PKB/Akt inhibits prostate cancer tumor growth in mice by blocking the PKB pathway. Biochemistry 46:4716-4724.

Liu D, Wen J, Liu J, Li L (1999) The roles of free radicals in amyotrophic lateral sclerosis: reactive oxygen species and elevated oxidation of protein, DNA, and membrane phospholipids. Faseb J 13:2318-2328.

Liu J, Lillo C, Jonsson PA, Vande Velde C, Ward CM, Miller TM, Subramaniam JR, Rothstein JD, Marklund S, Andersen PM, Brannstrom T, Gredal O, Wong PC, Williams DS, Cleveland DW (2004) Toxicity of familial ALS-linked SOD1 mutants from selective recruitment to spinal mitochondria. Neuron 43:5-17.

Liu Y, Hao W, Dawson A, Liu S, Fassbender K (2009) Expression of amyotrophic lateral sclerosis-linked SOD1 mutant increases the neurotoxic potential of microglia via TLR2. J Biol Chem 284:3691-3699.

Lobsiger CS, Boillee S, McAlonis-Downes M, Khan AM, Feltri ML, Yamanaka K, Cleveland DW (2009) Schwann cells expressing dismutase active mutant SOD1 unexpectedly slow disease progression in ALS mice. Proc Natl Acad Sci U S A 106:4465-4470.

Locatelli F, Corti S, Papadimitriou D, Fortunato F, Del Bo R, Donadoni C, Nizzardo M, Nardini M, Salani S, Ghezzi S, Strazzer S, Bresolin N, Comi GP (2007) Fas small interfering RNA reduces motoneuron death in amyotrophic lateral sclerosis mice. Ann Neurol 62:81-92.

Lomen-Hoerth C, Murphy J, Langmore S, Kramer JH, Olney RK, Miller B (2003) Are amyotrophic lateral sclerosis patients cognitively normal? Neurology 60:1094-1097.

Lowenberg M, Verhaar A, van den Blink B, ten Kate F, van Deventer S, Peppelenbosch M, Hommes D (2005) Specific inhibition of c-Raf activity by semapimod induces clinical remission in severe Crohn's disease. J Immunol 175:2293-2300.

Ludwig S, Hoffmeyer A, Goebeler M, Kilian K, Hafner H, Neufeld B, Han J, Rapp UR (1998) The stress inducer arsenite activates mitogen-activated protein kinases extracellular signal-regulated kinases 1 and 2 via a MAPK kinase 6/p38-dependent pathway. J Biol Chem 273:1917-1922.

Luo HR, Hattori H, Hossain MA, Hester L, Huang Y, Lee-Kwon W, Donowitz M, Nagata E, Snyder SH (2003) Akt as a mediator of cell death. Proc Natl Acad Sci U S A 100:11712-11717.

Luo Y, Shoemaker AR, Liu X, Woods KW, Thomas SA, de Jong R, Han EK, Li T, Stoll VS, Powlas JA, Oleksijew A, Mitten MJ, Shi Y, Guan R, McGonigal TP, Klinghofer V, Johnson EF, Leverson JD, Bouska JJ, Mamo M, Smith RA, Gramling-Evans EE, Zinker BA, Mika AK, Nguyen PT, Oltersdorf T, Rosenberg SH, Li Q, Giranda VL (2005) Potent and selective inhibitors of Akt kinases slow the progress of tumors in vivo. Mol Cancer Ther 4:977-986.

Mackay K, Mochly-Rosen D (1999) An inhibitor of p38 mitogen-activated protein kinase protects neonatal cardiac myocytes from ischemia. J Biol Chem 274:6272-6279.

Mackenzie IR, Bigio EH, Ince PG, Geser F, Neumann M, Cairns NJ, Kwong LK, Forman MS, Ravits J, Stewart H, Eisen A, McClusky L, Kretzschmar HA, Monoranu CM, Highley JR, Kirby J, Siddique T, Shaw PJ, Lee VM, Trojanowski JQ (2007) Pathological TDP-43 distinguishes sporadic amyotrophic lateral sclerosis from amyotrophic lateral sclerosis with SOD1 mutations. Ann Neurol 61:427-434.

MacKenzie TC, Kobinger GP, Louboutin JP, Radu A, Javazon EH, Sena-Esteves M, Wilson JM, Flake AW (2005) Transduction of satellite cells after prenatal intramuscular administration of lentiviral vectors. J Gene Med 7:50-58.

Maher P (1999) p38 mitogen-activated protein kinase activation is required for fibroblast growth factor-2-stimulated cell proliferation but not differentiation. J Biol Chem 274:17491-17498.

Majumder PK, Yeh JJ, George DJ, Febbo PG, Kum J, Xue Q, Bikoff R, Ma H, Kantoff PW, Golub TR, Loda M, Sellers WR (2003) Prostate intraepithelial neoplasia induced by prostate restricted Akt activation: the MPAKT model. Proc Natl Acad Sci U S A 100:7841-7846.

Malstrom S, Tili E, Kappes D, Ceci JD, Tsichlis PN (2001) Tumor induction by an Lck-MyrAkt transgene is delayed by mechanisms controlling the size of the thymus. Proc Natl Acad Sci U S A 98:14967-14972.

Manabe Y, Nagano I, Gazi MS, Murakami T, Shiote M, Shoji M, Kitagawa H, Setoguchi Y, Abe K (2002) Adenovirus-mediated gene transfer of glial cell line-derived neurotrophic factor prevents motor neuron loss of transgenic model mice for amyotrophic lateral sclerosis. Apoptosis 7:329-334.

Mangeot PE, Negre D, Dubois B, Winter AJ, Leissner P, Mehtali M, Kaiserlian D, Cosset FL, Darlix JL (2000) Development of minimal lentivirus vectors derived from simian immunodeficiency virus (SIVmac251) and their use for gene transfer into human dendritic cells. J Virol 74:8307-8315.

Mani N, Khaibullina A, Krum JM, Rosenstein JM (2005) Astrocyte growth effects of vascular endothelial growth factor (VEGF) application to perinatal neocortical explants: receptor mediation and signal transduction pathways. Exp Neurol 192:394-406.

Manilla P, Rebello T, Afable C, Lu X, Slepushkin V, Humeau LM, Schonely K, Ni Y, Binder GK, Levine BL, MacGregor RR, June CH, Dropulic B (2005) Regulatory considerations for novel gene therapy products: a review of the process leading to the first clinical lentiviral vector. Hum Gene Ther 16:17-25.

Manning BD, Cantley LC (2007) AKT/PKB signaling: navigating downstream. Cell 129:1261-1274.

Mantovani S, Garbelli S, Pasini A, Alimonti D, Perotti C, Melazzini M, Bendotti C, Mora G (2009) Immune system alterations in sporadic amyotrophic lateral sclerosis patients suggest an ongoing neuroinflammatory process. J Neuroimmunol 210:73-79.

Mao Z, Bonni A, Xia F, Nadal-Vicens M, Greenberg ME (1999) Neuronal activity-dependent cell survival mediated by transcription factor MEF2. Science 286:785-790.

Markevich NI, Tsyganov MA, Hoek JB, Kholodenko BN (2006) Long-range signaling by phosphoprotein waves arising from bistability in protein kinase cascades. Mol Syst Biol 2:61.

Martin N, Jaubert J, Gounon P, Salido E, Haase G, Szatanik M, Guenet JL (2002) A missense mutation in Tbce causes progressive motor neuronopathy in mice. Nat Genet 32:443-447.

Matsui T, Li L, Wu JC, Cook SA, Nagoshi T, Picard MH, Liao R, Rosenzweig A (2002) Phenotypic spectrum caused by transgenic overexpression of activated Akt in the heart. J Biol Chem 277:22896-22901.

Matsumoto A, Okada Y, Nakamichi M, Nakamura M, Toyama Y, Sobue G, Nagai M, Aoki M, Itoyama Y, Okano H (2006a) Disease progression of human SOD1 (G93A) transgenic ALS model rats. J Neurosci Res 83:119-133.

Matsumoto G, Kim S, Morimoto RI (2006b) Huntingtin and mutant SOD1 form aggregate structures with distinct molecular properties in human cells. J Biol Chem 281:4477-4485.

Matsumoto G, Stojanovic A, Holmberg CI, Kim S, Morimoto RI (2005) Structural properties and neuronal toxicity of amyotrophic lateral sclerosis-associated Cu/Zn superoxide dismutase 1 aggregates. J Cell Biol 171:75-85.

Matsuzawa A, Ichijo H (2001) Molecular mechanisms of the decision between life and death: regulation of apoptosis by apoptosis signal-regulating kinase 1. J Biochem 130:1-8.

Mazarakis ND, Azzouz M, Rohll JB, Ellard FM, Wilkes FJ, Olsen AL, Carter EE, Barber RD, Baban DF, Kingsman SM, Kingsman AJ, O'Malley K, Mitrophanous KA (2001) Rabies virus glycoprotein pseudotyping of lentiviral vectors enables retrograde axonal transport and access to the nervous system after peripheral delivery. Hum Mol Genet 10:2109-2121.

McGuire V, Longstreth WT, Jr., Koepsell TD, van Belle G (1996) Incidence of amyotrophic lateral sclerosis in three counties in western Washington state. Neurology 47:571-573.

Meister G, Tuschl T (2004) Mechanisms of gene silencing by double-stranded RNA. Nature 431:343-349.

Melani A, Gianfriddo M, Vannucchi MG, Cipriani S, Baraldi PG, Giovannini MG, Pedata F (2006) The selective A2A receptor antagonist SCH 58261 protects from neurological deficit, brain damage and activation of p38 MAPK in rat focal cerebral ischemia. Brain Res 1073-1074:470-480.

Mende I, Malstrom S, Tsichlis PN, Vogt PK, Aoki M (2001) Oncogenic transformation induced by membrane-targeted Akt2 and Akt3. Oncogene 20:4419-4423.

Mennini T, Bigini P, Ravizza T, Vezzani A, Calvaresi N, Tortarolo M, Bendotti C (2002) Expression of glutamate receptor subtypes in the spinal cord of control and mnd mice, a model of motor neuron disorder. J Neurosci Res 70:553-560.

Mentis GZ, Gravell M, Hamilton R, Shneider NA, O'Donovan MJ, Schubert M (2006) Transduction of motor neurons and muscle fibers by intramuscular injection of HIV-1-based vectors pseudotyped with select rabies virus glycoproteins. J Neurosci Methods 157:208-217.

Mercado PA, Ayala YM, Romano M, Buratti E, Baralle FE (2005) Depletion of TDP 43 overrides the need for exonic and intronic splicing enhancers in the human apoA-II gene. Nucleic Acids Res 33:6000-6010.

Messer A, Strominger NL, Mazurkiewicz JE (1987) Histopathology of the late-onset motor neuron degeneration (Mnd) mutant in the mouse. J Neurogenet 4:201-213.

Mi R, Chen W, Hoke A (2007) Pleiotrophin is a neurotrophic factor for spinal motor neurons. Proc Natl Acad Sci U S A 104:4664-4669.

Mielke K, Herdegen T (2000) JNK and p38 stresskinases--degenerative effectors of signal-transduction-cascades in the nervous system. Prog Neurobiol 61:45-60.

Migheli A, Piva R, Atzori C, Troost D, Schiffer D (1997) c-Jun, JNK/SAPK kinases and transcription factor NF-kappa B are selectively activated in astrocytes, but not motor neurons, in amyotrophic lateral sclerosis. J Neuropathol Exp Neurol 56:1314-1322.

Migheli A, Autilio-Gambetti L, Gambetti P, Mocellini C, Vigliani MC, Schiffer D (1990) Ubiquitinated filamentous inclusions in spinal cord of patients with motor neuron disease. Neurosci Lett 114:5-10.

Migheli A, Atzori C, Piva R, Tortarolo M, Girelli M, Schiffer D, Bendotti C (1999) Lack of apoptosis in mice with ALS. Nat Med 5:966-967.

Mika J, Osikowicz M, Rojewska E, Korostynski M, Wawrzczak-Bargiela A, Przewlocki R, Przewlocka B (2009) Differential activation of spinal microglial and astroglial cells in a mouse model of peripheral neuropathic pain. Eur J Pharmacol.

Milhorat TH, Clark RG, Hammock MK, McGrath PP (1970) Structural, ultrastructural, and permeability changes in the ependyma and surrounding brain favoring equilibration in progressive hydrocephalus. Arch Neurol 22:397-407.

Miller TM, Kim SH, Yamanaka K, Hester M, Umapathi P, Arnson H, Rizo L, Mendell JR, Gage FH, Cleveland DW, Kaspar BK (2006) Gene transfer demonstrates that muscle is not a primary target for non-cell-autonomous toxicity in familial amyotrophic lateral sclerosis. Proc Natl Acad Sci U S A 103:19546-19551.

Mitchell J, Paul P, Chen HJ, Morris A, Payling M, Falchi M, Habgood J, Panoutsou S, Winkler S, Tisato V, Hajitou A, Smith B, Vance C, Shaw C, Mazarakis ND, de Belleroche J Familial amyotrophic lateral sclerosis is associated with a mutation in D-amino acid oxidase. Proc Natl Acad Sci U S A 107:7556-7561.

Mitchell JD, Borasio GD (2007) Amyotrophic lateral sclerosis. Lancet 369:2031-2041.

Mitrophanous K, Yoon S, Rohll J, Patil D, Wilkes F, Kim V, Kingsman S, Kingsman A, Mazarakis N (1999) Stable gene transfer to the nervous system using a non-primate lentiviral vector. Gene Ther 6:1808-1818.

Mitsumoto H, Bradley WG (1982) Murine motor neuron disease (the wobbler mouse): degeneration and regeneration of the lower motor neuron. Brain 105 (Pt 4):811-834.

Mitsumoto H CD, Pioro EP (1998) Amyotrophic Lateral Sclerosis. New
York: Oxford Univ. Press.

Mitta B, Rimann M, Fussenegger M (2005) Detailed design and comparative analysis of protocols for optimized production of high-performance HIV-1-derived lentiviral particles. Metab Eng 7:426-436.

Miyoshi H, Blomer U, Takahashi M, Gage FH, Verma IM (1998) Development of a self-inactivating lentivirus vector. J Virol 72:8150-8157.

Morooka T, Nishida E (1998) Requirement of p38 mitogen-activated protein kinase for neuronal differentiation in PC12 cells. J Biol Chem 273:24285-24288.

Mourelatos Z, Hirano A, Rosenquist AC, Gonatas NK (1994) Fragmentation of the Golgi apparatus of motor neurons in amyotrophic lateral sclerosis (ALS). Clinical studies in ALS of Guam and experimental studies in deafferented neurons and in beta,beta'-iminodipropionitrile axonopathy. Am J Pathol 144:1288-1300.

Mourelatos Z, Adler H, Hirano A, Donnenfeld H, Gonatas JO, Gonatas NK (1990) Fragmentation of the Golgi apparatus of motor neurons in amyotrophic lateral

sclerosis revealed by organelle-specific antibodies. Proc Natl Acad Sci U S A 87:4393-4395.
Munch C, Rosenbohm A, Sperfeld AD, Uttner I, Reske S, Krause BJ, Sedlmeier R, Meyer T, Hanemann CO, Stumm G, Ludolph AC (2005) Heterozygous R1101K mutation of the DCTN1 gene in a family with ALS and FTD. Ann Neurol 58:777-780.
Murakami T, Warita H, Hayashi T, Sato K, Manabe Y, Mizuno S, Yamane K, Abe K (2001) A novel SOD1 gene mutation in familial ALS with low penetrance in females. J Neurol Sci 189:45-47.
Murashov AK, Ul Haq I, Hill C, Park E, Smith M, Wang X, Goldberg DJ, Wolgemuth DJ (2001) Crosstalk between p38, Hsp25 and Akt in spinal motor neurons after sciatic nerve injury. Brain Res Mol Brain Res 93:199-208.
Murphy JM, Henry RG, Langmore S, Kramer JH, Miller BL, Lomen-Hoerth C (2007) Continuum of frontal lobe impairment in amyotrophic lateral sclerosis. Arch Neurol 64:530-534.
Murray LM, Thomson D, Conklin A, Wishart TM, Gillingwater TH (2008) Loss of translation elongation factor (eEF1A2) expression in vivo differentiates between Wallerian degeneration and dying-back neuronal pathology. J Anat 213:633-645.
Muthumani K, Choo AY, Hwang DS, Premkumar A, Dayes NS, Harris C, Green DR, Wadsworth SA, Siekierka JJ, Weiner DB (2005) HIV-1 Nef-induced FasL induction and bystander killing requires p38 MAPK activation. Blood 106:2059-2068.
Naciff JM, Behbehani MM, Misawa H, Dedman JR (1999) Identification and transgenic analysis of a murine promoter that targets cholinergic neuron expression. J Neurochem 72:17-28.
Nagai M, Re DB, Nagata T, Chalazonitis A, Jessell TM, Wichterle H, Przedborski S (2007) Astrocytes expressing ALS-linked mutated SOD1 release factors selectively toxic to motor neurons. Nat Neurosci 10:615-622.
Nagai M, Aoki M, Miyoshi I, Kato M, Pasinelli P, Kasai N, Brown RH, Jr., Itoyama Y (2001) Rats expressing human cytosolic copper-zinc superoxide dismutase transgenes with amyotrophic lateral sclerosis: associated mutations develop motor neuron disease. J Neurosci 21:9246-9254.
Nagano I, Ilieva H, Shiote M, Murakami T, Yokoyama M, Shoji M, Abe K (2005) Therapeutic benefit of intrathecal injection of insulin-like growth factor-1 in a mouse model of Amyotrophic Lateral Sclerosis. J Neurol Sci 235:61-68.
Nakamura S, Kawamoto Y, Nakano S, Ikemoto A, Akiguchi I, Kimura J (1997) Cyclin-dependent kinase 5 in Lewy body-like inclusions in anterior horn cells of a patient with sporadic amyotrophic lateral sclerosis. Neurology 48:267-270.
Nakano I, Hirano A (1987) Atrophic cell processes of large motor neurons in the anterior horn in amyotrophic lateral sclerosis: observation with silver impregnation method. J Neuropathol Exp Neurol 46:40-49.
Nakano T, Windrem M, Zappavigna V, Goldman SA (2005) Identification of a conserved 125 base-pair Hb9 enhancer that specifies gene expression to spinal motor neurons. Dev Biol 283:474-485.
Naldini L, Blomer U, Gage FH, Trono D, Verma IM (1996a) Efficient transfer, integration, and sustained long-term expression of the transgene in adult rat brains injected with a lentiviral vector. Proc Natl Acad Sci U S A 93:11382-11388.
Naldini L, Blomer U, Gallay P, Ory D, Mulligan R, Gage FH, Verma IM, Trono D (1996b) In vivo gene delivery and stable transduction of nondividing cells by a lentiviral vector. Science 272:263-267.
Namikawa K, Honma M, Abe K, Takeda M, Mansur K, Obata T, Miwa A, Okado H, Kiyama H (2000) Akt/protein kinase B prevents injury-induced motoneuron death and accelerates axonal regeneration. J Neurosci 20:2875-2886.
Naviaux RK, Costanzi E, Haas M, Verma IM (1996) The pCL vector system: rapid production of helper-free, high-titer, recombinant retroviruses. J Virol 70:5701-5705.
Nawa M, Kanekura K, Hashimoto Y, Aiso S, Matsuoka M (2008) A novel Akt/PKB-interacting protein promotes cell adhesion and inhibits familial amyotrophic lateral sclerosis-linked mutant SOD1-induced neuronal death via inhibition of PP2A-mediated dephosphorylation of Akt/PKB. Cell Signal 20:493-505.
Neumann J, Gunzer M, Gutzeit HO, Ullrich O, Reymann KG, Dinkel K (2006a) Microglia provide neuroprotection after ischemia. Faseb J 20:714-716.
Neumann M, Sampathu DM, Kwong LK, Truax AC, Micsenyi MC, Chou TT, Bruce J, Schuck T, Grossman M, Clark CM, McCluskey LF, Miller BL, Masliah E,

Mackenzie IR, Feldman H, Feiden W, Kretzschmar HA, Trojanowski JQ, Lee VM (2006b) Ubiquitinated TDP-43 in frontotemporal lobar degeneration and amyotrophic lateral sclerosis. Science 314:130-133.

Newbery HJ, Gillingwater TH, Dharmasaroja P, Peters J, Wharton SB, Thomson D, Ribchester RR, Abbott CM (2005) Progressive loss of motor neuron function in wasted mice: effects of a spontaneous null mutation in the gene for the eEF1 A2 translation factor. J Neuropathol Exp Neurol 64:295-303.

Newton AC (2003) Regulation of the ABC kinases by phosphorylation: protein kinase C as a paradigm. Biochem J 370:361-371.

Nguyen MD, D'Aigle T, Gowing G, Julien JP, Rivest S (2004) Exacerbation of motor neuron disease by chronic stimulation of innate immunity in a mouse model of amyotrophic lateral sclerosis. J Neurosci 24:1340-1349.

Nishimura AL, Mitne-Neto M, Silva HC, Richieri-Costa A, Middleton S, Cascio D, Kok F, Oliveira JR, Gillingwater T, Webb J, Skehel P, Zatz M (2004) A mutation in the vesicle-trafficking protein VAPB causes late-onset spinal muscular atrophy and amyotrophic lateral sclerosis. Am J Hum Genet 75:822-831.

Nishitoh H, Kadowaki H, Nagai A, Maruyama T, Yokota T, Fukutomi H, Noguchi T, Matsuzawa A, Takeda K, Ichijo H (2008) ALS-linked mutant SOD1 induces ER stress- and ASK1-dependent motor neuron death by targeting Derlin-1. Genes Dev 22:1451-1464.

Ogura M, Kitamura M (1998) Oxidant stress incites spreading of macrophages via extracellular signal-regulated kinases and p38 mitogen-activated protein kinase. J Immunol 161:3569-3574.

Ohta Y, Kamiya T, Nagai M, Nagata T, Morimoto N, Miyazaki K, Murakami T, Kurata T, Takehisa Y, Ikeda Y, Asoh S, Ohta S, Abe K (2008) Therapeutic benefits of intrathecal protein therapy in a mouse model of amyotrophic lateral sclerosis. J Neurosci Res 86:3028-3037.

Okamoto K, Mizuno Y, Fujita Y (2008) Bunina bodies in amyotrophic lateral sclerosis. Neuropathology 28:109-115.

Okamoto K, Hirai S, Amari M, Watanabe M, Sakurai A (1993) Bunina bodies in amyotrophic lateral sclerosis immunostained with rabbit anti-cystatin C serum. Neurosci Lett 162:125-128.

Okamoto S, Krainc D, Sherman K, Lipton SA (2000) Antiapoptotic role of the p38 mitogen-activated protein kinase-myocyte enhancer factor 2 transcription factor pathway during neuronal differentiation. Proc Natl Acad Sci U S A 97:7561-7566.

O'Keefe SJ, Mudgett JS, Cupo S, Parsons JN, Chartrain NA, Fitzgerald C, Chen SL, Lowitz K, Rasa C, Visco D, Luell S, Carballo-Jane E, Owens K, Zaller DM (2007) Chemical genetics define the roles of p38alpha and p38beta in acute and chronic inflammation. J Biol Chem 282:34663-34671.

Oosthuyse B, Moons L, Storkebaum E, Beck H, Nuyens D, Brusselmans K, Van Dorpe J, Hellings P, Gorselink M, Heymans S, Theilmeier G, Dewerchin M, Laudenbach V, Vermylen P, Raat H, Acker T, Vleminckx V, Van Den Bosch L, Cashman N, Fujisawa H, Drost MR, Sciot R, Bruyninckx F, Hicklin DJ, Ince C, Gressens P, Lupu F, Plate KH, Robberecht W, Herbert JM, Collen D, Carmeliet P (2001) Deletion of the hypoxia-response element in the vascular endothelial growth factor promoter causes motor neuron degeneration. Nat Genet 28:131-138.

Orrell RW (2000) Amyotrophic lateral sclerosis: copper/zinc superoxide dismutase (SOD1) gene mutations. Neuromuscul Disord 10:63-68.

Otomo A, Hadano S, Okada T, Mizumura H, Kunita R, Nishijima H, Showguchi-Miyata J, Yanagisawa Y, Kohiki E, Suga E, Yasuda M, Osuga H, Nishimoto T, Narumiya S, Ikeda JE (2003) ALS2, a novel guanine nucleotide exchange factor for the small GTPase Rab5, is implicated in endosomal dynamics. Hum Mol Genet 12:1671-1687.

Oyanagi K, Wada M (1999) Neuropathology of parkinsonism-dementia complex and amyotrophic lateral sclerosis of Guam: an update. J Neurol 246 Suppl 2:II19-27.

Oyanagi K, Ikuta F, Horikawa Y (1989) Evidence for sequential degeneration of the neurons in the intermediate zone of the spinal cord in amyotrophic lateral sclerosis: a topographic and quantitative investigation. Acta Neuropathol 77:343-349.

Page KA, Landau NR, Littman DR (1990) Construction and use of a human immunodeficiency virus vector for analysis of virus infectivity. J Virol 64:5270-5276.

Palmer JA, Branston RH, Lilley CE, Robinson MJ, Groutsi F, Smith J, Latchman DS, Coffin RS (2000) Development and optimization of herpes simplex virus vectors for multiple long-term gene delivery to the peripheral nervous system. J Virol 74:5604-5618.

Pasinelli P, Belford ME, Lennon N, Bacskai BJ, Hyman BT, Trotti D, Brown RH, Jr. (2004) Amyotrophic lateral sclerosis-associated SOD1 mutant proteins bind and aggregate with Bcl-2 in spinal cord mitochondria. Neuron 43:19-30.

Peng XD, Xu PZ, Chen ML, Hahn-Windgassen A, Skeen J, Jacobs J, Sundararajan D, Chen WS, Crawford SE, Coleman KG, Hay N (2003) Dwarfism, impaired skin development, skeletal muscle atrophy, delayed bone development, and impeded adipogenesis in mice lacking Akt1 and Akt2. Genes Dev 17:1352-1365.

Perdiguero E, Ruiz-Bonilla V, Gresh L, Hui L, Ballestar E, Sousa-Victor P, Baeza-Raja B, Jardi M, Bosch-Comas A, Esteller M, Caelles C, Serrano AL, Wagner EF, Munoz-Canoves P (2007) Genetic analysis of p38 MAP kinases in myogenesis: fundamental role of p38alpha in abrogating myoblast proliferation. Embo J 26:1245-1256.

Perlson E, Hanz S, Ben-Yaakov K, Segal-Ruder Y, Seger R, Fainzilber M (2005) Vimentin-dependent spatial translocation of an activated MAP kinase in injured nerve. Neuron 45:715-726.

Persad S, Attwell S, Gray V, Mawji N, Deng JT, Leung D, Yan J, Sanghera J, Walsh MP, Dedhar S (2001) Regulation of protein kinase B/Akt-serine 473 phosphorylation by integrin-linked kinase: critical roles for kinase activity and amino acids arginine 211 and serine 343. J Biol Chem 276:27462-27469.

Petiot A, Ogier-Denis E, Blommaart EF, Meijer AJ, Codogno P (2000) Distinct classes of phosphatidylinositol 3'-kinases are involved in signaling pathways that control macroautophagy in HT-29 cells. J Biol Chem 275:992-998.

Peviani M, Cheroni C, Troglio F, Quarto M, Pelicci G, Bendotti C (2007) Lack of changes in the PI3K/AKT survival pathway in the spinal cord motor neurons of a mouse model of familial amyotrophic lateral sclerosis. Mol Cell Neurosci 34:592-602.

Piao CS, Che Y, Han PL, Lee JK (2002) Delayed and differential induction of p38 MAPK isoforms in microglia and astrocytes in the brain after transient global ischemia. Brain Res Mol Brain Res 107:137-144.

Piao CS, Kim JB, Han PL, Lee JK (2003) Administration of the p38 MAPK inhibitor SB203580 affords brain protection with a wide therapeutic window against focal ischemic insult. J Neurosci Res 73:537-544.

Pickering M, Cumiskey D, O'Connor JJ (2005) Actions of TNF-alpha on glutamatergic synaptic transmission in the central nervous system. Exp Physiol 90:663-670.

Piva R, Chiarle R, Manazza AD, Taulli R, Simmons W, Ambrogio C, D'Escamard V, Pellegrino E, Ponzetto C, Palestro G, Inghirami G (2006) Ablation of oncogenic ALK is a viable therapeutic approach for anaplastic large-cell lymphomas. Blood 107:689-697.

Plaitakis A, Caroscio JT (1987) Abnormal glutamate metabolism in amyotrophic lateral sclerosis. Ann Neurol 22:575-579.

Pramatarova A, Laganiere J, Roussel J, Brisebois K, Rouleau GA (2001) Neuron-specific expression of mutant superoxide dismutase 1 in transgenic mice does not lead to motor impairment. J Neurosci 21:3369-3374.

Prosch S, Stein J, Staak K, Liebenthal C, Volk HD, Kruger DH (1996) Inactivation of the very strong HCMV immediate early promoter by DNA CpG methylation in vitro. Biol Chem Hoppe Seyler 377:195-201.

Puls I, Jonnakuty C, LaMonte BH, Holzbaur EL, Tokito M, Mann E, Floeter MK, Bidus K, Drayna D, Oh SJ, Brown RH, Jr., Ludlow CL, Fischbeck KH (2003) Mutant dynactin in motor neuron disease. Nat Genet 33:455-456.

Pun S, Santos AF, Saxena S, Xu L, Caroni P (2006) Selective vulnerability and pruning of phasic motoneuron axons in motoneuron disease alleviated by CNTF. Nat Neurosci 9:408-419.

Pyra T, Hui B, Hanstock C, Concha L, Wong JC, Beaulieu C, Johnston W, Kalra S (2009) Combined structural and neurochemical evaluation of the corticospinal tract in amyotrophic lateral sclerosis. Amyotroph Lateral Scler:1-9.

Raibon E, Todd LM, Moller T (2008) Glial cells in ALS: the missing link? Phys Med Rehabil Clin N Am 19:441-459, vii-viii.

Raimondi A, Mangolini A, Rizzardini M, Tartari S, Massari S, Bendotti C, Francolini M, Borgese N, Cantoni L, Pietrini G (2006) Cell culture models to investigate the

selective vulnerability of motoneuronal mitochondria to familial ALS-linked G93ASOD1. Eur J Neurosci 24:387-399.
Ralph GS, Radcliffe PA, Day DM, Carthy JM, Leroux MA, Lee DC, Wong LF, Bilsland LG, Greensmith L, Kingsman SM, Mitrophanous KA, Mazarakis ND, Azzouz M (2005) Silencing mutant SOD1 using RNAi protects against neurodegeneration and extends survival in an ALS model. Nat Med 11:429-433.
Ranta S, Zhang Y, Ross B, Lonka L, Takkunen E, Messer A, Sharp J, Wheeler R, Kusumi K, Mole S, Liu W, Soares MB, Bonaldo MF, Hirvasniemi A, de la Chapelle A, Gilliam TC, Lehesjoki AE (1999) The neuronal ceroid lipofuscinoses in human EPMR and mnd mutant mice are associated with mutations in CLN8. Nat Genet 23:233-236.
Raoul C, Henderson CE, Pettmann B (1999) Programmed cell death of embryonic motoneurons triggered through the Fas death receptor. J Cell Biol 147:1049-1062.
Raoul C, Barthelemy C, Couzinet A, Hancock D, Pettmann B, Hueber AO (2005a) Expression of a dominant negative form of Daxx in vivo rescues motoneurons from Fas (CD95)-induced cell death. J Neurobiol 62:178-188.
Raoul C, Estevez AG, Nishimune H, Cleveland DW, deLapeyriere O, Henderson CE, Haase G, Pettmann B (2002) Motoneuron death triggered by a specific pathway downstream of Fas. potentiation by ALS-linked SOD1 mutations. Neuron 35:1067-1083.
Raoul C, Abbas-Terki T, Bensadoun JC, Guillot S, Haase G, Szulc J, Henderson CE, Aebischer P (2005b) Lentiviral-mediated silencing of SOD1 through RNA interference retards disease onset and progression in a mouse model of ALS. Nat Med 11:423-428.
Raoul C, Buhler E, Sadeghi C, Jacquier A, Aebischer P, Pettmann B, Henderson CE, Haase G (2006) Chronic activation in presymptomatic amyotrophic lateral sclerosis (ALS) mice of a feedback loop involving Fas, Daxx, and FasL. Proc Natl Acad Sci U S A 103:6007-6012.
Ravikumar B, Acevedo-Arozena A, Imarisio S, Berger Z, Vacher C, O'Kane CJ, Brown SD, Rubinsztein DC (2005) Dynein mutations impair autophagic clearance of aggregate-prone proteins. Nat Genet 37:771-776.
Ray SS, Nowak RJ, Strokovich K, Brown RH, Jr., Walz T, Lansbury PT, Jr. (2004) An intersubunit disulfide bond prevents in vitro aggregation of a superoxide dismutase-1 mutant linked to familial amytrophic lateral sclerosis. Biochemistry 43:4899-4905.
Raynor EM, Shefner JM (1994) Recurrent inhibition is decreased in patients with amyotrophic lateral sclerosis. Neurology 44:2148-2153.
Reaume AG, Elliott JL, Hoffman EK, Kowall NW, Ferrante RJ, Siwek DF, Wilcox HM, Flood DG, Beal MF, Brown RH, Jr., Scott RW, Snider WD (1996) Motor neurons in Cu/Zn superoxide dismutase-deficient mice develop normally but exhibit enhanced cell death after axonal injury. Nat Genet 13:43-47.
Reuveni H, Livnah N, Geiger T, Klein S, Ohne O, Cohen I, Benhar M, Gellerman G, Levitzki A (2002) Toward a PKB inhibitor: modification of a selective PKA inhibitor by rational design. Biochemistry 41:10304-10314.
Richard E, Douillard-Guilloux G, Batista L, Caillaud C (2008) Correction of glycogenosis type 2 by muscle-specific lentiviral vector. In Vitro Cell Dev Biol Anim 44:397-406.
Rippon GA, Scarmeas N, Gordon PH, Murphy PL, Albert SM, Mitsumoto H, Marder K, Rowland LP, Stern Y (2006) An observational study of cognitive impairment in amyotrophic lateral sclerosis. Arch Neurol 63:345-352.
Ripps ME, Huntley GW, Hof PR, Morrison JH, Gordon JW (1995) Transgenic mice expressing an altered murine superoxide dismutase gene provide an animal model of amyotrophic lateral sclerosis. Proc Natl Acad Sci U S A 92:689-693.
Robberecht W, Aguirre T, Van den Bosch L, Tilkin P, Cassiman JJ, Matthijs G (1996) D90A heterozygosity in the SOD1 gene is associated with familial and apparently sporadic amyotrophic lateral sclerosis. Neurology 47:1336-1339.
Robert H. Brown VM, Michael Swash (2000) Amyotrophic lateral sclerosis: Martin Dunitz.
Robertson J, Sanelli T, Xiao S, Yang W, Horne P, Hammond R, Pioro EP, Strong MJ (2007) Lack of TDP-43 abnormalities in mutant SOD1 transgenic mice shows disparity with ALS. Neurosci Lett 420:128-132.
Rodgers EE, Theibert AB (2002) Functions of PI 3-kinase in development of the nervous system. Int J Dev Neurosci 20:187-197.

Rodriguez JA, Valentine JS, Eggers DK, Roe JA, Tiwari A, Brown RH, Jr., Hayward LJ (2002) Familial amyotrophic lateral sclerosis-associated mutations decrease the thermal stability of distinctly metallated species of human copper/zinc superoxide dismutase. J Biol Chem 277:15932-15937.

Romanelli RJ, Wood TL (2008) Directing traffic in neural cells: determinants of receptor tyrosine kinase localization and cellular responses. J Neurochem.

Rosen DR, Siddique T, Patterson D, Figlewicz DA, Sapp P, Hentati A, Donaldson D, Goto J, O'Regan JP, Deng HX, et al. (1993) Mutations in Cu/Zn superoxide dismutase gene are associated with familial amyotrophic lateral sclerosis. Nature 362:59-62.

Ross CA, Poirier MA (2005) Opinion: What is the role of protein aggregation in neurodegeneration? Nat Rev Mol Cell Biol 6:891-898.

Rothstein JD, Jin L, Dykes-Hoberg M, Kuncl RW (1993) Chronic inhibition of glutamate uptake produces a model of slow neurotoxicity. Proc Natl Acad Sci U S A 90:6591-6595.

Rothstein JD, Van Kammen M, Levey AI, Martin LJ, Kuncl RW (1995) Selective loss of glial glutamate transporter GLT-1 in amyotrophic lateral sclerosis. Ann Neurol 38:73-84.

Rothstein JD, Kuncl R, Chaudhry V, Clawson L, Cornblath DR, Coyle JT, Drachman DB (1991) Excitatory amino acids in amyotrophic lateral sclerosis: an update. Ann Neurol 30:224-225.

Rouaux C, Panteleeva I, Rene F, Gonzalez de Aguilar JL, Echaniz-Laguna A, Dupuis L, Menger Y, Boutillier AL, Loeffler JP (2007) Sodium valproate exerts neuroprotective effects in vivo through CREB-binding protein-dependent mechanisms but does not improve survival in an amyotrophic lateral sclerosis mouse model. J Neurosci 27:5535-5545.

Rousseau S, Houle F, Landry J, Huot J (1997) p38 MAP kinase activation by vascular endothelial growth factor mediates actin reorganization and cell migration in human endothelial cells. Oncogene 15:2169-2177.

Roux PP, Blenis J (2004) ERK and p38 MAPK-activated protein kinases: a family of protein kinases with diverse biological functions. Microbiol Mol Biol Rev 68:320-344.

Ruddy DM, Parton MJ, Al-Chalabi A, Lewis CM, Vance C, Smith BN, Leigh PN, Powell JF, Siddique T, Meyjes EP, Baas F, de Jong V, Shaw CE (2003) Two families with familial amyotrophic lateral sclerosis are linked to a novel locus on chromosome 16q. Am J Hum Genet 73:390-396.

Rutherford AC, Traer C, Wassmer T, Pattni K, Bujny MV, Carlton JG, Stenmark H, Cullen PJ (2006) The mammalian phosphatidylinositol 3-phosphate 5-kinase (PIKfyve) regulates endosome-to-TGN retrograde transport. J Cell Sci 119:3944-3957.

Sabio G, Arthur JS, Kuma Y, Peggie M, Carr J, Murray-Tait V, Centeno F, Goedert M, Morrice NA, Cuenda A (2005) p38gamma regulates the localisation of SAP97 in the cytoskeleton by modulating its interaction with GKAP. Embo J 24:1134-1145.

Sagot Y, Rosse T, Vejsada R, Perrelet D, Kato AC (1998) Differential effects of neurotrophic factors on motoneuron retrograde labeling in a murine model of motoneuron disease. J Neurosci 18:1132-1141.

Sakurai M, Hayashi T, Abe K, Itoyuama Y, Tabayashi K (2001) Induction of phosphatidylinositol 3-kinase and serine-threonine kinase-like immunoreactivity in rabbit spinal cord after transient ischemia. Neurosci Lett 302:17-20.

Sale EM, Sale GJ (2008) Protein kinase B: signalling roles and therapeutic targeting. Cell Mol Life Sci 65:113-127.

Sale EM, Hodgkinson CP, Jones NP, Sale GJ (2006) A new strategy for studying protein kinase B and its three isoforms. Role of protein kinase B in phosphorylating glycogen synthase kinase-3, tuberin, WNK1, and ATP citrate lyase. Biochemistry 45:213-223.

Salvador JM, Mittelstadt PR, Guszczynski T, Copeland TD, Yamaguchi H, Appella E, Fornace AJ, Jr., Ashwell JD (2005) Alternative p38 activation pathway mediated by T cell receptor-proximal tyrosine kinases. Nat Immunol 6:390-395.

Sapp PC, Hosler BA, McKenna-Yasek D, Chin W, Gann A, Genise H, Gorenstein J, Huang M, Sailer W, Scheffler M, Valesky M, Haines JL, Pericak-Vance M, Siddique T, Horvitz HR, Brown RH, Jr. (2003) Identification of two novel loci for dominantly inherited familial amyotrophic lateral sclerosis. Am J Hum Genet 73:397-403.

Sarbassov DD, Guertin DA, Ali SM, Sabatini DM (2005) Phosphorylation and regulation of Akt/PKB by the rictor-mTOR complex. Science 307:1098-1101.
Sasabe J, Chiba T, Yamada M, Okamoto K, Nishimoto I, Matsuoka M, Aiso S (2007) D-serine is a key determinant of glutamate toxicity in amyotrophic lateral sclerosis. Embo J 26:4149-4159.
Sasaki S, Maruyama S (1991) Immunocytochemical and ultrastructural studies of hyaline inclusions in sporadic motor neuron disease. Acta Neuropathol 82:295-301.
Sasaki S, Maruyama S (1993) A fine structural study of Onuf's nucleus in sporadic amyotrophic lateral sclerosis. J Neurol Sci 119:28-37.
Sasaki S, Iwata M (1996) Synaptic loss in anterior horn neurons in lower motor neuron disease. Acta Neuropathol 91:416-421.
Sato T, Nakanishi T, Yamamoto Y, Andersen PM, Ogawa Y, Fukada K, Zhou Z, Aoike F, Sugai F, Nagano S, Hirata S, Ogawa M, Nakano R, Ohi T, Kato T, Nakagawa M, Hamasaki T, Shimizu A, Sakoda S (2005) Rapid disease progression correlates with instability of mutant SOD1 in familial ALS. Neurology 65:1954-1957.
Sato-Harada R, Okabe S, Umeyama T, Kanai Y, Hirokawa N (1996) Microtubule-associated proteins regulate microtubule function as the track for intracellular membrane organelle transports. Cell Struct Funct 21:283-295.
Sau D, De Biasi S, Vitellaro-Zuccarello L, Riso P, Guarnieri S, Porrini M, Simeoni S, Crippa V, Onesto E, Palazzolo I, Rusmini P, Bolzoni E, Bendotti C, Poletti A (2007) Mutation of SOD1 in ALS: a gain of a loss of function. Hum Mol Genet 16:1604-1618.
Saudou F, Finkbeiner S, Devys D, Greenberg ME (1998) Huntingtin acts in the nucleus to induce apoptosis but death does not correlate with the formation of intranuclear inclusions. Cell 95:55-66.
Scheid MP, Woodgett JR (2003) Unravelling the activation mechanisms of protein kinase B/Akt. FEBS Lett 546:108-112.
Scherer SS, Xu YT, Messing A, Willecke K, Fischbeck KH, Jeng LJ (2005) Transgenic expression of human connexin32 in myelinating Schwann cells prevents demyelination in connexin32-null mice. J Neurosci 25:1550-1559.
Schmalbruch H, Jensen HJ, Bjaerg M, Kamieniecka Z, Kurland L (1991) A new mouse mutant with progressive motor neuronopathy. J Neuropathol Exp Neurol 50:192-204.
Schmechel DE, Brightman MW, Marangos PJ (1980) Neurons switch from non-neuronal enolase to neuron-specific enolase during differentiation. Brain Res 190:195-214.
Schmitt-John T, Drepper C, Mussmann A, Hahn P, Kuhlmann M, Thiel C, Hafner M, Lengeling A, Heimann P, Jones JM, Meisler MH, Jockusch H (2005) Mutation of Vps54 causes motor neuron disease and defective spermiogenesis in the wobbler mouse. Nat Genet 37:1213-1215.
Schnell L, Fearn S, Klassen H, Schwab ME, Perry VH (1999) Acute inflammatory responses to mechanical lesions in the CNS: differences between brain and spinal cord. Eur J Neurosci 11:3648-3658.
Schnell T, Foley P, Wirth M, Munch J, Uberla K (2000) Development of a self-inactivating, minimal lentivirus vector based on simian immunodeficiency virus. Hum Gene Ther 11:439-447.
Schochet SS, Jr., Hardman JM, Ladewig PP, Earle KM (1969) Intraneuronal conglomerates in sporadic motor neuron disease. A light and electron microscopic study. Arch Neurol 20:548-553.
Schreiber H, Gaigalat T, Wiedemuth-Catrinescu U, Graf M, Uttner I, Muche R, Ludolph AC (2005) Cognitive function in bulbar- and spinal-onset amyotrophic lateral sclerosis. A longitudinal study in 52 patients. J Neurol 252:772-781.
Schwertfeger KL, McManaman JL, Palmer CA, Neville MC, Anderson SM (2003) Expression of constitutively activated Akt in the mammary gland leads to excess lipid synthesis during pregnancy and lactation. J Lipid Res 44:1100-1112.
Seimon TA, Wang Y, Han S, Senokuchi T, Schrijvers DM, Kuriakose G, Tall AR, Tabas IA (2009) Macrophage deficiency of p38alpha MAPK promotes apoptosis and plaque necrosis in advanced atherosclerotic lesions in mice. J Clin Invest 119:886-898.
Sekine Y, Takeda K, Ichijo H (2006) The ASK1-MAP kinase signaling in ER stress and neurodegenerative diseases. Curr Mol Med 6:87-97.

Sena-Esteves M, Tebbets JC, Steffens S, Crombleholme T, Flake AW (2004) Optimized large-scale production of high titer lentivirus vector pseudotypes. J Virol Methods 122:131-139.
Shan X, Vocadlo D, Krieger C (2009) Mislocalization of TDP-43 in the G93A mutant SOD1 transgenic mouse model of ALS. Neurosci Lett 458:70-74.
Shaw PJ, Ince PG, Falkous G, Mantle D (1995a) Oxidative damage to protein in sporadic motor neuron disease spinal cord. Ann Neurol 38:691-695.
Shaw PJ, Forrest V, Ince PG, Richardson JP, Wastell HJ (1995b) CSF and plasma amino acid levels in motor neuron disease: elevation of CSF glutamate in a subset of patients. Neurodegeneration 4:209-216.
Shibata M, Yamawaki T, Sasaki T, Hattori H, Hamada J, Fukuuchi Y, Okano H, Miura M (2002) Upregulation of Akt phosphorylation at the early stage of middle cerebral artery occlusion in mice. Brain Res 942:1-10.
Shibata N (2001) Transgenic mouse model for familial amyotrophic lateral sclerosis with superoxide dismutase-1 mutation. Neuropathology 21:82-92.
Siddique T, Hentati A (1995) Familial amyotrophic lateral sclerosis. Clin Neurosci 3:338-347.
Siegel A, Albers, Fisher, Uhler (1999) Basic Neurochemistry, Molecular, Cellular and Medical Aspects: Lippincott Williams and Wilkins.
Siklos L, Engelhardt J, Harati Y, Smith RG, Joo F, Appel SH (1996) Ultrastructural evidence for altered calcium in motor nerve terminals in amyotropic lateral sclerosis. Ann Neurol 39:203-216.
Siolas D, Lerner C, Burchard J, Ge W, Linsley PS, Paddison PJ, Hannon GJ, Cleary MA (2005) Synthetic shRNAs as potent RNAi triggers. Nat Biotechnol 23:227-231.
Sitaraman SV, Hoteit M, Gewirtz AT (2003) Semapimod. Cytokine. Curr Opin Investig Drugs 4:1363-1368.
Snove O, Jr., Rossi JJ (2006) Expressing short hairpin RNAs in vivo. Nat Methods 3:689-695.
Sobue G, Hashizume Y, Yasuda T, Mukai E, Kumagai T, Mitsuma T, Trojanowski JQ (1990) Phosphorylated high molecular weight neurofilament protein in lower motor neurons in amyotrophic lateral sclerosis and other neurodegenerative diseases involving ventral horn cells. Acta Neuropathol 79:402-408.
Soler RM, Egea J, Mintenig GM, Sanz-Rodriguez C, Iglesias M, Comella JX (1998) Calmodulin is involved in membrane depolarization-mediated survival of motoneurons by phosphatidylinositol-3 kinase- and MAPK-independent pathways. J Neurosci 18:1230-1239.
Son M, Puttaparthi K, Kawamata H, Rajendran B, Boyer PJ, Manfredi G, Elliott JL (2007) Overexpression of CCS in G93A-SOD1 mice leads to accelerated neurological deficits with severe mitochondrial pathology. Proc Natl Acad Sci U S A 104:6072-6077.
Soneoka Y, Cannon PM, Ramsdale EE, Griffiths JC, Romano G, Kingsman SM, Kingsman AJ (1995) A transient three-plasmid expression system for the production of high titer retroviral vectors. Nucleic Acids Res 23:628-633.
Soraru G, D'Ascenzo C, Nicolao P, Volpe M, Martignago S, Palmieri A, Romeo V, Koutsikos K, Piccione F, Cima V, Pegoraro E, Angelini C (2008) Muscle histopathology in upper motor neuron-dominant amyotrophic lateral sclerosis. Amyotroph Lateral Scler 9:287-293.
Spalloni A, Pascucci T, Albo F, Ferrari F, Puglisi-Allegra S, Zona C, Bernardi G, Longone P (2004) Altered vulnerability to kainate excitotoxicity of transgenic-Cu/Zn SOD1 neurones. Neuroreport 15:2477-2480.
Sreedharan J, Blair IP, Tripathi VB, Hu X, Vance C, Rogelj B, Ackerley S, Durnall JC, Williams KL, Buratti E, Baralle F, de Belleroche J, Mitchell JD, Leigh PN, Al-Chalabi A, Miller CC, Nicholson G, Shaw CE (2008) TDP-43 mutations in familial and sporadic amyotrophic lateral sclerosis. Science 319:1668-1672.
Steen E, Terry BM, Rivera EJ, Cannon JL, Neely TR, Tavares R, Xu XJ, Wands JR, de la Monte SM (2005) Impaired insulin and insulin-like growth factor expression and signaling mechanisms in Alzheimer's disease--is this type 3 diabetes? J Alzheimers Dis 7:63-80.
Stephens B, Guiloff RJ, Navarrete R, Newman P, Nikhar N, Lewis P (2006) Widespread loss of neuronal populations in the spinal ventral horn in sporadic motor neuron disease. A morphometric study. J Neurol Sci 244:41-58.

Stevenson A, Yates DM, Manser C, De Vos KJ, Vagnoni A, Leigh PN, McLoughlin DM, Miller CC (2009) Riluzole protects against glutamate-induced slowing of neurofilament axonal transport. Neurosci Lett 454:161-164.

Stieber A, Gonatas JO, Gonatas NK (2000) Aggregates of mutant protein appear progressively in dendrites, in periaxonal processes of oligodendrocytes, and in neuronal and astrocytic perikarya of mice expressing the SOD1(G93A) mutation of familial amyotrophic lateral sclerosis. J Neurol Sci 177:114-123.

Stokin GB, Lillo C, Falzone TL, Brusch RG, Rockenstein E, Mount SL, Raman R, Davies P, Masliah E, Williams DS, Goldstein LS (2005) Axonopathy and transport deficits early in the pathogenesis of Alzheimer's disease. Science 307:1282-1288.

Storkebaum E, Lambrechts D, Dewerchin M, Moreno-Murciano MP, Appelmans S, Oh H, Van Damme P, Rutten B, Man WY, De Mol M, Wyns S, Manka D, Vermeulen K, Van Den Bosch L, Mertens N, Schmitz C, Robberecht W, Conway EM, Collen D, Moons L, Carmeliet P (2005) Treatment of motoneuron degeneration by intracerebroventricular delivery of VEGF in a rat model of ALS. Nat Neurosci 8:85-92.

Strong MJ, Kesavapany S, Pant HC (2005) The pathobiology of amyotrophic lateral sclerosis: a proteinopathy? J Neuropathol Exp Neurol 64:649-664.

Subramaniam JR, Lyons WE, Liu J, Bartnikas TB, Rothstein J, Price DL, Cleveland DW, Gitlin JD, Wong PC (2002) Mutant SOD1 causes motor neuron disease independent of copper chaperone-mediated copper loading. Nat Neurosci 5:301-307.

Sullivan KA, Kim B, Feldman EL (2008) Insulin-like growth factors in the peripheral nervous system. Endocrinology 149:5963-5971.

Sumi H, Nagano S, Fujimura H, Kato S, Sakoda S (2006) Inverse correlation between the formation of mitochondria-derived vacuoles and Lewy-body-like hyaline inclusions in G93A superoxide-dismutase-transgenic mice. Acta Neuropathol 112:52-63.

Sussmuth SD, Brettschneider J, Ludolph AC, Tumani H (2008) Biochemical markers in CSF of ALS patients. Curr Med Chem 15:1788-1801.

Suzuki M, McHugh J, Tork C, Shelley B, Klein SM, Aebischer P, Svendsen CN (2007) GDNF secreting human neural progenitor cells protect dying motor neurons, but not their projection to muscle, in a rat model of familial ALS. PLoS One 2:e689.

Svensson CI, Fitzsimmons B, Azizi S, Powell HC, Hua XY, Yaksh TL (2005) Spinal p38beta isoform mediates tissue injury-induced hyperalgesia and spinal sensitization. J Neurochem 92:1508-1520.

Swash M, Desai J (2000) Motor neuron disease: classification and nomenclature. Amyotroph Lateral Scler Other Motor Neuron Disord 1:105-112.

Swerdlow RH, Parks JK, Cassarino DS, Trimmer PA, Miller SW, Maguire DJ, Sheehan JP, Maguire RS, Pattee G, Juel VC, Phillips LH, Tuttle JB, Bennett JP, Jr., Davis RE, Parker WD, Jr. (1998) Mitochondria in sporadic amyotrophic lateral sclerosis. Exp Neurol 153:135-142.

Takahashi K, Luo T, Saishin Y, Sung J, Hackett S, Brazzell RK, Kaleko M, Campochiaro PA (2002) Sustained transduction of ocular cells with a bovine immunodeficiency viral vector. Hum Gene Ther 13:1305-1316.

Takeda K, Hatai T, Hamazaki TS, Nishitoh H, Saitoh M, Ichijo H (2000) Apoptosis signal-regulating kinase 1 (ASK1) induces neuronal differentiation and survival of PC12 cells. J Biol Chem 275:9805-9813.

Takekawa M, Maeda T, Saito H (1998) Protein phosphatase 2Calpha inhibits the human stress-responsive p38 and JNK MAPK pathways. Embo J 17:4744-4752.

Takenaka K, Moriguchi T, Nishida E (1998) Activation of the protein kinase p38 in the spindle assembly checkpoint and mitotic arrest. Science 280:599-602.

Teuchert M, Fischer D, Schwalenstoecker B, Habisch HJ, Bockers TM, Ludolph AC (2006) A dynein mutation attenuates motor neuron degeneration in SOD1(G93A) mice. Exp Neurol 198:271-274.

Teuling E, van Dis V, Wulf PS, Haasdijk ED, Akhmanova A, Hoogenraad CC, Jaarsma D (2008) A novel mouse model with impaired dynein/dynactin function develops amyotrophic lateral sclerosis (ALS)-like features in motor neurons and improves lifespan in SOD1-ALS mice. Hum Mol Genet 17:2849-2862.

Thiel G, Lietz M, Bach K, Guethlein L, Cibelli G (2001) Biological activity of mammalian transcriptional repressors. Biol Chem 382:891-902.

Tibbles LA, Woodgett JR (1999) The stress-activated protein kinase pathways. Cell Mol Life Sci 55:1230-1254.

Tibbles LA, Ing YL, Kiefer F, Chan J, Iscove N, Woodgett JR, Lassam NJ (1996) MLK-3 activates the SAPK/JNK and p38/RK pathways via SEK1 and MKK3/6. Embo J 15:7026-7035.

Tijsterman M, Ketting RF, Plasterk RH (2002) The genetics of RNA silencing. Annu Rev Genet 36:489-519.

Toker A (2000) Protein kinases as mediators of phosphoinositide 3-kinase signaling. Mol Pharmacol 57:652-658.

Toker A, Newton AC (2000a) Cellular signaling: pivoting around PDK-1. Cell 103:185-188.

Toker A, Newton AC (2000b) Akt/protein kinase B is regulated by autophosphorylation at the hypothetical PDK-2 site. J Biol Chem 275:8271-8274.

Tomik B, Adamek D, Pierzchalski P, Banares S, Duda A, Partyka D, Pawlik W, Kaluza J, Krajewski S, Szczudlik A (2005) Does apoptosis occur in amyotrophic lateral sclerosis? TUNEL experience from human amyotrophic lateral sclerosis (ALS) tissues. Folia Neuropathol 43:75-80.

Topp JD, Gray NW, Gerard RD, Horazdovsky BF (2004) Alsin is a Rab5 and Rac1 guanine nucleotide exchange factor. J Biol Chem 279:24612-24623.

Tortarolo M, Crossthwaite AJ, Conforti L, Spencer JP, Williams RJ, Bendotti C, Rattray M (2004) Expression of SOD1 G93A or wild-type SOD1 in primary cultures of astrocytes down-regulates the glutamate transporter GLT-1: lack of involvement of oxidative stress. J Neurochem 88:481-493.

Tortarolo M, Veglianese P, Calvaresi N, Botturi A, Rossi C, Giorgini A, Migheli A, Bendotti C (2003) Persistent activation of p38 mitogen-activated protein kinase in a mouse model of familial amyotrophic lateral sclerosis correlates with disease progression. Mol Cell Neurosci 23:180-192.

Tortarolo M, Grignaschi G, Calvaresi N, Zennaro E, Spaltro G, Colovic M, Fracasso C, Guiso G, Elger B, Schneider H, Seilheimer B, Caccia S, Bendotti C (2006) Glutamate AMPA receptors change in motor neurons of SOD1G93A transgenic mice and their inhibition by a noncompetitive antagonist ameliorates the progression of amytrophic lateral sclerosis-like disease. J Neurosci Res 83:134-146.

Towne C, Raoul C, Schneider BL, Aebischer P (2008) Systemic AAV6 delivery mediating RNA interference against SOD1: neuromuscular transduction does not alter disease progression in fALS mice. Mol Ther 16:1018-1025.

Toyoshima I, Sugawara M, Kato K, Wada C, Hirota K, Hasegawa K, Kowa H, Sheetz MP, Masamune O (1998) Kinesin and cytoplasmic dynein in spinal spheroids with motor neuron disease. J Neurol Sci 159:38-44.

Trotti D, Rolfs A, Danbolt NC, Brown RH, Jr., Hediger MA (1999) SOD1 mutants linked to amyotrophic lateral sclerosis selectively inactivate a glial glutamate transporter. Nat Neurosci 2:848.

Tsiang H (1979) Evidence for an intraaxonal transport of fixed and street rabies virus. J Neuropathol Exp Neurol 38:286-299.

Tudor EL, Perkinton MS, Schmidt A, Ackerley S, Brownlees J, Jacobsen NJ, Byers HL, Ward M, Hall A, Leigh PN, Shaw CE, McLoughlin DM, Miller CC (2005) ALS2/Alsin regulates Rac-PAK signaling and neurite outgrowth. J Biol Chem 280:34735-34740.

Turner BJ, Baumer D, Parkinson NJ, Scaber J, Ansorge O, Talbot K (2008) TDP-43 expression in mouse models of amyotrophic lateral sclerosis and spinal muscular atrophy. BMC Neurosci 9:104.

Tuttle RL, Gill NS, Pugh W, Lee JP, Koeberlein B, Furth EE, Polonsky KS, Naji A, Birnbaum MJ (2001) Regulation of pancreatic beta-cell growth and survival by the serine/threonine protein kinase Akt1/PKBalpha. Nat Med 7:1133-1137.

Ugolini G (2008) Use of rabies virus as a transneuronal tracer of neuronal connections: implications for the understanding of rabies pathogenesis. Dev Biol (Basel) 131:493-506.

Van Damme P, Leyssen M, Callewaert G, Robberecht W, Van Den Bosch L (2003) The AMPA receptor antagonist NBQX prolongs survival in a transgenic mouse model of amyotrophic lateral sclerosis. Neurosci Lett 343:81-84.

Van Den Bosch L, Tilkin P, Lemmens G, Robberecht W (2002) Minocycline delays disease onset and mortality in a transgenic model of ALS. Neuroreport 13:1067-1070.

Van den Haute C, Eggermont K, Nuttin B, Debyser Z, Baekelandt V (2003) Lentiviral vector-mediated delivery of short hairpin RNA results in persistent knockdown of gene expression in mouse brain. Hum Gene Ther 14:1799-1807.

Vance C, Rogelj B, Hortobagyi T, De Vos KJ, Nishimura AL, Sreedharan J, Hu X, Smith B, Ruddy D, Wright P, Ganesalingam J, Williams KL, Tripathi V, Al-Saraj S, Al-Chalabi A, Leigh PN, Blair IP, Nicholson G, de Belleroche J, Gallo JM, Miller CC, Shaw CE (2009) Mutations in FUS, an RNA processing protein, cause familial amyotrophic lateral sclerosis type 6. Science 323:1208-1211.

Veglianese P, Lo Coco D, Bao Cutrona M, Magnoni R, Pennacchini D, Pozzi B, Gowing G, Julien JP, Tortarolo M, Bendotti C (2006) Activation of the p38MAPK cascade is associated with upregulation of TNF alpha receptors in the spinal motor neurons of mouse models of familial ALS. Mol Cell Neurosci 31:218-231.

Veldink JH, Kalmijn S, Van der Hout AH, Lemmink HH, Groeneveld GJ, Lummen C, Scheffer H, Wokke JH, Van den Berg LH (2005) SMN genotypes producing less SMN protein increase susceptibility to and severity of sporadic ALS. Neurology 65:820-825.

Vilar JM, Saiz L (2005) DNA looping in gene regulation: from the assembly of macromolecular complexes to the control of transcriptional noise. Curr Opin Genet Dev 15:136-144.

Wagey R, Pelech SL, Duronio V, Krieger C (1998) Phosphatidylinositol 3-kinase: increased activity and protein level in amyotrophic lateral sclerosis. J Neurochem 71:716-722.

Wagey R, Lurot S, Perrelet D, Pelech SL, Sagot Y, Krieger C (2001) Phosphatidylinositol 3-kinase activity in murine motoneuron disease: the progressive motor neuropathy mouse. Neuroscience 103:257-266.

Wang H, Ghosh A, Baigude H, Yang CS, Qiu L, Xia X, Zhou H, Rana TM, Xu Z (2008) Therapeutic gene silencing delivered by a chemically modified small interfering RNA against mutant SOD1 slows amyotrophic lateral sclerosis progression. J Biol Chem 283:15845-15852.

Wang J, Xu G, Slunt HH, Gonzales V, Coonfield M, Fromholt D, Copeland NG, Jenkins NA, Borchelt DR (2005) Coincident thresholds of mutant protein for paralytic disease and protein aggregation caused by restrictively expressed superoxide dismutase cDNA. Neurobiol Dis 20:943-952.

Wang LJ, Lu YY, Muramatsu S, Ikeguchi K, Fujimoto K, Okada T, Mizukami H, Matsushita T, Hanazono Y, Kume A, Nagatsu T, Ozawa K, Nakano I (2002) Neuroprotective effects of glial cell line-derived neurotrophic factor mediated by an adeno-associated virus vector in a transgenic animal model of amyotrophic lateral sclerosis. J Neurosci 22:6920-6928.

Wang Y, Su B, Sah VP, Brown JH, Han J, Chien KR (1998) Cardiac hypertrophy induced by mitogen-activated protein kinase kinase 7, a specific activator for c-Jun NH2-terminal kinase in ventricular muscle cells. J Biol Chem 273:5423-5426.

Wang Z, Harkins PC, Ulevitch RJ, Han J, Cobb MH, Goldsmith EJ (1997) The structure of mitogen-activated protein kinase p38 at 2.1-A resolution. Proc Natl Acad Sci U S A 94:2327-2332.

Warita H, Manabe Y, Murakami T, Shiro Y, Nagano I, Abe K (2001) Early decrease of survival signal-related proteins in spinal motor neurons of presymptomatic transgenic mice with a mutant SOD1 gene. Apoptosis 6:345-352.

Watanabe M, Dykes-Hoberg M, Culotta VC, Price DL, Wong PC, Rothstein JD (2001) Histological evidence of protein aggregation in mutant SOD1 transgenic mice and in amyotrophic lateral sclerosis neural tissues. Neurobiol Dis 8:933-941.

Watson DJ, Kobinger GP, Passini MA, Wilson JM, Wolfe JH (2002) Targeted transduction patterns in the mouse brain by lentivirus vectors pseudotyped with VSV, Ebola, Mokola, LCMV, or MuLV envelope proteins. Mol Ther 5:528-537.

Wengenack TM, Holasek SS, Montano CM, Gregor D, Curran GL, Poduslo JF (2004) Activation of programmed cell death markers in ventral horn motor neurons during early presymptomatic stages of amyotrophic lateral sclerosis in a transgenic mouse model. Brain Res 1027:73-86.

West M, Mhatre M, Ceballos A, Floyd RA, Grammas P, Gabbita SP, Hamdheydari L, Mai T, Mou S, Pye QN, Stewart C, West S, Williamson KS, Zemlan F, Hensley K (2004) The arachidonic acid 5-lipoxygenase inhibitor nordihydroguaiaretic acid inhibits tumor necrosis factor alpha activation of microglia and extends survival of G93A-SOD1 transgenic mice. J Neurochem 91:133-143.

Wharton S (2003) Pathology of motor neuron disorders. Philadelphia: Butterworth-Heinemann.
White MR, Masuko M, Amet L, Elliott G, Braddock M, Kingsman AJ, Kingsman SM (1995) Real-time analysis of the transcriptional regulation of HIV and hCMV promoters in single mammalian cells. J Cell Sci 108 (Pt 2):441-455.
Whitely (1996) Herpes simplex viruses: Lippincott.
Wiedau-Pazos M, Goto JJ, Rabizadeh S, Gralla EB, Roe JA, Lee MK, Valentine JS, Bredesen DE (1996) Altered reactivity of superoxide dismutase in familial amyotrophic lateral sclerosis. Science 271:515-518.
Wijesekera LC, Leigh PN (2009) Amyotrophic lateral sclerosis. Orphanet J Rare Dis 4:3.
Wilhelmsen KC, Forman MS, Rosen HJ, Alving LI, Goldman J, Feiger J, Lee JV, Segall SK, Kramer JH, Lomen-Hoerth C, Rankin KP, Johnson J, Feiler HS, Weiner MW, Lee VM, Trojanowski JQ, Miller BL (2004) 17q-linked frontotemporal dementia-amyotrophic lateral sclerosis without tau mutations with tau and alpha-synuclein inclusions. Arch Neurol 61:398-406.
Williamson TL, Cleveland DW (1999) Slowing of axonal transport is a very early event in the toxicity of ALS-linked SOD1 mutants to motor neurons. Nat Neurosci 2:50-56.
Williamson TL, Bruijn LI, Zhu Q, Anderson KL, Anderson SD, Julien JP, Cleveland DW (1998) Absence of neurofilaments reduces the selective vulnerability of motor neurons and slows disease caused by a familial amyotrophic lateral sclerosis-linked superoxide dismutase 1 mutant. Proc Natl Acad Sci U S A 95:9631-9636.
Willing AE, Garbuzova-Davis S, Saporta S, Milliken M, Cahill DW, Sanberg PR (2001) hNT neurons delay onset of motor deficits in a model of amyotrophic lateral sclerosis. Brain Res Bull 56:525-530.
Wilson KP, Fitzgibbon MJ, Caron PR, Griffith JP, Chen W, McCaffrey PG, Chambers SP, Su MS (1996) Crystal structure of p38 mitogen-activated protein kinase. J Biol Chem 271:27696-27700.
Witherden AS, Hafezparast M, Nicholson SJ, Ahmad-Annuar A, Bermingham N, Arac D, Rankin J, Iravani M, Ball S, Peters J, Martin JE, Huntley D, Hummerich H, Sergot M, Fisher EM (2002) An integrated genetic, radiation hybrid, physical and transcription map of a region of distal mouse chromosome 12, including an imprinted locus and the 'Legs at odd angles' (Loa) mutation. Gene 283:71-82.
Wong GH (1995) Protective roles of cytokines against radiation: induction of mitochondrial MnSOD. Biochim Biophys Acta 1271:205-209.
Wong LF, Azzouz M, Walmsley LE, Askham Z, Wilkes FJ, Mitrophanous KA, Kingsman SM, Mazarakis ND (2004) Transduction patterns of pseudotyped lentiviral vectors in the nervous system. Mol Ther 9:101-111.
Wong PC, Waggoner D, Subramaniam JR, Tessarollo L, Bartnikas TB, Culotta VC, Price DL, Rothstein J, Gitlin JD (2000) Copper chaperone for superoxide dismutase is essential to activate mammalian Cu/Zn superoxide dismutase. Proc Natl Acad Sci U S A 97:2886-2891.
Worms PM (2001) The epidemiology of motor neuron diseases: a review of recent studies. J Neurol Sci 191:3-9.
Wu R, Wang H, Xia XG, Zhou H, Liu C, Castro MG, Xu Z (2009) Nerve injection of viral vectors efficiently transfers transgenes into motor neurons and delivers RNAi therapy against ALS. Antioxid Redox Signal.
Wu X, Franka R, Velasco-Villa A, Rupprecht CE (2007) Are all lyssavirus genes equal for phylogenetic analyses? Virus Res 129:91-103.
Wuolikainen A, Hedenstrom M, Moritz T, Marklund SL, Antti H, Andersen PM (2009) Optimization of procedures for collecting and storing of CSF for studying the metabolome in ALS. Amyotroph Lateral Scler 10:229-236.
Xiao Q, Zhao W, Beers DR, Yen AA, Xie W, Henkel JS, Appel SH (2007) Mutant SOD1(G93A) microglia are more neurotoxic relative to wild-type microglia. J Neurochem 102:2008-2019.
Xu Z, Cork LC, Griffin JW, Cleveland DW (1993) Involvement of neurofilaments in motor neuron disease. J Cell Sci Suppl 17:101-108.
Yamanaka K, Miller TM, McAlonis-Downes M, Chun SJ, Cleveland DW (2006) Progressive spinal axonal degeneration and slowness in ALS2-deficient mice. Ann Neurol 60:95-104.
Yamanaka K, Vande Velde C, Eymard-Pierre E, Bertini E, Boespflug-Tanguy O, Cleveland DW (2003) Unstable mutants in the peripheral endosomal membrane component

ALS2 cause early-onset motor neuron disease. Proc Natl Acad Sci U S A 100:16041-16046.
Yamanaka K, Chun SJ, Boillee S, Fujimori-Tonou N, Yamashita H, Gutmann DH, Takahashi R, Misawa H, Cleveland DW (2008) Astrocytes as determinants of disease progression in inherited amyotrophic lateral sclerosis. Nat Neurosci 11:251-253.
Yan X, Mohankumar PS, Dietzschold B, Schnell MJ, Fu ZF (2002) The rabies virus glycoprotein determines the distribution of different rabies virus strains in the brain. J Neurovirol 8:345-352.
Yanagisawa M, Nakashima K, Takeda K, Ochiai W, Takizawa T, Ueno M, Takizawa M, Shibuya H, Taga T (2001) Inhibition of BMP2-induced, TAK1 kinase-mediated neurite outgrowth by Smad6 and Smad7. Genes Cells 6:1091-1099.
Yang Y, Zhu X, Chen Y, Wang X, Chen R (2007) p38 and JNK MAPK, but not ERK1/2 MAPK, play important role in colchicine-induced cortical neurons apoptosis. Eur J Pharmacol 576:26-33.
Yang Y, Hentati A, Deng HX, Dabbagh O, Sasaki T, Hirano M, Hung WY, Ouahchi K, Yan J, Azim AC, Cole N, Gascon G, Yagmour A, Ben-Hamida M, Pericak-Vance M, Hentati F, Siddique T (2001) The gene encoding alsin, a protein with three guanine-nucleotide exchange factor domains, is mutated in a form of recessive amyotrophic lateral sclerosis. Nat Genet 29:160-165.
Yang ZZ, Tschopp O, Hemmings-Mieszczak M, Feng J, Brodbeck D, Perentes E, Hemmings BA (2003) Protein kinase B alpha/Akt1 regulates placental development and fetal growth. J Biol Chem 278:32124-32131.
Yang ZZ, Tschopp O, Di-Poi N, Bruder E, Baudry A, Dummler B, Wahli W, Hemmings BA (2005) Dosage-dependent effects of Akt1/protein kinase Balpha (PKBalpha) and Akt3/PKBgamma on thymus, skin, and cardiovascular and nervous system development in mice. Mol Cell Biol 25:10407-10418.
Zarubin T, Han J (2005) Activation and signaling of the p38 MAP kinase pathway. Cell Res 15:11-18.
Zavada J (1982) The pseudotypic paradox. J Gen Virol 63 (Pt 1):15-24.
Zetser A, Gredinger E, Bengal E (1999) p38 mitogen-activated protein kinase pathway promotes skeletal muscle differentiation. Participation of the Mef2c transcription factor. J Biol Chem 274:5193-5200.
Zhang M, Fang X, Liu H, Wang S, Yang D (2007) Blockade of AKT activation in prostate cancer cells with a small molecule inhibitor, 9-chloro-2-methylellipticinium acetate (CMEP). Biochem Pharmacol 73:15-24.
Zhang S, Han J, Sells MA, Chernoff J, Knaus UG, Ulevitch RJ, Bokoch GM (1995) Rho family GTPases regulate p38 mitogen-activated protein kinase through the downstream mediator Pak1. J Biol Chem 270:23934-23936.
Zhao C, Strappe PM, Lever AM, Franklin RJ (2003) Lentiviral vectors for gene delivery to normal and demyelinated white matter. Glia 42:59-67.
Zhou H, Li XM, Meinkoth J, Pittman RN (2000) Akt regulates cell survival and apoptosis at a postmitochondrial level. J Cell Biol 151:483-494.
Zhu Q, Couillard-Despres S, Julien JP (1997) Delayed maturation of regenerating myelinated axons in mice lacking neurofilaments. Exp Neurol 148:299-316.
Zhu S, Stavrovskaya IG, Drozda M, Kim BY, Ona V, Li M, Sarang S, Liu AS, Hartley DM, Wu DC, Gullans S, Ferrante RJ, Przedborski S, Kristal BS, Friedlander RM (2002) Minocycline inhibits cytochrome c release and delays progression of amyotrophic lateral sclerosis in mice. Nature 417:74-78.
Zufferey R, Dull T, Mandel RJ, Bukovsky A, Quiroz D, Naldini L, Trono D (1998) Self-inactivating lentivirus vector for safe and efficient in vivo gene delivery. J Virol 72:9873-9880.

LIST OF PUBLICATIONS

Publications arisen from this thesis

Although no parts of this thesis have yet been published, a manuscript comprising the results described in chapters 3 and 4 is already in preparation.

Publications related to this thesis

Peviani M, Cheroni C, Troglio F, Quarto M, Pelicci G, Bendotti C (2007) Lack of changes in the PI3K/AKT survival pathway in the spinal cord motor neurons of a mouse model of familial amyotrophic lateral sclerosis. Mol Cell Neurosci 34:592-602

Publications not strictly related to this thesis

Cheroni C, Peviani M, Cascio P, Debiasi S, Monti C, Bendotti C (2005) Accumulation of human SOD1 and ubiquitinated deposits in the spinal cord of SOD1G93A mice during motor neuron disease progression correlates with a decrease of proteasome. Neurobiol Dis 18:509-522.

Bendotti C, Bao Cutrona M, Cheroni C, Grignaschi G, Lo Coco D, Peviani M, Tortarolo M, Veglianese P, Zennaro E (2005)
Inter- and intracellular signaling in amyotrophic lateral sclerosis: role of p38 mitogen-activated protein kinase. Neurodegener Dis 2:128-134.